LV-2013-016

Landsvirkjun

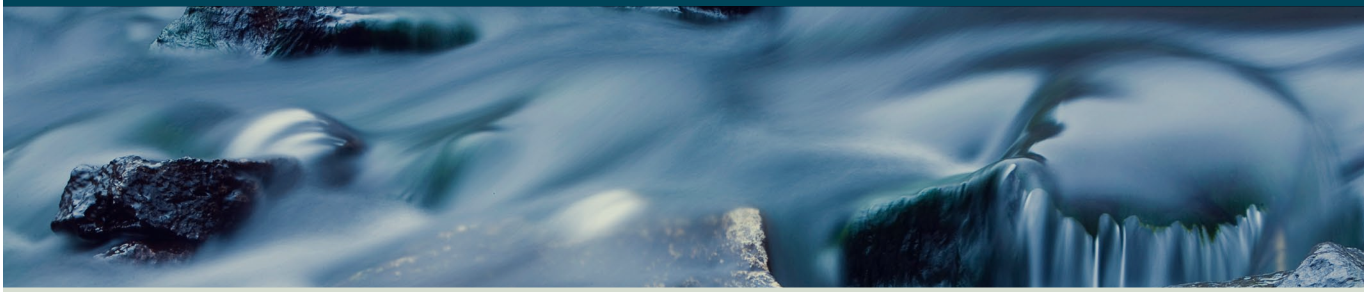

Urriðafoss HEP Lower Þjórsá Physical Model Investigation on the Spillway and Juvenile Fish Passage

Final Report

Key page Landsvirkjun

LV report no: LV-2013-016 Date: March 2013

Number of pages: 217 Copies: 20 Distribution: ☒ On www.lv.is ☒ Open ☐ Limited until

Title: Urriðafoss HEP Lower Þjórsá
Physical Model Investigation on the Spillway and Juvenile Fish Passage

Authors / Company: Gunnar Guðni Tómasson / Reykjavík Univ., Sigurður Magnús Garðarsson / Univ. of Iceland, Andri Gunnarsson / Univ. of Iceland, Gísli Steinn Pétursson / Univ. of Iceland and Ágúst Guðmundsson / Univ. of Iceland

Project manager: Helgi Jóhannesson

Prepared for: Landsvirkjun

Co operators: Verkís, Mannvit and Icelandic Maritime Administration

Abstract: In this report results of model tests of the Urriðafoss HEP spillway and juvenile fish passage are presented. The model was built at a scale of 1:40 in order to investigate and optimize the design of the spillway and downstream conditions and to verify the performance of the proposed juvenile fish passage system. Improvements and technical optimizations of the original reference design are described. The hydraulic performance of the hydraulic structures over the entire range of possible operating conditions is verified. The results of a numerical model investigation of the juvenile fish passage system are presented in a separate report LV-2013-017.

Keywords: Þjórsá, Urriðafoss, spillway, model, roller bucket, juvenile fish passage.

ISBN no:

Approved by Landsvirkjun's project manager:

Helgi Jóhannesson

LV-2013-016

Landsvirkjun

Urriðafoss HEP Lower Þjórsá Physical Model Investigation on the Spillway and Juvenile Fish Passage

Final Report

March 2013

Summary

The National Power Company of Iceland (LV), is planning to construct three power plants in the Lower Þjórsa River, Hvammur Hydro Electric Project (HEP), Holt HEP and Urriðafoss HEP. The projects are run of the river power plants with small intake ponds. Urriðafoss HEP is the lowest of the three projects utilizing the head between elevations of 50 m a.s.l. and 9.4 m a.s.l. The design discharge is 370 m^3/s providing installed capacity of approximately 128 MW, and energy-generating capacity of 980 GWh/a with two Kaplan turbines.

The University of Iceland and Reykjavik University joined forces in performing model tests at a scale of 1:40 to investigate and optimize the design of the spillway, downstream conditions and juvenile fish passage facility. The main characteristics of the final design resulting from the model tests are described below:

The standard profile weir of the gated spillway is in three 12 m wide sections. The sections are divided by piers with side wall configurations at the sides. The crest elevation is 41 m a.s.l. with 12 x 10 m radial gates (w x h). The maximum reservoir waterlevel elevation for the design flood of 2250 m^3/s is 51.2 m a.s.l. as measured in the model. For the normal regulated reservoir elevation of 50.0 m a.s.l. the discharge capacity of the spillway with all three gates fully open is 1720 m^3/s.

The transition from supercritcal to subcritical flow takes place in the slotted roller bucket energy dissipator for all discharges. The high velocity low Froude number jet disperses within the bucket geometry. For higher flows a surface boiler is observed but is absent for low and mid to low flows. The bucket has a radius of 11 m with the bucket invert at 26 m a.s.l. In total 22 teeth are applied to disperse the incoming jet. Dimensions of the slotted bucket are according to USBR recommendations.

For low discharges the flow in the downstream natural river channel is stable, with a relatively smooth surface and subcritical flow. For mid to high discharges the surface in the upstream part of the river channel is irregular and partly critical and for high discharges the flow characteristics in the natural river channel are fluctuating with periodical waves but not unsatisfactory.

The intake is a conventional structure with a juvenile fish bypass system incorporated at the top of the structure. The intake has four 5.95 m wide entrances, uniting in pairs, into two separate draft tubes. The juvenile fish facility has four 5.95 m wide entrances, each with a smooth rounded crest at an elevation of 49.1 m a.s.l. The approach flow and efficiency of the juvenile fish passage facility based on various operation parameters is summarized in this report.

Contents

1. Introduction

1.1. Project description

The National Power Company of Iceland (LV), is planning to construct three power plants in the Lower Þjórsa River, Hvammur Hydro Electric Project (HEP), Holt HEP and Urriðafoss HEP. The projects are run of the river power plants with small intake ponds. Urriðafoss HEP is the lowest of the three projects utilizing the head between elevations of 50 m a.s.l. and 9.4 m a.s.l. The design discharge is 370 m^3/s providing installed capacity of approximately 128 MW, and energy-generating capacity of 980 GWh/a with two Kaplan turbines.

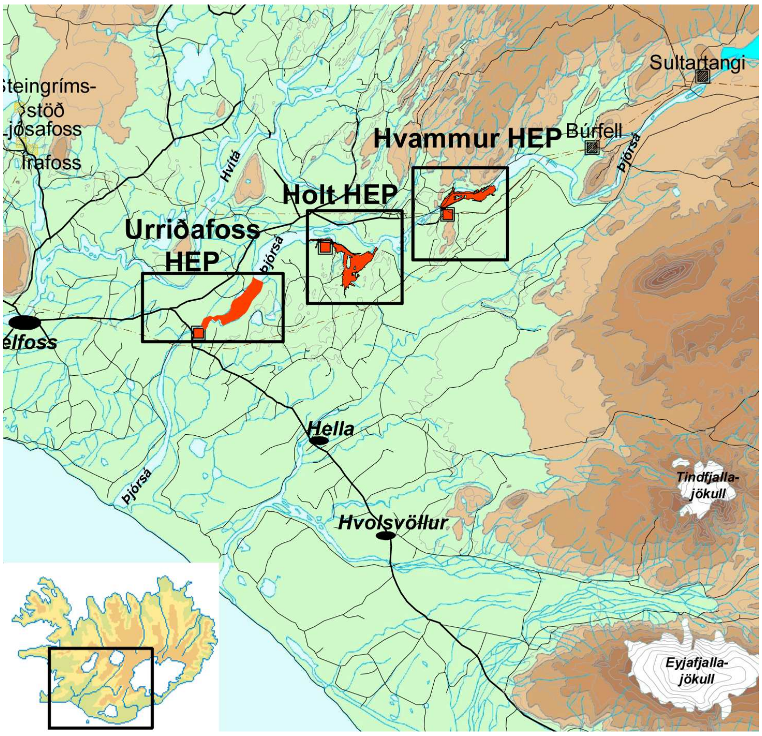

Figure 1.1: *General overview of the hydro electric project in Lower Þjórsá*

Heiðarlón, the intake reservoir for Urriðafoss HEP, will be formed by a dam across Þjórsá river, located at Heiðartangi point and by dykes along the west bank of the river. The intake structures will be at Heiðartangi point with the powerhouse underground, near Þjórsártún farm, while the tailrace tunnel leading from the powerhouse will open into Þjórsá river somewhat downstream of Urriðafoss waterfall.

A gated spillway is proposed to bypass floods and regulate reservoir elevation. The gated section of the spillway is ogee shaped with a crest elevation of 41 m a.s.l. and equipped with three 10 m high and 12 m wide radial gates. A proposed slotted roller bucket downstream of the radial gates dissipates excess energy and protects the dam and the gated structure from erosion. The design assumes a roller to form within the bucket geometry for all normal gate openings and discharges up to Q_{1000} (2250 m^3/s). The water is then routed back to the original river channel downstream of the roller bucket by an excavated channel. The water through the power plant is routed back to the river by a tailrace tunnel 3 km downstream of the dam itself.

The Urridafoss HEP is located in the migratory pathways of the North Atlantic salmon, requiring mitigating measures to ensure satisfactory fish passage up and down the river. A surface flow outlet (SFO) type juvenile fish bypass system is proposed as part of the project to aid the downstream migration of juvenile salmon to the ocean. The SFO is located above the powerhouse intake. From the SFO the water is united in a single sideway channel and routed through a separate channel to the original riverbed downstream of the dam.

As part of the design process for Urriðafoss HEP hydraulic model tests of the hydraulic structures in the system are conducted to validate and optimize the proposed design. These structures include the main gated spillway, roller bucket energy dissipator, downstream channel, intake to power plant, SFO and general approach flow conditions in the upstream area of the intake and spillway. Results from hydraulic model tests at Urriðafoss HEP are presented in this report.

1.2. Tendering and contract

Verkís Engineering and Mannvit Engineering (the designers) where hired as consultants by the client responsible for the design of the structure. A contract agreement, based on contract documents NTH-81 (Verkís & Mannvit 2010) prepared by the designers, was made in September 2010 between the National Power Company of Iceland (the client), University of Iceland, Reykjavik University and the National Maritime Administration of Iceland (the modeling group). The scope of this agreement was to fulfill the needs of physical modeling at Hvammur HEP and Urriðafoss HEP. Preparations started early fall 2011 and the building of the model started late January 2012. Model tests started in May 2012 and investigations on the final design at Urriðafoss finished in October 2012.

1.3. Co-ordination groups

Two co-ordination groups where established, The first group was responsible for co-ordination of the model construction and time schedule for the project (modeling group):

- Dr. Helgi Jóhannesson, The National Power Company of Iceland (LV).
- Prof. Sigurdur M. Garðarsson, University of Iceland (UI).
- Dr. Gunnar G. Tómasson, Reykjavik University (RU).
- Mr. Pétur Sveinbjörnsson, Icelandic Maritime Adm. (SI).
- Mr. Andri Gunnarsson, Head of Laboratory. (UI/RU)
- Mr. Gísli Steinn Pétursson, Laboratory assistant. (UI/RU)
- Mr. Ágúst Guðmundsson, Laboratory assistant. (UI/RU)

The second co-ordination group was initiated to review model results and suggest improvements (client, the modeling group and the designers). The group was composed of the following participants:

- Dr. Helgi Jóhannesson, The National Power Company of Iceland (LV).
- Prof. Sigurdur M. Garðarsson, University of Iceland (UI.)
- Dr. Gunnar G. Tómasson, Reykjavik University (RU.)
- Mr. Þorbergur S. Leifsson, Verkis Engineering.
- Ms. Ólöf Rós Káradóttir, Verkis Engineering.
- Mr. Einar Júliusson, Mannvit Engineering.
- Dr. Sigurður Guðjónsson
- Mr. Andri Gunnarsson, Head of Laboratory. (UI/RU)
- Mr. Gísli Steinn Pétursson, Laboratory assistant. (UI/RU)
- Mr. Ágúst Guðmundsson, Laboratory assistant. (UI/RU)

1.4. Design criteria and scope of investigation

The general objectives of the hydraulic investigations are, as listed in the contract documents, (Verkís & Mannvit 2010):

- Verification of the hydraulic performance of the hydraulic structures over the entire range of possible operating conditions.
- Possible improvements and technical optimization of the original reference design by hydraulic investigations and testing of design alternatives.

The spillway structure must meet the following design criteria:

- Pass the design flood without any damage to the spillway.
- The operation condition of the roller bucket energy dissipator needs to be satisfactory for all flow scenarios

Table 1.1: *Return periods for floods in Lower Þjórsá at Urriðafoss HEP. The design flood is 2250 m^3/s (Q_{1000}) with the associated maximum allowable reservoir elevation of 51.5 m .a.s.l.*

Prototype	Return Period	Allowable Reservoir Elevation
m^3/s	Years	m a.s.l.
1000	2	50
1250	5	50
1350	10	50
1700	50	50
2250	1000	51.5

Further more the scope of the investigation contains the following aspects:

Upstream reservoir:

- Flow conditions in the approach area of the spillway and in the approach zone of the powerhouse intake at various combinations of operation.

Spillway structure:

- Discharge capacity at normal and maximum flood level.
- Optimal geometry of Spillway approach zone, bottom elevation, pier and abutment geometry.
- Optimal spillway crest elevation and ogee shape.
- Operation conditions with partial gate opening and relevant combinations of gate opening, including discharge curves for all gate openings.

Roller bucket:

- Roller bucket invert elevation and bucket radius.
- Optimal geometry of excavated channel invert downstream of the roller bucket.

Downstream discharge channel:

- Minimum required excavation of the downstream part of discharge canal.
- Flow conditions in the river channel.

Surface flow outlet (juvenile fish passage):

- Flow through the surface flow outlet
- Extent of the area in the reservoir delivering water to the surface flow outlet and velocity distribution within that specified area.
- Extent of the area in the reservoir delivering water to the spillway and velocity distribution within that specified area.
- Local stagnant velocity zones in the upstream reservoir
- Local zones with large change in flow velocity, i.e. acceleration zones.

1.5. General overview of the study

The investigation presented in this report lasted over a period of 4 months. This excludes the building of the model which took a period of 3 months and a 2 month period of review of and modifications to the initial design prior to physical research. The initial design was handed in by the designers and reviewed by the modeling group, with some modifications made prior to model investigation (see discussion in Chapter 3, review of design). The design handed in was optimized in various steps and the model was modified several times.

1.6. Schedule of investigation for Urriðafoss HEP

The modeling group was commissioned by LV to do the physical model tests with a contract(nr.1100) dating 3. September 2010. Due to review of the initial design at Urriðarfoss based on results from the model work at Hvammur HEP, the model construction for Urriðarfoss was delayed and finally completed 1. May 2012. During the experimental process the modeling group, consultant and client met on a weekly basis to review and discuss the experimental work.

First results from the physical model of Urriðarfoss according to the measurement program (Tómasson, Garðarsson & Gunnarsson 2012*b*) were presented in a meeting 07.05.2012. The spillway capacity was sufficient and in general the approach flow was satisfactory. A decision was made to investigate conditions immediately downstream of the bucket with more detail than suggested in the measurement program, both to assess the scour potential and the required minimum excavation. In a meeting 14.05.2012 results from the preliminary measurement program for the spillway were presented with the exception of the final invert elevation and layout downstream of the roller bucket. An extensive program to estimate the necessary minimum excavation was designed. The consultant provided more layouts of the suggested downstream profile. In meetings 18.05.2012 and 04.06.2012 results from this detailed program where presented and finally on 12.06.2012 the downstream layout of the profile was selected and the preliminary testing of the spillway was complete. Following this the preliminary investigation for the powerhouse intake and associated juvenile fish passage facility was conducted. In a meeting 25.06.2012 the results from the preliminary measurement program for the intake and associated juvenile fish passage were presented. In that meeting a decision was made that the preliminary program had been completed and the detailed measurement program could be started. Results from the detailed measurement program, both for the spillway and intake structure and the associated juvenile fish passage were presented in meetings 02.07.2012, 09.07.2012 and 08.08.2012. On 22.08.2012 the physical modeling of Urriðarfoss HEP according to the contract documents was completed.

2. Hydraulic model

2.1. Model purpose and scope

A physical hydraulic model of Urriðafoss HEP includes the main dam spillway structure, the intake to the powerhouse, a part of the upstream reservoir and a part of the downstream Þjórsá river section. Figure 2.1 shows the area that is represented in the model and which part of the proposed project area is constructed. The laboratory system is a closed loop system, pumping water from one tank downstream of the model to an upstream reservoir tank. Discharge in the model is regulated by three high capacity pumps which are controlled by frequency inverters.

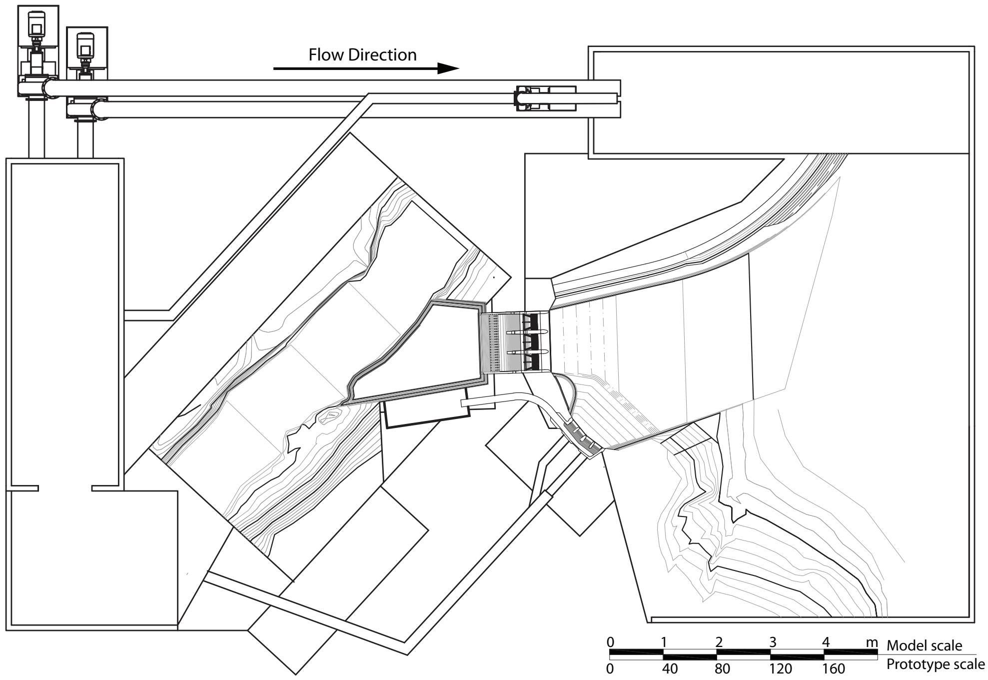

Figure 2.1: *Overview of the modeled area for Urriðafoss HEP. Water flows from right to left through the hydraulic structures.*

Figure 2.2: *Overview of the laboratory model for Urriðafoss HEP.*

2.2. Model construction

The model construction can be divided into two parts. First the landscape of the original riverbed, approach flow channels and downstream discharge channel are made of fiber reinforced concrete and mortar. Contour lines and positions of the designed structures are positioned using a total station with accuracy in position (xyz) less than 1 mm. The second part includes the spillway structure and the intake. Both are constructed of industrial plastics (PE) and made in computer numerical controlled (CNC) milling machines. The side walls of the roller bucket basin are made out of perplex to make the flow behavior in the basin visible. This construction method for the structures made it also easy to install measuring equipment at desired locations and its highly modular parts were easy to change and modify in the optimization process. Figures 2.3 and 2.4 show the intake structure after assembly and the spillway structure during assembly.

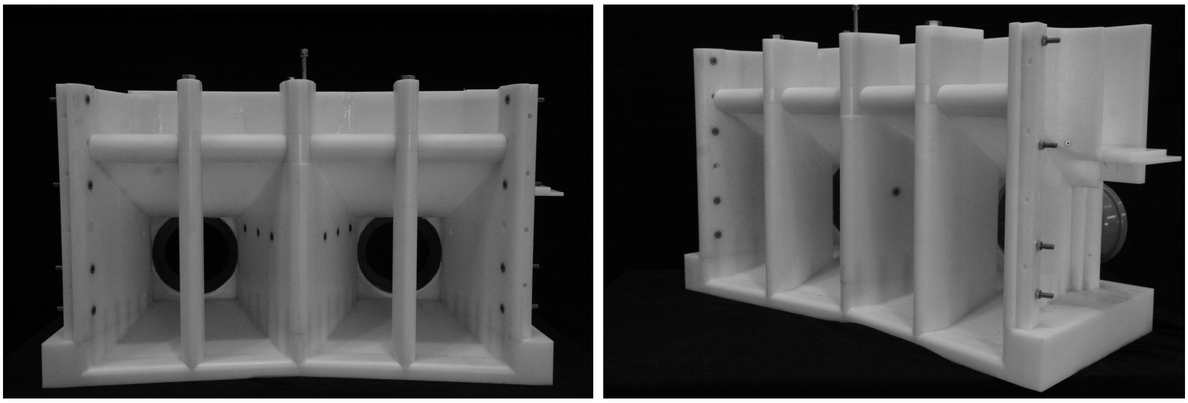

Figure 2.3: *The intake and juvenile fish passage facility in the model for Urriðafoss HEP.*

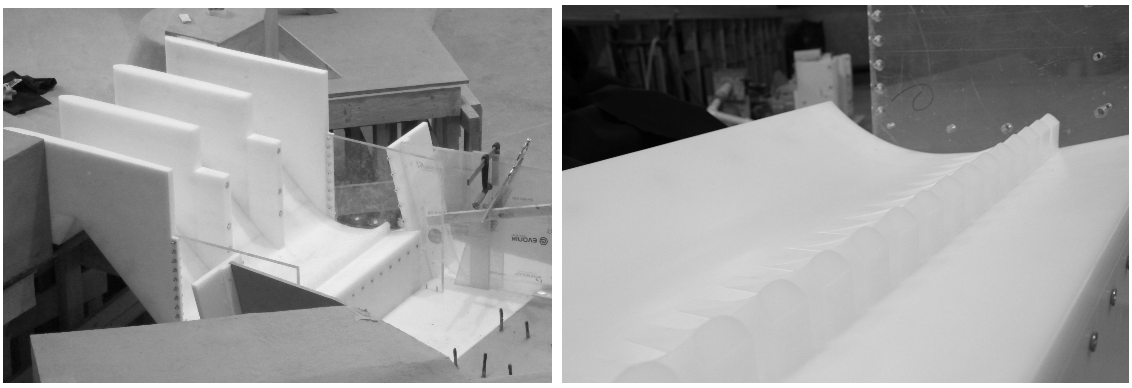

Figure 2.4: *The spillway during assembly in the model for Urriðafoss HEP.*

The laboratory model was constructed within a 3 month period from February to May 2012 in the facilities of the Icelandic Maritime Administration in Kópavogur.

2.3. Model calibration

A flow straightness structure was located at the outlet of the upstream reservoir tank. The flow straightness structure was used to direct the flow entering the approach flow channel more along the right approach bank which was in accordance with preliminary results from the numerical model. The flow straightness structure was applied for all scenarios and discharges tested in the model.

2.4. Model instrumentation

2.4.1. Discharge

Two high capacity pumps transport the water from the downstream reservoir tank to the upstream reservoir tank. The pumps are located at the downstream tank, see Figure 2.1, and two DN250 PE pipes link the two reservoirs. Discharge in the model is measured with two ultra sonic acoustic discharge meters fitted to the DN250 PE pipes which recirculate water in the model. The meters where factory calibrated before installation and calibration verified after installation. Additionally, a portable ultra sonic acoustic discharge meter was used for verification. Accuracy of the instruments is 1% for the given range. A third smaller pump which transports water from the intake to the downstream reservoir tank was fitted with a ultra sonic acoustic discharge meter to allow for determination of flow through the intake structure.

2.4.2. Velocity

Velocity was measured using an acoustic Doppler velocimeter (ADV). The ADV has a sampling rate up to 50 Hz and acquires both instantaneous values and mean value with its statistical properties. Accuracy of the instrument is 1% of the selected measurable range. The instrument ranges from 0.001 m/s to 2.5 m/s and has a sampling volume of 0.1 cm^3.

2.4.3. Water levels and flow depths

Water levels and flow depths were measured with various gauges. A conventional point gauge was used to measure reservoir elevation. For flow depths in the stilling basin and downstream channel manual gauges were used.

2.4.4. Pressure

Hydrostatic pressure is measured with pinhole relative pressure transducers. The sampling rate varies depending on the scenario being tested. All sensors were calibrated before operation. Full measuring range of the sensors is 1 mH_2O with accuracy of 0.1 % of full range.

2.4.5. Particle test

Plastic particles, 1 cm diameter by 1 cm long cylinders were scattered upstream in the model, for a given case, and the movements of the particles in the approach flow channel were documented by a video. The paths of the particles were computed from the videos by image processing program written in Matlab. The image processing program takes each frame of the video subtracts it from the previous frame, filters out noise and locates movement in the video. A single image showing particle tracks was obtained from the image processing, the images and videos were then used to derive schematic drawings of the approach flow characteristics. The aim was to identify irregularities and stagnant velocity zones in the approach flow and focus on general flow characteristics in the system. The scattering of particles took place immediately downstream of the flow straightness structures in the model.

2.4.6. Dye test

A dye was released through a pitot tube at depths ranging from 0.5 m to 3 m immediately upstream of the SFO crest. The dye was a solution of potassium permanganate dissolved in water which has approximately the same buoyancy as water. The dye was used to assess the streamline separation immediately upstream of the SFO crest and quantify the surface layer transported by the SFO. The streamline separation was documented by a video. The depths at which water was completely transported by the SFO, equally transported by the intake and SFO and where water was completely transported by the intake were determined.

2.4.7. Other measurements

Photographs and videos were documented systematically through the project to allow for comparison between different scenarios.

2.5. Model similitude

Similitude between the model and the prototype is achieved when the ratios of the major forces controlling the physical processes are kept equal in the model and prototype. For clear water flow a model scale of 1:40 represents well turbulent prototype conditions for open channel hydraulic jump and channel flow. Since gravitational and inertial forces dominate the physics of open channel flow, Froude-scale similitude was used to establish a kinematic relationship between the model and the prototype. Air bubbles and air pockets as well as the flux of air in the mixture flow cannot however be adequately modeled. This is due to the applicable similarity laws (Froude: pure water flow; Weber: surface tension, entrained air) preventing each other from being fulfilled at the same time.

The Froude number is a dimensionless classification of open channel flow measuring the ratio of channel flow velocity to the speed of propagation of small disturbance wave in the channel and is defined by Equation 2.1:

$$Fr = \frac{\text{flow velocity}}{\text{surface wave speed}} = \frac{V}{\sqrt{gy}} \tag{2.1}$$

where V is the velocity average over depth [m/s], g is gravitational acceleration [m/s^2], and y is the flow depth [m]. When Froude-scale modelling is used, the following relationship needs to be fulfilled between the model and prototype.

$$Fr_{model} = Fr_{prototype} \tag{2.2}$$

Equation 2.2 needs to be fulfilled for all operational conditions. Relations between model and prototype are shown in Table 2.1.

Table 2.1: *Scale factors for Froude similarity. λ is the scale ratio.*

Parameter	Unit	Scale factor	$\lambda = 40$
Length	[m]	λ	40
Velocity	[m/s]	$\sqrt{\lambda}$	$\sqrt{40}$
Time	[s]	$\sqrt{\lambda}$	$\sqrt{40}$
Discharge	[m^3/s]	$\lambda^{5/2}$	$40^{5/2}$

3. Review of design

3.1. Review of proposed design

Before building of the physical model started the design proposed by the designers was reviewed by the modeling group. This includes both the design for the spillway structure itself and the energy dissipation method suggested downstream of the spillway. Furthermore, the design and layout of the intake with its associated juvenile fish passage was reviewed, partly with theory and mainly based on pre-investigations in the Hvammur physical model. This chapter summarizes the review of the design for hydraulic structures at Urriðarfoss HEP and the discussion that led to the final design.

3.2. Review of spillway and energy dissipation design

According to the contract documents for the hydraulic model tests (Verkís & Mannvit 2010) the spillway and energy dissipation layout for Urriðarfoss was to be a gated ogee crest spillway with three radial gates and a 25 m long shallow USBR stilling basin. Also, the details of the design should be based on results from Hvammur HEP physical model. The design of the gated section of the spillway, its discharge capacity and overall dimensions where confirmed by a general review of the project (Tómasson, Garðarsson & Gunnarsson 2010) although a marginal increase in the discharge capacity was required. The majority of the review at Urriðarfoss was focused on the concept of energy dissipation as the results from Hvammur HEP and further investigation indicated that the energy dissipation concept proposed was not feasible. Another difference from the conditions at Hvammur HEP is the local geology. At Urriðarfoss it is estimated that a weak 4-6 m thick scoria layer is located in a mildly sloping plane ranging from 28 m a.s.l. to 36 m a.s.l. approximately. This layer is unstable and believed to be to erosive if not protected or excavated. This needed to be taken into account when designing the final layout of the energy dissipation method.

3.2.1. Energy dissipation at Urriðarfoss HEP

Based on results from Hvammur HEP physical model (Tómasson, Garðarsson & Gunnarsson 2012*a*) an acceptably functioning stilling basin is dependent to the available tailwater level downstream of the stilling basin. At Hvammur HEP a man-made hydraulic control is applied to ensure the necessary tailwater elevation. At Urriðarfoss spillway, the natural tailwater elevations are not sufficient to facilitate a conventional stilling basin as proposed in the contract documents. Furthermore, if to adopt the solution from Hvammur HEP, the physical space available in the nearby topography is insufficient to excavate and build a man-made hydraulic control. Based on this, a complete review was conducted by the designers to reassess and redesign the concept and mechanism of energy dissipation at Urriðarfoss. In (Verkís 2011) the design at Urriðafoss HEP is reviewed by the designers and in total six design layouts put forward, five of which are different versions of a stilling basin, including a design based on that proposed for Hvammur HEP. The sixth suggestion is a flip bucket concept and the one preferred by the designers. Table 3.1 summarizes the options proposed and their main parameters.

	Basin level	Fro-ude	Jet depth	Calc. basin Length	Endwall el.	Side wall el.	Energy dissip. (max flow)	Pot. Vel. In river	Constr cost
	m a.s.l	-	m	m	m a.s.l	m a.s.l	%	m/s	Mkr
Proposal 1	35,0	2,80	3,29	(25)	38,3 (39,6)	48,5	32%	15	189
Proposal 2.1	35,0	2,80	3,29	47,4	38,6	48,5	31%	15	346
Proposal 2.2 (DL1)	32,5	3,26	2,99	54,1	36,8	46,7	49%	13,5	462
Proposal 2.3 (Dl2)	29,0	3,83	2,69	60,9	34,1	44,3	77%	10,5	619
Proposal 2.4	26,5	4,21	2,53	65,0	(32)	42,2	100%	(8)	706
Proposal 3	(35)	1,9*	4,2*	(15,0)	(40)	45,0	~ 0%	(17)	194
*) At lip end for 40 m a.s.l									

Figure 3.1: *Summary of energy dissipation options reviewed by the designers. Table from (Verkís 2011)*

Some of the stilling basin layouts proposed were not investigated further due to high construction cost (Proposals 2.4 and 2.3). For all stilling basin layouts suggested except for proposal 2.4, the natural tailwater elevation is insufficient and the topography and river geometry do not facilitate similar solutions as applied at Hvammur HEP. This means that for the stilling basins proposed a hydraulic control forms at the end sill creating a plunging jet from the end sill to the excavated downstream channel invert. Also, the end sill top elevation needs to be much higher than for a conventional stilling basin design to dissipate the energy from the incoming jet without behaving like a flip in a flip bucket.

A shallow short stilling basin layout (Proposal 2.2 in Table 3.1) was tested roughly in the physical model to assess the conditions and hydraulics of the layout. The stilling basin invert elevation is kept fixed at 32.5 m a.s.l. but the end sill height is varied from 3 - 5 m below the crest elevation of the spillway (crest elevation: 41 m a.s.l.). In general a plunging jet is formed at the end sill for all discharges. This means the hydraulic load on the rock immediately downstream of the end sill is continuous for spillway operation. With higher discharges and low end sill height the hydraulic jump moves closer to the end sill, until at approximately 700 m^3/s the function of the end sill becomes a flip for the incoming jet with even higher hydraulic loads on the downstream rock. To ensure the hydraulic jump to form within the stilling basin for all discharges, the end sill height required is 3 m below the crest elevation. This means very limited energy dissipation within the system.

Figure 3.2 shows the plunging jet from the end sill for a low flow condition discharge 350 m^3/s and the end sill height 3 m below the crest elevation (5.5 m above the basin invert). This character prevails out through the whole discharge regime. Figure 3.3 shows the character for a low elevation end sill, 5.5 m below the crest elevation (3 m above the stilling basin invert). Here the high velocity incoming jet plunges off the end sill as a flip and out to the downstream channel. Visual observations and preliminary measurements indicate that this is a very unsatisfactory system, with high downstream velocities and loads on the rock invert. Also the stilling basin has very limited energy dissipation and the functionality of the stilling basin is not conventional.

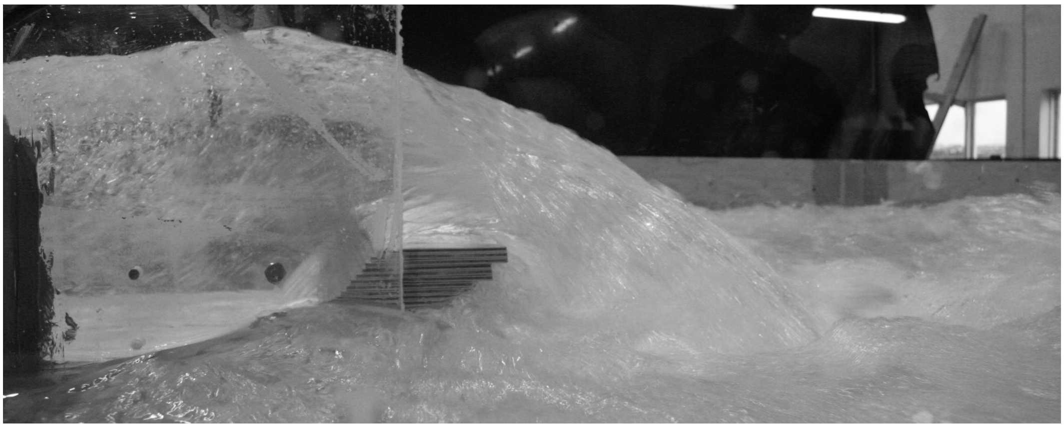

Figure 3.2: ***Q = 350 m^3/s:*** *The plunging jet from the end sill. The end sill is 5.5 m above the stilling basin invert.*

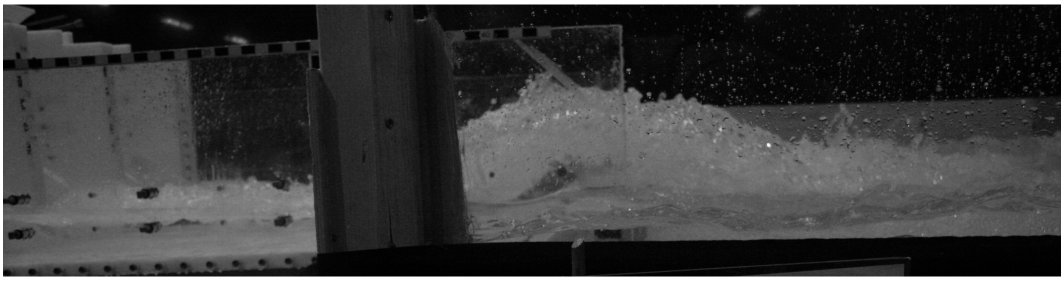

Figure 3.3: ***Q = 2250 m^3/s:*** *The hydraulic jump moves towards the end sill with the end sill functioning as a flip for mid to high and high discharges. The end sill is 3 m above the stilling basin invert.*

In (Tómasson, Garðarsson & Gunnarsson 2011) the modeling group reviewed the suggested energy dissipation method with emphasis on the proposed flip bucket. The proposed flip bucket design seems only to work properly for a limited range of discharges, but may act as an underdesigned stilling basin for low flows and non-optimally designed roller bucket for high flow conditions. Hence, the proposed design mixes together several hydraulic design concepts with associated uncertainties in flow behavior for the improperly designed conditions as well as for transition between the concepts. The proposed flip bucket was preliminary tested in the physical model, modeling only the geometry of the bucket itself but not the downstream topography.

Figure 3.4 shows the results from preliminary testing of the flip bucket. For low flow conditions the backwater is lower than the downstream end of the flip bucket. However, due to the low energy head of the inflow jet, the hydraulic jump will be within the bucket, hence creating uncertain flow conditions, both upstream of the end of the flip bucket as well as immediately downstream of the flip. These conditions lead to a fluctuating jump, and/or the flip bucket acting as an under designed stilling basin. Figure 3.5 shows the character for mid-range flow conditions. The tailwater is sufficiently low not to influence the flip and the throw distance is sufficient to protect the structure. For these conditions the flip bucket is probably an acceptable design. Finally, Figure 3.6 shows high flow conditions. The tailwater elevation is higher than the elevation of the flip bucket lip, creating a backwater effect for the flip. Generally, design recommendations suggest placing the lip of the flip above the tail water level for all flow conditions (Vischer & Hager, 1995) , (Khatsuria, 2005), (USBR, 1978), a condition which is not fulfilled here for high flow conditions. A high tail water elevation can create cavitation potential at the tip of the bucket when the jet separates from the lip. For these conditions, the flip bucket could act more as a roller bucket with potentially unpredictable behavior when the flow conditions change from flip conditions to roller bucket conditions.

The proposed flip bucket design seems only to work properly for a limited range of discharges, but may act as an underdesigned stilling basin for low flows and non-optimally designed roller bucket for high flow conditions. Based on the expected behavior of the flip bucket (multi flow regime) a more stable and predictable operation of an energy dissipation structure may be achieved with a roller bucket. Therefore, an investigation of a roller bucket layout at Urriðafoss HEP was suggested although the conditions at the site place such design at the boundary of or outside the design charts. With a successful roller bucket design, more controlled operating conditions can be achieved with a submerged hydraulic jump for the entire flow regime.

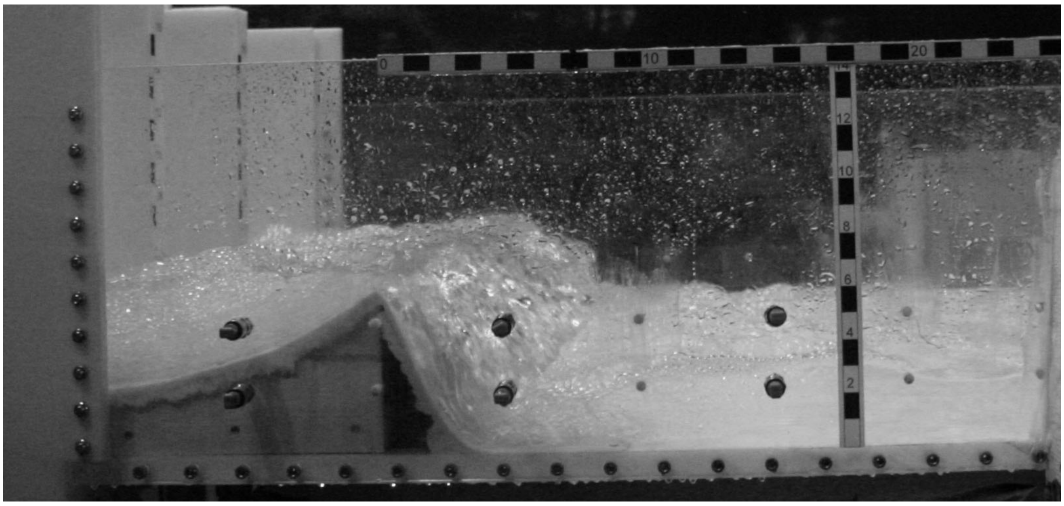

Figure 3.4:* $Q = 150$ *m*^{3}*/s: *Low flow condition for the flip bucket.*

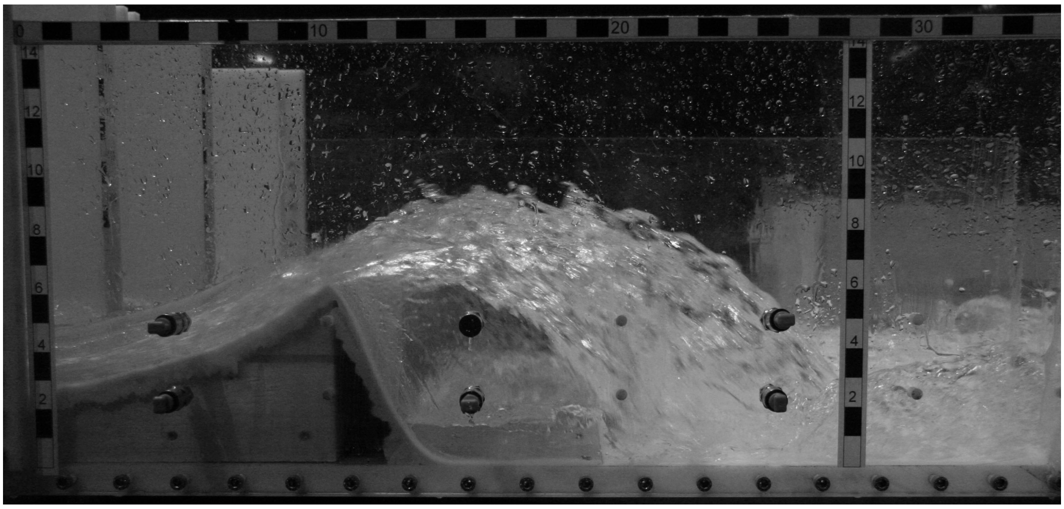

Figure 3.5:* $Q = 350$ *m*^{3}*/s: *Mid-range flow conditions for the flip bucket.*

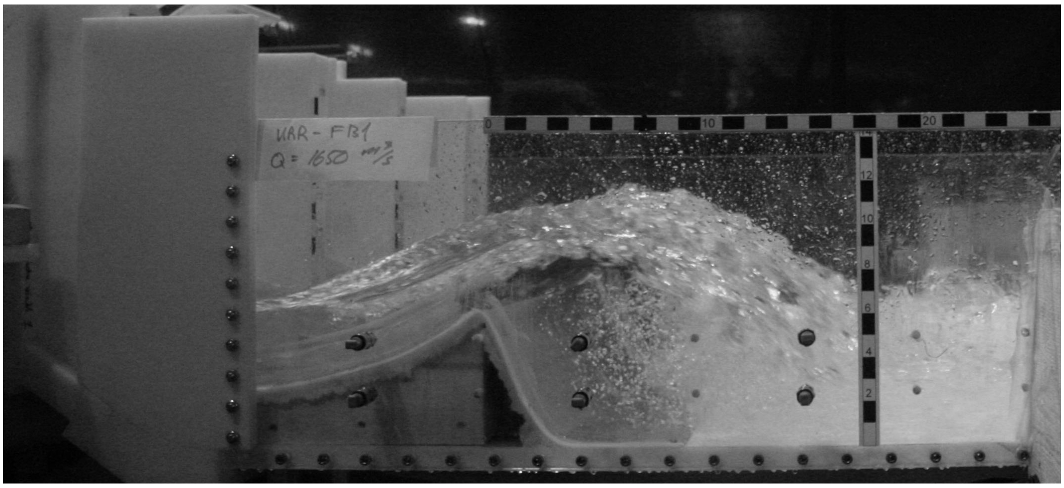

Figure 3.6: ***Q = 1650 m^3/s:*** *High flow condition for the flip bucket. This indicates a unstable design over the discharge operating regime.*

Based on the review and testing summarized above a roller bucket layout for energy dissipation was preliminary designed. Description of the design proposed is summarized in (Verkís 2012). Where the main parameters for the roller bucket layout are described as well as the proposed layout of the downstream discharge channel. This is the layout that was tested in the preliminary phase of the physical model work for Urriðarfoss HEP. It should be noted that the total cost of the roller bucket solution is similar to the total cost for the flip bucket solution[1].

3.3. Review of intake and juvenile fish passage design

A preliminary design of the SFO and the approach channel was released in 2010 (Verkís & Mannvit 2010). In the design a funnel shaped approach channel approximately 130 m wide 200 m upstream of the spillway gradually narrows down to 45 m width in front of the spillway. The approach channel towards the spillway is at a single elevation of 39 m a.s.l. From the left side of the spillway approach channel another separate channel heads towards the power intake and SFO structure. The intake approach channel slopes gradually from the spillway approach invert down to an elevation of 31.5 m a.s.l. in front of the intake. Another distinct feature of the 2010 design is a large sheltered off shallow water area in front of the fuse plug. The layout of the preliminary design from 2010 can be seen in Figure 3.7.

The 2010 design of the SFO had a sharp crest as seen in Figure 3.8. Inside the SFO channel structural blocks and different invert elevations divided the channel into pairs as seen in Figure 3.9.

The designers at Verkís reviewed the original design from 2010 in January 2012 prior the building of the physical model of Urriðafoss HEP. Following the review both the approach channel and SFO structure were changed in order to make the design more effective in terms of fish passage. The power intake and SFO structure was rotated for the SFO entrance to take the main current head on and to provide a more direct path for the juvenile salmon towards the SFO. The approach channel was widened to smooth the approach to the SFO. The curb between the spillway and power intake in the 2010 design was reduced and lowered to a elevation of 48

[1]Minutes of meeting, 23.1.2012

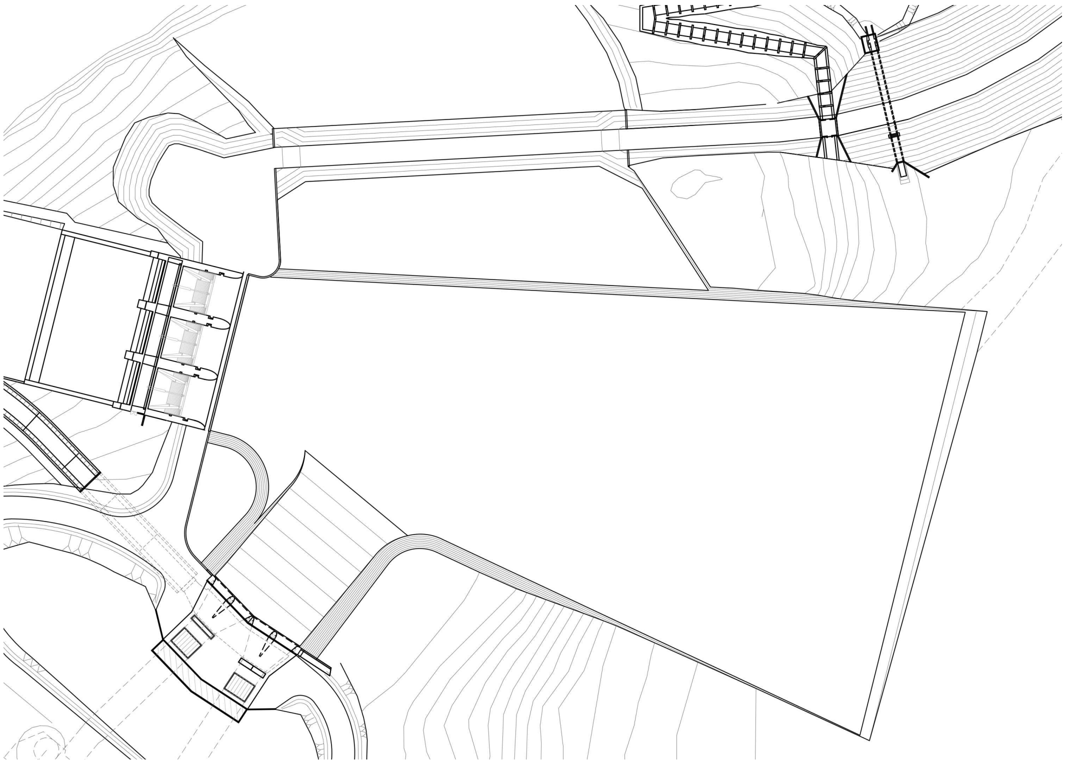

Figure 3.7: *Overview of the Urriðafoss HEP design layout from 2010 (Landsvirkjun, 2010).*

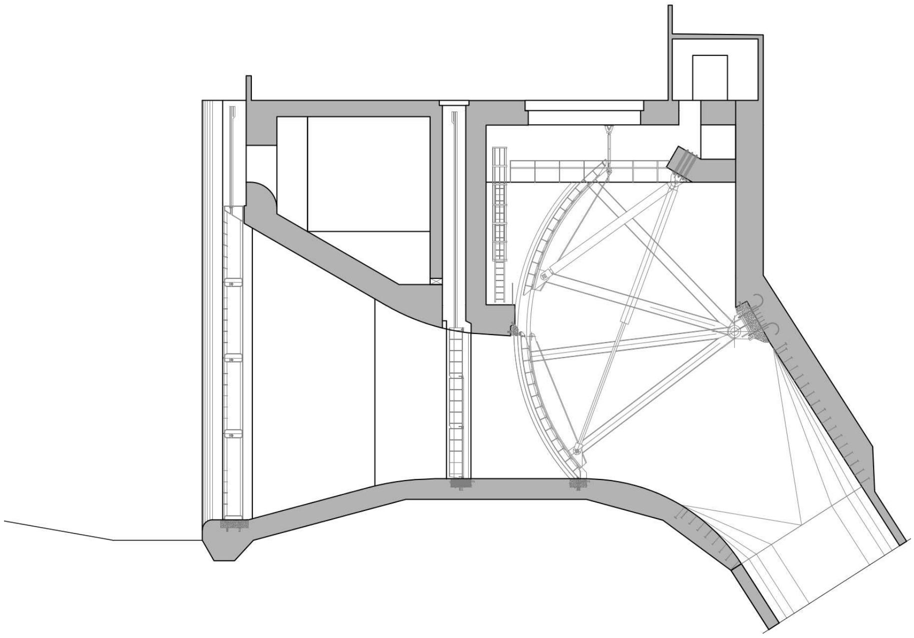

Figure 3.8: *A longitudinal view of the 2010 SFO design (Landsvirkjun, 2010).*

m a.s.l. to open a path for juvenile salmon which might get lost in front of the spillway. The large shallow area in front of the fuse plug was thought likely to become a stagnant velocity zone where the juvenile salmon might get lost. Because of this the fuse plug was moved closer to the approach channel. The layout of the reviewed design can be seen in Figure 3.10.

The sharp crest of the SFO entrance was changed to a rounded nose to make the entrance flow transition more smooth as seen in Figure 3.11. Inside the SFO the different invert elevations and structural blocks in the 2010 design where thought to lead to abrasion or other injury of

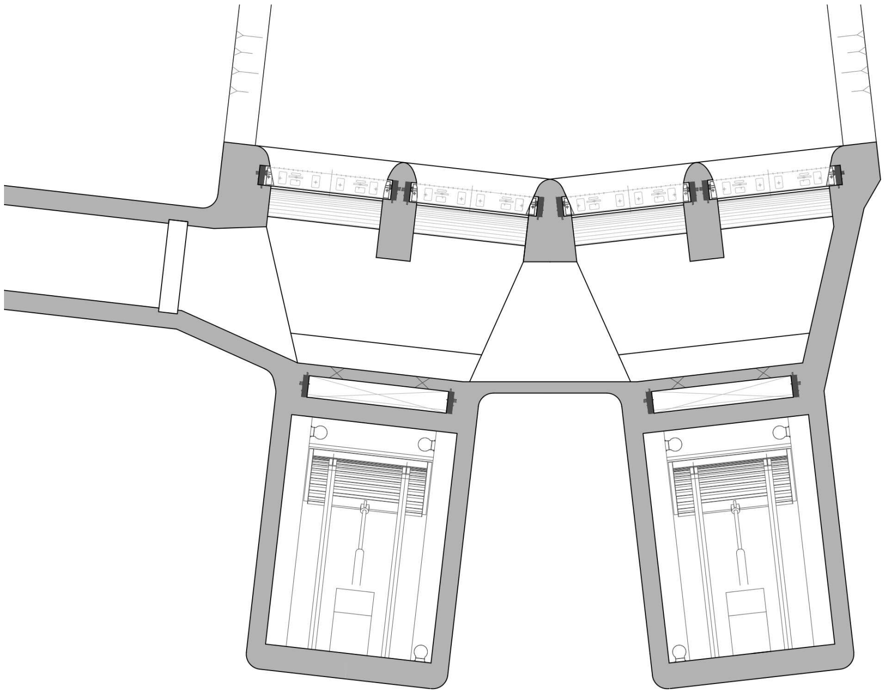

Figure 3.9: *A plan view of the 2010 SFO design (Landsvirkjun, 2010).*

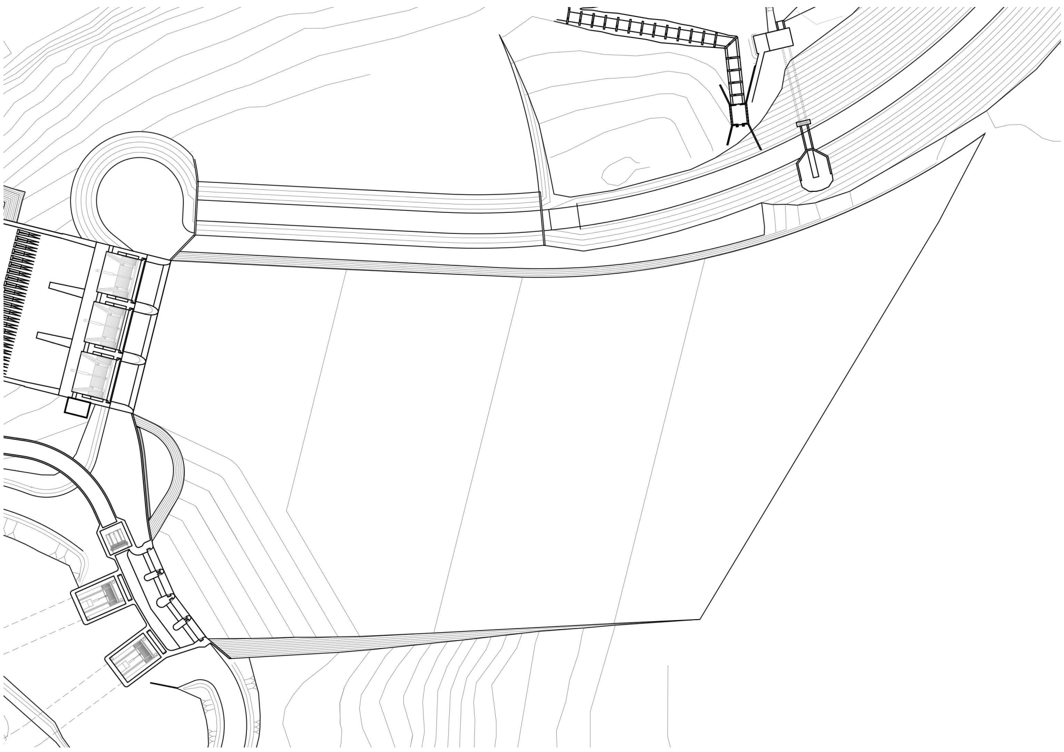

Figure 3.10: *Reviewed layout of approach channel with modifications from february 2012 (Landsvirkjun, 2010).*

juvenile salmon and possible accumulation of debris and trash which might also be harmful for the fish. Because of this the structural blocks where removed and the SFO channel invert leveled out into a single elevation of 45 m a.s.l. As to further improve the design all corners where made rounded and more streamlined as seen in Figure 3.12.

Parallel with the physical model of Urriðafoss HEP a numerical model was set up according to the revised design to study flow condition in the pond and the approach flow for the SFO.

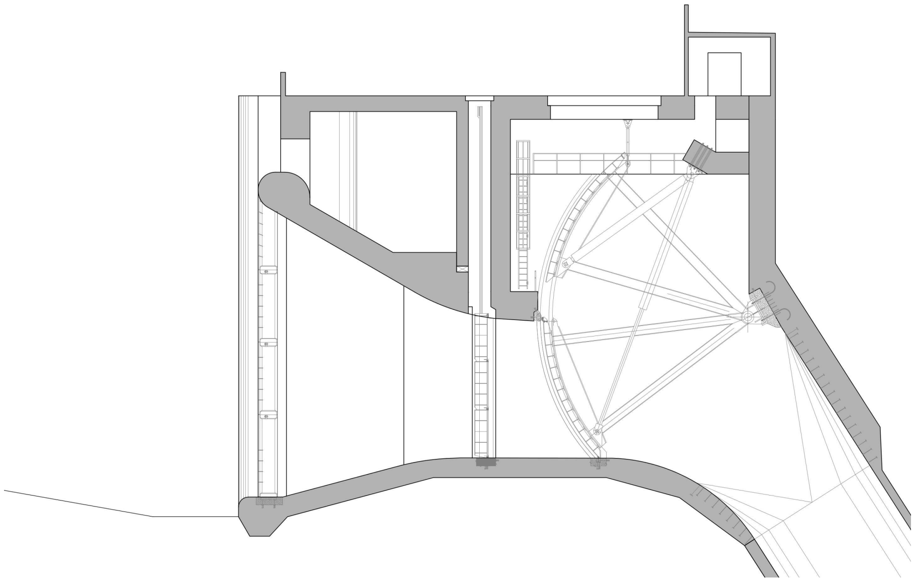

Figure 3.11: *A longitudinal view of the revised SFO design (Landsvirkjun, 2010).*

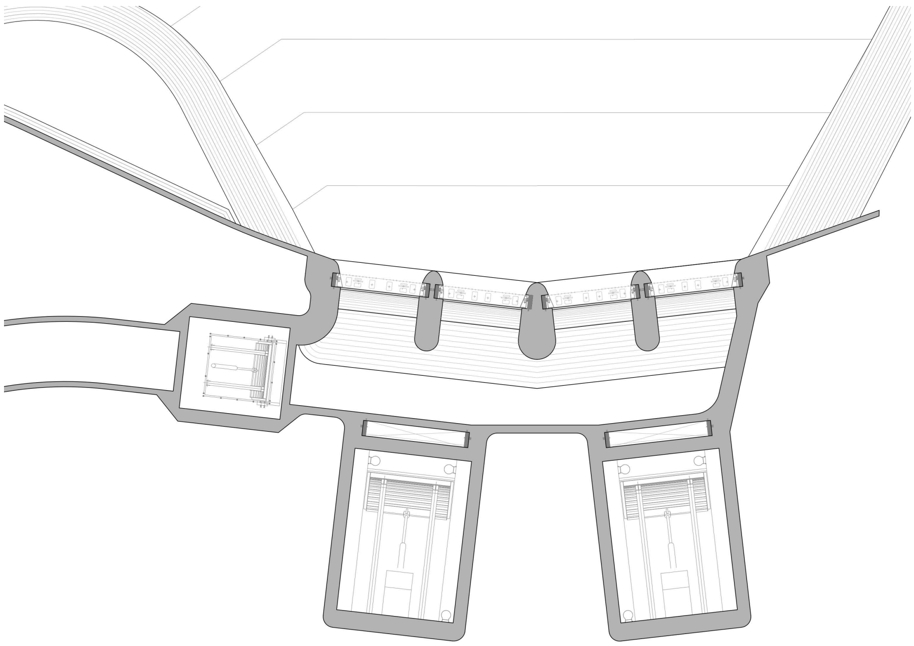

Figure 3.12: *A plan view of the revised SFO design (Landsvirkjun, 2010).*

Description and results from the numerical model can be found in Tómasson et al. 2013.

Preliminary tests in the physical model and preliminary results from the numerical model showed irregularities forming at the left approach bank (looking downstream). Where the topography sways upstream forcing the flow along the bank to flow in near opposite direction to the incoming main current in the approach flow channel. Because of this irregularities form around the left approach bank with the main current diverted from the bank into the center of the approach flow channel. A velocity contour plot from the preliminary numerical model can be seen in Figure 3.13(b). The diversion of flow from the left approach bank can be seen in Figure 3.13(a), taken during preliminary tests in the physical model.

(a) Photograph of a dye test from preliminary tests in the physical model showing diversion of flow away from left bank.

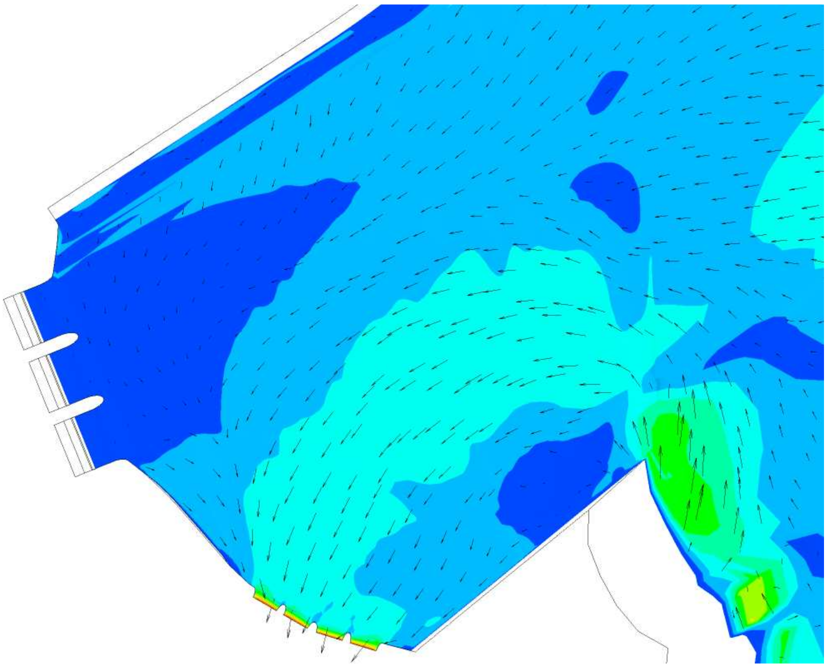

(b) Contour and vector plot from a preliminary numerical model showing flow diversion from the left bank.

Figure 3.13: *Dye test from preliminary test phase and velocity distribution of approach flow from preliminary test.*

In light of the irregularities forming at the left bank modifications were made in attempt to get the flow to follow better the left bank limiting the formation of vortices and stagnant velocity zones under the left approach bank. The modifications consisted of changes in the left bank geometry. The angle of the left abutment of the power intake was also increased to limit the potential of a stagnant velocity zone forming at the left abutment.

This summarizes the modifications and changes to the layout of the combined intake and juvenile fish passage structure at Urriðarfoss HEP which led to the preliminary design tested in the preliminary testing phase in the physical model.

4. Spillway final design

4.1. Description of spillway final design for Urriðafoss HEP

The scope of the study conducted by the physical modelling of the spillway structure at Urriðafoss HEP is to verify the general design criteria set forth in Section 1.4. The final design layout for Urriðafoss HEP and the spillway structure is shown in Figures 4.1 and 4.2 as an overview of the project and longitudinal sections of the spillway.

The Heiðarlón reservoir is formed by a dam crossing the river at Heiðartangi point and dykes along the west bank of the river. The spillway and the intake structures are located at Heiðartangi point. In general, the overall layout of the approach flow channel and the spillway structure (including the roller bucket type energy dissipator and downstream channel and river section) is studied. The elements under investigation and relevant to this study are as follows (numbers refer to Figure 4.1):

- (1) the original river bed of Þjórsá River
- (2) an excavated approach flow channel for the spillway and intake. The approach flow channel invert slopes towards the spillway from an elevation of 41 m a.s.l. to 37 m a.s.l. in front of the spillway. The channel is approximately 120 m wide excavated in an arch shape starting at the original riverbank approximately 200 m upstream of the spillway crest. The sides of the channel have a steep 4:1 slope. At the right side of the channel the side walls reach a plan at an elevation of 49 m a.s.l. where the fuse plug and dykes continue to elevations of 51.8 m a.s.l. and 53.5 m a.s.l. respectively.
- (3) a gated spillway with three radial gates for reservoir regulation and flood passing. The spillway has three 12 by 10 m radial gates (width x height) with a crest elevation of 41 m a.s.l.
- (4) a slotted roller bucket energy dissipator. The 42.94 m wide bucket has 11 m radius and 22 teeth in the bucket. The bucket has a variable invert elevation depending on the layout being investigated. The elevation of the bucket invert is defined as it's lowest point. For the final design a bucket elevation of 26 m a.s.l. is selected.
- (5) a excavated downstream discharge channel to pass of the water from the spillway and roller bucket back to the original riverbed. The channel is excavated in bedrock and has 1:4 side slope, the variable bottom invert is dependent on the case of investigation.
- (6) a fuse plug with crest elevation at 51.8 m a.s.l. to pass larger floods than Q_{1000}.

– (7) a mandatory release structure which provides constant discharge of 10 m^3/s to the riverbed downstream of the dam.

– (8) Urriðafoss dam forming Heiðarlón Reservoir.

– (9) an excavated approach flow channel for the intake and SFO structure. The approach flow channel slopes downward to the left of the main approach channel towards the intake and SFO structure to an elevation of 31.5 m a.s.l. in front of the intake. On the right of the channel a curb reaching an elevation 48 m a.s.l. separates the intake and spillway. The sides of the channel are steep with 4:1 slopes.

– (10) a power intake and SFO structure. The intake is a conventional power intake structure with a SFO type juvenile bypass system incorporated into the top of the structure. The power intake has four 5.95 m wide entrances uniting in pairs into two separate draft tubes. The design discharge for the intake is 370 m^3/s. The SFO has four 5.95 m wide entrances, each with a smooth rounded crest at an elevation of 49.1 m a.s.l. providing an estimated discharge of 40 m^3/s at normal reservoir water level of 50 m a.s.l. From the crest the water from the four entrances is united in a single sideways channel and routed through a 4.5 m wide concrete channel to the original riverbed downstream of the dam.

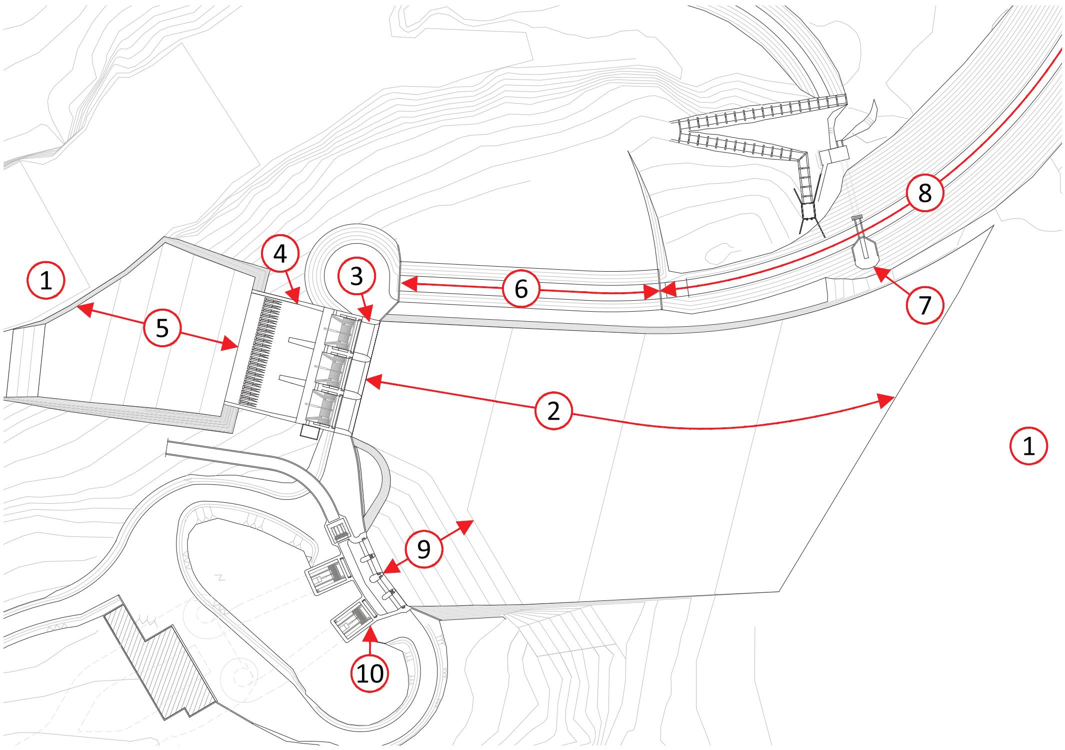

Figure 4.1: *Overview of the Urriðafoss HEP final design: (1) original riverbed, (2) spillway approach flow channel, (3) gated spillway, (4) roller bucket, (5) downstream discharge channel, (6) fuse plug, (7) mandatory release structure, (8) Urriðafoss dam, (9) intake and SFO approach flow channel, (10) intake to the power house and SFO structure.*

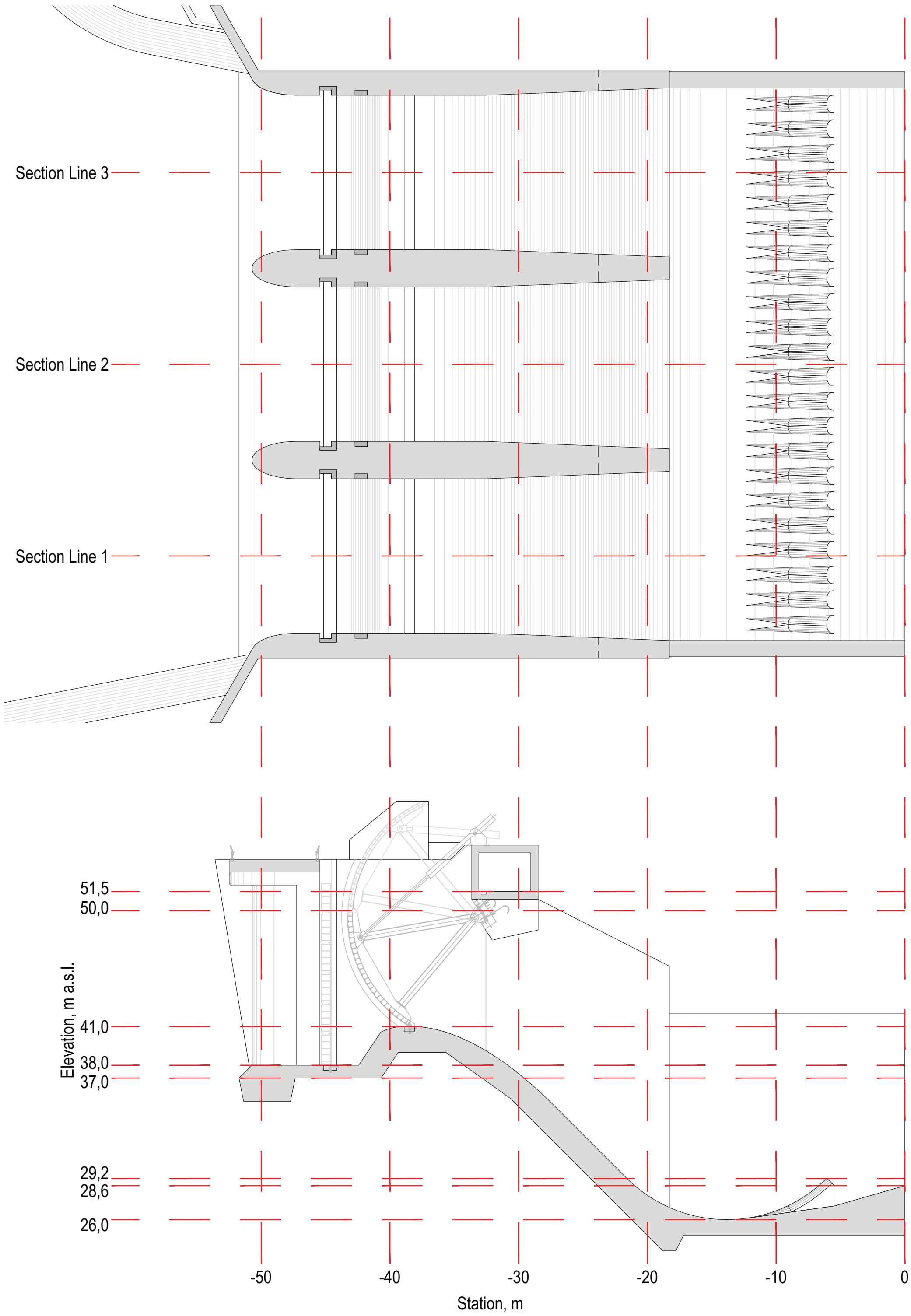

Figure 4.2: *Top view and longitudinal section of the spillway structure.*

4.2. Overview of final design

The investigations presented in this chapter of the selected final design are divided into three main parts in the detailed measurement program. In total four test series are defined, Discharge test series 1, 2, 3 and 4 (DT1, DT2 DT3 and DT4, respectively). Detailed description of each individual test series is shown in the measurement program in Appendix A. The investigation of the final design is divided into six main parts which consists of

1) layout of the excavated downstream channel, bottom profile

2) approach flow of the spillway and upstream conditions

3) the gated spillway structure and its discharge capacity

4) the roller bucket, the downstream channel and the river section

5) asymmetric operation of the spillway gates

6) tailwater sensitivity

These parts were investigated individually so the results chapter is divided into four main sections:

- **Bottom profile layout** (Section 4.3)
- **Approach flow** (Section 4.4)
- **Spillway Capacity** (Section 4.5)
- **Roller bucket, downstream channel and river section** (Section 4.6)
- **Asymmetric gate operation** (Section 4.7)

4.3. Bottom profile in the downstream channel

At Urriðafoss HEP a roller bucket is suggested to dissipate excess energy from upstream to downstream. Roller buckets in general tend to move loose material from the downstream channel into the bucket itself, especially during asymmetric operation (United States Army Corps of Engineers 1992), therefore the design of the downstream channel is relatively critical to assure acceptable performance of the structure and to prevent unnecessary damage risk of the structure. Three preliminary bottom profiles for the downstream discharge channel were proposed for testing as summarized in (Verkís 2012). In total 11 layouts of the downstream channel were tested that were categorized in 8 groups or profiles, all profiles were tested with the design flood of 2250 m^3/s. Bottom profile 1 and 2 were a gravel bed while 3-8 were a fixed bed made out of plywood. For all cases, except for Bottom profiles 5 and 6, a measured velocity approximately 1 m above the bottom and water elevations were documented, all cases were documented with photos. The bottom profiles with gravel bed (Bottom profile 1 and 2) were suggested to estimate scouring profile from the secondary roller.

4.3.1. Water elevation in the downstream channel

The water elevations for Section line 2 can be seen for Bottom profile 1-4, 7 and 8 in Figure 4.3, water elevations for Section line 1 and 3 can be seen in Appendix J. The bottom velocities can be found in Appendix K.

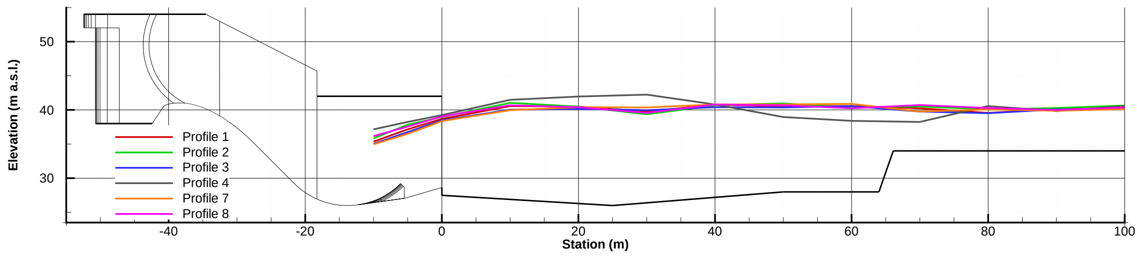

Figure 4.3: *Water elevations for Section Line 2 in the downstream channel for the preliminary cases investigated in the model. Data shown for $Q = 2250\ m^3/s$.*

4.3.2. Bottom profile 1

Bottom profile 1, shown in Figure 4.4, was a gravel bed at elevation of 28 m a.s.l. at beginning of testing. The design flood was tested for 2 hours and the scouring profile, velocity near the bottom and water elevations were documented. Although the ground roller was not visible during testing, the scouring indicate that at least a weak ground roller is formed.

The scouring profile is shown in Figure 4.5, the water elevations is shown in Figure 4.3 and RMS of velocity on Figure 4.14 - 4.16.

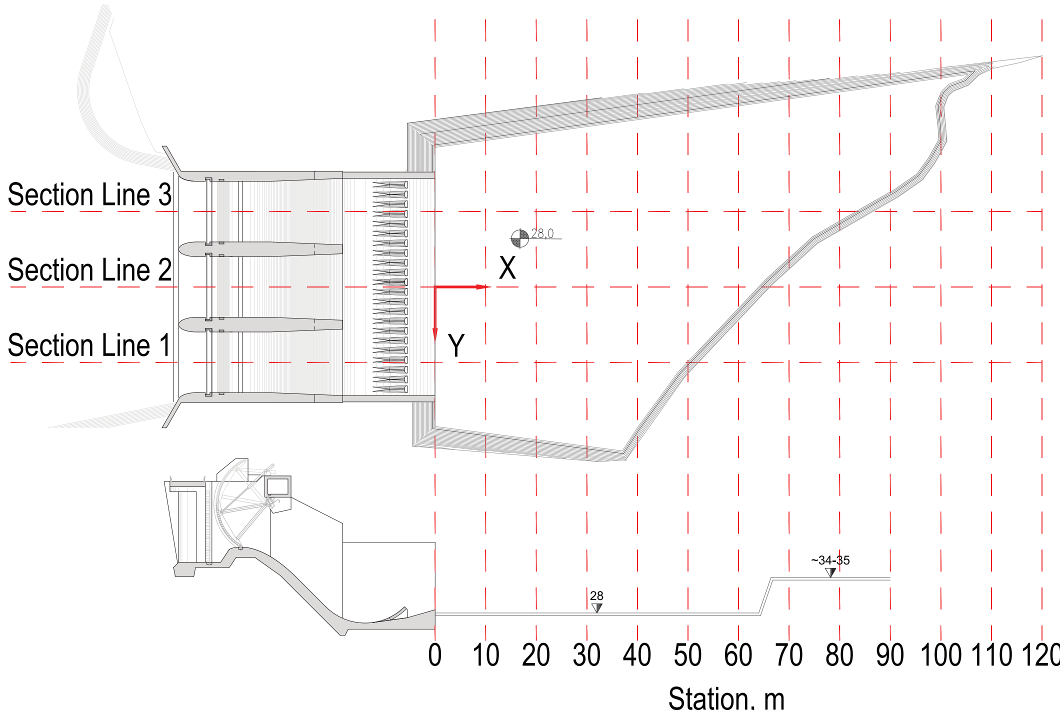

Figure 4.4: *Downstream channel for bottom profile 1.*

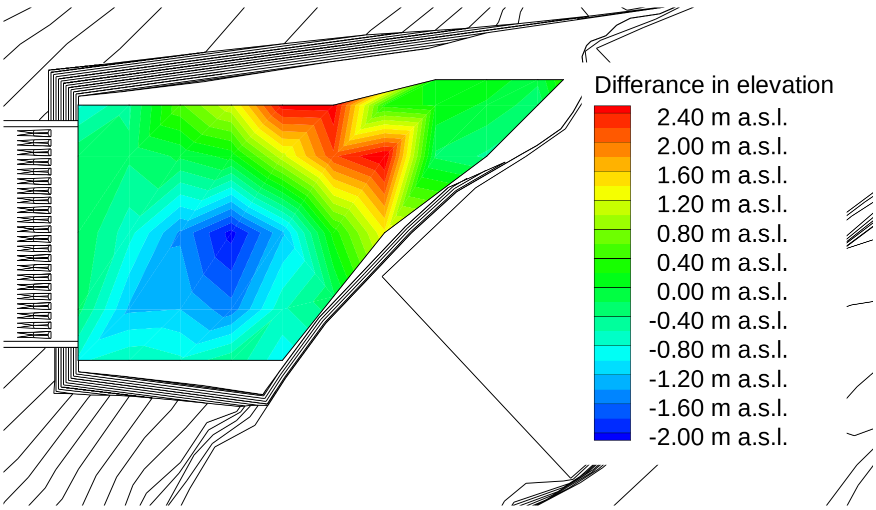

Figure 4.5: *Scouring on the downstream invert for bottom profile 1.*

4.3.3. Bottom profile 2

Bottom profile 2, shown in Figure 4.6, was a gravel bed at elevation of 26 m a.s.l. at beginning of testing. The design flood was tested for 2 hours and the scouring profile, velocity near the bottom and water elevations were documented. Although the ground roller was not visible during testing, the scouring indicate that at least a weak ground roller is formed. By comparing Bottom profile 1 and 2 the sensitivity of the bottom profile layout is quite clear, the results indicate that the ground roller location is a function of the depth of the bed downstream of the roller bucket structure.

The scouring profile is shown in Figure 4.7, the water elevations is shown in Figure 4.3 and RMS of velocity on Figure 4.14 - 4.16.

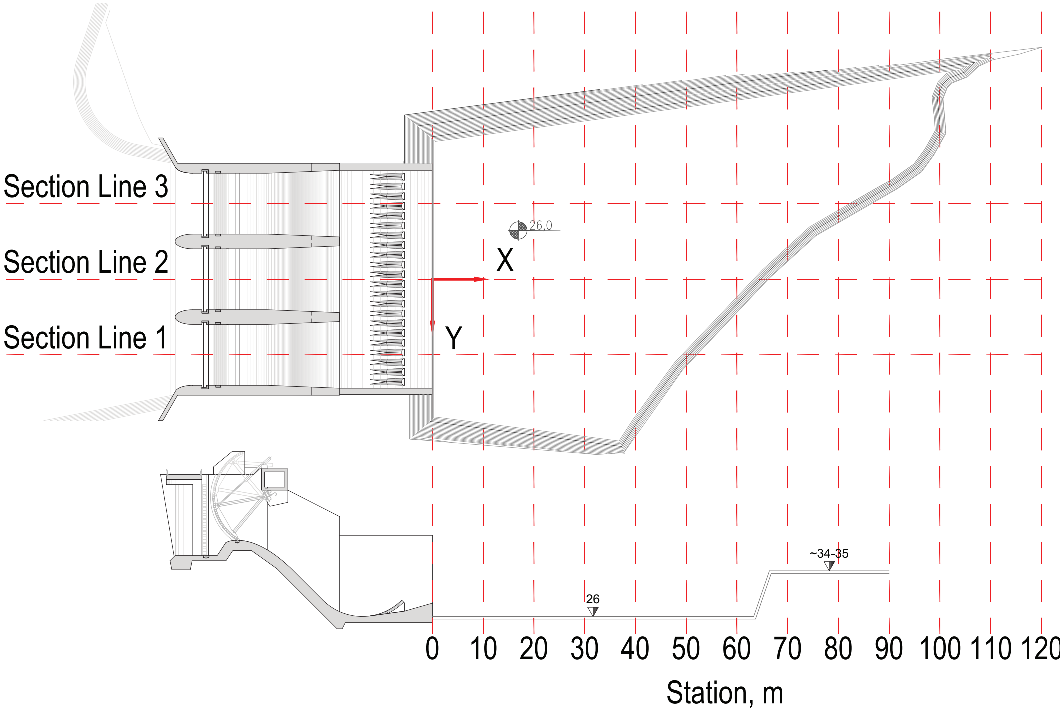

Figure 4.6: *Downstream channel for bottom profile 2.*

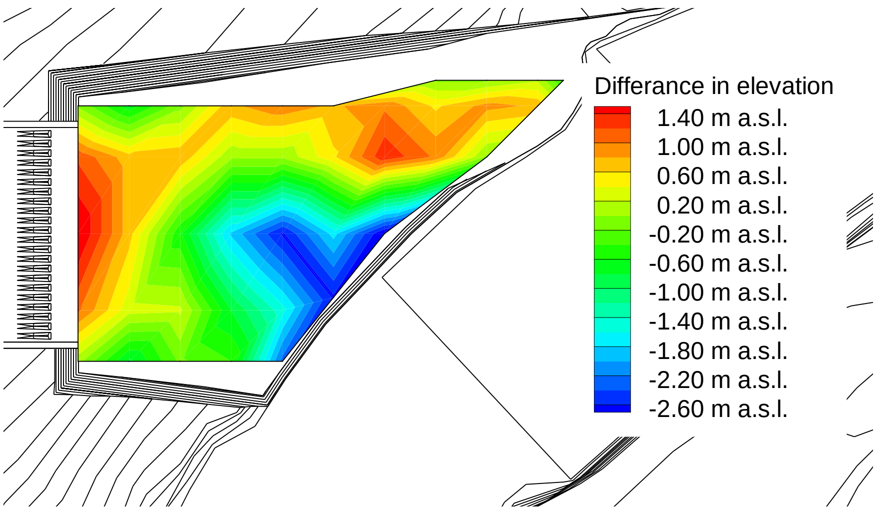

Figure 4.7: *Scouring on the downstream invert for bottom profile 2.*

4.3.4. Bottom profile 3

Bottom profile 3, shown in Figure 4.8, was a fixed bed made out of plywood. The complex layout of the bottom profile was proposed as the maximum excavation case, excavating through the weak scoria layer down to the lower basalt layer. This layout was the first proposal from the designers and was aimed to follow the estimated geology at the site. The design flood was tested and the velocity near the bottom and water elevations were documented. The water elevation is shown in Figure 4.3 and RMS of velocity on Figure 4.14 - 4.16.

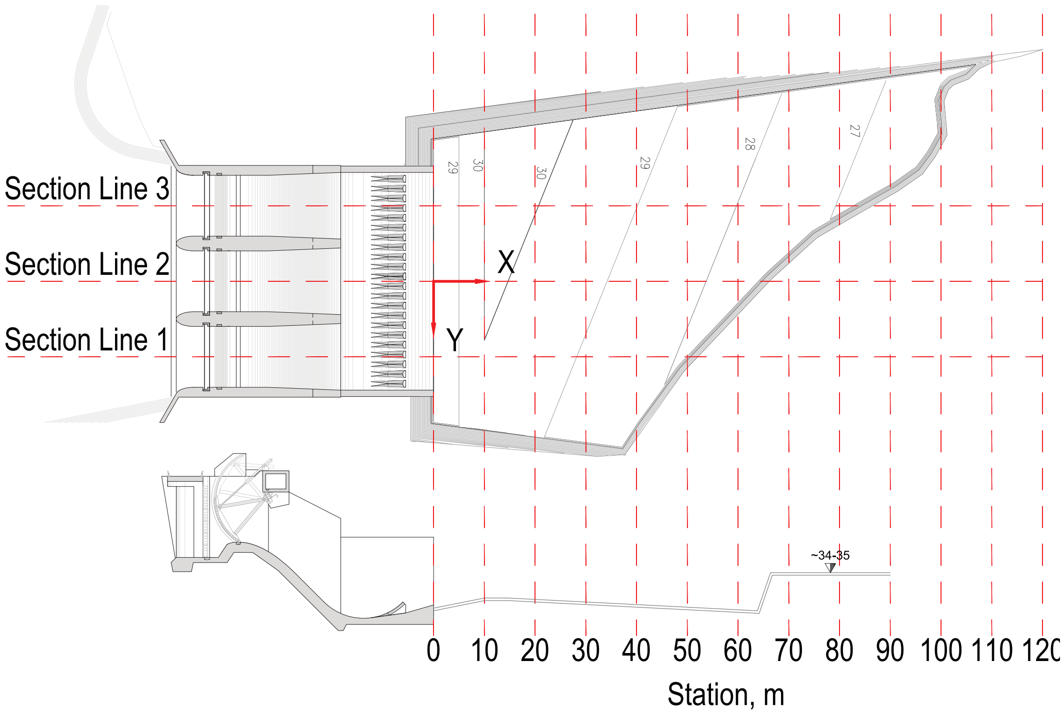

Figure 4.8: *Downstream channel for bottom profile 3. Drawing C-11-3.101-P4.*

4.3.5. Bottom profile 4

Bottom profile 4, shown in Figure 4.9, was a fixed bed made out of plywood. The complex layout of the proposed bottom profile was aimed to avoid exposure of the weak scoria layer similar to Bottom profile 3 but reducing the length of the excavated channel to minimize the excavation. This layout was the second proposal from the designers and was aimed to follow the estimated geology at the site. The design flood was tested and the velocity near the bottom and water elevations were documented. The water elevation is shown in Figure 4.3 and RMS of velocity on Figure 4.14 - 4.16.

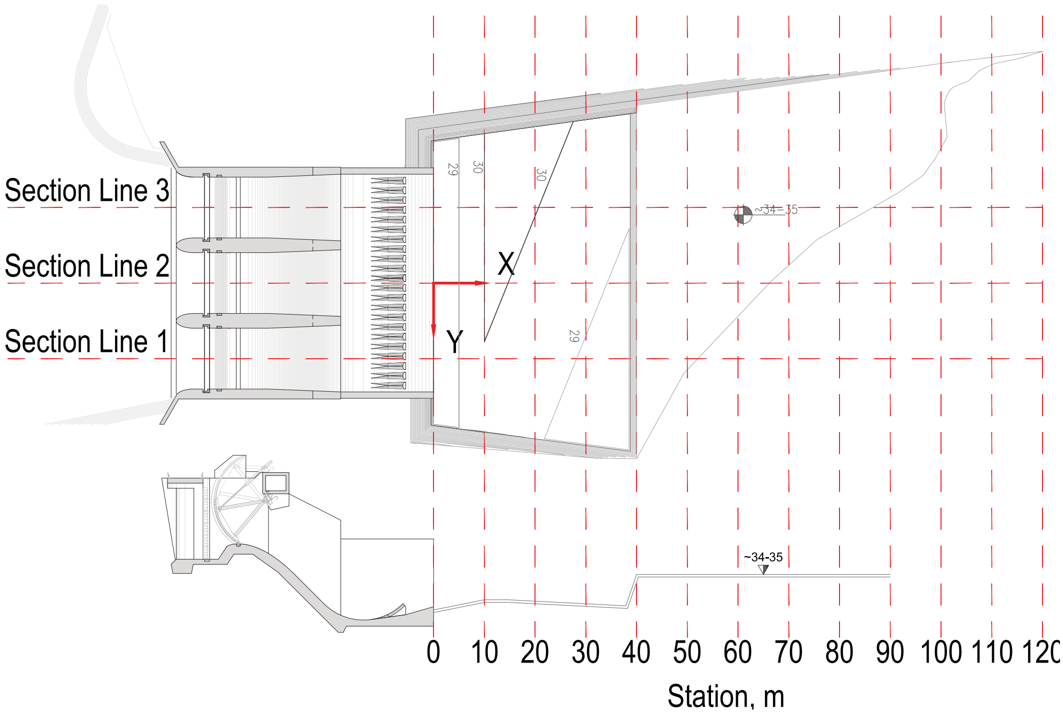

Figure 4.9: *Downstream channel for bottom profile 4. Drawing C-11-3.103-P2.*

4.3.6. Bottom profile 5

Due to unfavourable flow characteristics in Bottom profile 3 and 4, the bottom profile layout was made more uniform. Bottom profile 5, shown in Figure 4.10, was a fixed bed made out of plywood. Directly downstream of the bucket the downstream invert had an elevation of 28 m a.s.l. extending approximately 40 m out where the bottom started to slope upwards with a uniform slope of 2(H):1(V) until it matched the elevation of the river. The design flow was tested and the layout performance was assessed with visual observations and documented with photos. The preliminary results indicated a very unsatisfactory behavior with a unstable character in the flow and limited capability for the incoming jet to form the rollers needed for energy dissipation. The characteristics between profile 5 and 6 are very similar.

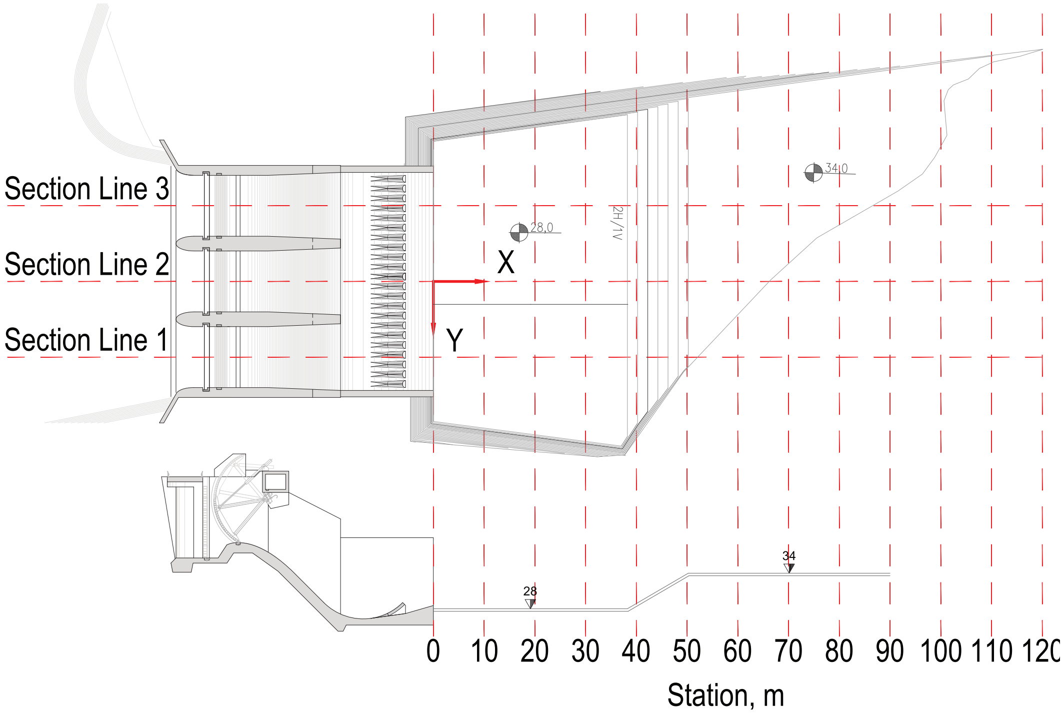

Figure 4.10: Downstream channel for bottom profile 5. Drawing C-11-3.104-P1.

4.3.7. Bottom profile 6

Bottom profile 6, shown in Figure 4.11, consisted of four layouts: 6.0 was a fixed bed at elevation of 28 m a.s.l. made out of plywood, 6.1 was 20 m shorter, 6.2 was 40 m shorter and 6.3 was 52 m shorter (as illustrated on Figure 4.11). This layout was proposed as an sensitivity analysis for the channel length to minimize the excavation without compromising the performance of the bucket. The design flood was tested and these layouts performance was assessed with visual observations and documented with photos. The preliminary results indicated a very unsatisfactory behavior with a unstable character in the flow and limited capability for the incoming jet to form the rollers needed for energy dissipation. The characteristics between profile 5 and 6 are very similar.

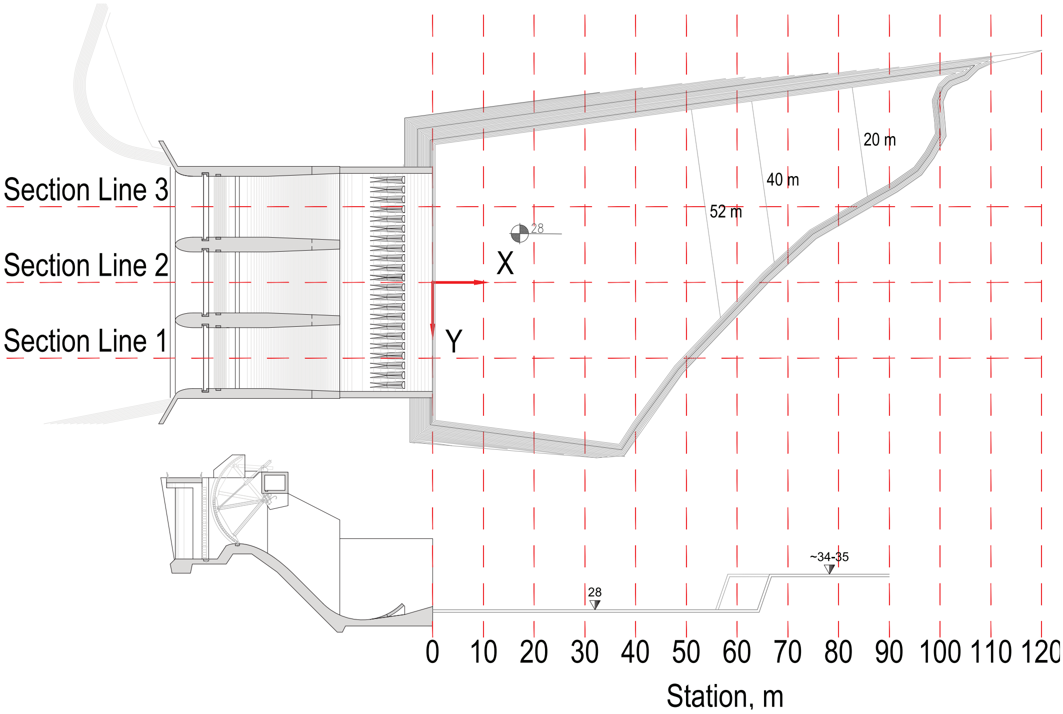

Figure 4.11: *Downstream channel for bottom profiles 6.*

4.3.8. Bottom profile 7

Bottom profile 7, shown in Figure 4.12, was the result of the sensitivity analysis from Bottom profiles 6.0-6.3. The length of the invert was 82 m measured from the downstream end of the bucket (20 m shorter as in Bottom profile 6.1). A small edge at the top of the wall were the river meets the excavated channel (marked as a cloud in Figure 4.12) was lowered to the same elevation as the river section. The design flood was tested and the velocity near the bottom and water elevations were documented. The water elevation is shown in Figure 4.3 and RMS of velocity on Figure 4.14 - 4.16.

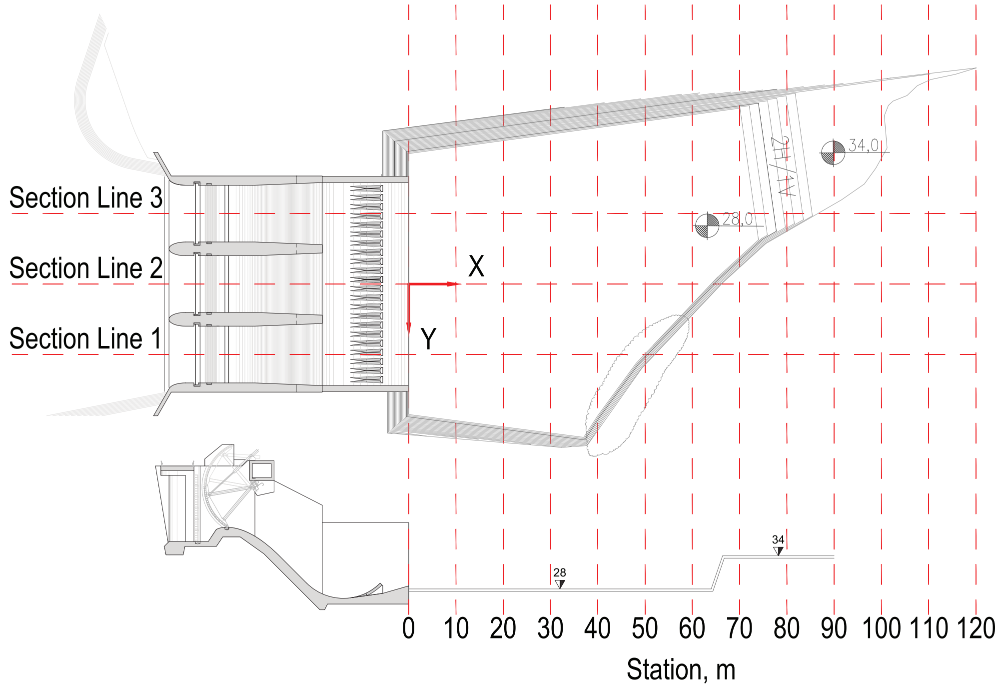

Figure 4.12: Downstream channel for bottom profile 7.

4.3.9. Bottom profile 8

Bottom profile 8, shown in Figure 4.13, was a fixed plywood profile that was aimed at combining Bottom profiles 1,2 and 7 for best performance. The bottom profile had an elevation of 27.5 m a.s.l. immediately downstream of the bucket lip and a uniform slope down to 26 m a.s.l. over the next 25 m. From there it had a uniform slope upwards over a 25 m distance to 28 m a.s.l. The invert remained at elevation 28 m a.s.l., after which it sloped up to the original river bed of 34 m a.s.l. with a uniform slope of 1:2. The end of the excavated channel was asymmetric as shown in Figure 4.13 and therefore a high end wall was located at the downstream end of the channel for most part of the channel as in previous cases. This V-shaped dent at station 25 m was aimed to simulate the scouring pit of Bottom profiles 1 and 2. The design flood was tested and the velocity near the bottom and water elevations were documented. The water elevation is shown in Figure 4.3 and RMS of velocity on Figure 4.14 - 4.16. This profile was selected as the final design.

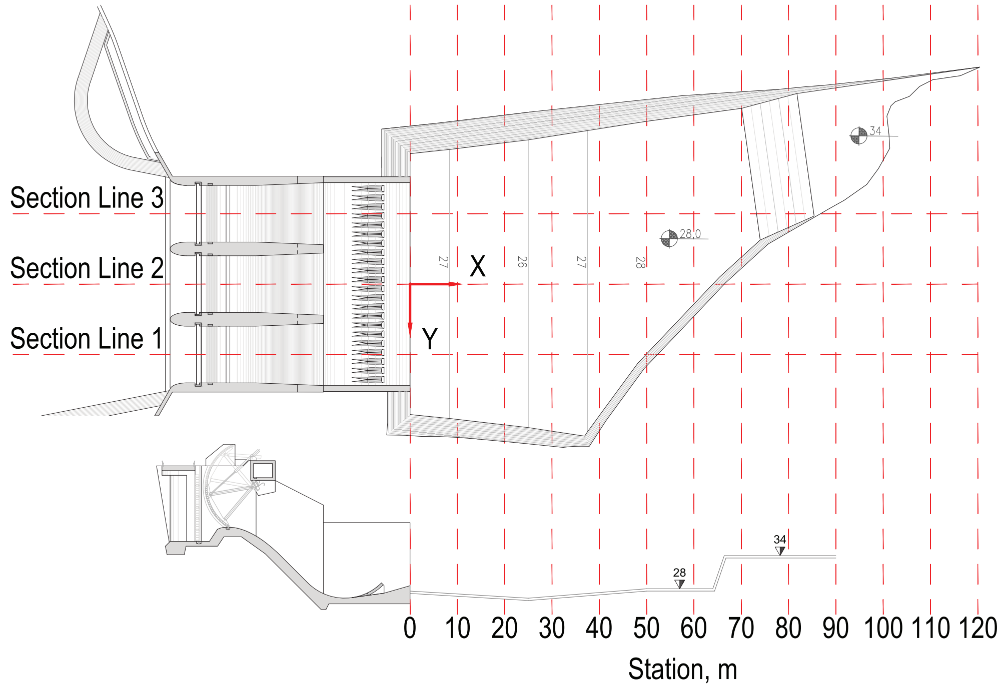

Figure 4.13: *Downstream channel for bottom profile 8. Drawing C-11-3.101-P7.*

4.3.10. Selection of the final bottom profile

The bottom profiles with gravel bed (Bottom profile 1 and 2) were suggested to estimate scouring profile from the secondary roller. Following the gravel beds, a series of fixed bed profiles were tested as previously discussed and the fixed bed layouts compared to the gravel bed. The comparison was done visually and with calculated RMS values from velocity measurements near the bottom of the downstream channel during the design flood. The comparison of the RMS values for Bottom profile 1-4, 7 and 8 are shown in Figures 4.14 - 4.16 for Section line 1-3 respectively. Bottom profile 1 and 2 gave a relatively low peak RMS value for the velocity. Bottom profile 3, 4 and 7 gave a lot higher peak RMS value than the gravel bed, the surface of Bottom profile 3 was less violent than Bottom profile 4 and Bottom profile 7 was even less violent. Bottom profile 8 was aimed to simulate the scouring profile of the gravel layouts, this layout gave a similar RMS values to those from the gravel bottom and had the best performance of all of the fixed bed profiles. Bottom profile 8 was selected as the final design.

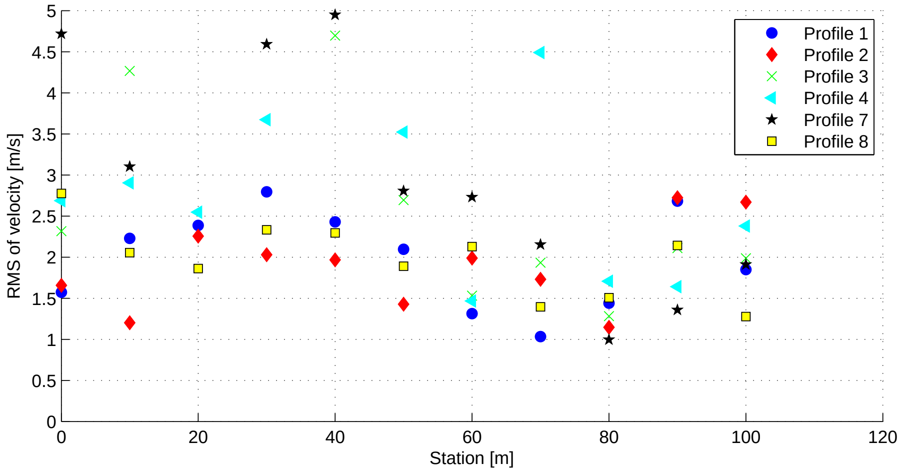

Figure 4.14: *RMS of the velocity approximately 1 m above the bottom of the downstream channel for section 1.*

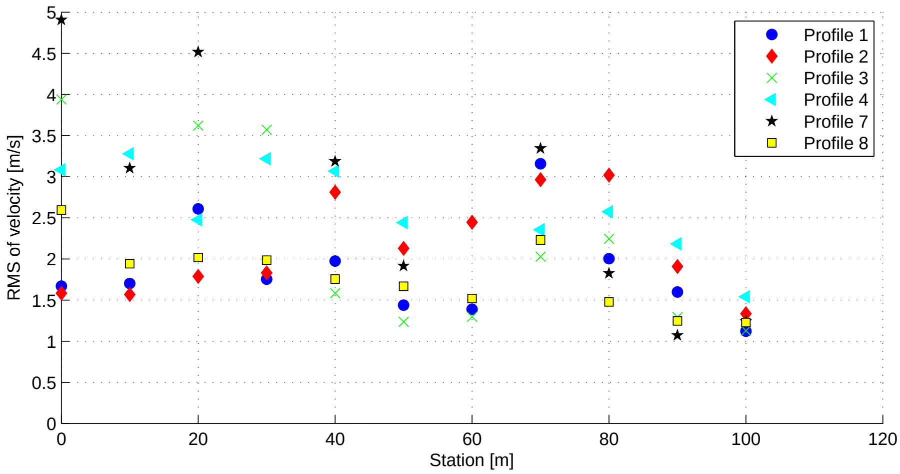

Figure 4.15: *RMS of the velocity approximately 1 m above the bottom of the downstream channel for section 2.*

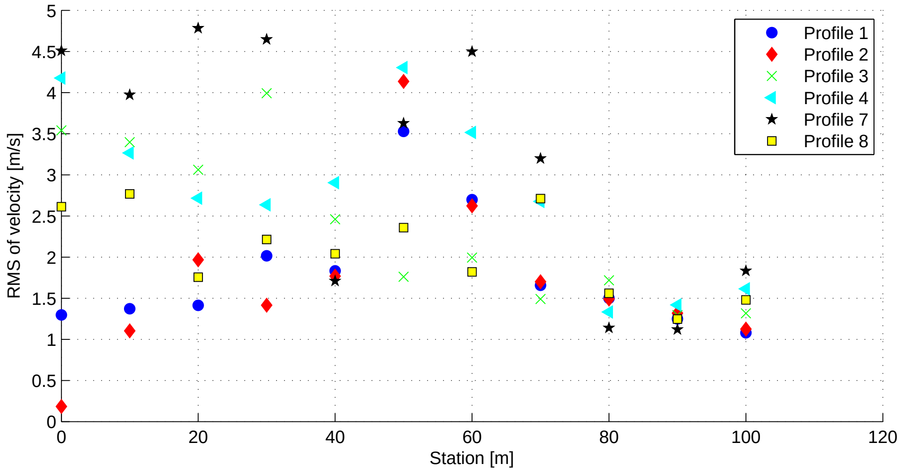

Figure 4.16: *RMS of the velocity approximately 1 m above the bottom of the downstream channel for section 3.*

4.4. Approach flow

The main approach flow channel for the spillway and intake has an invert elevation of 41 m a.s.l., decreasing to 37 m a.s.l. immediately upstream of the spillway crest. The channel is approximately 120 m wide channel excavated in an arch shape starting at the original riverbank approximately 200 m upstream of the spillway crest.

An excavated approach flow channel for the intake and the SFO slopes downward to the left of the main approach flow channel to an invert elevation of 31.5 m a.s.l. in front of the intake. A curb separates the intake and spillway structures with steep walls 4:1 slope.

The approach flow is defined as the flow conditions upstream of the spillway crest and intake opening. As these two structures are in close proximity to each other interference between them can influence flow distribution in the approach area and create unwanted conditions. To assess the approach flow conditions in the vicinity of the spillway and intake, velocities were measured at an elevation plan of 47.6 m a.s.l. for different discharges. About 50 points were measured on a 20 m grid in the upstream part of the approach flow channel and 10 m grid immediately upstream of the spillway and intake.

The investigation is dived into two sections, 1) spillway approach flow and 2) intake approach flow.

4.4.1. Spillway Approach Flow

Apart from the elevation and size of the spillway gates, the discharge capacity of the spillway is controlled by conditions upstream of the crest, i.e. the layout and geometric configuration of the excavated approach channel, side wall and layout of abutments. Figure 4.17 shows the naming convention for the spillway structure while Figure 4.18 shows the approach flow configuration as built in the model and the associated spillway structure.

In general, quantifying the approach flow conditions in close proximity of the spillway is hard

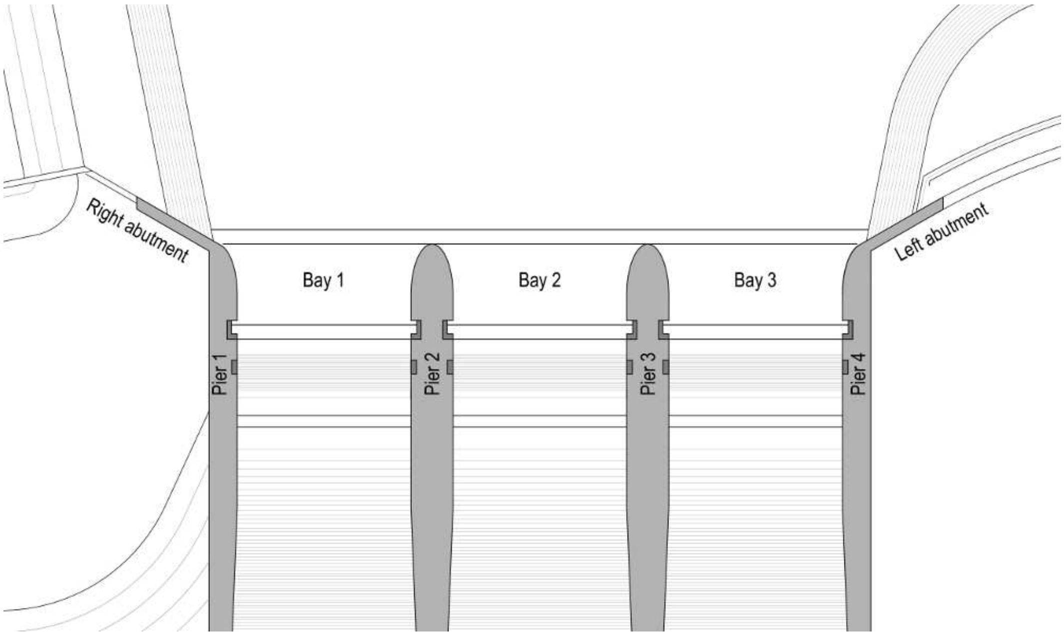

Figure 4.17: *Top view of the spillway. The spillway has two main abutments. Between the side walls four piers create a sitting for three radial gates. Between each pair of piers is a bay, in total 3 bays. Definition of left and right is such that the viewer looks downstream. At the right abutment, the mandatory release spillway is located left of Pier 1 in the figure (Landsvirkjun 2010).*

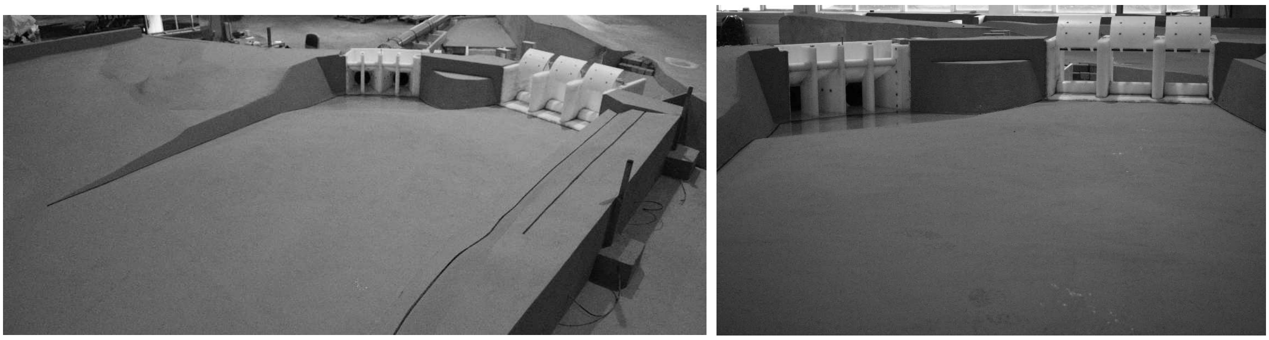

Figure 4.18: *On left: Approach channels to intake and spillway in the model for the final design. View is from upstream in the reservoir. On right: Main approach channel to intake and spillway in the model for the final design. View is from upstream in the reservoir.*

and for this study mainly based on visual observations rather than direct measurements.

The approach flow conditions for the spillway were in general good and no improvements were necessary. For spillway discharges ranging from 100 m^3/s to 700 m^3/s the surface of the approach flow channel is relatively smooth, but with increasing discharge the surface became more rippled, being very rippled at 2250 m^3/s. During spill of 500 m^3/s to 1300 m^3/s shallow, unsteady and weak vortices formed,(class VT-4 as described by (Vischer & Hager 1995): Figure 4.19) inside spillway bay 3 by pier 4 as shown in Figure 4.20 (left) for spillway discharge of 1050 m^3/s. Notice is made that the results can not be scaled directly to prototype due to the influence of surface tension and viscosity effect on vortex formation and properties. In the model, no full air core being pulled under the gate was observed but in prototype floating trash or ice might be pulled down. The vortices may also cause additional entrance loss.

At 1300 m^3/s drawdown at endwalls and piers became noticeable and increased with increased

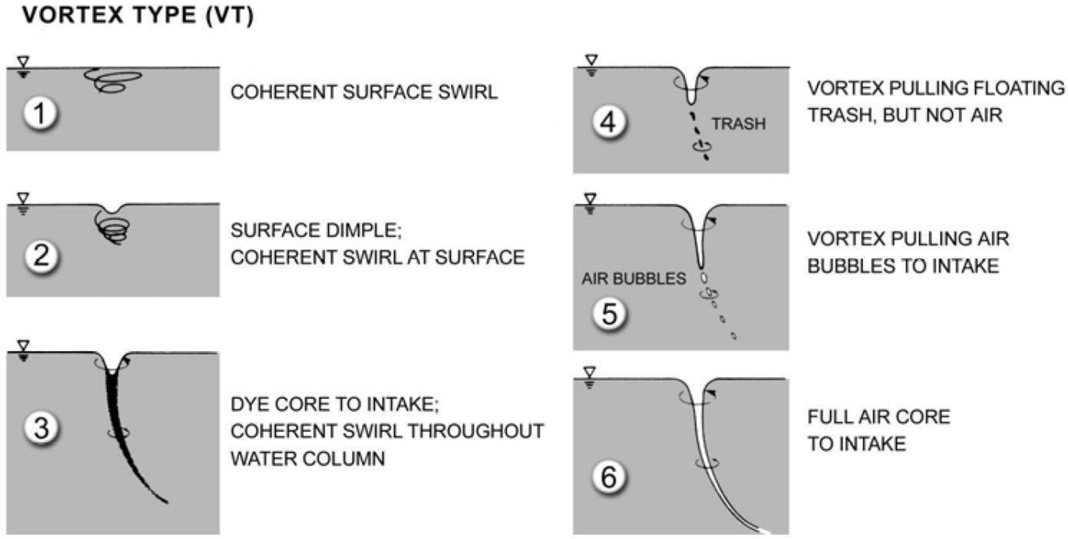

Figure 4.19: *Vortex classification set forth by Vischer & Hager (1995)*

spillway discharge. At 2250 m^3/s a small interruption in the drawdown was observed at pier 4 (noticeably more than at other piers) as shown in Figure 4.20 (right). At 1700 m^3/s spillway discharge the spillway gate operation is in a transient zone where the gates stop influencing the spillway flow. Because of this, bulking of water was observed in front of the gates as shown in Figure 4.21 (left). Bulking of water in front of spillway piers started at 1900 m^3/s and increased in magnitude with increased discharge, bulking in front of piers at 2250 m^3/s is shown in Figure 4.21 (right). At 1900 m^3/s spillway discharge a small irregular draw down was observed at the left abutment. As the flow comes over the curb between the spillway and intake a small drawdown and then rise forms as shown in Figure 4.22 (left). As mentioned above the approach flow conditions were in general good as shown in Figure 4.22 (right) for the design discharge Q_{1000} = 2250 m^3/s.

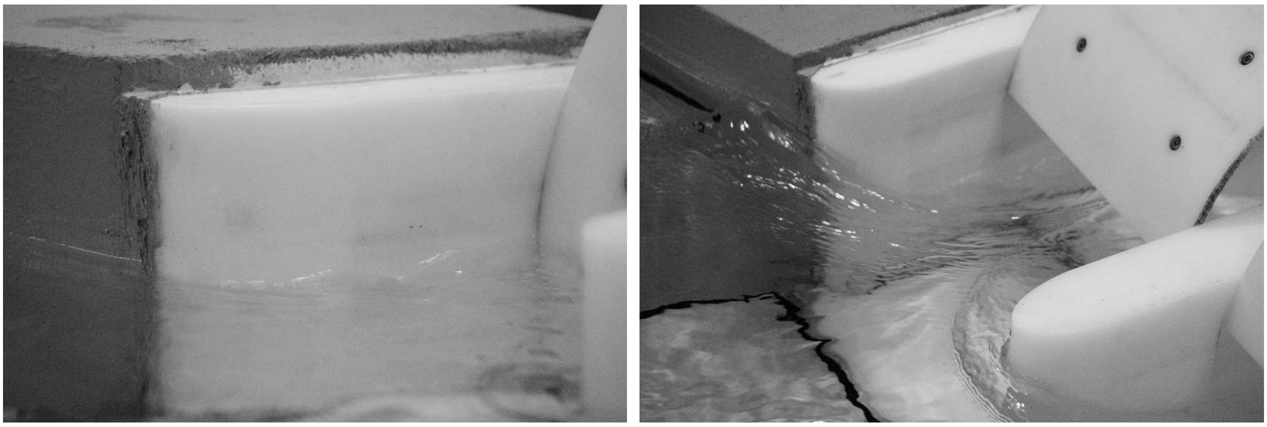

Figure 4.20: *On left: Vortex formation at pier 4 in spillway bay 3 at 1050 m^3/s. On right: Small interruption in drawdown at spillway pier 4 during 2250 m^3/s spillway discharge.*

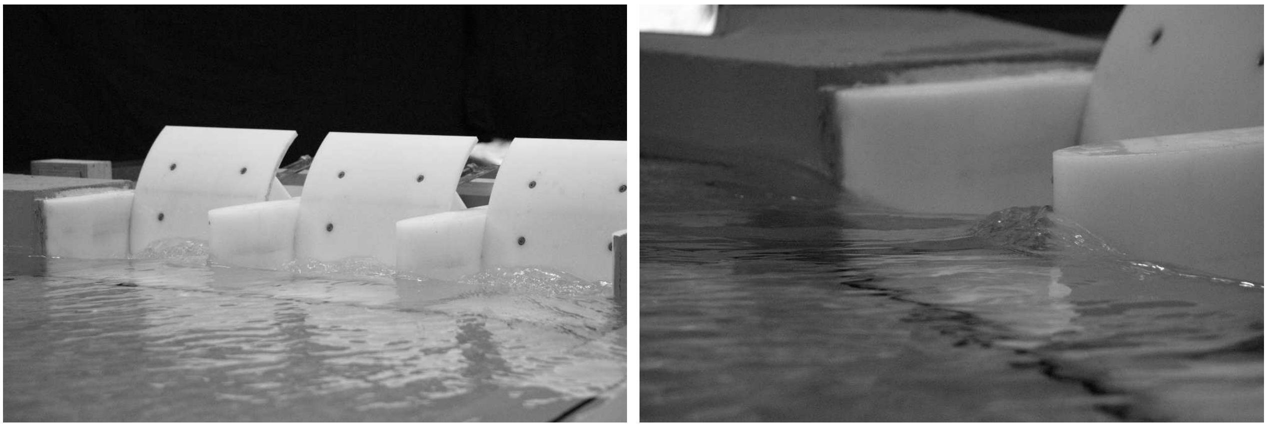

Figure 4.21: *On left: Bulking of water in front of spillway gates at 1700 m^3/s spillway discharge. On right: Bulking of water in front of spillway piers at 2250 m^3/s spillway discharge.*

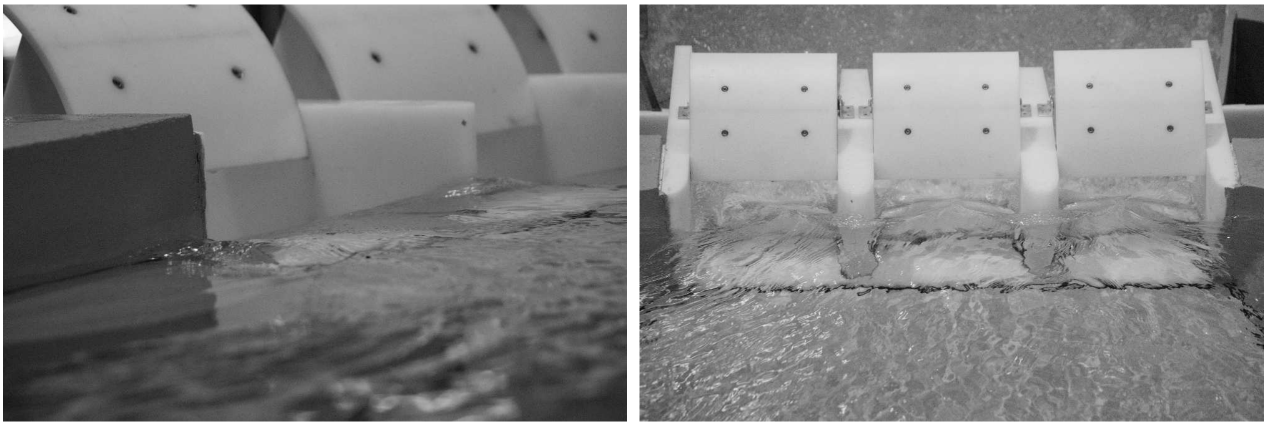

Figure 4.22: *On left: Abnormal drawdown at left abutment during 1900 m^3/s spillway discharge. On right: Spillway approach flow conditions at 2250 m^3/s spillway discharge.*

4.4.2. Velocity Distribution

In Figure 4.23 the velocity distribution at elevation 47.2 m a.s.l., 2.8 m depth, in the approach flow channel is shown at spillway discharge 350 m^3/s and intake design discharge of 370 m^3/s As seen in the figure the main current heads straight for the spillway with velocities ranging between 0.45 m/s and 0.5 m/s. Two other locations show high velocity components, one in front of the intake and the other at the left bank where a current flowing along the bank perpendicular to the main current and intersects the main approach flow creating disturbances in the flow. Figure 4.23 (right) shows the velocity distribution at 2.5 m depth, 47.5 m a.s.l., in the approach flow channel is shown at spillway discharge 1050 m^3/s and intake design discharge of 370 m^3/s. The increased discharge to the spillway dominates the approach flow conditions with the velocity reaching a maximum value of 1.7 m/s in front of the spillway. The increased discharge creates a stagnant velocity zone at the left bank just upstream of the intake, where flow coming along the left bank is drawn further into the center of the approach flow channel towards the spillway.

In Figure 4.24 the velocity distribution at an elevation 46.9 m a.s.l., 3.1 m depth, in the approach flow channel is shown at spillway discharge 1700 m^3/s without power intake operation Water in the approach flow channel is drawn towards the spillway with maximum velocity of 3 m/s immediately upstream of the spillway. A stagnant velocity zone forms upstream off the power intake reaching approximately 90 m upstream along the left bank. Figure 4.24 (right) shows velocity distribution at an elevation 48.4 m a.s.l., 3.1 m depth, in the approach flow channel at spillway discharge 2250 m^3/s without power intake operation. Similar characteristics are observed as during 1700 m^3/s spillway discharge but with larger velocities, reaching maximum of 3.7 m/s in front of the spillway.

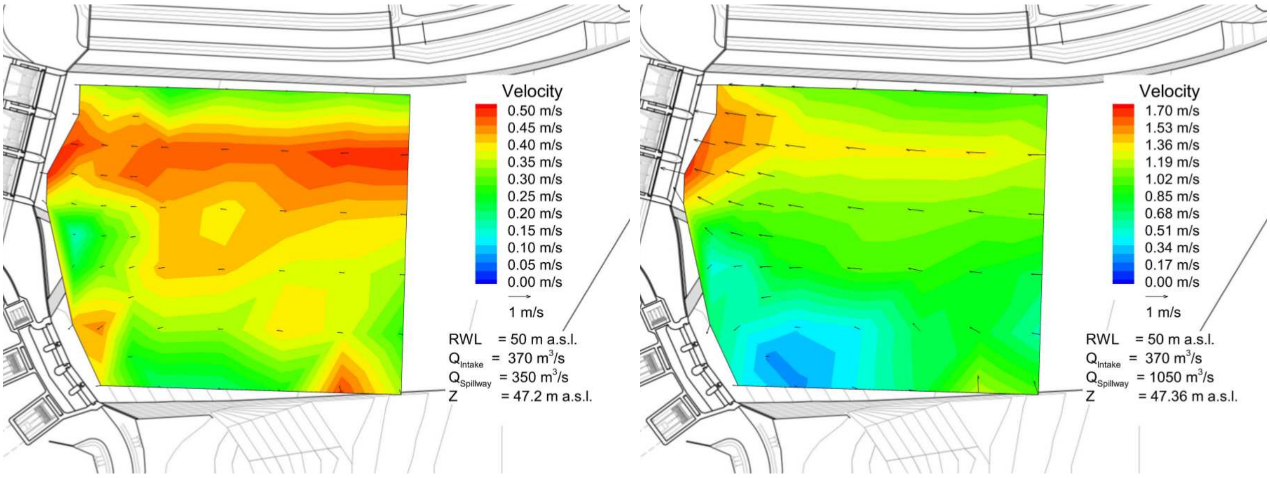

Figure 4.23: *On left: Velocity distribution in approach flow channel at spillway discharge 350 m^3/s and normal intake operation of 370 m^3/s. On right: Velocity distribution in approach flow channel at spillway discharge 1050 m^3/s and normal intake operation of 370 m^3/s.*

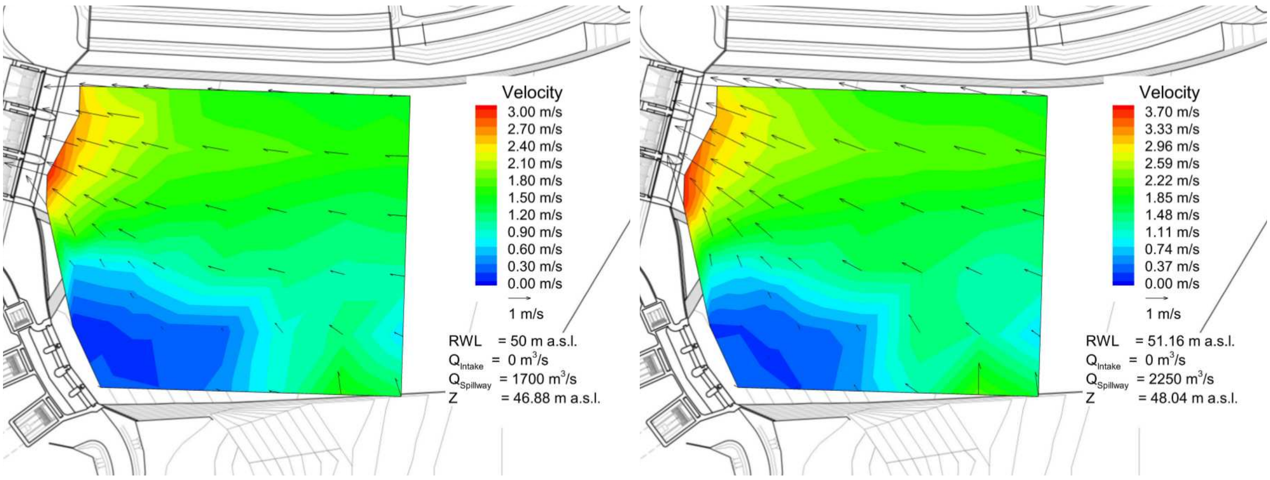

Figure 4.24: *On left: Velocity distribution in approach flow channel at spillway discharge 1700 m^3/s without power intake operation. On right: Velocity distribution in approach flow channel at spillway discharge 2250 m^3/s without power intake operation.*

4.4.3. Intake Approach Flow

At the intake, for its design discharge of 370 m^3/s, no drawdown was measured upstream of the intake entrance for any of the flow cases. Swirls or surface dimples, VT-2 type vortices (see Figure 4.19) were observed in front of all intake entrances but more frequently in front of Entrances 3 and 4 for all cases. The vortices shown in Figure 4.25 were defined as weak surface vortices which do not draw air. A more detailed description of intake and SFO approach flow conditions is presented in Chapter 5.

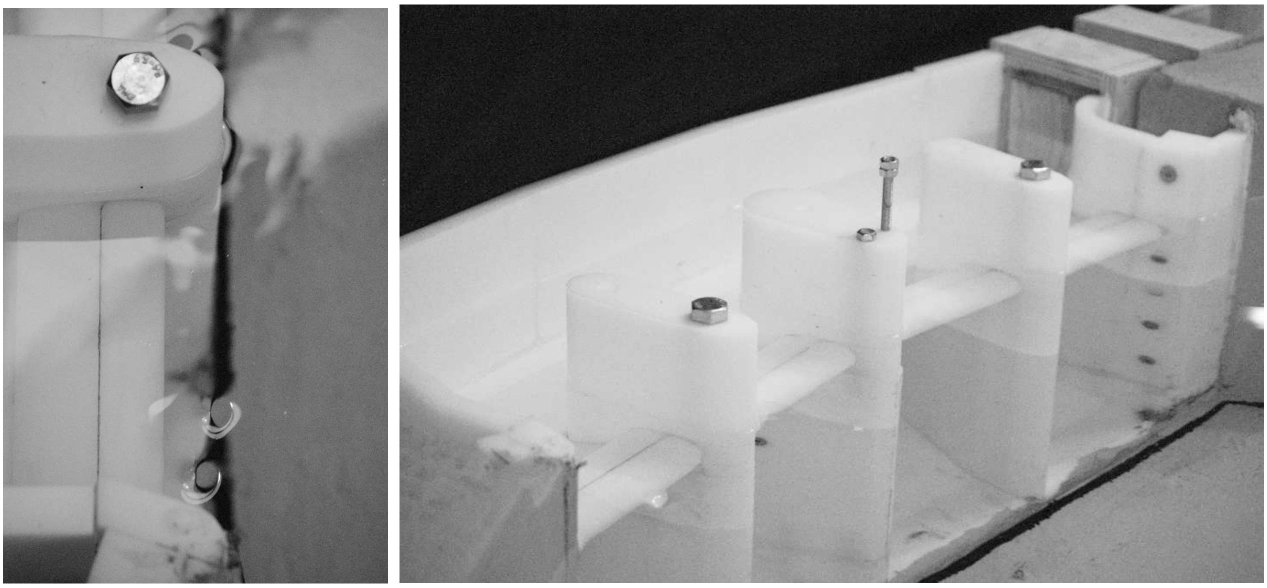

Figure 4.25: *Surface dimples forming in front of intake entrances.*

4.5. Spillway capacity

The discharge capacity of the proposed spillway at Heiðarlón pond was verified in the model studies. A manual point gauge was used to measure pond elevation and monitor stability, the gate opening in the model was measured with a custom made gauge. Calibration was made for the gate opening gauge so that vertical gate opening could be derived.

Measurements were conducted to establish discharge capacity of the structure in various operating modes. In total three scenarios were tested: (1) each gate of the three independently; (2) all three gates interlocked (all three gates equally open); and (3) all gates fully open and pond elevation ranging from crest elevation (41,0 m a.s.l.) to normal water level (NWL, 50,0 m a.s.l.). For cases (1) and (2), elevations from approximately 46.5 m a.s.l. to approximately 50 m a.s.l. were tested to cover all operation conditions. For discharges larger than 1850 m^3/s the operation of the structure is non-gated and pond elevation can rise to HRWL.

The discharge through a gated structure with radial gates can be expressed according to USBR (1987) and NVE (2005) as:

$$Q = C_g D L \sqrt{2 g H_g} \tag{4.1}$$

where Q is the discharge, C_g is a dimensionless discharge coefficient, dependant on various features of the design such as gate lip angle and shape, gate radius and trunnion pin point height; D is gate opening, L is the total length of gate, g is the acceleration of gravity and H_g is the head at the center of the gate opening including the dynamic head. Figure 4.26 shows the definitions adopted in this study for gate regulated flow for the parameters of Equation 4.1. In the model the reservoir elevation is measured at a zero velocity zone approximately 400 m southeast of the intake structure. Energy loss in the approach channel is insignificant for the design discharge.

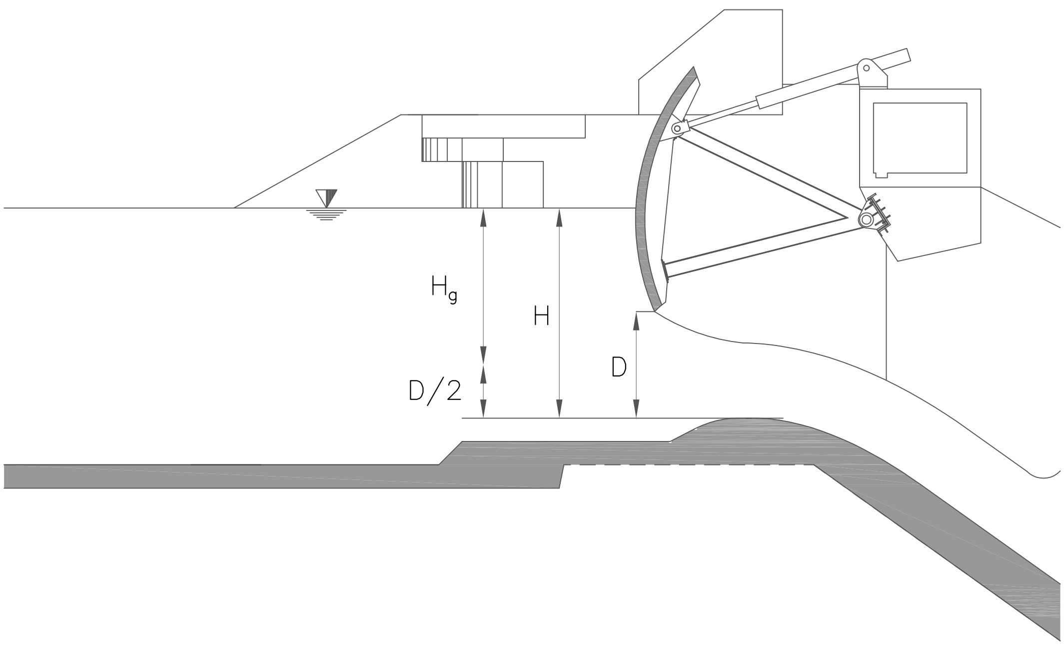

Figure 4.26: *Definiton of parameters for Equation 4.1.*

The main design criteria for Urriðafoss spillway is to convey 1700 m^3/s (Q_{50}) at 50,0 m a.s.l. and 2250 m^3/s (Q_{1000}) at 51.5 m a.s.l. or lower. For discharges higher than approximately 1850 m^3/s the gate opening of the radial gate exceeds the critical flow depth for the given discharge. This mean that the gate does not influence the flow. The discharge Q over a non-gated spillway can be expressed according to USBR (1987) and Peterka (1958) as:

$$Q = C_d L_{eff} H^{3/2} \tag{4.2}$$

where Q is the discharge, C_d is a dimensionless discharge coefficient, dependant on various features of the design such as approach flow geometry, downstream apron elevation, downstream submergence, ratio of dynamic and static head in the approach flow and the relation of the actual crest shape to the ideal nappe shape; H is the actual head on the crest, including the dynamic head of approach; L_{eff} is the effective length of the crest and is less than the physical length, L. The reduction of the physical length to the effective length is controlled by the number and layout of the piers in the structure and the abutments of the spillway. For the free flow conditions at Urriðafoss spillway the reduction from physical length is about 7 percent according to the referred literature.

A comparison between the criteria of Heiðarlón pond levels and the values measured in the model is shown in Table 4.1. In general the spillway meets the criteria, both the Q_{50} and the Q_{1000} pass through the spillway with pond levels lower than required. The pond reaches the fuse plug level of 51.8 m a.s.l. at discharge trough the spillway measured at 2450 m^3/s.

Table 4.1: *Criteria and measured water surface levels in the Heiðarlón pond.*

	Unit	Q_{50}	Q_{1000}	$Q_{\text{Fuse plug elevation}}$
Discharge	m^3/s	1700	2250	2450
Pond level, criteria	m a.s.l.	50.0	51.5	-
Measured pond level in the model	m a.s.l.	49.56	51.2	51.8

Figure 4.27 shows the calculated discharge coefficient derived from Equation 4.2. In the operation of the spillway, discharges greater than approximately 1800 m^3/s are unregulated by the radial gates of the structure. In this region in Figure 4.27 the calculated discharge coefficient is relatively constant and averages as 1.916 for discharges above 1800 m^3/s. This indicates that a constant discharge coefficient gives acceptable results for calculation of un-gated discharges with Equation 4.2. For these derivations the effective length of the crest is assumed the physical length, 36 m. The discharge coefficient, C_d, for discharges less than 1800 m^3/s is not as important as the flow is regulated by the gates and therefore the discharge coefficient C_g (see Equation 4.1) should be used.

Figure 4.28 shows the measured head-discharge relationship (non-gated crest flow) for Urriðafoss spillway, the measured data is fitted according to Equation 4.2 with a constant discharge coefficient, C_d as 1.916. The crest length for the calculated curve is 36 m, i.e. the effect of crest length reduction, L_{eff}, is included in the discharge coefficient. The crest elevation is at 41 m a.s.l. as previously shown in Figure 4.2 in Section 4.1.

The concreted part immediately upstream of the spillway crest was raised by 2 m to validate its influence on the discharge capacity. This modification lowered the discharge coefficient from 1.916 to 1.752, reducing the discharge capacity by approximately 9%. This modification at Hvammur HEP spillway could provide additional discharge capacity as the structure bypasses the design discharge marginally.

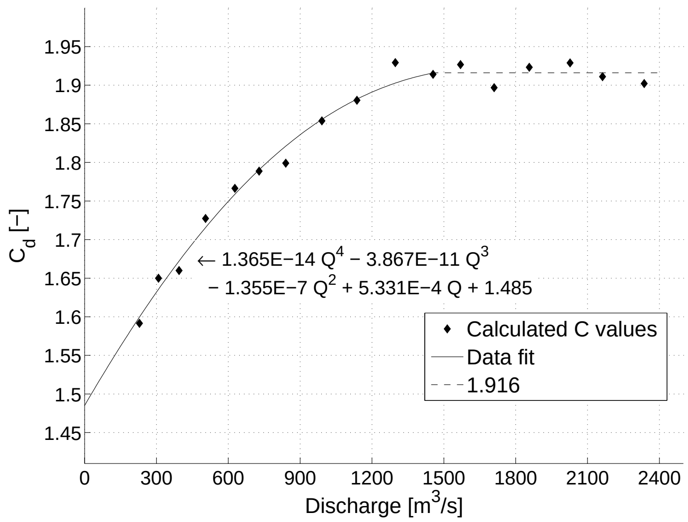

Figure 4.27: *Calculated discharge coefficient C_d from ungated crest flow measurements in the model. For ungated flow and discharges lower than 1350 - 1400 m^3/s the discharge coefficient follows the function provided in the graph but for higher flows the discharge coefficient can be assumed constant, 1.916. For normal operation the ungated discharge coefficient should be taken as a constant because for flows less than 1800 m^3/s the flow is regulated by the radial gates.*

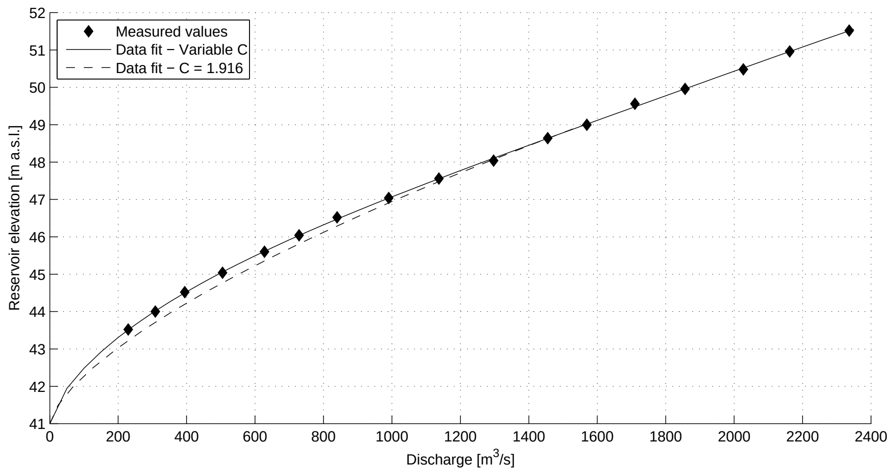

Figure 4.28: *Measured pond water level in Heiðarlón pond as a function of discharge for all three gates fully open, non-gated crest flow. Points indicate measurements in the model and the solid line shows a calculated rating curve with a varying discharge coefficient as seen in the function in Figure 4.27. The dotted line shows the fit through the measurements in the model by using a constant discharge coefficient as 1.916.*

Discharge capacity measurements were made for all three gates independently and no significant variance between gates was observed. The single gate data presented is therefore applicable to any of the three gates. Figure 4.29 shows the discharge capacity as a function of the pond elevation for different gate opening, the measured data is fitted with Equation 4.1 with the discharge coefficient as the average discharge coefficient calculated from the measured data for each gate opening. One gate can regulate discharge for up to a 6 m gate opening which corresponds to a discharge of 520 m^3/s at the NWL. By increasing the gate opening beyond that point the flow enters a regime of fluctuating pulses and transition to critical non-gated flow. At the NWL and a fully open single gate the discharge capacity is about 625 m^3/s.

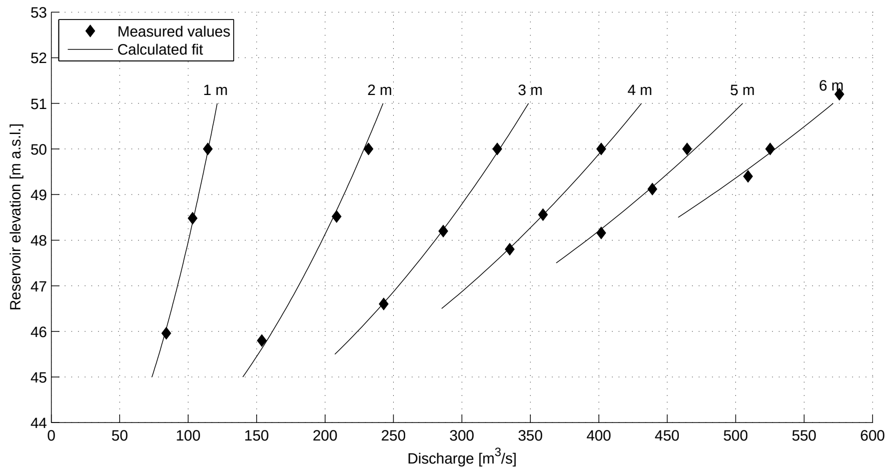

Figure 4.29: *Rating curves for single gate operation for variable gate openings. The curves are applicable to all gates individually. Points show measurements while the solid lines are calculated from Equation 4.1.*

Interlocked gates operation is the recommended operation for the spillway structure for all discharges greater than 200 m^3/s. A detailed investigation of asymmetric gate operation was performed in accordance with the measurement program and is discussed in Section 4.7.

For interlocked operation, discharge capacity as a function of gate openings and pond elevation is presented in Figure 4.30. The measured data is fitted with Equation 4.1 with the discharge coefficient as the average discharge coefficient calculated from the measured data for each gate opening. For gate openings up to 6 m the gates regulate the flow but for D greater than 6 m the system enters a transition regime to critical flow.

Figure 4.31 is the recommended rating curve that should be used for the spillway structure, made from the calculated fit from the measured data as previously described. The black dots in Figure 4.30 and 4.28 show the measured data points, the fitted data is extrapolated according to Equations 4.1 and 4.2. The rating curve on Figure 4.31 is presented in more detail in Appendix L. Because of the scale ratio of the model (1/40) care must be taken as the discharge coefficient varies with the layout of the gate lip. In a model scaled at 1/40 it is impossible to represent accurately the gate lip and its effect on the discharge coefficient. Table 4.2 shows the discharge coefficient for gate operation, both single and interlocked, as a function of gate opening.

Table 4.2: *Discharge coefficient (C_g) for single and interlocked operation.*

Single gate		Interlocked gate	
D [m]	C_g [-]	D [m]	C_g [-]
1	0.769	1	0.740
2	0.759	2	0.760
3	0.734	3	0.750
4	0.705	4	0.717
5	0.682	5	0.694
6	0.670	6	0.677

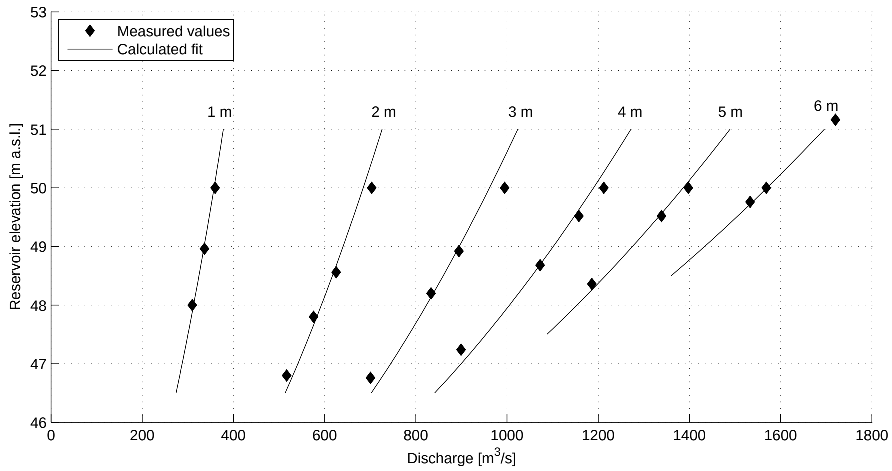

Figure 4.30: *Rating curves for interlocked gates operation for variable gate openings. The points show measurements while the solid lines are calculated from Equation 4.1.*

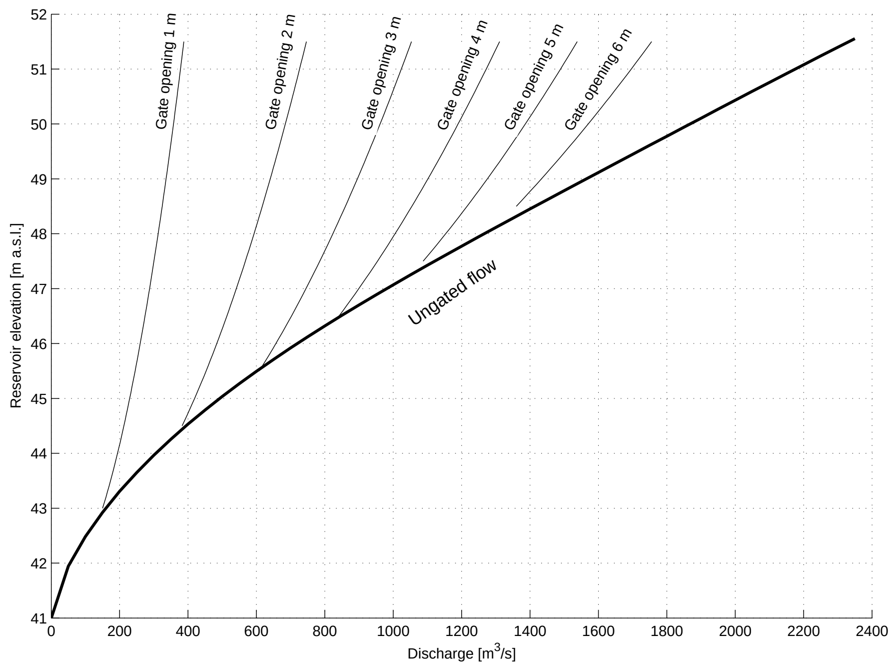

Figure 4.31: *Rating curves for interlocked gate operation for variable gate openings. The bold line shows free flow conditions (ungated flow). The other lines show gate regulated flow at variable gate openings as a function of pond elevation and flow.*

4.6. Roller bucket

A slotted roller bucket downstream of the gated section was selected for the final design with an invert elevation of 26 m a.s.l., a radius of 11 m and an exit angle of 16°. Downstream of the bucket an excavated channel will transport the water to the original riverbed. The excavated channel has an elevation of 27.5 m a.s.l. immediately downstream of the lip and a uniform slope down to 26 m a.s.l. over the next 25 m. From there it slopes uniformly upwards over a 25 m distance to 28 m a.s.l. The invert remains at elevation 28 m a.s.l., after which it slopes up to the original river bed of 34 m a.s.l. with a uniform slope of 1:2. The downstream end of the excavated channel is asymmetric as shown in Figure 4.32 and therefore a high end wall is located at the downstream end of the channel. The side walls of the excavated channel have a uniform slope of 4:1 and expand outwards from the roller bucket. Figure 4.32 shows an overview of the structures and the coordinate system and stationing adopted in the study. It should be noted that a different coordination system from that used in the laboratory study is used by the design group. Detailed drawings of the layout are presented in Appendix G.

The measurement program (Appendix A) describes the measurement procedures for the final design. Four main discharges were investigated, 350, 1050, 1700 and 2250 m^3/s and detailed measurements conducted to document the hydraulics, flow conditions and performance of the structures. Additionally six discharges were tested, ≈100, 200, 500, 700, 1300, 1900 m^3/s, but with less extensive measurements. Water level, velocity and pressure measurements were conducted as well as visual observations.

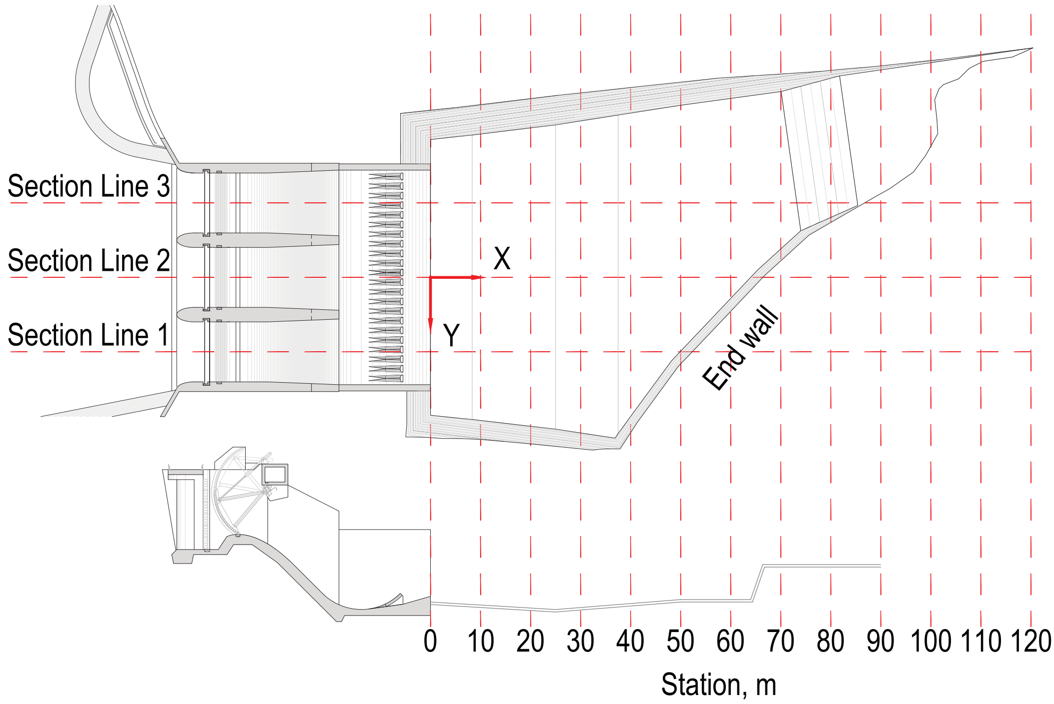

Figure 4.32: *Spillway, roller bucket and downstream channel according to the final design at Urriðafoss. The coordinate system adopted in the laboratory study is shown. It should be noted that a different coordination system from that used in the laboratory study is used by the design group. Drawing C-11-3.101-P7.*

4.6.1. Flow conditions in the bucket and downstream channel

The flow conditions in the downstream channel are highly dependant on the flow conditions in the bucket and its performance. For a slotted roller bucket, as is present at Urriðafoss spillway, the high velocity jet is spread laterally between the teeth of the bucket only with a part of the high velocity reaching the surface. The high velocity that reaches the surface will result in a surface boil that may induce wave propagation in the downstream channel.

For low discharges tested, less then 200 m^3/s, the flow conditions in the system were stable, with a smooth surface in the downstream channel and a boiling, but stable surface inside the bucket. Inside the bucket, a stable but weak roller was formed. At 350, 500 and 700 m^3/s some irregularities were observed in the downstream channel but the surface was still stable.

For 1050 and 1300 m^3/s the bucket roller starts to show submerged jet characteristics and the boiling behaviour inside the bucket starts to move out of the bucket with the surface inside the bucket a little lower than in the downstream channel. For 1700 m^3/s the surface in the downstream channel gets rippled and quite wavy with a boiling surface approximately 9 meters downstream of the end of the bucket.

For 2250 m^3/s, the bucket roller is less visible and a submerged jet has formed. The surface in the downstream channel is wavy and irregular with a boiling surface approximately 11 meters downstream of the bucket lip. The surface inside the bucket is irregular and significantly lower than in the downstream channel.

Figure 4.33 shows the surface of the downstream channel for 200, 500, 700 and 1700 m^3/s. Figures 4.34 and 4.35 show the measured water elevation for Section Line 2 in the system (see Figure 4.32). With increasing discharge the elevation difference between the water surface elevation in the downstream channel and the bucket increases. Water elevation for Section Lines 1 and 3 can be found in Appendix J and tables with water elevation measurements for 350, 1050, 1700 and 2250 m^3/s. In Appendix C the calculated tailwater elevations from the designers are compared to the results from the model and from field measurements during a flood in March 2013.

The flow velocity in the downstream channel was measured with an ADV at a sampling rate of 10 Hz for a period of 60 seconds. Velocity was measured from station 0 to 120, at 10 m interval for 3-5 elevations, as possible, for the three section lines shown in Figure 4.32 and eight cross sections located at stations 10 to 80 m at 10 m intervals.

Figure 4.36 shows the average velocity at each station for 350, 1050, 1700 and 2250 m^3/s. All measured values are used at each station to derive a mean value. When the discharge is less than 1050 m^3/s the depth in the original riverbed was insufficient to make a velocity measurement with the ADV probe. The sudden change in the average velocity for section line 1 at station 50 m is where the downstream channel meets the original riverbed with the high end wall. This happens again for Section Line 2 between station 60 and 70 m where Section Line 2 enters the original riverbed.

Figures 4.37-4.40 show the velocity distribution in each section line for 350, 1050, 1700 and 2250 m^3/s.

Figure 4.37 shows the velocity distribution for 350 m^3/s in each section line. The velocity is

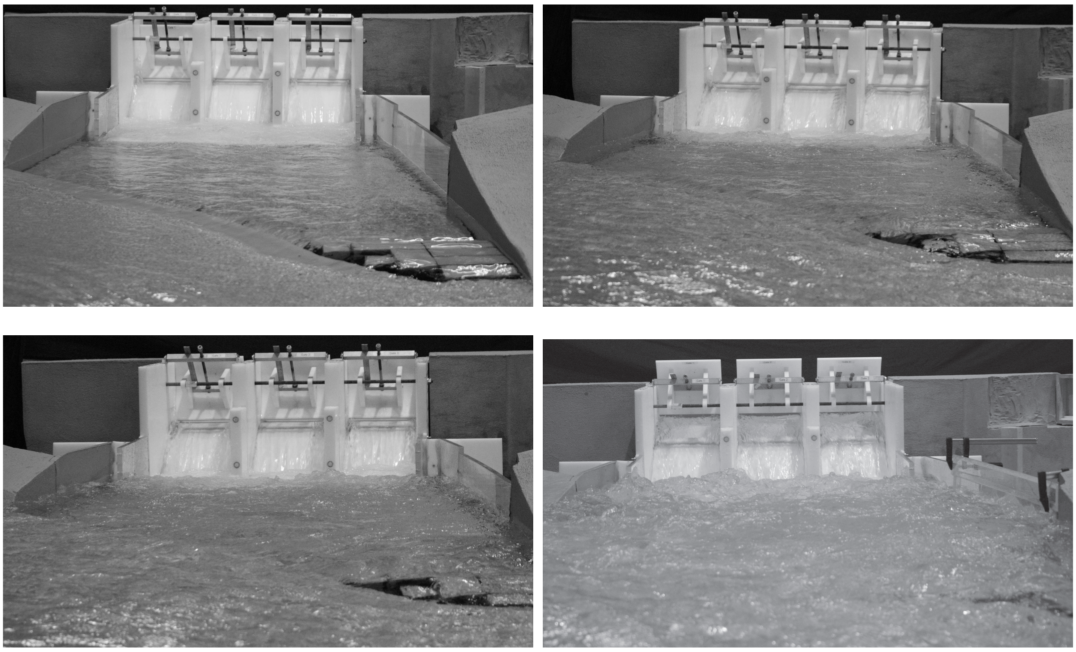

Figure 4.33: Surface of the downstream channel for 200 m^3/s (top left), 500 m^3/s (top right), 700 m^3/s (bottom left) and 1700 m^3/s (bottom right).

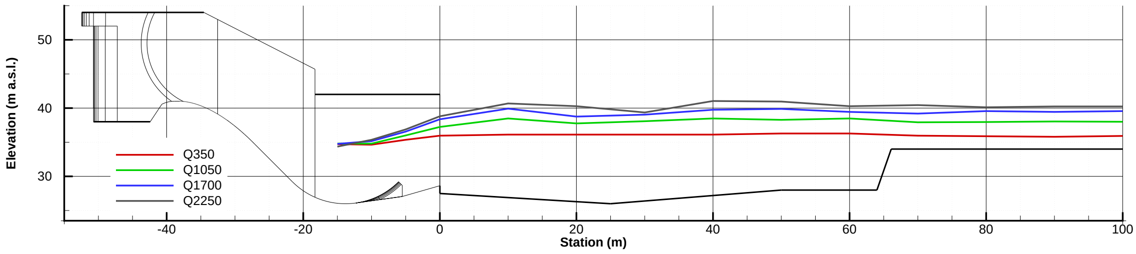

Figure 4.34: Water elevations for Section Line 2 in the system for the main discharges investigated in the model.

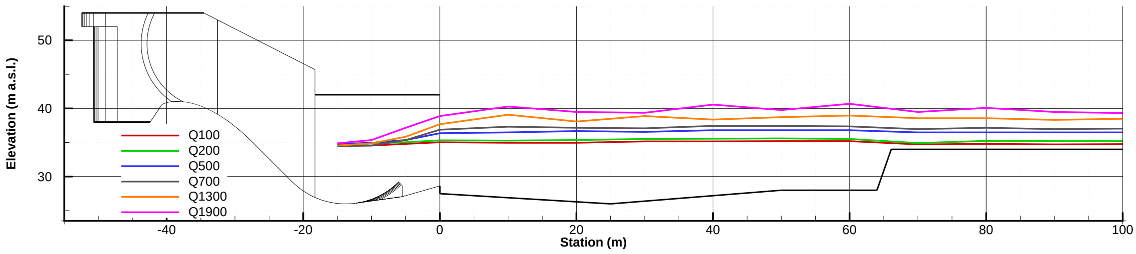

Figure 4.35: Water elevations for Section Line 2 in the system for the secondary discharges investigated in the model.

generally quite low (less than 1 m/s). The surface velocity directly downstream of the bucket lip is not uniform which could be related to the asymmetric downstream channel. One vector can be seen in opposite direction to the main flow direction indicating a very weak ground roller directly downstream of the bucket, this is at Section Line 2 (middle figure), station 10 m and closest to the bottom. Figure 4.38 shows the velocity distribution for 1050 m^3/s in each section line. The weak ground roller is more visible but is not uniform, the ground roller seams to be more compressed to the bottom in Section Line 2 as compared to Section Lines 1 and 3. This can be explained by the sudden expansion of the downstream channel. Figure 4.39 shows the velocity distribution for 1700 m^3/s in each section line. The ground roller has reduced and is barley noticeable, however the layer near the bottom of near stagnant water indicates that the ground roller is still there to some extent. Figure 4.40 shows the velocity distribution for 2250 m^3/s in each section line. The ground roller is more visible in Section Lines 1 and 3. It is noted that the contour levels are not synchronized between the figures. Figures 4.37-4.40 are shown with synchronized contour levels in Appendix K.

The root mean square (RMS) of the turbulent velocity fluctuations around the mean velocity are computed for use in determining turbulence intensities and levels of turbulent kinetic energy. The RMS value is equal to the standard deviation of the individual velocity measurements and is believed to indicate energy dissipation intensity. Figure 4.41 shows the calculated average root mean square (RMS) of velocity at each station for 350, 1050, 1700 and 2250 m^3/s. All measured values are used at each station to derive the RMS value.

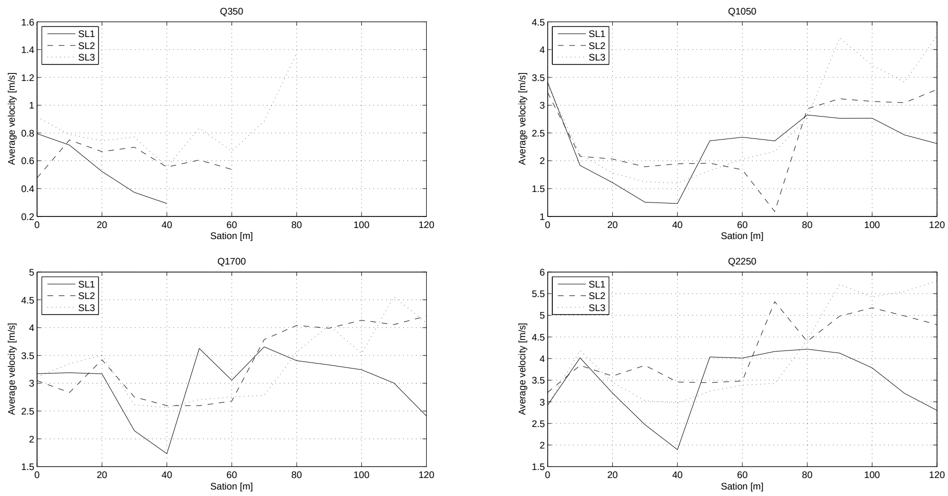

Figure 4.36: *Measured average velocity at each station for 350, 1050, 1700 and 2250 m^3/s.*

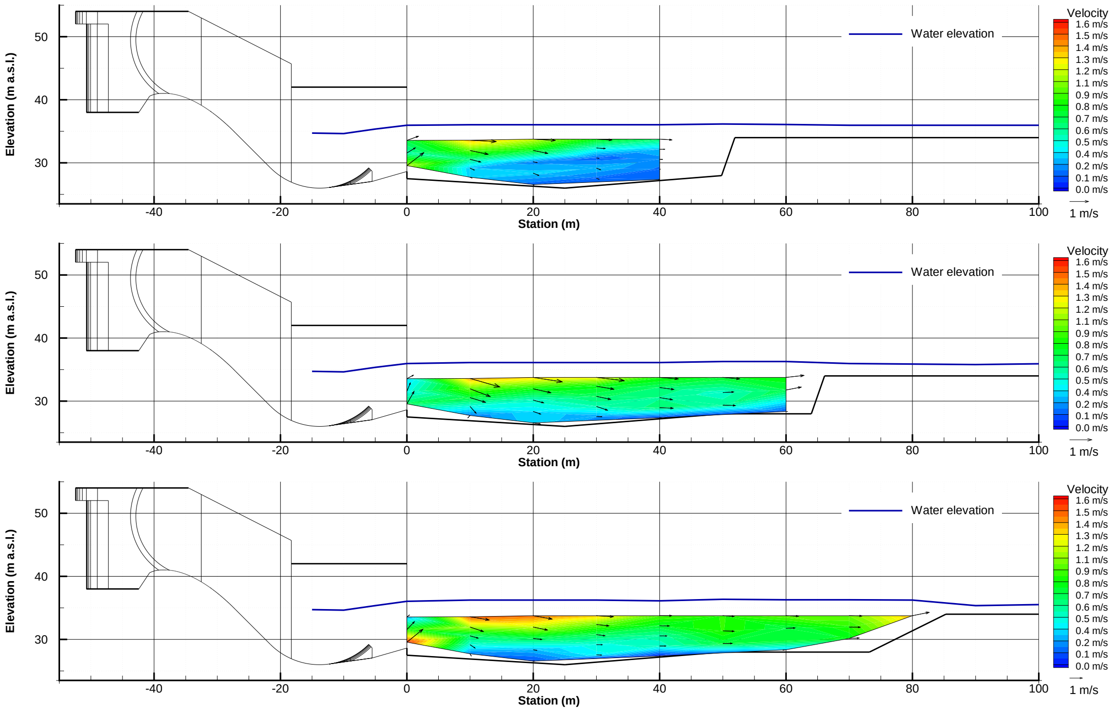

Figure 4.37: *Velocity measurements along the three section lines for 350 m^3/s.*

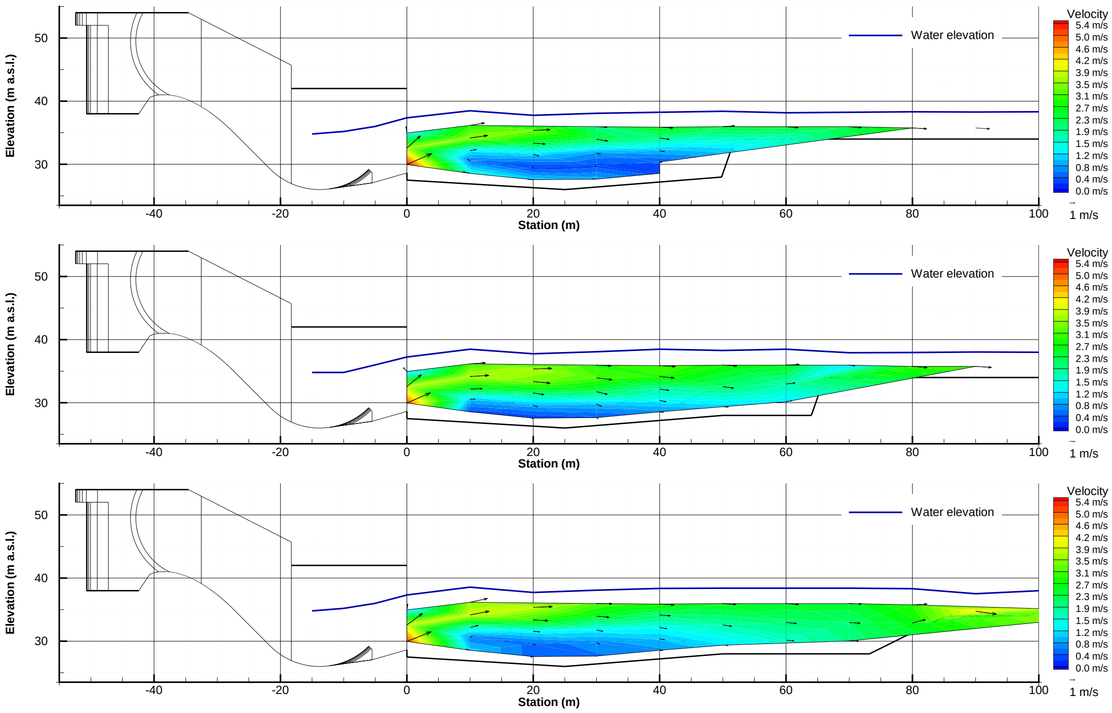

Figure 4.38: *Velocity measurements along the three section lines for 1050 m^3/s.*

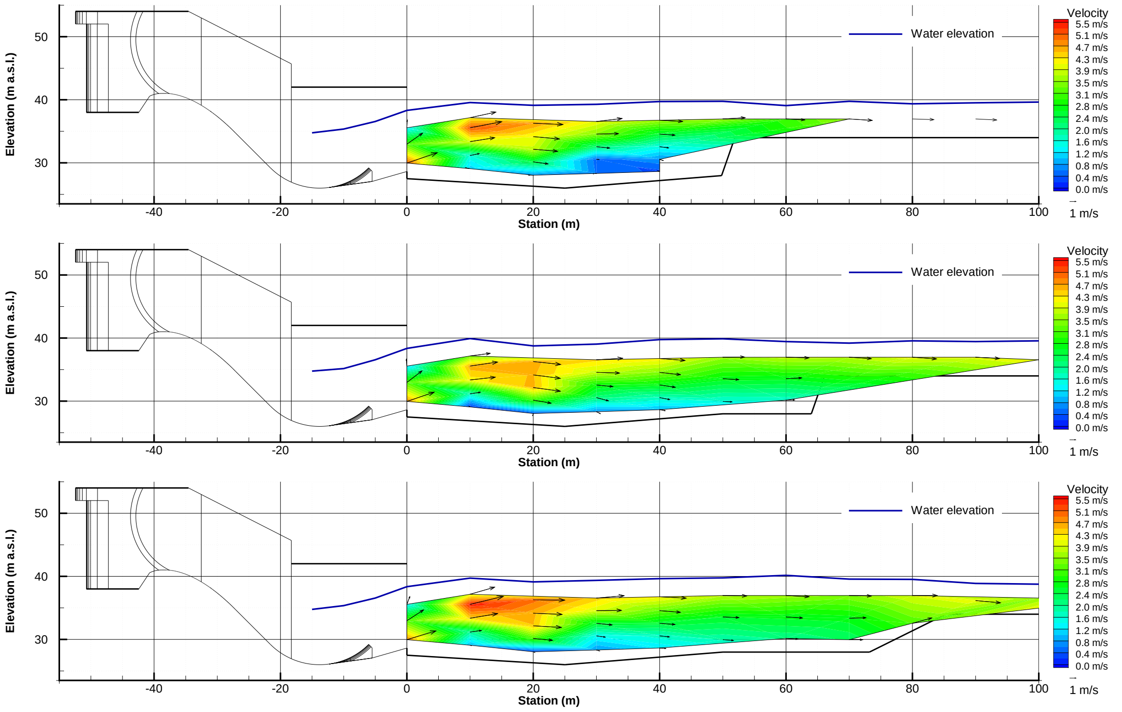

Figure 4.39: *Velocity measurements along the three section lines for 1700 m^3/s.*

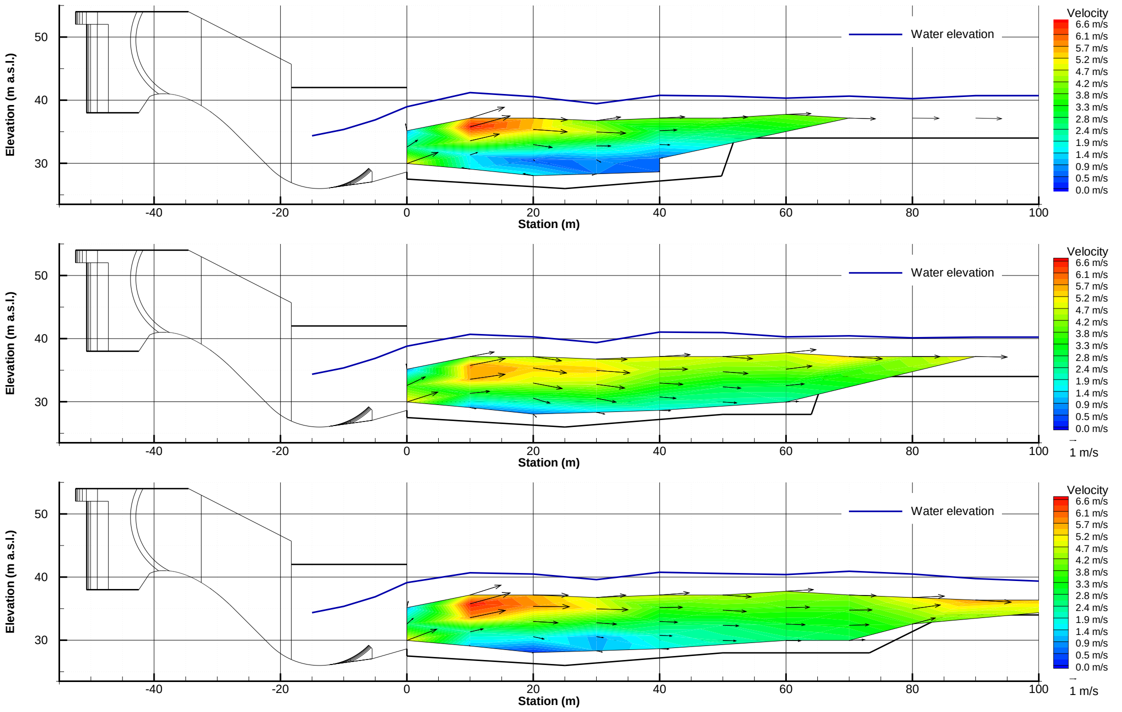

Figure 4.40: *Velocity measurements along the three section lines for 2250 m^3/s.*

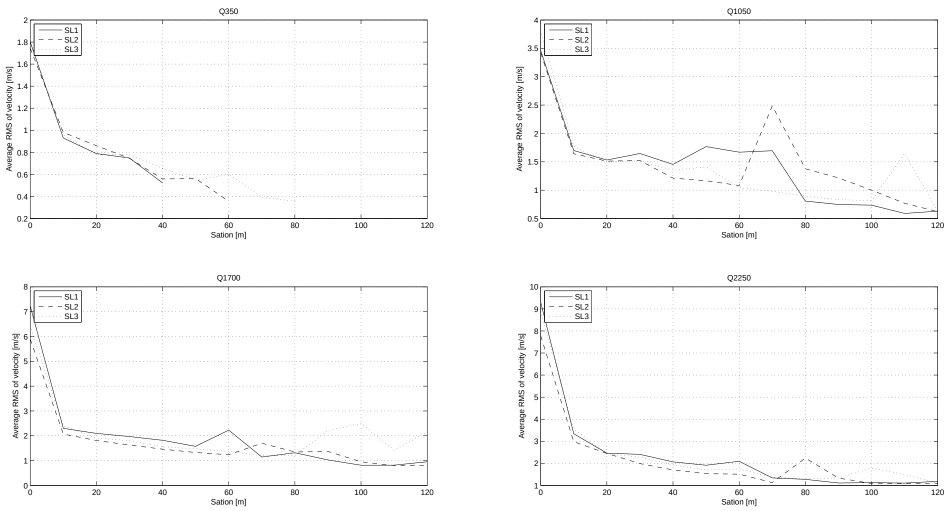

Figure 4.41: *Measured average root mean square (RMS) of the velocity at each station for 350, 1050, 1700 and 2250 m^3/s.*

4.6.2. Flow conditions in the receiving river section

For low discharges tested, less than 350 m^3/s the flow conditions in the original riverbed are stable, with a relatively smooth surface. A small hydraulic jump forms immediately after the end wall, stretching over the cross section where the downstream channel meets the riverbed. Figure 4.42 shows the hydraulic jump at 200 m^3/s. The jump forms approximately 8 meters downstream of the end wall for 100 m^3/s and moves closer to the end wall as the discharge is increased. The hydraulic jump vanished at discharge between 700 and 1050 m^3/s.

For discharges higher or equal to 700 m^3/s the surface of the upstream part of the river section (upstream of where the channel enters the riverbed) is irregular. In the downstream section the river surface is rippled for these cases.

For 1300 m^3/s the water elevation reaches the lowest part (flood plane elevation) of the riverbank directly opposite to the excavated channel. With increasing discharge the water elevation increases, reaching further into the flood plane of the riverbank opposite to the spillway structure at discharge between 1700 and 1900 m^3/s. At 2250 m^3/s the water elevation reaches approximately 10 - 15 meters inland (plan view, about 2.5 m elevation change from the flood bank elevation) directly opposite the excavated channel.

Figure 4.43 shows the surface of the downstream river section for 350, 1050, 1300 and 2250 m^3/s. The water elevation in the system for 350, 1050, 1700 and 2250 m^3/s can be seen in Figures 4.44 - 4.47. It is noted that the contour levels are not synchronized between figures. The measured water elevations for each data point is shown in Table J.1 - J.4 in Appendix J.

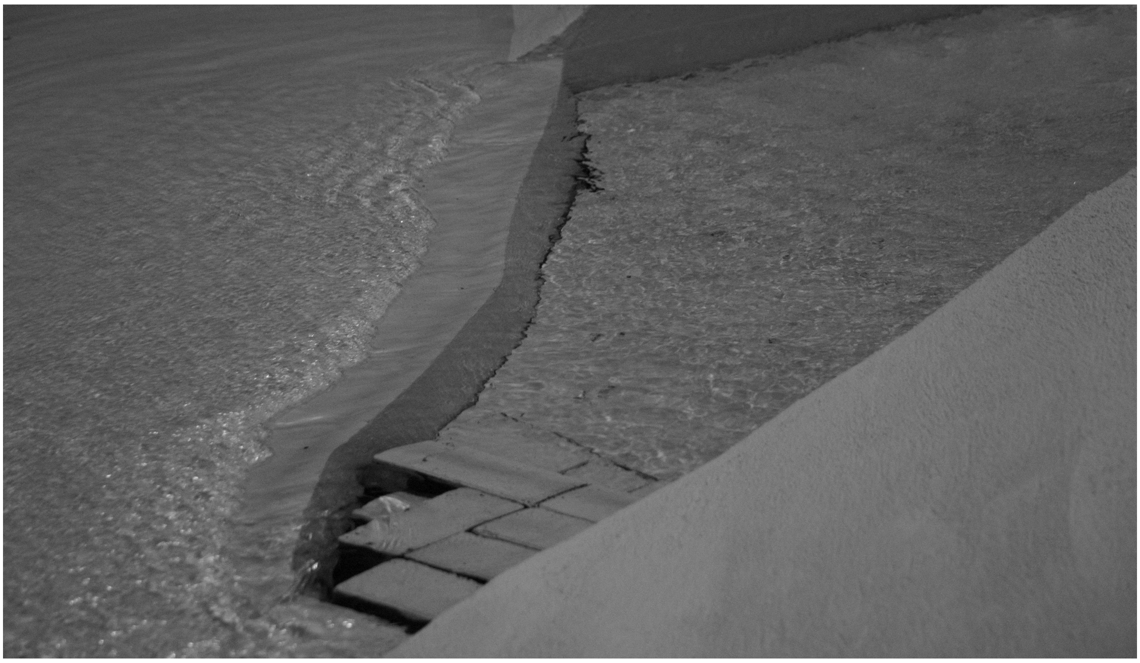

Figure 4.42: *Small hydraulic jump immediately at the end wall for 200 m*^{3}*/s.*

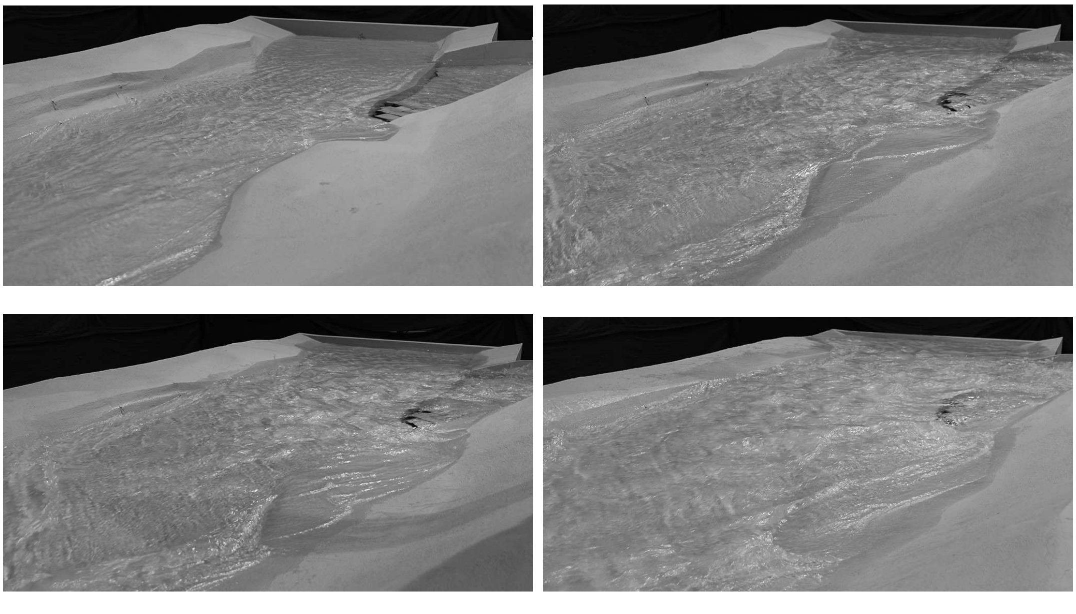

Figure 4.43: *The downstream river section for 350 m*^{3}*/s (top left), 1050 m*^{3}*/s (top right), 1300 m*^{3}*/s (bottom left) and 2250 m*^{3}*/s (bottom right).*

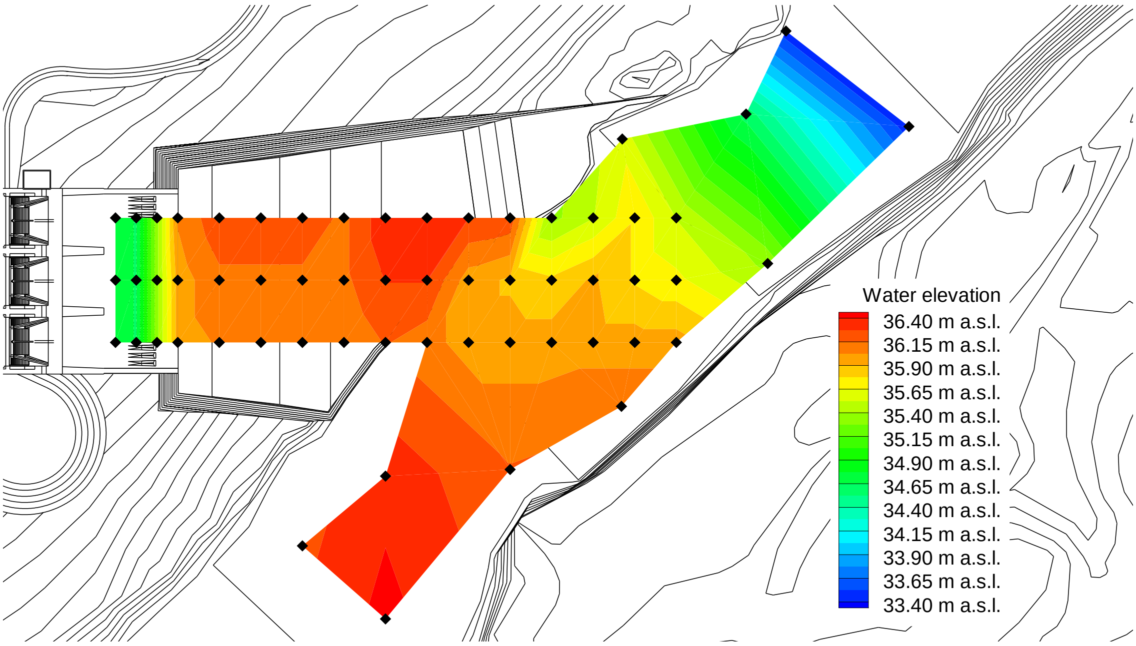

Figure 4.44: *Water elevations in the downstream river section for 350 m^3/s, the black dots indicate measurement points.*

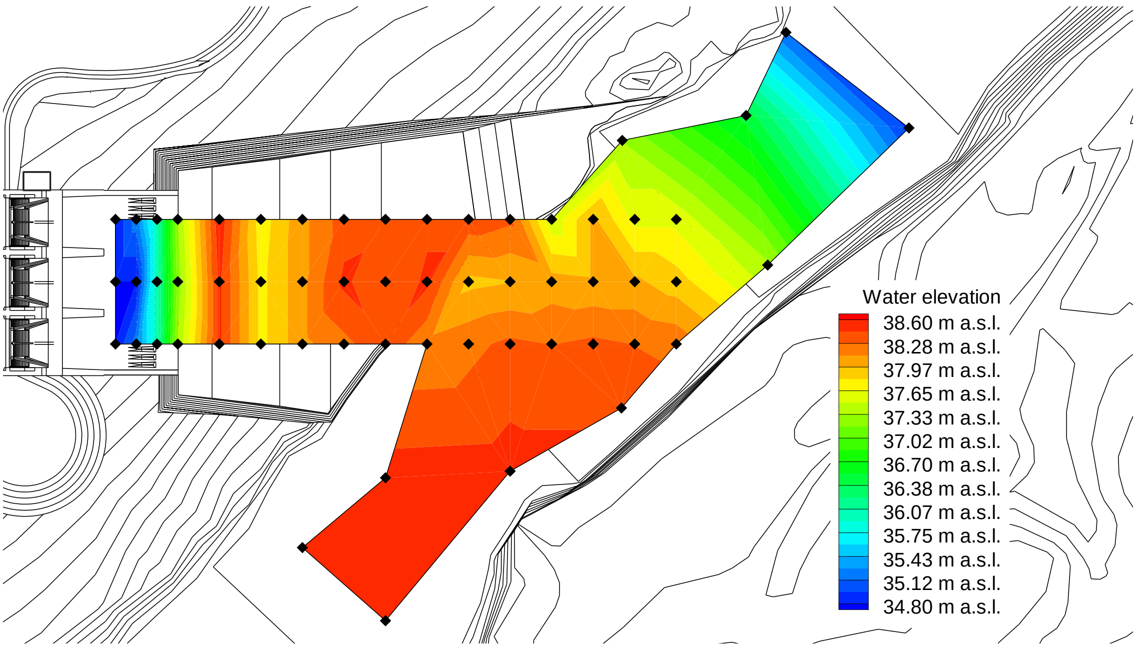

Figure 4.45: *Water elevations in the downstream river section for 1050 m^3/s, the black dots indicate measurement points.*

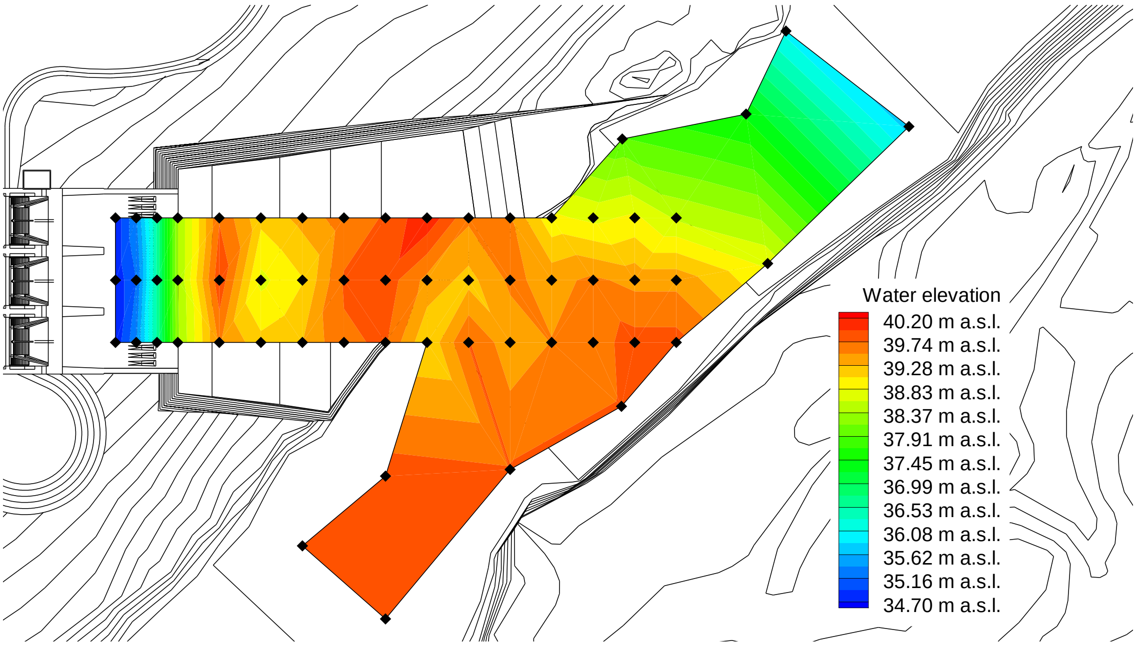

Figure 4.46: *Water elevations in the downstream river section for 1700 m^3/s, the black dots indicate measurement points.*

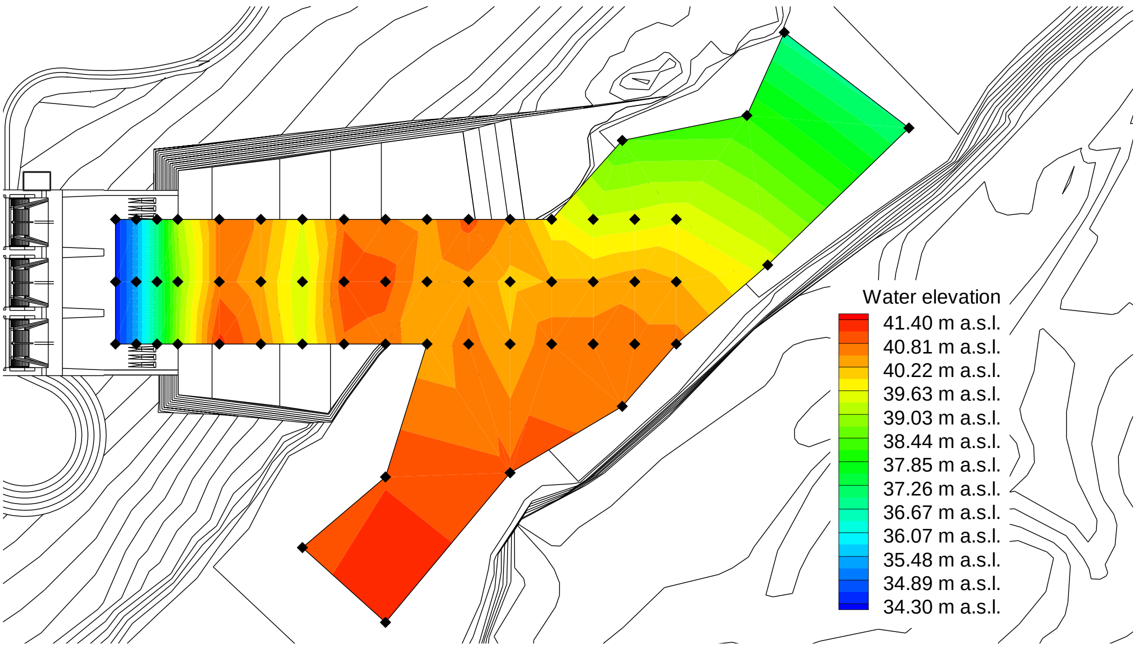

Figure 4.47: *Water elevations in the downstream river section for 2250 m^3/s, the black dots indicate measurement point.*

The flow velocity in the river was measured for 1700 and 2250 m^3/s, but the depth of the water for 350 and 1050 m^3/s was insufficient for the ADV probe to operate. The flow velocity downstream of the excavated channel was too great for an accurate measurement to be made, however it can be assumed that the depth is critical and by that assumption the velocity can be estimated from the depth of the water.

Figures 4.48 and 4.49 show the measured velocity in the river section at approximately 2 m depth for 1700 and 2250 m^3/s, respectively. The velocities shown in the excavated channel are depth averaged velocity. Within the downstream channel is a vertical circular motion along the section lines as previously discussed in Section 4.6.1, this could affect the average velocity and its direction. It is noted that the contour levels are not synchronized between the figures.

The upstream part of the river section has a stagnant zone with a slow clockwise circular movement but in the downstream section the flow is critical with high velocities. The flow turns after it reaches the original riverbed without hitting the opposite riverbank directly.

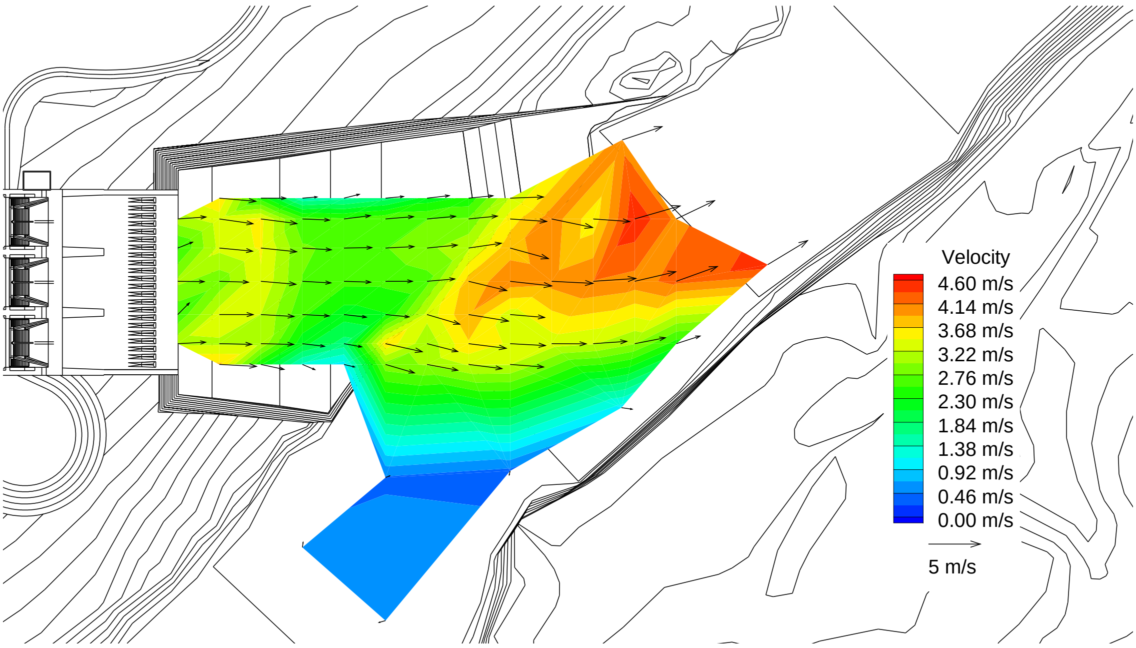

Figure 4.48: *Measured velocity in the river section for 1700 m^3/s, the velocity shown in the excavated channel is depth averaged velocity.*

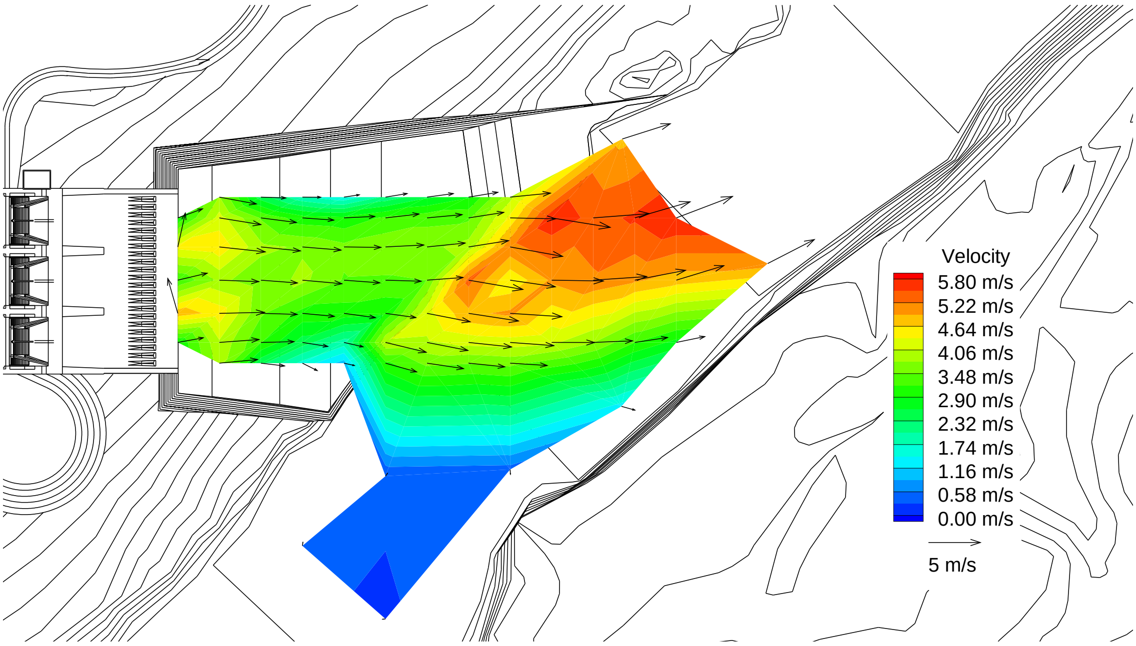

Figure 4.49: *Measured velocity in the river section for 2250 m^3/s, the velocity shown in the excavated channel is depth averaged velocity.*

4.6.3. Pressure measurements

Bottom pressure was measured with pressure transducers mounted on 15 locations in the downstream channel. The distribution of standard deviation of pressure is shown in Figures 4.50, 4.51, 4.52 and 4.53 for 350, 1050, 1700 and 2250 m^3/s, respectively. Note that the contour levels are not synchronized between the figures.

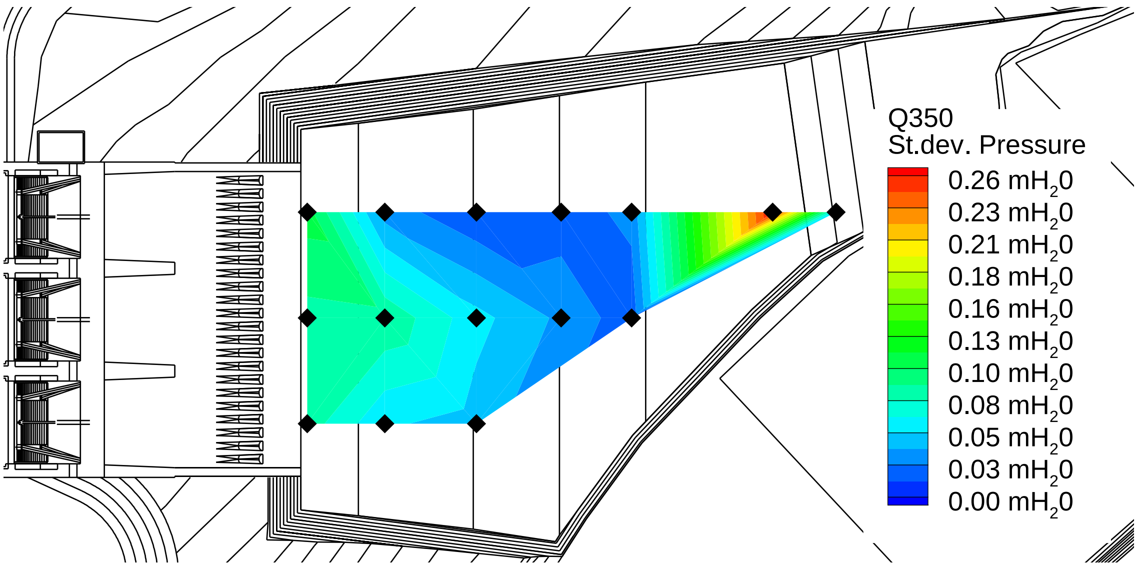

Figure 4.50: *Standard deviation of bottom pressure in the downstream channel for 350 m^3/s.*

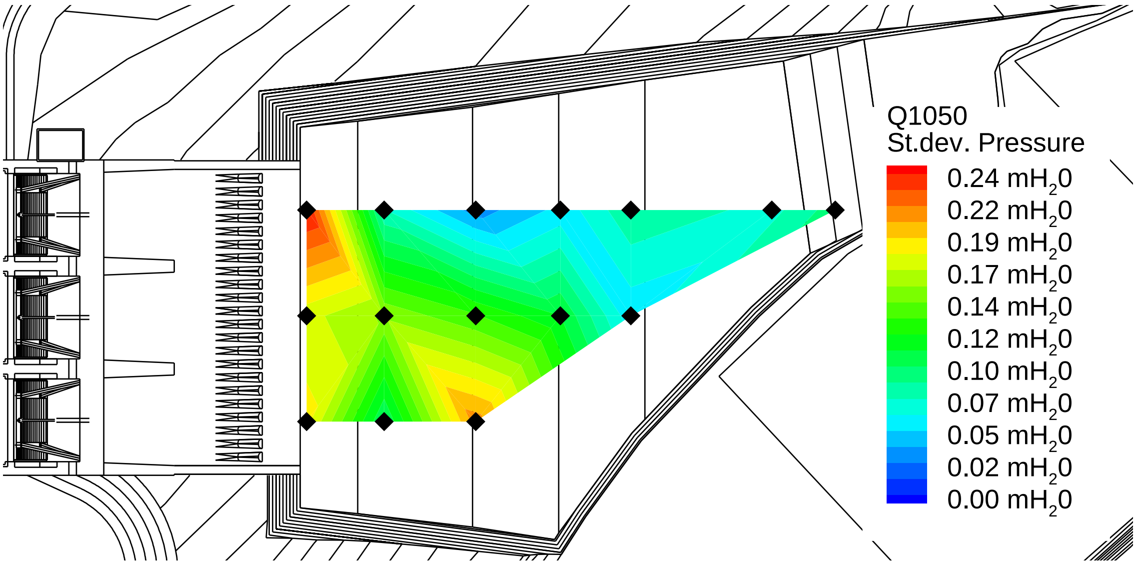

Figure 4.51: *Standard deviation of bottom pressure in the downstream channel for 1050 m^3/s.*

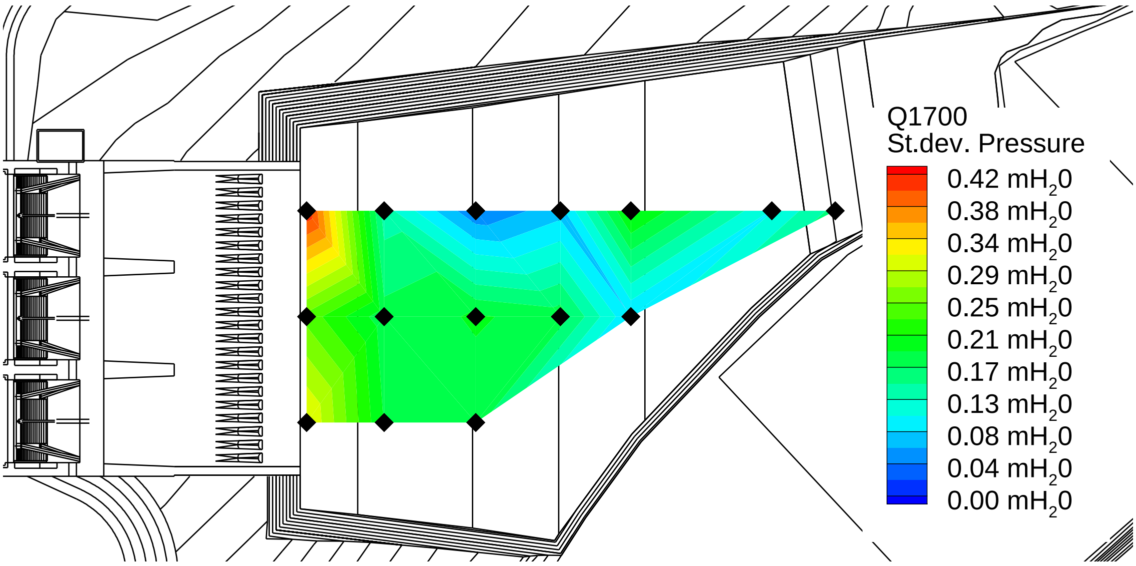

Figure 4.52: *Standard deviation of bottom pressure in the downstream channel for 1700 m^3/s.*

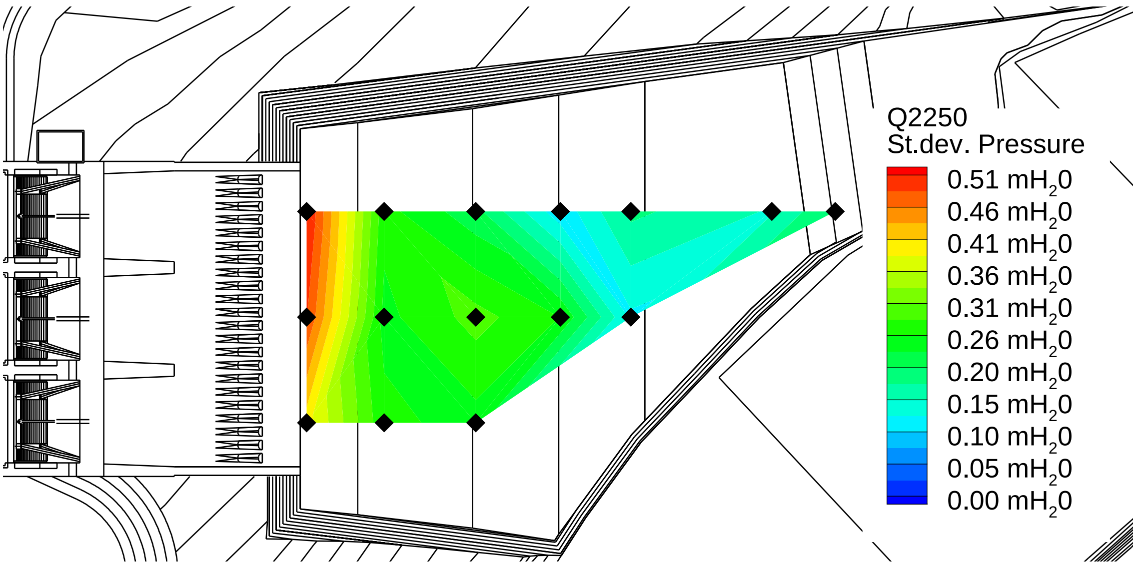

Figure 4.53: *Standard deviation of bottom pressure in the downstream channel for 2250 m^3/s.*

Pressure at the left side wall of the downstream channel was measured at six locations, three at elevation of 29.6 m a.s.l. and three at 32 m a.s.l. for four discharges, 350, 1050, 1700 and 2250 m^3/s. Measurements were made at stations 15, 25 and 35 m. Table 4.3 shows the standard deviation of the pressure measurements at the side wall of the downstream channel, the measurements are in mH_20. The standard deviation of the pressure measurements increases with increasing discharge as expected.

Table 4.3: *Standard deviation of pressure measurements at the left side wall of the downstream channel.*

Discharge	m^3/s	350		1050		1700		2250	
Elevation	m a.s.l.	29.6	32	29.6	32	29.6	32	29.6	32
St. 15	mH_20	0.05	0.08	0.11	0.16	0.16	0.15	0.20	0.18
St. 25	mH_20	0.05	0.06	0.11	0.15	0.16	0.20	0.28	0.26
St. 35	mH_20	0.04	0.05	0.10	0.12	0.16	0.18	0.50	0.31

Pressure at the end wall where the downstream channel and the riverbed meet was measured at two locations, both points are at elevation 30 m a.s.l., located 8 meters from the center line of the roller bucket (Y= $\pm$8 m, see Figure 4.32). The maximum and minimum fluctuation from the mean as well as the standard deviations are shown in Table 4.4.

Table 4.4: *Maximum and minimum fluctuation from the mean as well as standard deviation of pressure measurements at the end wall of the downstream channel.*

Discharge	m^3/s	350		1050		1700		2250	
Y	m	8	-8	8	-8	8	-8	8	-8
Max amp.	mH_20	0.12	0.09	0.40	0.31	0.55	0.40	0.93	0.61
Min amp.	mH_20	-0.07	-0.07	-0.30	-0.27	-0.66	-0.28	-0.74	-0.56
St.dev.	mH_20	0.02	0.02	0.07	0.07	0.13	0.10	0.21	0.14

4.6.4. Sensitivity to bucket elevation

Slotted roller bucket structures are sensitive to the tailwater elevation. With lower tailwater the energy of the incoming jet will be greater than the resistive energy of the tailwater, this can cause the bucket roller to leave the bucket yielding a *sweepout* condition. During sweepout conditions the roller bucket will thus form a high velocity ski-jump type jet. When the tailwater elevation is too great the energy of the incoming jet is weaker than the resistive energy of the tailwater, this can cause the incoming jet to dive from the bucket lip yielding a *diving flow* condition. With diving flow the flow may cause severe scouring of the downstream bed. When the downstream bed has become sufficiently scoured a bottom roller will be generated, lifting the flow to the water surface. The ground roller will move material down to the scouring pit causing the ground roller to reduce to the point where it will not divert the flow to the surface, causing the flow to dive again (Peterka 1958).

To simulate different tailwater elevations, the bucket invert was elevated 2 meters above the final design (final design has bucket invert at 26 m a.s.l.) and lowered 2 and 4 meters below the final design elevation. The performance of these four bucket invert elevations, 22, 24, 26 and 28 m a.s.l. are compared visually for four discharges 350, 1050, 1700 and 2250 m^3/s.

Figures 4.54 - 4.57 show the character of the system for different elevation of the bucket for 350 m^3/s, 1050 m^3/s, 1700m^3/s and 2250 m^3/s respectively.

For the elevations tested the character improves with increasing depth. The performance of the bucket for discharges of 1050 m^3/s and lower is satisfactory for all bucket elevations. For bucket elevation of 26 m a.s.l., the discharges of 1700 m^3/s and higher yield a marginally acceptable performance for a roller bucket where the bucket roller has mostly been substituted for a submerged jet, this also applies to 1700 m^3/s at bucket elevation of 28 m a.s.l. At 2250 m^3/s a sweepout occurred for bucket invert at 28 m a.s.l. as seen in Figure 4.57(d). This case can also be used to simulate a 2 meters scouring of the original riverbed. This condition indicates that the final design has less than 2 meters of margin to tailwater elevation and/or riverbed invert elevation.

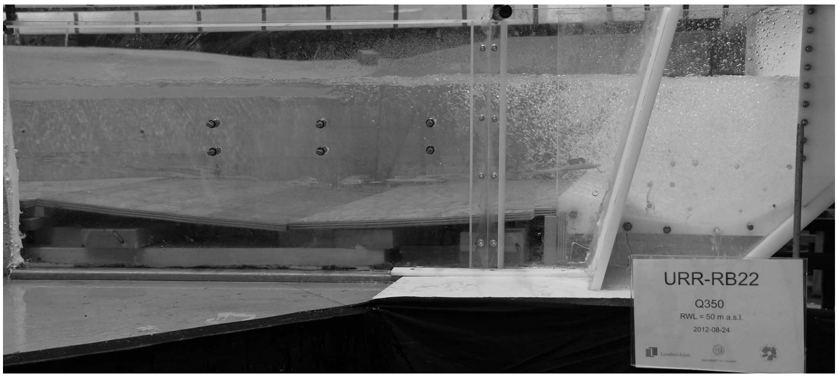

(a) Bucket elevation of 22 m a.s.l.

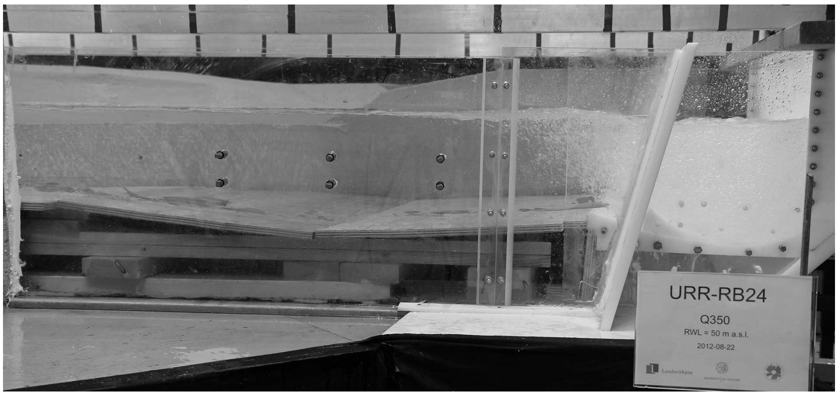

(b) Bucket elevation of 24 m a.s.l.

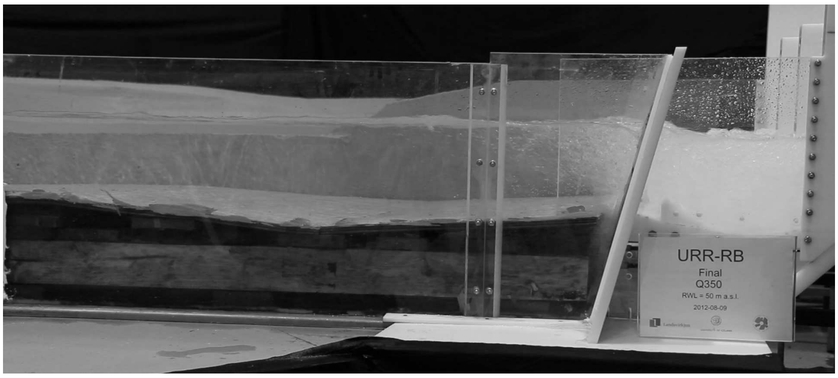

(c) Bucket elevation of 26 m a.s.l.

(d) Bucket elevation of 28 m a.s.l.

Figure 4.54: *Flow behaviour for different bucket invert elevations for 350 m^3/s.*

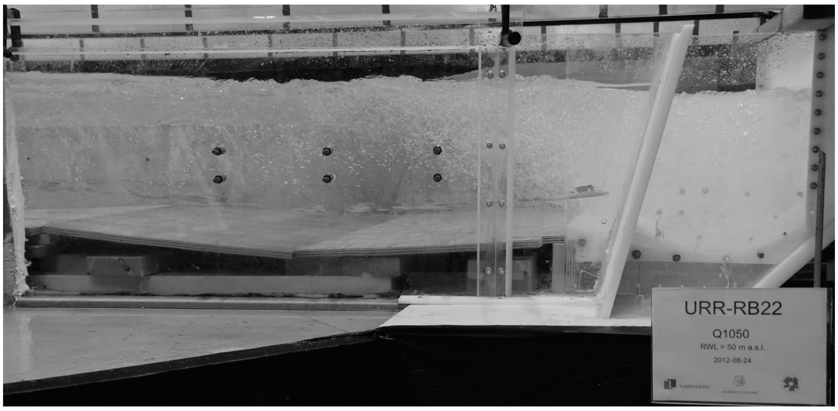

(a) Bucket elevation of 22 m a.s.l.

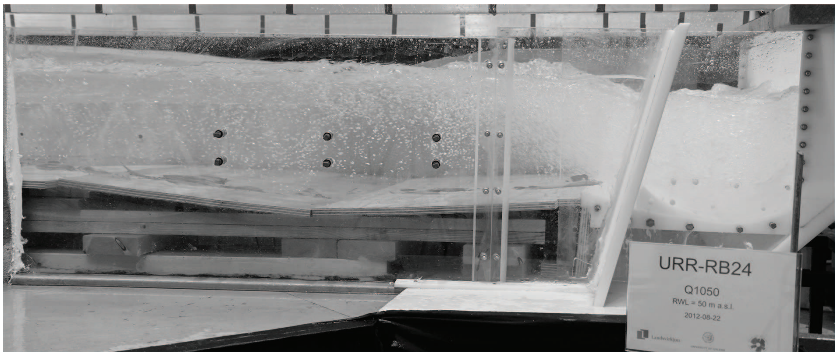

(b) Bucket elevation of 24 m a.s.l.

(c) Bucket elevation of 26 m a.s.l.

(d) Bucket elevation of 28 m a.s.l.

Figure 4.55: *Flow behaviour for different bucket invert elevations for 1050 m^3/s.*

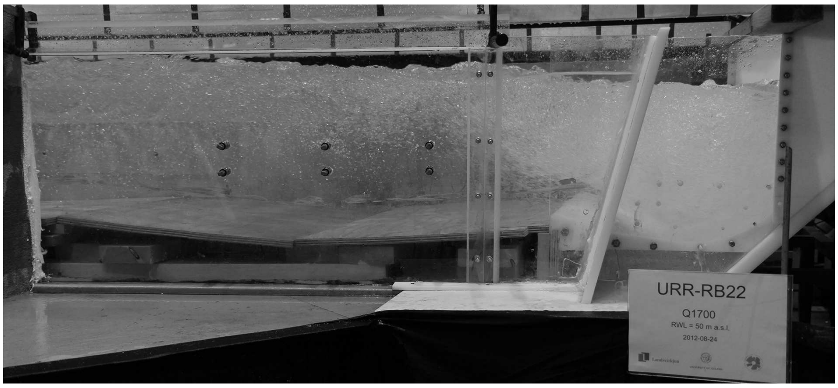

(a) Bucket elevation of 22 m a.s.l.

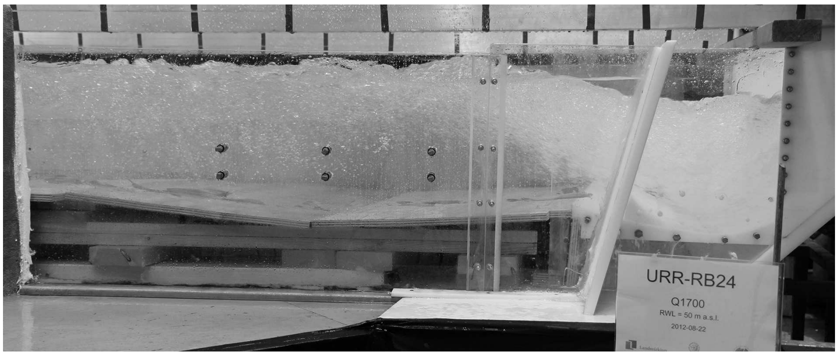

(b) Bucket elevation of 24 m a.s.l.

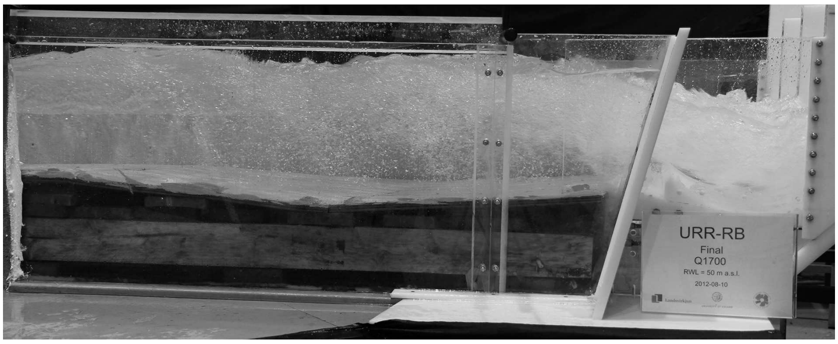

(c) Bucket elevation of 26 m a.s.l.

(d) Bucket elevation of 28 m a.s.l.

Figure 4.56: *Flow behaviour for different bucket invert elevations for 1700 m^3/s.*

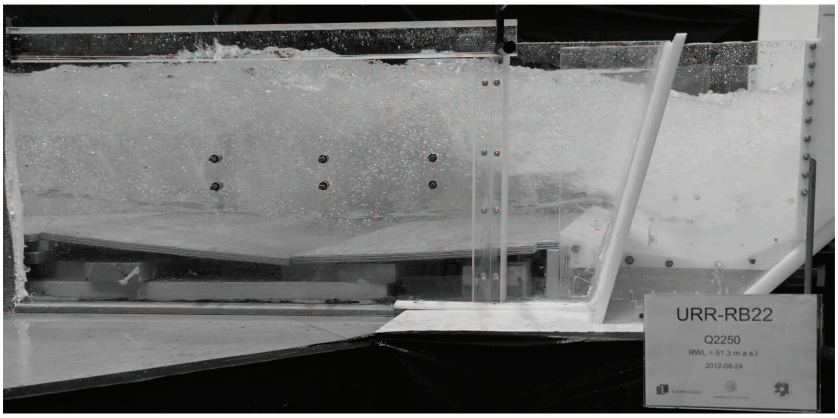

(a) Bucket elevation of 22 m a.s.l.

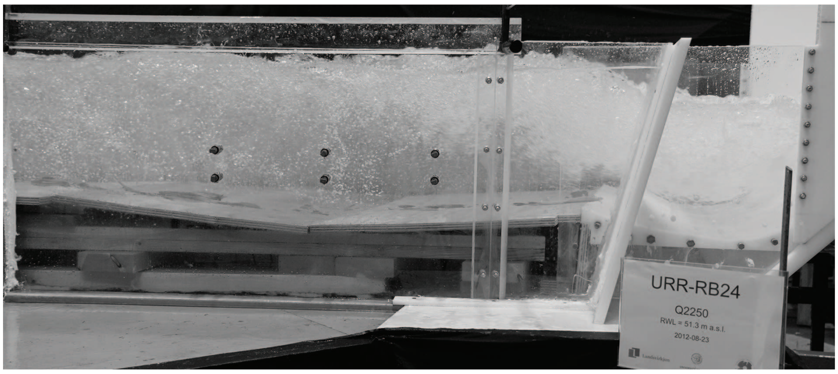

(b) Bucket elevation of 24 m a.s.l.

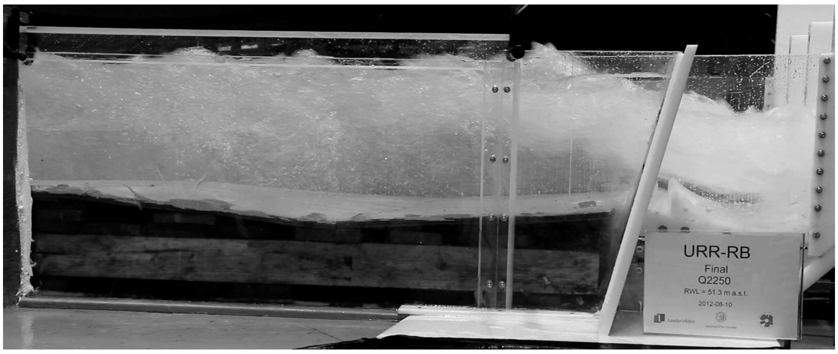

(c) Bucket elevation of 26 m a.s.l.

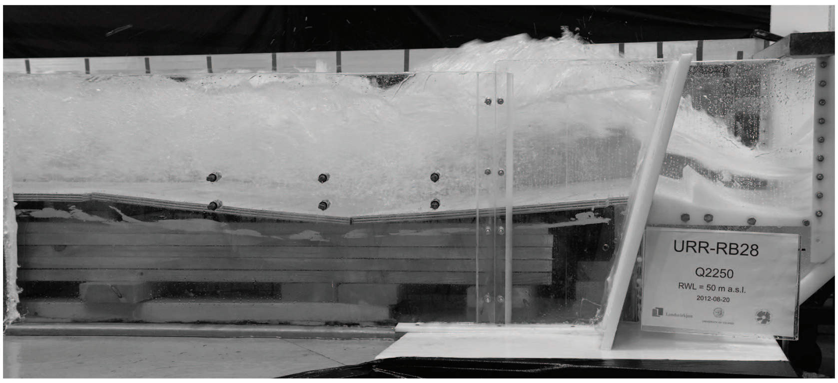

(d) Bucket elevation of 28 m a.s.l.

Figure 4.57: *Flow behaviour for different bucket invert elevations for 2250* m^3/s.

4.7. Asymmetric operation

Due to unfavourable flow characteristics with asymmetric gate operation for medium to high discharges a special measurement series was conducted to assess and observe the effect of this operational scheme. The interlocked operation is the recommended operational method for the gated spillway. The other operational schemes result in asymmetric operation and are further described below. Determination of operation conditions and assessment of the hydraulic conditions is mainly done visually in the laboratory but additionally photos and videos were used for systematic documentation.

Table 4.5 shows the asymmetric cases that were tested. Gate operation is shown as closed, marked with X, or open, marked with the corresponding gate number (1,2 or 3). All cases were tested for pond elevation of 50 m a.s.l. (NWL). It is noted that the scheme for the cases tested is a modified version of that originally proposed in the measurement plan.

A total of 6 asymmetrical cases were tested for different discharges. Because of the asymmetry in the downstream channel all six cases need to be discussed individually. Observations are made in the roller bucket, the downstream channel and the river section. Figure 4.58 shows the naming convention for observation and description of the asymmetric flow.

Table 4.5: *Tested cases for the asymmetric operation study*

Discharge			Gate operation																	
			Case 1			Case 2			Case 3			Case 4			Case 5			Case 6*		
	700	m^3/s	X	X	X	X	X	X	X	X	X	1	2	X	1	X	3	X	2	3
	500	m^3/s	1	X	X	X	2	X	X	X	3	1	2	X	1	X	3	X	2	3
Q_{ave}	350	m^3/s	1	X	X	X	2	X	X	X	3	1	2	X	1	X	3	X	2	3
	200	m^3/s	1	X	X	X	2	X	X	X	3	1	2	X	1	X	3	X	2	3
Q_{min}	~100	m^3/s	1	X	X	X	2	X	X	X	3	X	X	X	X	X	X	X	X	X
Number of cases			4			4			4			4			4			4		

* Only visual observation, no documentation with videos or photos

- Interlocked operation: all three gates operated at the same gate opening

- Paired operation: any two gates operated at the same gate opening

- Single operation: any single gate operated at any gate opening

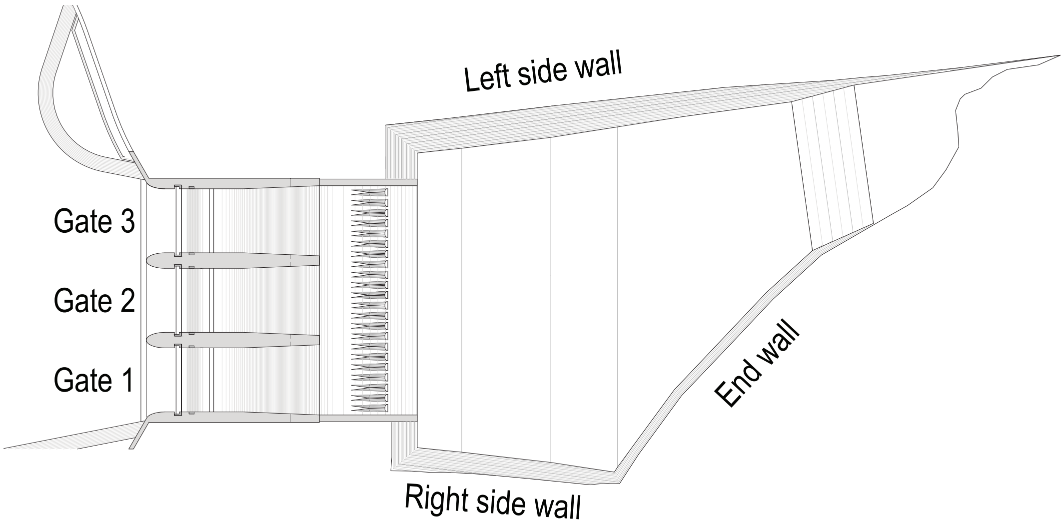

Figure 4.58: *Naming convention for observation description of the asymmetric flow.*

Single gate operation

When gate 1 is operated with gates 2 and 3 closed (case 1) a big anti-clockwise circulation is observed within the downstream channel. A small fluctuating hydraulic jump formed downstream of the end wall.

For gate 2 in single operation (case 2) a high velocity jet enters the downstream channel with circular movement on each side. A hydraulic jump is formed downstream of the end wall of the channel. A violent boiler is observed directly downstream of the bucket resulting in a very irregular surface inside the downstream channel.

For gate 3 in single operation (case 3) a clockwise circulation is observed in the downstream channel. For larger discharges (>350 m^3/s) the circular movement causes water to re-enter to the downstream channel near the right side wall. A small fluctuating hydraulic jump forms downstream of the end wall.

This circular movement could lead to piling up of loose material towards the bucket lip or even being transported into the bucket. Loose material brought into the bucket while in asymmetric operation could cause severe damage to the bucket invert or teeth as the asymmetric flow is not able to clear the loose material out of the bucket.

Figure 4.59 shows a schematic figure of the behaviour of the system for these operational cases. Tables 4.6 - 4.8 describe the behaviour for different discharges for cases 1, 2 and 3, respectively.

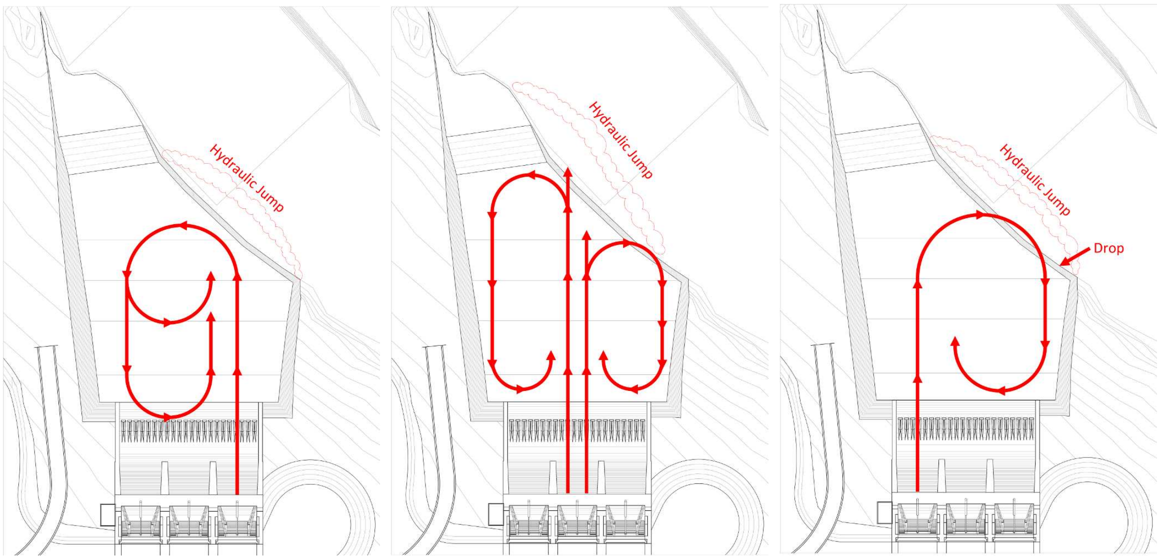

Figure 4.59: *Single gate operation (from left to right: case 1, case 2 and case 3).*

Table 4.6: *Description of single gate operation for case 1.*

Discharge	Description of case 1
100 m^3/s	Slow circular movement is observed in the excavated channel. Weak hydraulic jump is observed downstream of the end wall of the channel, the jump is non-uniformly distributed over the cross section.
200 m^3/s	Circular movement is observed in the excavated channel. Hydraulic jump downstream of the end wall of the channel, the jump is non-uniformly distributed over the cross section. There is one jump on the right hand side and another are where the excavated channel is longer. The jump reaches more upstream the river than in previous case. The circular movement has a tiny drawdown in the middle of the circle.
350 m^3/s	Circular movement in the excavated channel. Hydraulic jump downstream of the end wall of the channel, the jump is non-uniformly distributed over the cross section. There is one jump on the right hand side and another where the excavated channel is longer. The circular movement has a rather deep drawdown in the middle of the circle. Inside the bucket there is a boiling surface that reaches out to the end wall of the excavated channel.
500 m^3/s	Similar to 350 m^3/s

Table 4.7: *Description of single gate operation for case 2.*

Discharge	Description of case 2
100 m^3/s	A weak jet extends from the bucket with a circular movement on each side. A weak hydraulic jump is formed downstream of the end wall of the channel, the jump is almost uniformly distributed over the cross section. Small boiling behaviour is observed in the bucket.
200 m^3/s	A jet extends from the gate with a circular movement on each side. A hydraulic jump is formed downstream of the end wall of the channel, the jump is almost uniformly distributed over the cross section. Small boiling behaviour is observed in the bucket.
350 m^3/s	A jet extends from the gate with a circular movement on each side. A hydraulic jump is formed downstream of the end wall of the channel, the jump is almost uniformly distributed over the cross section. Boiling behaviour is observed in the bucket and a short distance downstream of the bucket. Surface inside the excavated channel is irregular.
500 m^3/s	Similar to 350 m^3/s.

Table 4.8: *Description of single gate operation for case 3.*

Discharge	Description of case 3
100 m^3/s	Slow circular movement in the excavated channel. Small and weak hydraulic jump is observed downstream of the end wall of the channel, the jump is non-uniformly distributed over the cross section.
200 m^3/s	Circular movement in the excavated channel. Hydraulic jump is formed downstream of the end wall of the channel, the jump is non-uniformly distributed over the cross section and the supercritical section downstream of the end wall reaches a little bit further than before. The jump reaches more upstream the river than in previous case. The circular movement has a small drawdown in the middle of the circle.
350 m^3/s	Circular movement in the excavated channel. Hydraulic jump is formed downstream of the end wall of the channel, the jump is non-uniformly distributed over the cross section. The circular movement has a drawdown in the middle of the circle. Water is drawn into the excavated channel from the upstream river section due to the drawdown from the circular movement.
500 m^3/s	Similar to 350 m^3/s with deeper drawdown and increased flow of returning water into the downstream channel.

Paired gate operation

When gates 1 and 2 are operated with gate 3 closed (case 4) a circular movement is observed near the left side wall of the downstream channel. A hydraulic jump is formed downstream of the end wall of the channel. The circular movement breaks up inside the bucket.

When gate 1 and 3 are operated with gate 2 closed (case 5) two jets extendes from the gates with circular movement in between the jets, the circular movement breaks up inside the middle of the bucket. A weak hydraulic jump is formed directly downstream of the end wall of the channel

When gate 2 and 3 are operated with gate 1 closed (case 6) the behaviour of the system is similar to that described in case 4, the main difference being that for larger discharges the drawdown from the circular movement causes the water to flow back into the downstream channel as described for case 3 in the single gate operation.

The circular movement, breaking up inside the bucket, could cause loose material to be brought into the bucket yielding a possibly severe damage to the bucket invert or teeth as the asymmetric flow could not clear the loose material out of the bucket.

Figure 4.60 shows a schematic figure of the behaviour of the system for these operational cases. Tables 4.9 and 4.10 describe the behaviour for different discharges for case 4 and 5 respectively, case 6 has similar behaviour as case 4.

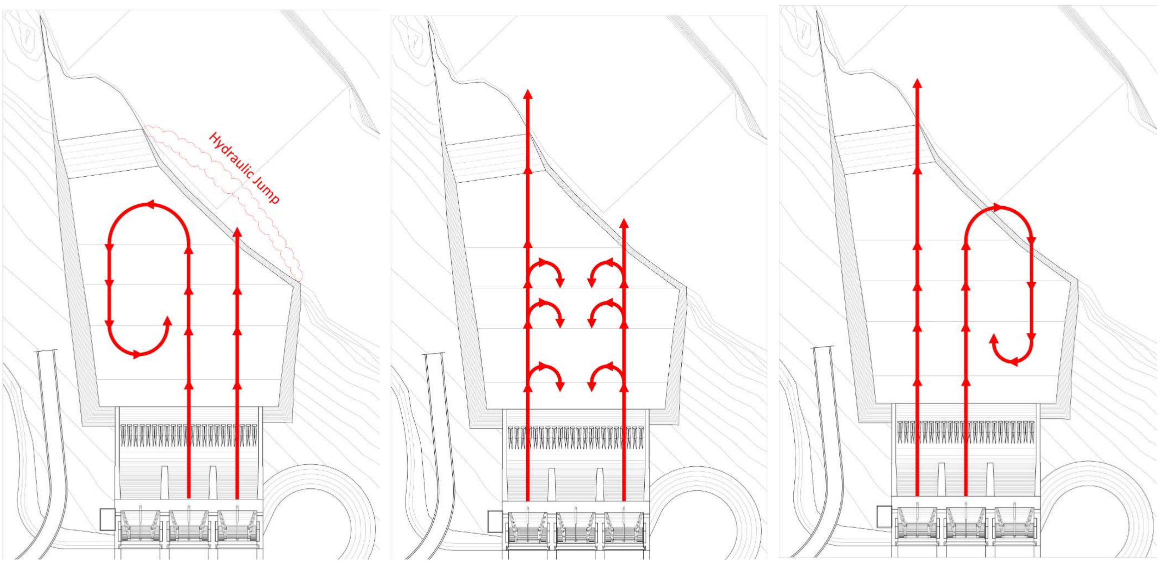

Figure 4.60: *Paired gate operation (from left to right: case 4, case 5 and case 6).*

Table 4.9: *Description of paired gate operation for case 4.*

Discharge	Description of case 4
200 m^3/s	Circular movement in the left side of the excavated channel. Hydraulic jump forms downstream of the end wall of the channel, the jump is quite uniformly distributed over the cross section.
350 m^3/s	Circular movement in the left side of the excavated channel with tiny drawdown in its center. Hydraulic jump is formed downstream of the end wall of the channel, the jump is quite uniformly distributed over the cross section.
500 m^3/s	Circular movement in the left side of the excavated channel with small drawdown in its center. Hydraulic jump is formed downstream of the end wall of the channel, the jump is quite uniformly distributed over the cross section. The circular movement breaks up inside the bucket.
700 m^3/s	Similar to 500 m^3/s with more drawdown, some indication of returning water near the right side wall.

Table 4.10: *Description of paired gate operation for case 5.*

Discharge	Description of case 5
200 m^3/s	Two jets extend from the gates with some circular movement in between them heading towards the bucket. The circular movement breaks up inside the bucket. Hydraulic jump is formed downstream of the end wall of the channel, the jump is quite uniformly distributed over the cross section.
350 m^3/s	Two jets extend from the gates with some circular movement in between them heading towards the bucket. The circular movement breaks up inside the bucket. Hydraulic jump forms downstream of the end wall of the channel, the jump is quite uniformly distributed over the cross section.
500 m^3/s	Two jets extend from the gates with some circular movement in between them heading towards the bucket. The circular movement breaks up inside the bucket. Weak hydraulic jump forms downstream of the end wall of the channel, the jump is quite uniformly distributed over the cross section. On the right hand side the hydraulic jump is very unstable and fluctuating.
700 m^3/s	Two jets extend from the gates with some circular movement in between them heading towards the bucket. The circular movement breaks up inside the bucket and forms a boiling surface in line with the middle gate. Irregularities are observed directly downstream of the end wall (where the hydraulic jump was before, the hydraulic jump is gone).

4.8. Summary

The previous sections present the results from measurements of the approach flow conditions, the spillway capacity, the roller bucket performance and the conditions in the downstream channel and the river section. This is summarized as follows:

Approach flow and capacity

- The approach flow to the spillway is acceptable with no observed abnormalities that limit the capacity of the spillway or pose a threat to the structure. The maximum velocity in the approach channel is about 3.7 m/s at 2250 m^3/s.
- The spillway capacity is sufficient, both the Q_{50} and the Q_{1000} pass through the spillway with pond levels lower than required.
- Increasing the elevation directly upstream of the crest of the spillway results in a poorer performance with regards to spillway capacity. Based on these results it is recommended that the area directly upstream of the spillway crest at Hvammur be lowered to increase the spillway capacity.

Roller bucket and downstream conditions

- All discharges tested pass without sweepout or diving flow for the Final design, indicating a sufficient tailwater level.
- For the Final design, the roller bucket performance is satisfactory for discharges up to 1300 - 1700 m^3/s after which the roller behaviour has mostly been substituted by a submerged jet characteristics. For higher discharges the roller bucket performance is marginally acceptable. Lower bucket elevation, 22 or 24 m a.s.l., result in improved flow conditions.
- For bucket elevation of 28 m a.s.l. (2 m increase from final design) a sweep out occurs for Q_{1000}, indicating a near sweep out limit for the Final design. Lowering of the bucket invert elevation to 25 m a.s.l. is recommended to further prevent sweep out, improve the performance of the bucket and the overall flow condition.
- Acceptable conditions in the river section and the downstream channel are observed for all discharges tested.
- At 2250 m^3/s the maximum measured velocity in the downstream channel is about 6.6 m/s and the average velocity in the downstream channel is about 3.3 m/s.
- A weak ground roller is formed immediately downstream of the bucket for lower discharges but is less evident for higher discharges.

Asymmetric gate operation

- Paired gate operation is in general not recommended. The asymmetric flow will result in returning water flowing towards the bucket which could bring loose material into the bucket and possibly cause damage to the bucket invert or bucket teeth.

- If single gate operation can not be avoided due to maintenance or malfunctions of other gates, operation of gate 2 is advised. Operation of a single gate should be limited to discharges less than 200 m^3/s.

5. Intake and SFO final design

The investigation presented in this chapter is focused on describing approach flow conditions and SFO performance for a wide range of operational schemes for Urriðafoss HEP. In the approach flow channel, the characteristics of the flow are described and quantified by velocity measurements, particle tests and visual observations. Abnormalities such as vortex zones and stagnant velocity zones which can lead juvenile salmon off course and away from the SFO were located and documented. The discharge capacity of the SFO was measured. The streamline separation immediately upstream of the SFO crest and quantification of the surface layer transported by the SFO were estimated by a dye test. The following zones were defined:

i) Approach zone

ii) Discovery zone

iii) Decision zone

The zones relate to fish behaviour and flow characteristics in a reservoir. Further clarification of the zones is presented in (Ágúst Guðmundsson & Garðarsson 2011). Measurement and observation methods used to describe and quantify characteristics relating to fish passage in the system are listed in the following sections. The design criteria for the SFO are summarized by the designers (Káradottir & Guðjónsson 2012):

Design criteria:

- the main surface current within the approach zone should be towards the SFO
- the SFO intake geometry is determined by the extends (width and depth) of the main surface current which is needed to ensure that all water within the discovery and decision zone from the surface to a depth of 1 m is bypassed by the SFO.
- the flow towards the SFO should be equally distributed, with a positive acceleration with a maximum value of 1 m/s^2 within the decision zone.
- the flow velocity 0 - 1 m upstream of the SFO crest is not less than 2.5 m/s
- no irregularities and zero flow velocity zones should be apparent where the juvenile fish could be trapped
- juvenile fish that has entered the SFO should not be capable of returning to the reservoir
- equally distributed water velocity within the SFO

- free surface flow within the SFO
- no blocks or sharp edges within the SFO which could damage the juvenile fish

Table 5.1 gives an overview of the cases in the final design measurement program for the intake and associated surface outlet flow (SFO) structure. Investigations were mostly focused on Cases 1.1 to 1.5 (see (Káradottir & Guðjónsson 2012)) as they represented the normal operating conditions of the structures.

The cases in Table 5.1 have the following definition and are further discussed in (Káradottir & Guðjónsson 2012):

1.1-1.5 Normal operating conditions of the structures

2.1-2.3 Power Plant inoperable, spillway and SFO operational

3.1-3.2 Reservoir water level $<$ NWL and power plant operable

4.1-4.2 SFO closed, intake operable

Table 5.1: *Overview of the cases. Columns 6 to 9 show the type of documentation made for each test case*

Case	RWL [m a.s.l.]	Q_{Intake} [m^3/s]	$Q_{Spillway}$ [m^3/s]	Q_{SFO} [m^3/s]	Q_{Total} [m^3/s]	% Time of Q => Q_{Total}**	Particle test	Velocity distri bution	Docu ment ation	Dye test
1.1	50.2*	240	0	40	280	99.9	x	x	x	x
1.2	50.2*	370	0	40	410	41	x	x	x	x
1.3	50.2*	370	70	40	480	25	x	x	x	x
1.4	50.2*	370	235	40	645	5	x	x	x	x
1.4 SG	50.2*	370	235***	40	645	5	x	x	x	x
1.5	50.2*	370	515	40	925	0.1	x	x	x	x
2.1	50.2*	0	260	40	300	95	x	-	x	-
2.2	50.2*	0	335	40	375	50	x	-	x	-
2.3	50.2*	0	605	40	645	5	x	-	x	-
3.1	49.9	260	0	20	280	99.9	x	x	x	x
3.2	49.9	370	0	20	390	46	x	x	x	x
4.1	50.2*	370	0	0	370	53	-	-	x	-
4.2	50.2*	370	270	0	640	5	-	-	x	-

* The required discharge capacity of the SFO is not met for NWL (50.0 m a.s.l.) but by operating the reservoir at 50.2 m .a.s.l. the design discharge for the SFO is fulfilled. See further discussion in Section 5.5.
** Percentage of time with equal or more discharge, (Káradottir & Guðjónsson 2012).
*** Spillway discharge routed through a single gate, gate 3.

5.1. Description of Intake Final Design for Urriðafoss HEP

The scope of the study conducted by the physical modelling of the intake and SFO structure at Urriðafoss HEP is to verify the general design criteria set forth in (Káradottir & Guðjónsson 2012). The final design layout for Urriðafoss HEP and detailed drawings of the intake and Surface Flow Outlet (SFO) type juvenile fish bypass structure are shown in Figures 5.1 and 5.2.

The Heiðarlón Pond is formed by a dam crossing the river at Heiðartangi point and dykes along the west banks of the river. The spillway and the intake structures are located at Heiðartangi point. In general, the overall layout of the approach flow channel, the intake to the powerhouse and a SFO type juvenile bypass structure are under investigation. The elements investigated and relevant to this study are as follows (numbers refer to Figure 5.1):

– (1) the original river bed of Þjórsá River upstream of the dam

– (2) the excavated Approach Flow Channel (AFC) for the spillway and intake. The AFC invert slopes towards the spillway from an elevation of 41 m a.s.l. to 37 m a.s.l. in front of the spillway. It is an approximately 120 m wide channel, excavated in an arch shape, starting at the original riverbank approximately 200 m upstream of the spillway crest. The sides of the channel have a steep 4:1 (vertical:horizontal) slope. At the right side of the channel (looking downstream) the side walls reach an elevation of 49 m a.s.l. From 49 m a.s.l. the fuse plug and dykes start to rise above the right approach bank and continue to elevations of 51.8 m a.s.l. and 53.5 m a.s.l. respectively.

– (3) the excavated AFC for the intake and SFO structure. The AFC slopes downward to the left of the main AFC towards the intake and SFO structure to an elevation of 31.5 m a.s.l. in front of the intake. On the right side of the channel, a curb, reaching an elevation 48 m a.s.l. separates the intake and spillway. The side walls of the channel are steep with 4:1 slopes.

- (4) the power intake and the SFO structure are shown in detail in Figure 5.2. The intake is a conventional structure with a SFO type juvenile bypass system incorporated at the top of the structure. The intake has four 5.95 m wide entrances, uniting in pairs, into two separate draft tubes. The design discharge for the intake is 370 m^3/s. The SFO has four 5.95 m wide entrances, each with a smooth rounded crest at an elevation of 49.1 m a.s.l., providing an estimated discharge of 40 m^3/s at Normal Water Level (NWL) is 50 m a.s.l. From the crest the water from the four entrances is united in a single sideway channel and routed through a 4.5 m wide concrete channel to the original riverbed downstream of the dam.

- (5) a gated spillway with three radial gates for reservoir regulation and flood passing. The spillway has three 12 by 10 m radial gates (width x height). The spillway crest is at an elevation of 41 m a.s.l.

- (6) a fuse plug with crest elevation at 51.8 m a.s.l. to pass larger floods than Q_{1000}.

- (7) an upstream fishway to aid the migration of salmon up the river.

- (8) a mandatory release structure which provides constant discharge of 10 m^3/s to the riverbed downstream of the dam.

- (9) Urriðafoss Dam forming Heiðarlón Pond.

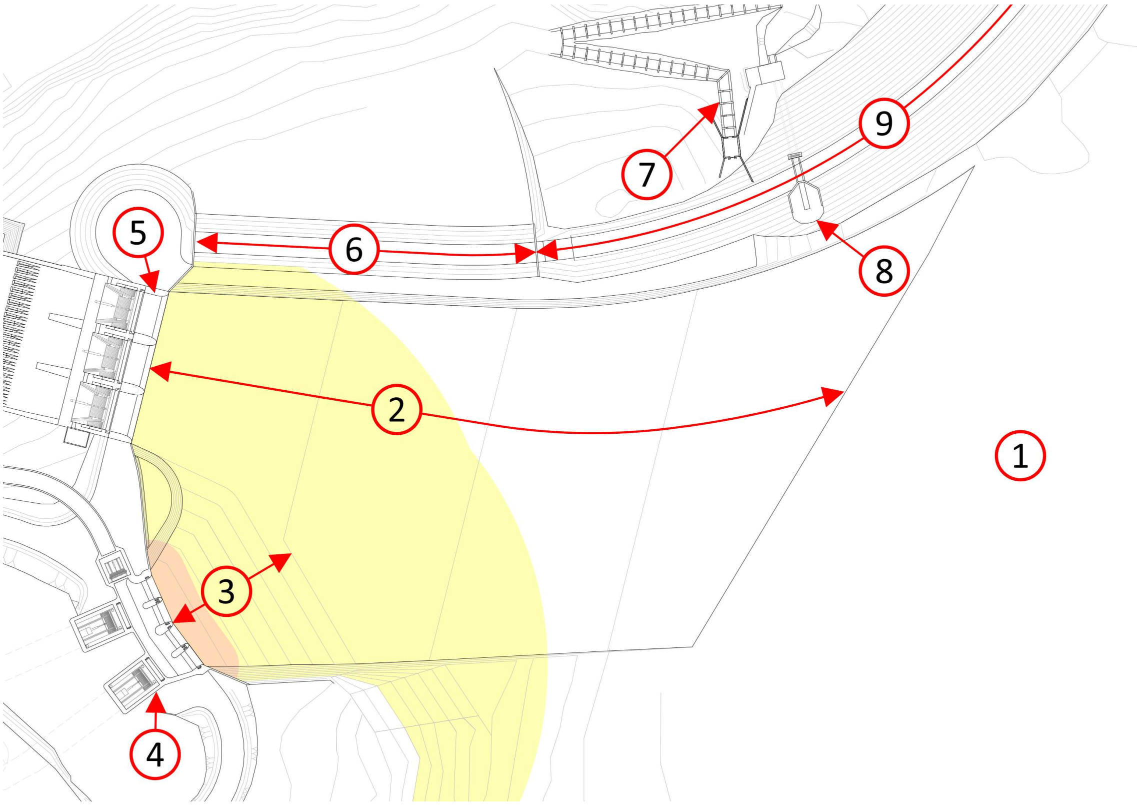

Figure 5.1: *Overview of the Urriðafoss HEP final design: (1) the original riverbed, (2) the spillway approach flow channel, (3) the intake and SFO approach flow channel, (4) the intake to the power house and SFO structure, (5) the spillway structure, (6) the fuse plug, (7) the upstream fishway, (8) the mandatory release structure, (9) Urriðafoss dam. Discovery zone shown in yellow and decision zone shown in orange.*

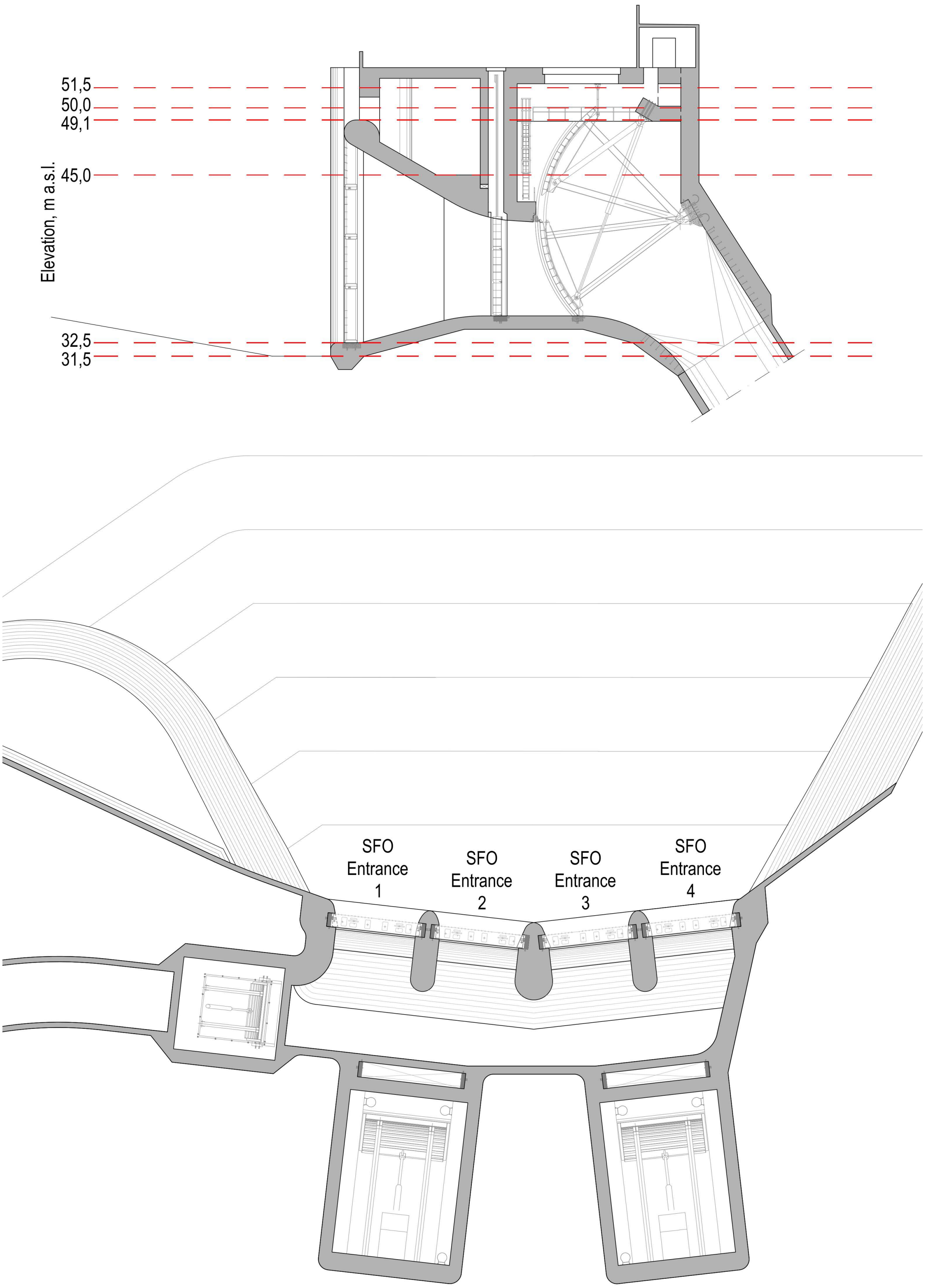

Figure 5.2: *Top view and longitudinal section of intake and SFO structure*

5.2. Particle Tests

Particle tests were conducted for eleven cases which represent a variety of operational conditions where SFO operation is included. Key parameters for all cases tested are listed in Table 5.1.

Figure 5.3 shows the results for Case 1.2 which represents conditions for normal operation, Q_{Intake} = 370 m^3/s, Q_{SFO} = 40 m^3/s and $Q_{Spillway}$ = 0. In Figure 5.3 the extent of the attraction flow is observed, most of the approach channel flow is drawn towards the intake and SFO. Two zones of irregularities are observed, labelled stagnant zone and vortex zone in the figure. The stagnant zone, located immediately upstream of spillway, is occupied by a slowly moving water body. Particles entering the zone may linger for some time until finally drawn towards the intake and the SFO. In the vortex zone, located by the Left Approach Bank (LAB), irregularities formed where different currents intersect with steady formation of small shallow vortices. The irregularities were formed by topographic features at the LAB and by the flow conditions at the LAB where the main current in the AFC and a current coming over the LAB intersect.

In Cases 1.1, 3.1 and 3.2 spillway discharge is zero as in Case 1.2. The general flow behaviour of the system for these cases is in accordance to the observed characteristics of Case 1.2. For cases where discharge to the intake is less than during normal operation, Cases 1.1 and 3.1, the main difference from Cases 1.2 and 3.2 is the overall reduction in velocity, i.e. the particles approached the intake and the SFO at a much slower pace. No distinct differences exist between Cases 1.2 and 3.2. Results of particle tests Cases 1.1, 3.1 and 3.2 are shown in Appendix H.

In Figure 5.4 the particle test results of Case 1.3 for operation with spillway, Q_{Intake} = 370 m^3/s, Q_{SFO} = 40 m^3/s and $Q_{Spillway}$ = 70 m^3/s. The figure shows that the spillway affects the approach flow conditions to the SFO. The large extent of the attraction flow in Case 1.2 heading towards the intake and SFO has been reduced. Water from the stagnant zone immediately upstream of the spillway is drawn towards the spillway. The irregularities at the LAB still exist.

In Cases 1.4. and 1.5 similar characteristics as in Case 1.3 are observed. The main difference is that with increased spillway discharge more water is drawn towards the spillway reducing the attraction flow zone. With increased discharge through the spillway the flow coming over the LAB extends farther into the main AFC towards the spillway. An extra case labelled Case 1.4 SG was requested by the designers. The case has the same set up as Case 1.4 with the exception of a single gated operation, i.e. all spillway discharge is routed through a single gate instead of three gated operation. The change to a single gate operation does not affect the flow conditions considerably as the flow drawn to the three gates in Case 1.4 is drawn to a single gate and the attraction flow has the same character as before. Results for particle tests for Cases 1.4, 1.4 SG and 1.5 are shown in Appendix H.

Figure 5.5 shows the particle test results for case 2.1, Q_{Intake} = 0 m^3/s, Q_{SFO} = 40 m^3/s and $Q_{Spillway}$ = 260 m^3/s. The figure shows that most of the approach flow is drawn towards the spillway and the SFO is only capable of transporting water from the decision zone (shown orange). No irregularities in the approach flow are observed.

Cases 2.2 and 2.3 show the same characteristic flow behavior as in Case 2.1 with the exception of irregularities forming at the left approach bank. Results of particle tests for Cases 2.2 and

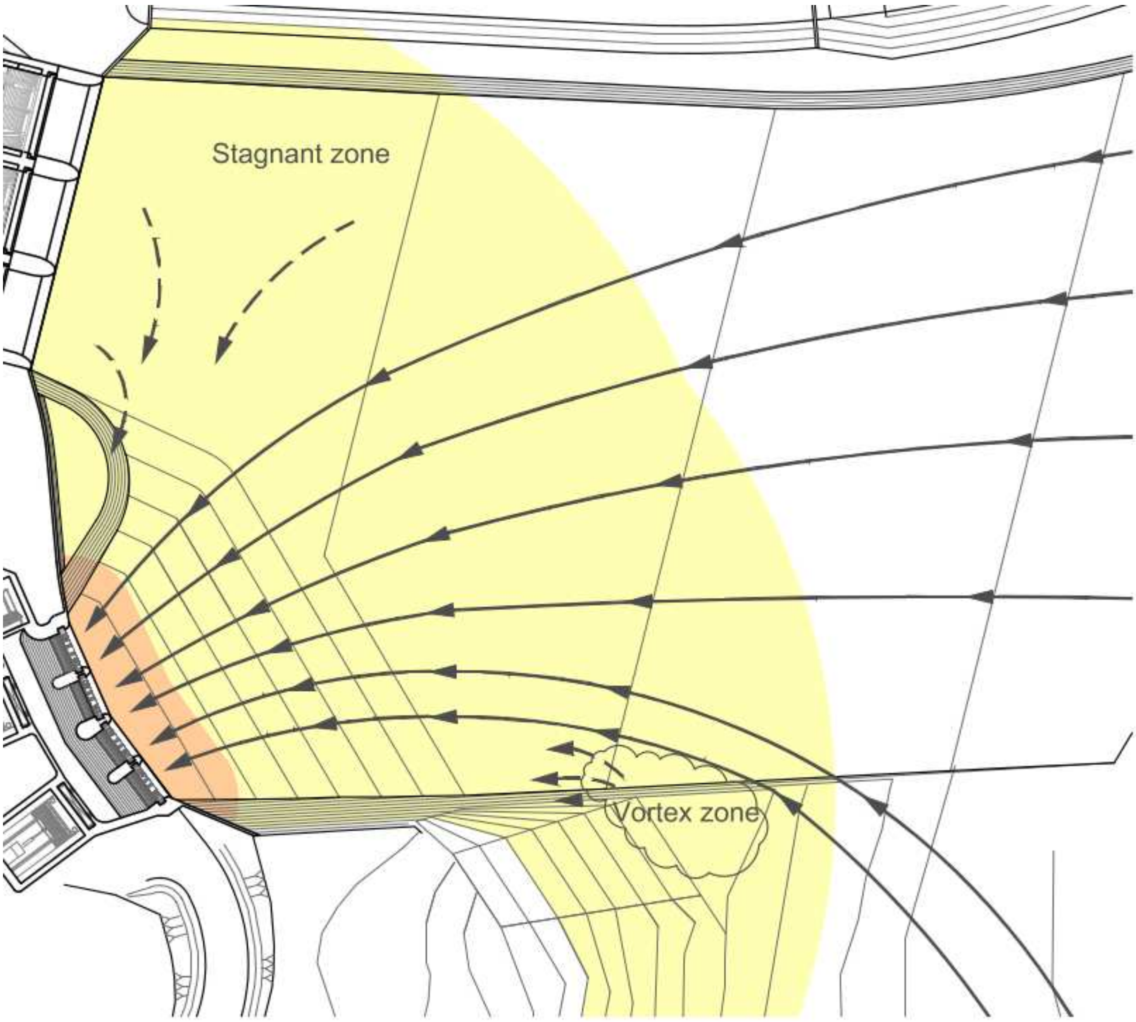

Figure 5.3: *Results from particle tests for Case 1.2., Q_{Intake} = 370 m^3/s, Q_{SFO} = 40 m^3/s and $Q_{Spillway}$ = 0 m^3/s. Lines with arrows represent general flow characteristics, the decision zone is shown in orange and the discovery zone in yellow.*

2.3 are shown in Appendix H.

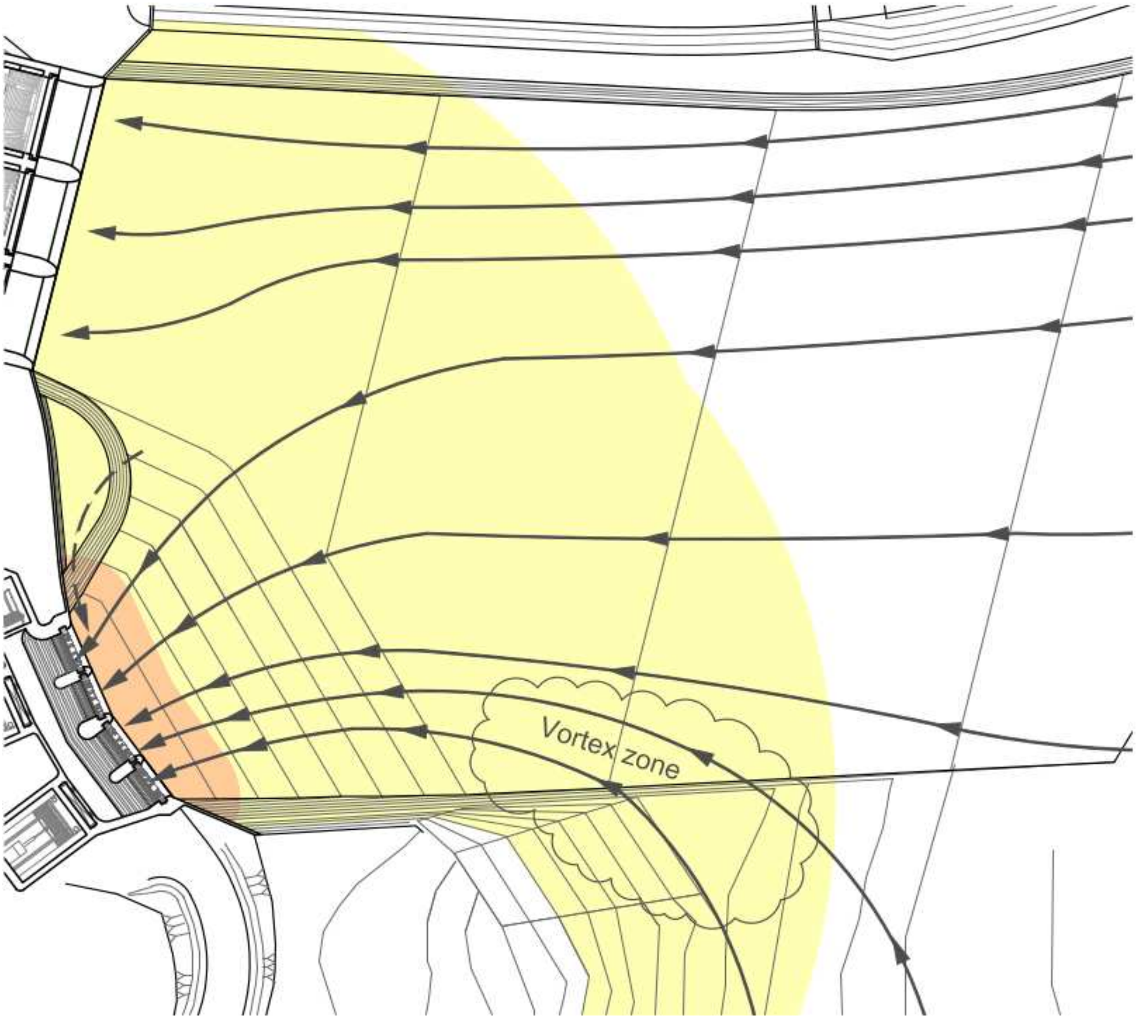

Figure 5.4: *Results from particle tests for Case 1.3., Q_{Intake} = 370 m^3/s, Q_{SFO} = 40 m^3/s and $Q_{Spillway}$ = 70 m^3/s. Lines with arrows represent general flow characteristics, the decision zone is shown in orange and the discovery zone in yellow.*

Figure 5.5: *Results from particle tests for Case 2.1., $Q_{Intake} = 0\ m^3/s$, $Q_{SFO} = 40\ m^3/s$ and $Q_{Spillway} = 260\ m^3/s$. Lines with arrows represent general flow characteristics, the decision zone is shown in orange and the discovery zone in yellow.*

5.3. Velocity Distribution

Velocity measurements were conducted for normal operational condition cases, Cases 1.1-1.5, and for cases where the reservoir water levels are below NWL, Cases 3.1 and 3.2. Key parameters for all cases are listed in Table 5.1.

Figure 5.6 shows the velocity distribution at 2.6 m depth, 47.6 m a.s.l. elevation, in the AFC for Case 1.1. A gradual increase in velocity of the attraction flow is observed with velocities taking maximum values around 0.4 m/s in front of the SFO. A stagnant velocity zone exists in front of the spillway reaching approximately 50 m upstream from spillway gate 2. A significant velocity component with direction perpendicular to the main approach flow current is observed at the LAB.

Figure 5.7 shows the velocity distribution at 2.6 m depth, 47.6 m a.s.l. elevation, in the AFC for Case 1.2. Compared to Case 1.1 shown in Figure 5.6 the increased discharge to the intake has the effect of increased approach flow velocity with the maximum value of 0.6 m/s immediately upstream of the intake. The increased discharge leads to more water getting drawn towards the intake and extends the attraction flow spatially which reduces the stagnant zone in front of the spillway. A significant velocity component at the LAB is observed as in Case 1.1, the component is similar in magnitude as in Case 1.1 but observed 20 m upstream from the previous location.

Figure 5.8 shows the velocity distribution in the AFC at 2.5 m depth, 47.7 m a.s.l. elevation, for case 1.3. In the figure the effect the spillway discharge has on the approach flow characteristics is evident. As before, velocity gradually increases towards the SFO and intake with maximum values being reached in front of the intake. The stagnant zone immediately upstream of the spillway has reduced considerably as water is drawn towards the spillway. The main current in the AFC is still directed towards the intake and SFO. As in Case 1.2, a significant velocity component is observed at the LAB with direction perpendicular to the main current in the approach flow channel.

Figure 5.9 shows the velocity distribution in the AFC at 2.5 m depth, 47.7 m a.s.l. elevation, for Case 1.4. In Case 1.4 the main current in the approach flow channel is divided between the spillway and intake with more water being drawn towards the intake and SFO. A high velocity zone at the center of the AFC is observed. As the current divides closer to the spillway and intake the velocity reduces but increases again immediately upstream of the intake and spillway. As before a significant velocity component is observed at the LAB with direction perpendicular to the main current. The component has increased in magnitude from Case 1.3.

Figure 5.10 shows velocity distribution in the AFC at 3 m depth, 47.2 m a.s.l., for Case 1.4 SG. Spillway discharge is routed through a single gate, gate 3. The approach flow character is almost identical to Case 1.4 except for water in front of the spillway structure being only drawn towards gate 3. A small stagnant velocity zone forms immediately upstream of gate 1.

Figure 5.11 shows velocity distribution in the AFC at 2.5 m depth, 47.7 m a.s.l. elevation, for Case 1.5. For this case more water is drawn towards the spillway with the flow being more directly divided between the intake and spillway. A high velocity zone is observed in the center of the approach flow channel with velocities reducing considerably in front of the intake and SFO. The high velocity zone extends towards the spillway with minimal decrease in velocity. The velocity takes a maximum value at the LAB as in Cases 1.3 and 1.4 with direction perpendicular to the main current in the approach channel.

Figure 5.12 shows velocity distribution in the AFC for Case 3.1 at 3 m depth, 46.9 m a.s.l. elevation. The case represents conditions when reservoir level is lower than NWL, 49.9 m a.s.l. The velocity distribution for Case 3.1 is nearly identical to Case 1.1 shown in Figure 5.6. The lowered reservoir water level does not seem to affect the characteristic of the flow in the AFC.

Figure 5.13 shows velocity distribution in the AFC for Case 3.2 at 3 m depth, 46.9 m a.s.l. elevation. The case represents conditions when reservoir level is lower than NWL, 49.9 m a.s.l. The velocity distribution for Case 3.2 is nearly identical to Case 1.2 shown in Figure 5.7. The lowered water level elevation does not seem to affect the characteristic of the flow in the AFC.

Figures 5.6 to 5.13 are shown with synchronized contour levels in Appendix I.

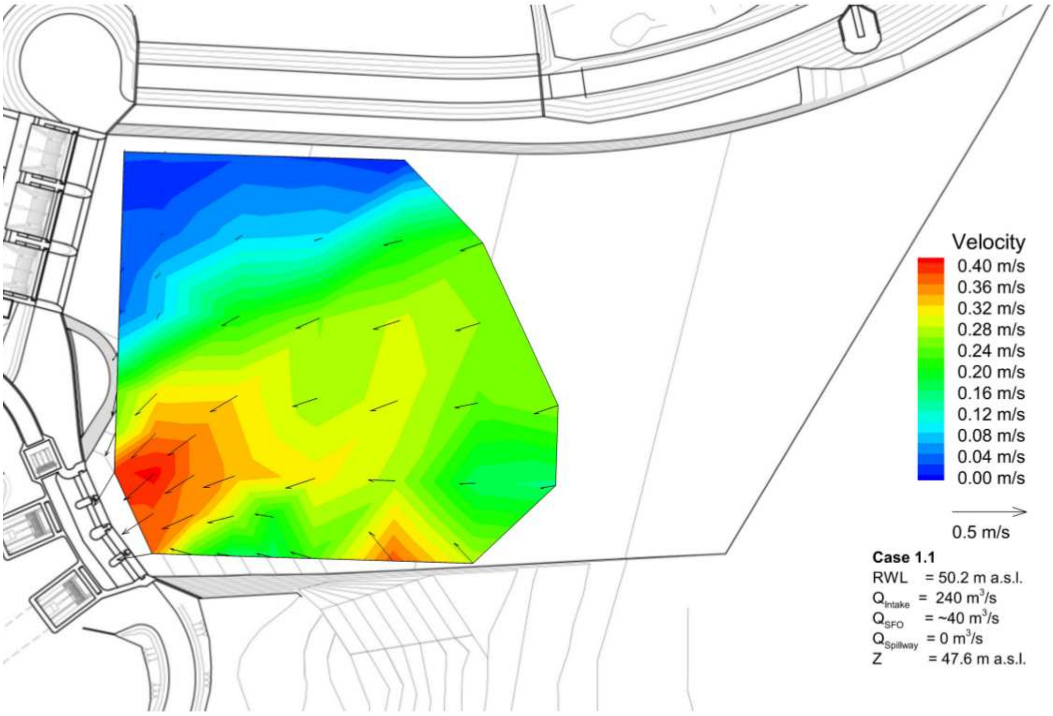

Figure 5.6: *Velocity distribution in the approach flow channel for Case 1.1, $Q_{Intake} = 240$ m^3/s, $Q_{SFO} = 40$ m^3/s and $Q_{Spillway} = 0$ m^3/s. (Note that contour levels are not synchronized between Figures 5.6-5.13)*

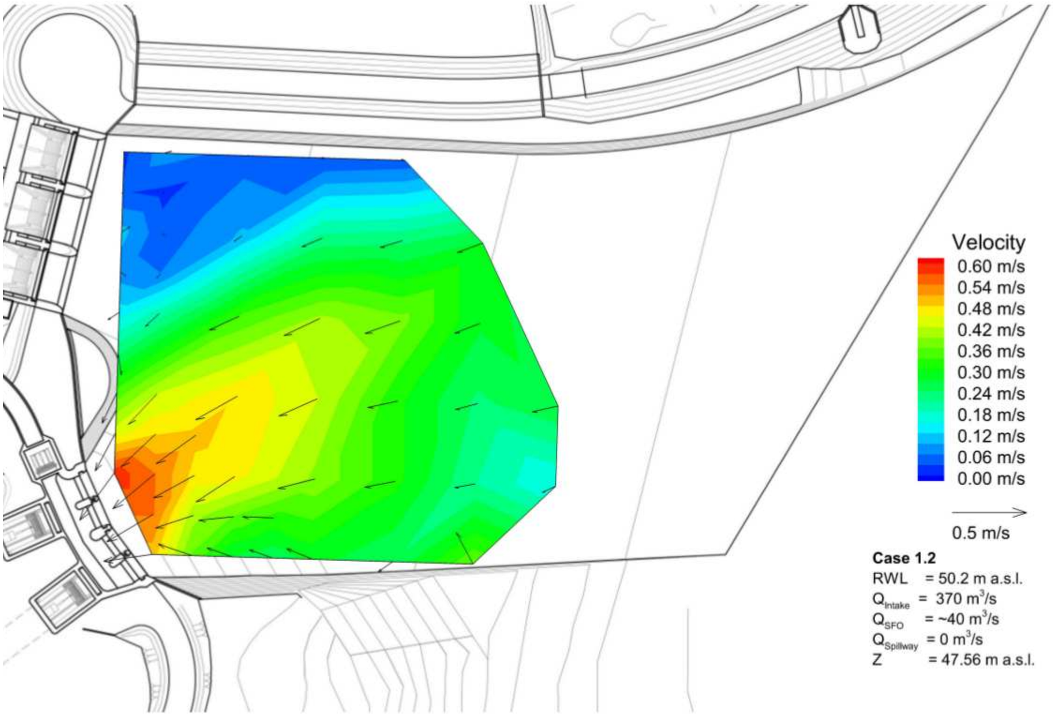

Figure 5.7: *Velocity distribution in the approach flow channel for Case 1.2, $Q_{Intake} = 370$ m^3/s, $Q_{SFO} = 40$ m^3/s and $Q_{Spillway} = 0$ m^3/s. (Note that contour levels are not synchronized between Figures 5.6-5.13)*

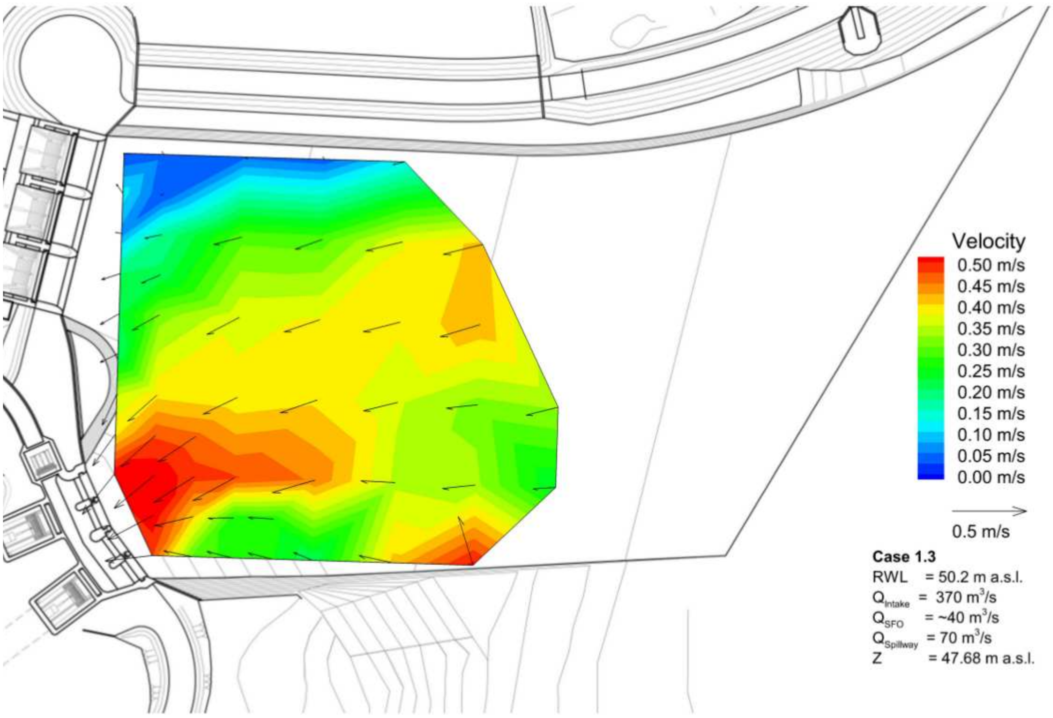

Figure 5.8: *Velocity distribution in the approach flow channel for Case 1.3, $Q_{Intake} = 370$ m^3/s, $Q_{SFO} = 40$ m^3/s and $Q_{Spillway} = 70$ m^3/s. (Note that contour levels are not synchronized between Figures 5.6-5.13)*

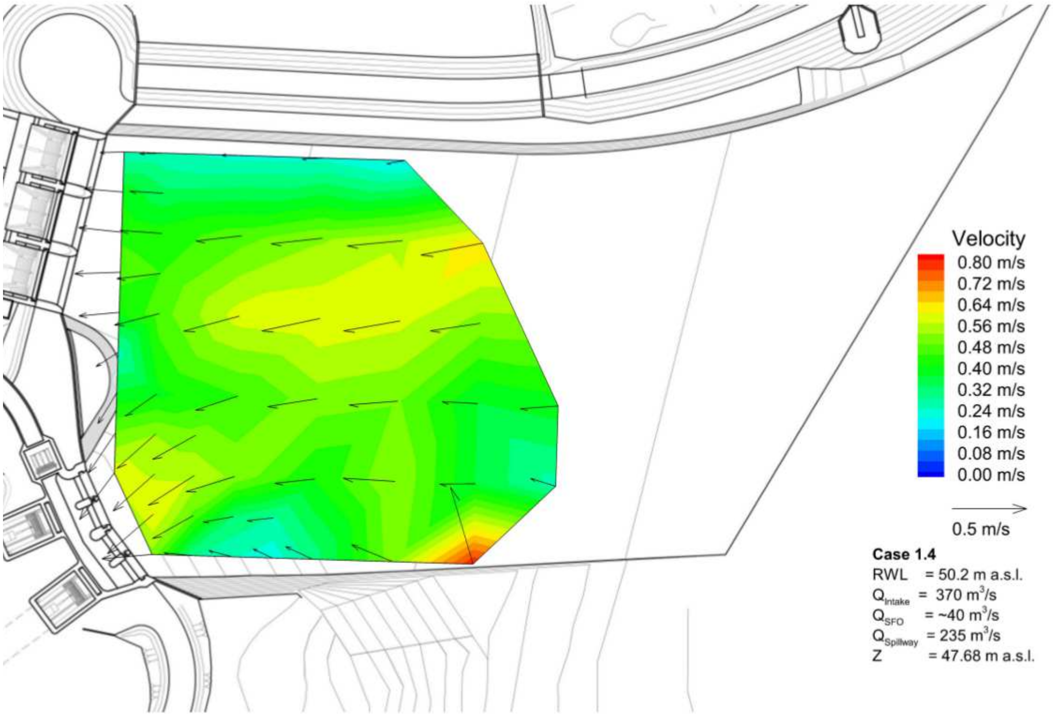

Figure 5.9: *Velocity distribution in the approach flow channel for Case 1.4, Q_{Intake} = 370 m^3/s, Q_{SFO} = 40 m^3/s and $Q_{Spillway}$ = 235 m^3/s. (Note that contour levels are not synchronized between Figures 5.6-5.13)*

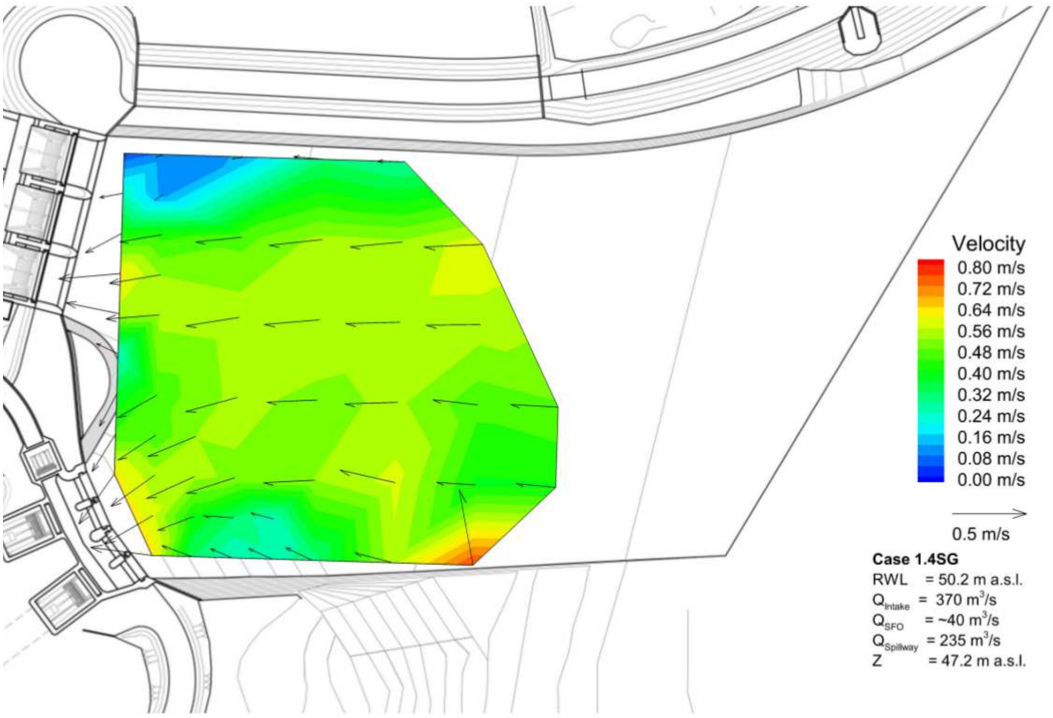

Figure 5.10: *Velocity distribution in the approach flow channel for Case 1.4 SG, Q_{Intake} = 370 m^3/s, Q_{SFO} = 40 m^3/s and $Q_{Spillway}$ = 235 m^3/s. Spillway discharge routed through a single gate, gate 3. (Note that contour levels are not synchronized between Figures 5.6-5.13)*

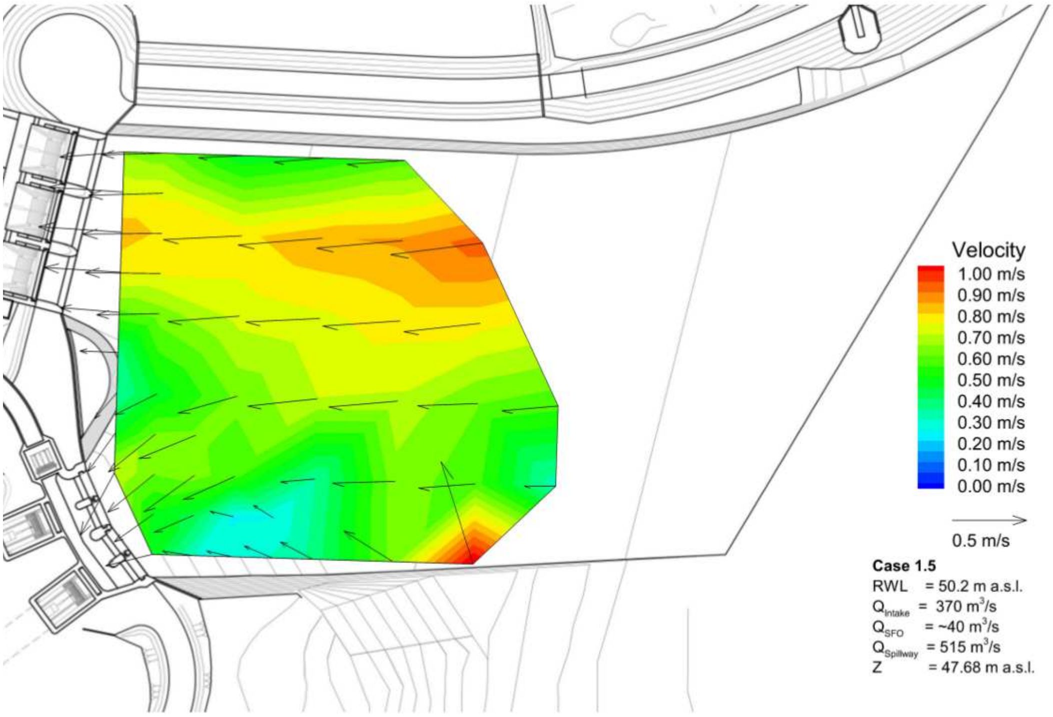

Figure 5.11: *Velocity distribution in the approach flow channel for Case 1.5, Q_{Intake} = 370 m^3/s, Q_{SFO} = 40 m^3/s and $Q_{Spillway}$ = 515 m^3/s. (Note that contour levels are not synchronized between Figures 5.6-5.13)*

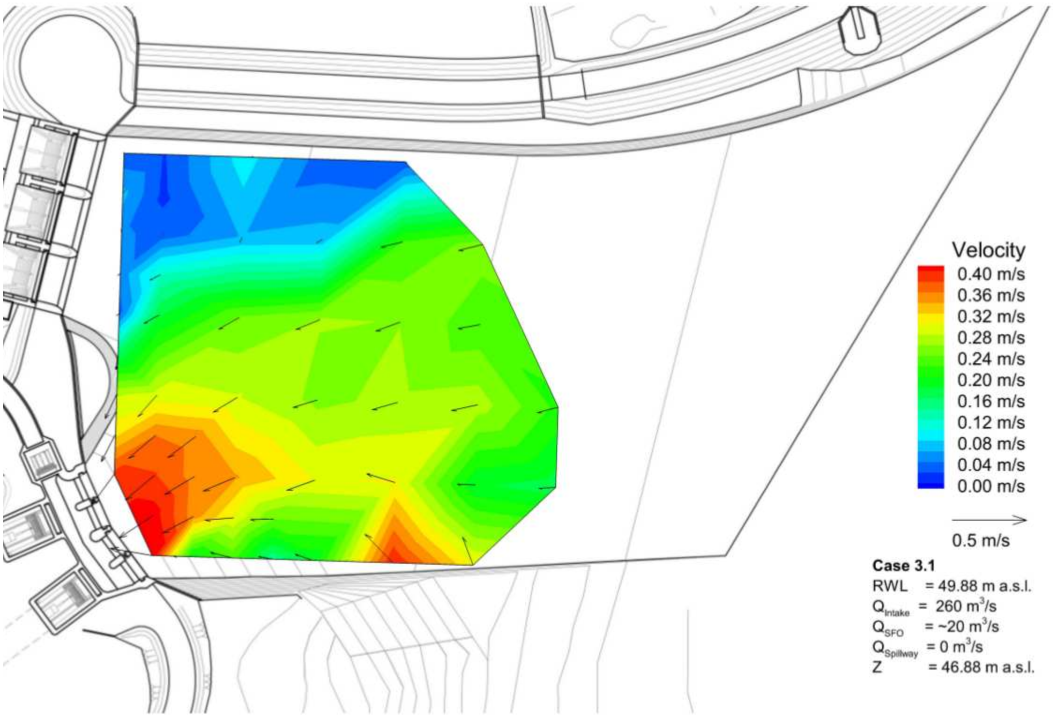

Figure 5.12: *Velocity distribution in the approach flow channel for Case 3.1, Q_{Intake} = 260 m^3/s, Q_{SFO} = 20 m^3/s and $Q_{Spillway}$ = 0 m^3/s. (Note that contour levels are not synchronized between Figures 5.6-5.13)*

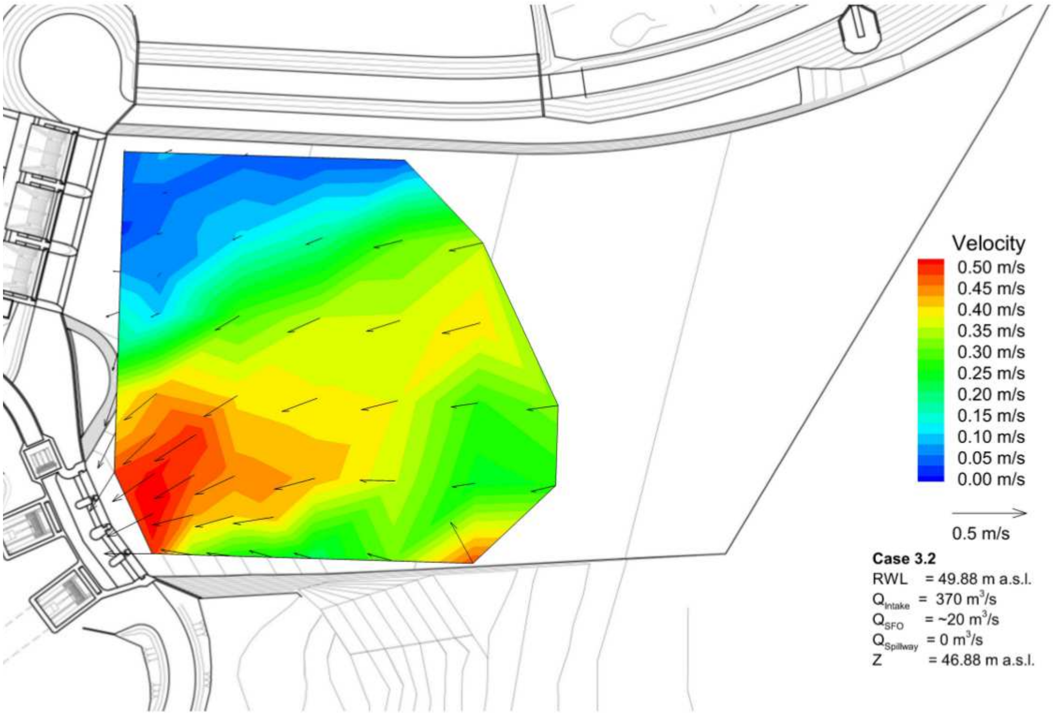

Figure 5.13: *Velocity distribution in the approach flow channel for Case 3.2, $Q_{Intake} = 370$ m^3/s, $Q_{SFO} = 20$ m^3/s and $Q_{Spillway} = 0$ m^3/s. (Note that contour levels are not synchronized between Figures 5.6-5.13)*

5.4. Dye Tests

Results of dye tests are shown in Table 5.2. The results show that the depth of water which the SFO attracts ranges between 0.7 m and 1.5 m. The depth at which half of the water is transported by the SFO and half by the intake ranges between 0.7 m and 2.5 m. The depth at which the power intake starts solely to draw water ranges between 1.2 m and 3 m. The effect of reservoir water level and intake discharge is evident, the lower reservoir water level in Cases 3.1 and 3.2 reduces the discharge to the SFO which in turn reduces the depth of water the SFO transports. With increased discharge to the power intake the increased downward current of the intake reduces the depth of water the SFO attracts.

Table 5.2: *Results from dye tests showing Reservoir Water Level RWL, depth at which water flows only to the SFO (Only SFO), depth at which the flow is divided evenly between intake and SFO (50/50) and the depth at which water flows only to the intake (Only Intake).*

Case	RWL [m a.s.l.]	Q_{Intake} [m^3/s]	$Q_{Spillway}$ [m^3/s]	Q_{SFO} [m^3/s]	Q_{Total} [m^3/s]	Only SFO [m] depth	50/50 [m] depth	Only Intake [m] depth
1.1	50.2	240	0	40	280	1.5	2-2.5	3
1.2	50.2	370	0	40	410	1-1.5	1.5-2	>2
1.3	50.2	370	70	40	480	1-1.5	1.5-2	>2
1.4	50.2	370	235	40	645	<1	1.5	>2
1.5	50.2	370	515	40	925	<1	1.5	>2
3.1	49.9	260	0	20	280	0.7-1.2	1.2-1.7	>1.7
3.2	49.9	370	0	20	390	<0.7	0.7-1.2	>1.2

During the dye test a distinct behavior was observed immediately upstream of the SFO crest where a dye released perpendicular to SFO Entrances 1 and 4 was drawn toward the center entrances, Entrances 2 and 3. The observed behavior shown in Figure 5.14 is caused by lateral flow.

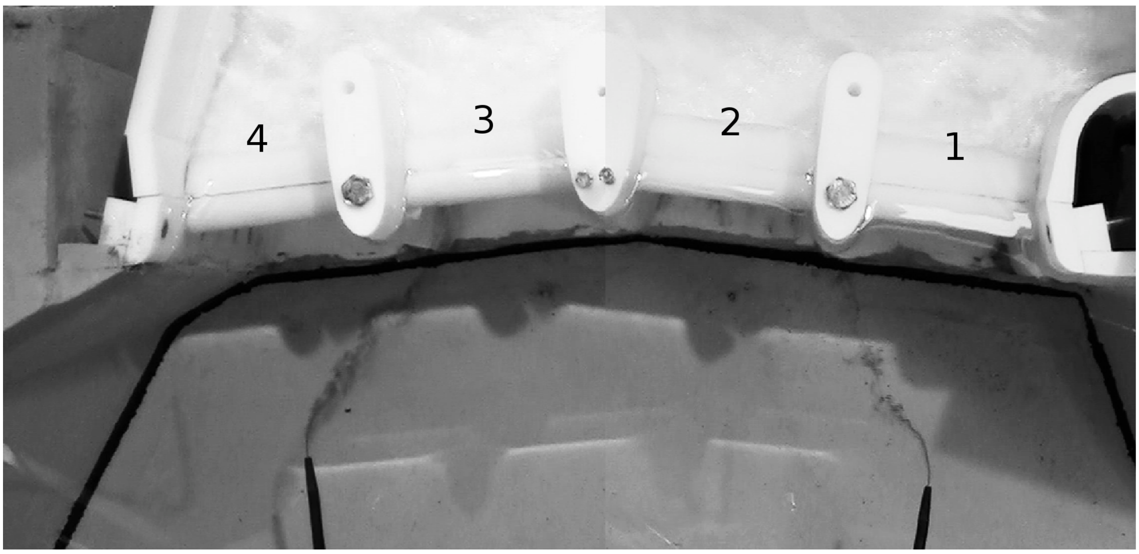

Figure 5.14: *Streamlines drawn towards SFO Entrances 2 and 3 during a dye test.*

5.5. SFO Capacity

Figure 5.15 shows measured SFO discharge as a function of RWL and a fitted curve where the discharge coefficient C from Equation 4.2 is derived as 1.518 for best fit. The figure shows that the discharge capacity of the SFO at NWL is around 31 m^3/s which is less than the 40 m^3/s the designers expected. The SFO conveys 40 m^3/s at RWL between 50.1 m a.s.l. and 50.2 m a.s.l.

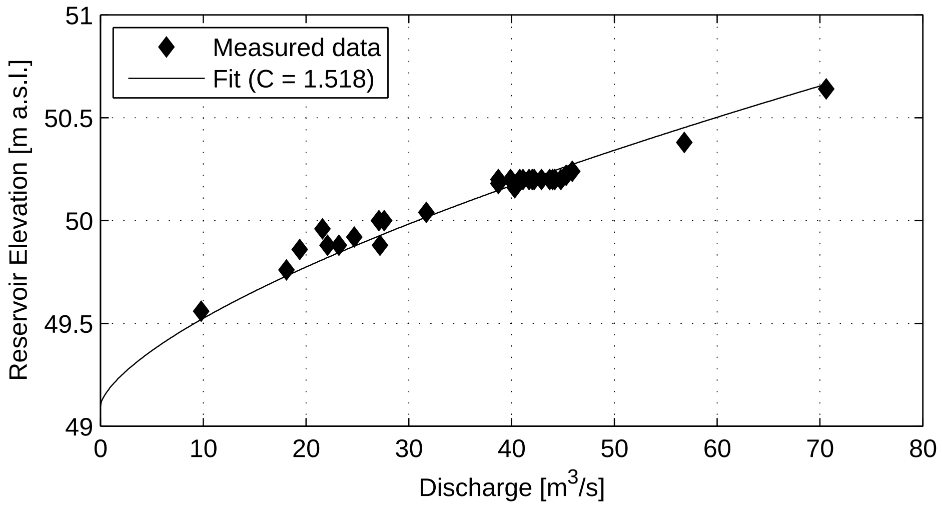

Figure 5.15: *Discharge rating curve for SFO. Diamonds show measured values and data fit is shown as a solid line*

The lower discharge capacity measured compared to the expected design capacity of 40 m^3/s may be due to unconventional features of the SFO and approach flow conditions. The inward angle of the structure and location of power intake below the SFO crest are not incorporated into the conventional discharge capacity equation for ungated spillways (Equation 4.2). The intake does however not affect the discharge capacity of the SFO as discharge measurements with the power intake closed showed no improvements in discharge capacity. The lower discharge capacity is not believed to be due to scale effects. Appendix E.4 discusses scale effects in SFO and possible reasons for the reduction in discharge capacity.

5.6. Visual Observations

Results from particle and velocity tests show irregularities forming at the LAB. The irregularities were observed for all cases excluding Case 2.1. Steady formation of coherent surface swirl, type VT-1 vortices as classified by (Vischer & Hager 1995) are shown in Figure 5.16, is observed at the LAB. VT-1 vortices are transported towards the intake, increase in intensity and travel further downstream with increased discharge through the system. The irregularities were formed by topographic features upstream of the LAB which direct the flow away from the LAB. As water flows over the LAB perpendicular to the main current in the AFC, irregularities form and the current is drawn away from the LAB into the middle of the AFC. Figure 5.17 shows the aforementioned irregularities forming at the LAB heading into the main AFC. The water surface in the approach flow channel is smooth for lower discharge cases but with increased discharge the surface becomes slightly rippled.

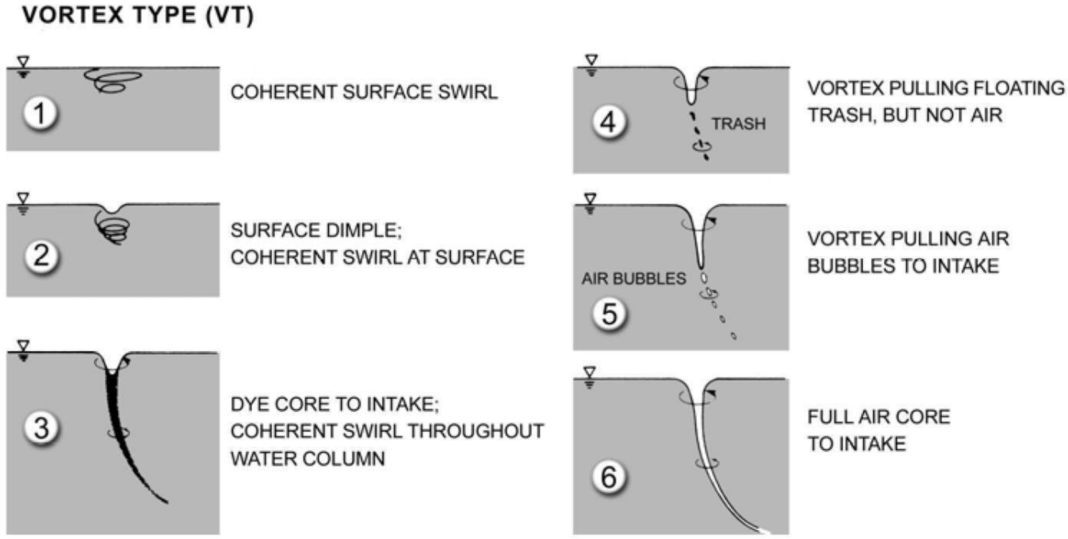

Figure 5.16: *Vortex classification set forth by Vischer & Hager (1995).*

Figure 5.17: *Irregularities forming at the left approach bank.*

For Cases 4.1 and 4.2, no SFO operation, only visual observations were made. The approach flow channel water surface is smooth with irregularities forming at the LAB. With the SFO closed, small vortices, surface dimples type VT-2 as shown in Figure 5.16, form and decay in front of the intake and SFO entrances, most frequently in front of intake Entrances 3 and 4. Figure 5.18 shows the surface dimples forming in front of intake and SFO Entrances 3 and 4 during documentation of Case 4.1. In order to locate the origin of the vortices, reservoir water elevation (RWL) was lowered and elevated from NWL and plugs used to block the SFO entrances. With lowered RWL vortex formation reduced and increased when RWL was increased above NWL. When the SFO entrances are completely blocked no vortex formation was observed. The results indicate that the vortex formation is not caused by the intake. The increased vortex formation at higher RWL points towards slow currents inside the SFO contributing to vortex formation.

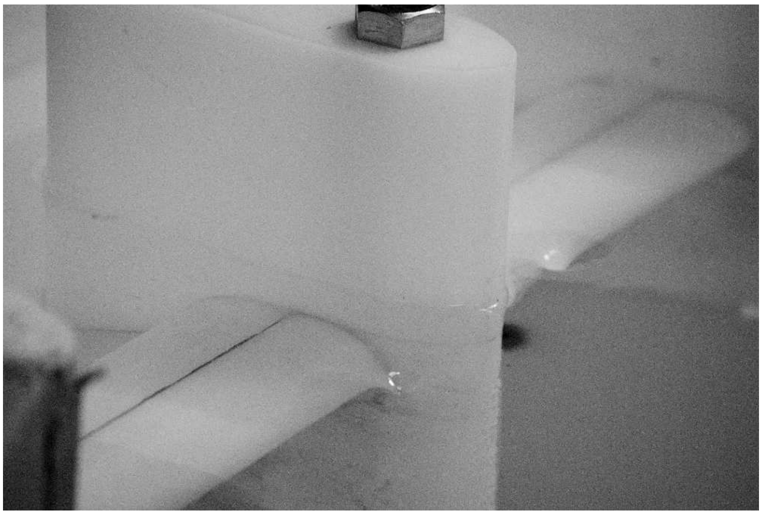

Figure 5.18: *Surface dimples forming in front of the intake and the SFO Entrances 3 and 4 during documentation of Case 4.1, Q_{Intake} = 370 m^3/s, Q_{SFO} = 0 m^3/s and $Q_{Spillway}$ = 0 m^3/s*

5.7. Summary

In the previous sections results from particle tests, velocity measurements, dye tests and visual observations for the SFO and the intake are described. The characteristics of the approach flow conditions were thoroughly mapped by particle and velocity tests. The following conclusions are made regarding the approach flow conditions and the effectiveness of the SFO design and the approach layout:

- In general the approach flow channel layout and the SFO design are effective in creating conditions favorable in attracting juvenile salmon towards the SFO type juvenile fish bypass. Locating the SFO on top of the power intake is an effective solution and is crucial as discharge to the power plant creates the attraction flow which guides the juvenile salmon towards the SFO entrance.

- The SFO attracts water from depths ranging between 0.7 m and 2.5 m depending on reservoir water levels and power intake operation. Increased discharge to the power intake decreases the depth of water which the SFO is able to attract. Lower reservoir water levels also limit the water depth the SFO is able to attract.

- The attraction flow towards the intake and SFO is extensive, reaching far upstream into the discovery zone with gradual acceleration towards the intake and SFO.

- Bulk of the flow in the approach flow channel splits into two branches immediately upstream of the curb located between the intake and spillway structures when the spillway is in operation. With increasing spillway discharge the extent of the attraction flow towards the intake and SFO reduces.

- A stagnant velocity zone forms immediately upstream of the spillway during periods of zero spillway discharge.

- Irregularities are observed in flow forming at the left approach bank (LAB). Water flowing over the LAB enters the approach flow channel (AFC) perpendicular to the main current in the AFC producing irregularities as the different currents intersect. Other features producing disturbances in the flow are topographic features at the LAB and vertical disturbances forming as water flows over the LAB perpendicular to the AFC.

- The discharge capacity of the SFO is lower than the designers expected at NWL. The cause of the lower discharge capacity can not be pinpointed directly as there are many unknowns regarding calculation of such a complex spillway structure. The requested discharge capacity of 40 m^3/s can be achieved by lowering the SFO crest by 15 cm to 20 cm.

- The SFO is not able to create the attraction flow alone and is only able to attract water approximately 10-20 m upstream of the SFO entrance if discharge to the power plant is not active.

Numerical investigation for the SFO at Urriðafoss can be found in (Tómasson, Garðarsson, Ágúst Guðmundsson & Gunnarsson 2013)

6. Conclusion

A comprehensive study has been done to validate the hydraulics at Urriðafoss HEP spillway, roller bucket for energy dissipation and the intake with its associated juvenile fish passage facility. Detailed description of the final design can be found in Section 4.1.

The flow conditions in the reservoir, the approach area of the spillway and the intake are validated and quantified. Spillway approach flow is acceptable with no observed abnormalities that limit the capacity of the spillway or pose a threat to the spillway structure. The attraction flow towards the intake and the juvenile fish passage is extensive reaching far upstream into the reservoir with gradual acceleration towards the intake and the juvenile fish passage. When the spillway is in operation, the bulk flow in the main approach flow channel splits into two branches immediately upstream of the curb located between the intake and spillway structures. During periods of zero spillway discharge and operation of the intake and juvenile fish passage a stagnant velocity zone forms immediately upstream of the spillway. Irregularities in flow form at the left approach bank of the intake due to topographic features. The discharge capacity of the spillway at the normal regulated water level (50 m a.s.l.) and the highest regulated water level (51.5 m a.s.l.) is tested. The capacity is sufficient without exceeding allowable reservoir elevations, both for Q_{50} and Q_{1000}.

The roller bucket performs satisfactorily for all discharges with no sweepout or diving flow for bucket elevation at 26 m a.s.l. (final design). The characteristic of the roller is conventional for discharges less than 1300 m^3/s. For discharges in the range of 1300 to 1700 m^3/s the roller behavior is substituted by submerged jet characteristics. For higher discharges the performance of the roller bucket is marginally acceptable. Lowering the invert of the roller bucket by 1-2 m (25-24 m a.s.l.) would improve the hydraulic performance significantly for higher discharges. A weak ground roller is formed immediately downstream of the bucket for lower discharges but is less evident for higher discharges. Interlocked operation (all gates at equal openings) of the gated structure is strongly advised. If single gate operation is used, various forms of flow abnormalities and vortices are formed in the excavated downstream channel. This could potentially lead to unpredictable consequences for the structures. Material could also be carried into the bucket by the asymmetric flow causing damage to the bucket invert or bucket teeth.

The discharge capacity of the juvenile fish passage (Surface Flow Outlet, SFO) does not meet the design criteria (40 m^3/s) at the normal water level. The geometric complexity of the juvenile fish passage causes difficulty in identifying exactly the cause of the lower capacity. The required discharge capacity of 40 m^3/s can be achieved by lowering the juvenile fish passage crest by 0.15 m, from 49.10 to 48.95 m a.s.l. This would provide a conservative discharge capacity of the juvenile fish passage which can then be regulated to some extent with reservoir elevation during periods of fish passage.

In general the approach flow channel layout and the juvenile fish passage design are effective in creating conditions favorable in attracting juvenile salmon towards the juvenile fish passage.

Locating the juvenile fish passage on top of the power intake is an effective solution and is crucial as discharge to the power plant creates the attraction flow which guides the juvenile salmon towards the juvenile fish passage entrance. For the design discharge of the juvenile fish passage (40 m^3/s) and intake (370 m^3/s), the juvenile fish passage attracts water from depths up to 1-1.5 m upstream of the structure. If discharge to the power plant is zero, the juvenile fish passage is only able to attract water approximately 10-20 m upstream of the juvenile fish passage entrance.

To summarize, the following aspects of the spillway, roller bucket, intake and juvenile fish passage associated structures are observed for the final design:

Approach flow conditions

- The approach flow to the spillway is acceptable with no observed abnormalities that limit the capacity of the spillway. The maximum velocity in the approach channel is about 3.7 m/s at 2250 m^3/s.

- The approach flow towards the intake and juvenile fish passage is extensive, reaching well upstream into the reservoir with gradual acceleration towards the intake and juvenile fish passage.

- A stagnant velocity zone forms immediately upstream of the spillway during periods of zero spillway discharge

Discharge characteristics

- The spillway capacity is sufficient, both the Q_{50} and the Q_{1000} pass through the spillway with reservoir levels lower than required.

- Interlocked operation (all gates at equal openings) of the gated structure is strongly advised.

- The discharge capacity of the juvenile fish passage does not meet the design criteria (40 m^3/s) at the normal water level.

Roller bucket and downstream conditions

- All discharges tested pass without sweepout or diving flow, indicating a sufficient tailwater level.

- For low flows (less than 1300 m^3/s) the roller bucket performance is satisfactory.

- For mid to high discharges (1300 to 1700 m^3/s) the roller behavior has mostly been substituted by a submerged jet characteristics.

- For high discharges (greater than 1700 m^3/s) the roller bucket performance is marginally acceptable.

Downstream discharge channel

- Hydraulic conditions in the downstream excavated channel and the receiving river section are acceptable for all discharges tested.

- At 2250 m^3/s the maximum measured velocity in the downstream channel is about 6.6 m/s and the average velocity is about 3.3 m/s.

Juvenile fish passage

- In general the approach flow channel layout and the SFO design are effective in creating conditions favorable in attracting juvenile salmon towards the SFO type juvenile fish bypass. Locating the SFO on top of the power intake is an effective solution and is crucial as discharge to the power plant creates the attraction flow which guides the juvenile salmon towards the SFO entrance.

- The SFO attracts water from depths ranging between 0.7 m and 2.5 m depending on reservoir water levels and power intake operation. Increased discharge to the power intake decreases the depth of water which the SFO is able to attract. Lower reservoir water levels also limit the water depth the SFO is able to attract.

- The attraction flow towards the intake and SFO is extensive, reaching far upstream into the discovery zone with gradual acceleration towards the intake and SFO.

- Bulk of the flow in the approach flow channel splits into two branches immediately upstream of the curb located between the intake and spillway structures when the spillway is in operation. With increasing spillway discharge the extent of the attraction flow towards the intake and SFO reduces.

- A stagnant velocity zone forms immediately upstream of the spillway during periods of zero spillway discharge.

- Irregularities are observed in flow forming at the left approach bank (LAB). Water flowing over the LAB enters the approach flow channel (AFC) perpendicular to the main current in the AFC producing irregularities as the different currents intersect. Other features producing disturbances in the flow are topographic features at the LAB and vertical disturbances forming as water flows over the LAB perpendicular to the AFC.

- The discharge capacity of the SFO is lower than the designers expected at NWL. The cause of the lower discharge capacity can not be pinpointed directly as there are many unknowns regarding calculation of such a complex spillway structure. The requested discharge capacity of 40 m^3/s can be achieved by lowering the SFO crest by 15 cm to 20 cm.

- The SFO is not able to create the attraction flow alone and is only able to attract water approximately 10-20 m upstream of the SFO entrance if discharge to the power plant is not active.

Hvammur HEP Spillway layout

At Hvammur HEP, the first part of the model investigation project for Lower Þjórsá River, a low Froude inflow stilling basin is optimized. Based on the results at Urriðafoss a further investigation of a roller bucket layout at Hvammur HEP is advised. Both parametric and geometric conditions at Hvammur are similar to Urriðafoss so the complex structure previously optimized at Hvammur could possibly be replaced by a less complex and less expensive structure by investigating the possibility for a low Froude inflow roller bucket layout.

References

ASCE (2000), 'Hydraulic Modeling; Concepts and Pratice, ASCE Manuals and Reports on Engineering Pratice no.97', *ASCE Press,Reston, VA, USA* .

Chanson, H. (2004), 'The Hydraulics of Open Channel Flow: An Introduction', *Elsevier Butterworth-Heinemann* .

Chanson, H. (2006), 'Bubbly Flow Structure in Hydraulic Jump', *European Journal of Mechanics B/Fluids 26* .

Chanson, H. & Gualtieri, C. (2008), 'Similitude and scale effects of air entrainment in hydraulic jumps', *Journal of Hydraulic Research, Vol 46, No.1, pp.35-44* .

Falvey, H. (1980), 'Air-Water flow in Hydraulic Structures, Engineering Monograph 41', *United States Department of the Interior, USBR, Denver, USA* .

García, C. M., Cantero, M. I., Nino, Y. & Garcia, M. H. (2005), 'Turbulence Measurements with Acoustic Doppler Delocimeters', *Journal of Hydraulic Engineering, ASCE p.1062* .

Ágúst Guðmundsson & Garðarsson, S. M. (2011), Hönnunarforsendur seiðafleytu - minnisblað.

Khatsuria, R. (2005), 'Hydraulics of Spillways and Energy Dissipators', *Marcel Dekker, NY, USA* .

Káradottir, l. R. & Guðjónsson, S. (2012), NTH-60 Neðri Þjórsá minnisblað, Málefni: Seiðafleyta Urriðafossvirkjun - líkanprófanir, Technical report, Landsvirkjun, Verkís, Veiðimálastofnun. Verknúmer: 11036-001.

Liu, M., Zhu, D. Z. & Rajaratnam, N. (2004), 'Evaluation of ADV Measurements in Bubbly Two-Phase Flows', *Journal of Hydraulic Engineering, ASCE* .

NVE (2005), 'Retningslinjer for flomløp til §§ 4-6 og 4-13 i forskrift om sikkerhet og tilsyn med vassdragsanlegg', *Norges vassdrags- og energidirektorat, Utgave 2* .

Peterka, A. J. (1958), 'Hydraulic Design of Stilling Basins and Energy Dissipators, Enineering Monograph no.25', *United States Department of the Interior, USBR* .

Pfister, M. & Hager, W. (2010), 'Chute Aerators.I:Air Transport Characteristics', *J. Hydraul. Eng. 136, 352* .

Sontek (2001), Sontek/YSI ADVField/Hydra Acoustic Doppler Velocimeter (Field) Technical Documentation, Technical report, Sontek, YSI Inc.

Tómasson, G. G., Garðarsson, S. M., Ágúst Guðmundsson & Gunnarsson, A. (2013), 'Urriðafoss HEP Lower Þjórsá: Numerical investigation of a Juvenile Fish Passage system, LV-2013-017'.

Tómasson, G. G., Garðarsson, S. M. & Gunnarsson, A. (2010), 'Hydraulic Model tests: Spillways at Hvammur and Urriðafoss Lower Þjórsá, Memorandum: Evaluation of Proposed Design'.

Tómasson, G. G., Garðarsson, S. M. & Gunnarsson, A. (2011), 'Hydraulic Model tests: Preliminary review of proposed design at Urriðarfoss HEP'.

Tómasson, G. G., Garðarsson, S. M. & Gunnarsson, A. (2012*a*), 'Hvammur HEP Lower Þjórsá: Physical Model investigation on the Spillway and Intake, Final report, LV-2012-111'.

Tómasson, G. G., Garðarsson, S. M. & Gunnarsson, A. (2012*b*), 'Hydraulic Model tests: Spillways at Hvammur and Urriðafoss Lower Þjórsá, Memorandum: Measurement Program for Urriðarfoss HEP'.

United States Army Corps of Engineers (1992), *Hydraulic Design of Spillways*, EM (Series) (United States Army Corps of Engineers), Headquarters, Department of the Army, Office of the Chief of Engineers.

Urban, A. L., Wilhelms, S. C. & Gulliver, J. S. (2005), 'Decay of Turbulence Downstream of a Stilling Basin', *Journal of Hydraulic Engineering, ASCE* .

USBR (1987), 'Design of Small Dams', *United States Department of the Interior, USBR, Denver, USA* .

Verkís (2011), 'NTH-60 HPP in Neðri-Þjórsá: Energy dissipation for Urriðafoss Spillway: Memo - MB-0511, Revision 2, 2011-12-06'.

Verkís (2012), 'NTH-60 HPP in Neðri-Þjórsá: Roller bucket energy dissipater for Urriðafoss Spillway: Memo - MB-0529, 2012-03-01'.

Verkís & Mannvit (2010), 'Hydraulic Model tests: Spillways at Hvammur and Urriðafoss - LV 2008/102'.

Vischer, D. & Hager, W. H. (1995), 'Energy Dissipators - Hydraulic Structure Manual - International Association for Hydraulic Research, IAHR'.

Wahl, T. L. (2000), 'Analyzing ADV Data Using WinADV', *Joint Conference on Water Resources Engineering and Water Resources Planning and Management, July 30 - August 2nd, 2000 — Minneapolis, Minnesota* .

A. Measurement program

HYDRAULIC MODEL TESTS
SPILLWAY AT HVAMMUR AND URRIÐAFOSS
LOWER ÞJÓRSÁ

LABORATORY MEASUREMENT PROGRAM FOR URRIÐAFOSS HEP

MEMORANDUM

DATE: 2012-03-17

FROM: Gunnar Guðni Tómasson, Sigurður Magnús Garðarsson, Andri Gunnarsson

TO: Helgi Jóhannesson, LV

Modifications:

2012-03-17: Memo first issued
2012-03-26: Revisions after meeting with the designers

The scope of this memo is to specify details of the hydraulic laboratory model and testing scheme for the spillway at Urriðafoss in the Lower-Þjórsá Hydroelectric Project. The memo discusses a proposed measurement program to validate and quantify the hydraulic structures at Urriðafoss based on the experience from physical model tests at Hvammur HEP. The measurement program is divided into two main parts, preliminary investigations of the proposed design, including necessary modifications; and a detailed measurement program for the final design. The measurement program is divided into two parts, the intake structure and the associated surface flow outlet (SFO) for fish passage, and the spillway structure and downstream conditions.

DOCUMENTS

This memo is written based on information and design memorandums supplied by the designers together with memorandums issued by the modeling group:

[1] LV-2008/102 Hydraulic model tests - Spillways at Hvammur and Urriðafoss (NTH-81). (Date: Jan. 2010)

[2] MB-0529 / Roller bucket energy dissipater for Urriðafoss Spillway (07028-036). (Date: March 1, 2012)

[3] MB-0040 / Seiðafleyta Urriðafossvirkjun – líkanprófanir (11036-001). (Date: 2012-05-16)

[4] Preliminary review of proposed design at Urriðafoss HEP, memo issued by the modeling group. (Date: 2011-12-29)

[5] Hönnunarforsendur seiðafleytu í Urriðafossvirkjun, memo issued by the modeling group. (Date: 2011-11-08)

[4] Drawings issued according to Table 1

Table 1 – list of drawings issued for building of Urriðafoss physical model.

Drawing number	Version	Text
C-11-3.101	P3	Power station, river dam, overview
C-11-3.102	P1	Hydraulic model tests, general sections
C-11-3.201	P2	Hydraulic model tests, structural drawing, plan at el. 41,0
C-11-3.202	P2	Hydraulic model tests, structural drawing, section
C-11-3.252	P6	Power station, power intake, layout, plan at el. 50,80
C-11-3.261	P4	Power station, power intake, laout, section a1
C-11.3.272	P3	Power station, power intake, laout, section b1
CAD file		Tversnid2_snið dypkuð.dwg (cross sections in river)

BASIC PARAMETERS

The laboratory model will be built in the scale 1:40 using Froude scaling.

In all tests discharge through the power intake will correspond to full design discharge for the station (370 m^3/s for Urriðafoss,). This condition will however not necessarily be met at the largest discharges on the spillway (combined spillway and power intake discharge is not required to exceed 2250 m^3/s).

Reservoir elevation will be measured at various locations, 2-4 points, in the upstream reservoir at a location with near-zero velocity.

For reference in this memo the spillway gates are labeled 1 to 3 from west to east.

Figure 1 shows the extent of the laboratory model. At the upstream end of the approach channel for the spillway flow straighteners will be positioned aimed at minimizing waves and stabilizing the flow in the system.

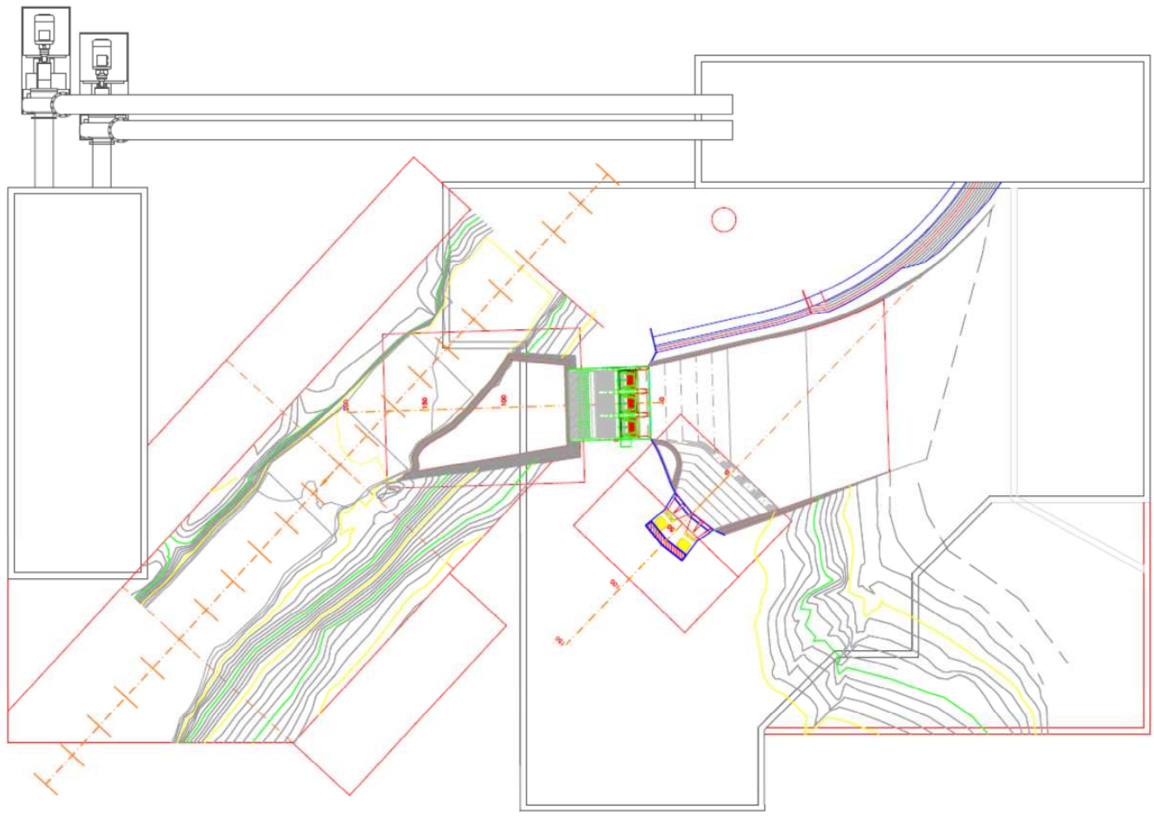

Figure 1 – The layout and extent of the laboratory model. Flow direction is from right to left.

INSTRUMENTATION

Table 2 shows number and type of instrumentation that will be used.

Table 2: Instrumentation

Type	***Range***	***Number***	***Accuracy***
Static Pressure	± 1-2 mWc	16	0.05% FS
Flow	0 – 280 l/s	2	1%
Velocity	± 3 m/s	2	1%
ADCP/ADV	Velocity Profiling	1	1%

Pressure sensors measure static pressure and can be placed in various locations in the model. For velocity measurements ADV and ADCP devices will be used. If the flow is highly aerated as can be expected in parts of the model a calibrated mechanical current meter will be used. ADV instruments provide velocity vectors in three dimensions (x,y,z) relative to its probe. The mechanical current meter provides only velocity vector in the direction of its body.

In observations of the intake structure, dye and trace material will be used to represent streamlines where applicable. To estimate surface currents and possible existence of stagnant velocity zones, small spherical particles (Particle test) will be used (3-8 mm in diameter), scattered in the flow and their traces documented.

GENERAL MEASURMENT PLAN

The measurement plan has the following structure:

General measurement plan:

1. **Preliminary measurement program – Proposed design**
    a. *Preliminary investigation for the proposed spillway design*
    b. *Preliminary investigation for the proposed intake and SFO design*

2. **Detailed measurement program – Final design**
    a. *Final investigation for the spillway final design*
    b. *Final investigation for the intake and SFO final design*

The proposed design of the hydraulic structures and their layout has been issued by the designers. The preliminary measurement program aims at validating the structures and quantifying their behavior. With satisfactory results from the preliminary measurement program including, if any, modifications, the detailed measurement program is conducted for the final design.

[1.a] Preliminary measurement program – Proposed Spillway design

The preliminary measurements test the overall hydraulic conditions for the spillway structure. On the basis of these measurements the design of the structures downstream of the spillway will be modified so as to obtain best hydraulic performance.

The discharge cases for the preliminary phase are listed in Table 2.

Table 3 - discharge cases for the preliminary phase

Discharge on spillway Urriðafoss			**Gate operation** Interlocked			**Res. elev.**
Q_{1000}	2250	**m^3/s**	1	2	3	HWL
Q_{50}	1700	**m^3/s**	1	2	3	NWL
Q_5	900	**m^3/s**	1	2	3	NWL
Q	350	**m^3/s**	1	2	3	NWL

Approach flow

Approach flow conditions will be observed visually and documented. If necessary, modifications aimed at improving the upstream hydraulics will be made in close collaboration with the designers.

Furthermore, by raising the concreted part immediately upstream of the spillway crest by 2 m measurements will be done to validate its influence on the discharge capacity.

Gated structure

The required discharge capacity will be measured and preliminary stage discharge relationships derived to identify if the spillway meets the necessary capacity set forth in the design criteria [1]. This means four combinations of reservoir elevation and gate opening will be derived, according to Table 3. If the capacity is insufficient, modifications aimed at increasing the capacity will be tested.

At Hvammur HEP an interlocked gate operation was advised based on experience from the hydraulic model test. The preliminary tests will identify if interlocked operation of the spillway gates is also a necessary operating condition at Urriðafoss HEP. The preliminary program will be based on interlocked operation of the gates while single gate operation will be tested to identify unwanted operating conditions. The detailed measurement program will document asymmetric operation.

Roller bucket

The performance of the roller bucket and formation of the rollers will be observed visually and flow characteristics documented (sweep out, jet flow). If necessary, velocity measurements will be made in the downstream area of the roller bucket to assist in flow characteristic identification. Water elevations will be measured at 10 m intervals downstream of the roller bucket.

No pressure or pressure fluctuations measurements will be conducted.

If the proposed bucket invert elevation, 26 m a.s.l., results in a satisfactory behavior no other elevations will be tested in the preliminary program. If 26 m a.s.l. is insufficient, 24 m a.s.l. and/or 22 m a.s.l. will be tested.

Bottom profile in the downstream canal

Downstream of the roller bucket three types of bottom profiles will be tested for Q_{1000}:

1. Initial tests will be done with a horizontal invert at 18 m a.s.l. for further decision making.
2. The recommended bottom profile by the designers according to [2].
3. Invert at 28 m a.s.l. with loose material aimed at identifying a stable bottom scour profile.

For Case 1 and 2, a fixed bed will be applied, while for cases 3 a homogenous material will be distributed in the downstream canal and the flow allowed to stabilize at a certain bottom profile. Further investigation on the scouring pattern and suggested downstream layout of the canal invert will be tested in the detailed measurement program. It is assumed that Q_{1000} will result in the most extreme bottom profile in the canal and should therefore be used as a design guideline for the final design.

[1.b] Preliminary measurement program – Intake and SFO – Proposed design

The preliminary measurement program for the intake and the SFO aims at identifying stagnant and unfavorable zones in the reservoir upstream of the intake for juvenile fish. Table 4 lists the discharge cases that will be tested. The performance will mainly be observed and documented visually by inserting floating particles in the approach flow and observing the flow patterns (particle test). In some cases flow visualization with dye might be necessary. Identification of zones with high acceleration and velocities will be documented and necessary modifications to the design made in cooperation with the designers.

The zone under investigation is from the SFO spillway crest and approximately 200 m upstream of the crest.

Table 4 – Discharges tested as proposed in reference [3]. Reservoir elevation is kept at NWL.

Case	Q_{Intake}	$Q_{spillway}$	Q_{total}
	[m^3/s]	[m^3/s]	[m^3/s]
1.1	240	0	280
1.2	370	0	410
1.3	370	70	480
1.4	370	235	645
1.5	370	515	925

No velocity measurements, pressure measurements or water elevations will be documented. The discharge capacity of the SFO will be determined for NWL.

[2.a] Detailed measurement program – Spillway – Final design

When final design has been accepted for the spillway layout based on the preliminary measurements, detailed measurements will be made to test and document the hydraulic performance of the structures for all important flow conditions.

The detailed measurements are divided into the following parts:

Discharge test series 1- [DT1]

This series of measurements is designed to produce a head-discharge relationship for the gates (Q-H plots for gate openings 0.25, 0.5, 0.75 and 1.0 and free flow under the gate). Reservoir elevation will range from 46 to 50 m a.s.l.

Tests will be made for the following:

- Each of the three gates independently as flow conditions upstream of the gates vary.
- All three gates interlocked.
- All three gates fully open and reservoir elevation ranges from 41 m a.s.l. to 51.5 m a.s.l. in 0.5 m intervals (an ungated crest head-discharge relationship).

Discharge test series 2- [DT2]

This series of measurements is designed to simulate optimum operational conditions at the gates for the range of possible discharges. Here it is assumed that the spillway gates will be operated such that all three gates are interlocked.

Discharge test series 2 is divided into two parts, part A and part B, as shown in Table 5.

For ***part A*** the following measurements will be execute:

- Approach flow velocity to spillway and power intake
    - A dense grid of velocity points will be acquired along the spillway/intake approach channel. In total 40-60 points will be acquired. Visual observations will be made to ensure acceptable flow conditions in the entire upstream region and notice made of any irregularities.

- Flow velocity in the canal downstream of the roller bucket
    - Velocity will be measured from the roller bucket along the canal at ~10 m intervals at 3-5 elevations at each station. 5 cross sections will be measured at relevant locations. Each cross section will have 15-25 points while the section line will have 35-45 points.

- Flow velocity in the river
    - Velocity will be measured in the river. Distribution of points will vary depending on conditions but the main focus will be on measuring the interaction of the excavated canal, the river and at the river bank opposite to the excavated canal.

- Pressure measurements
    - Pressure will be measured at 10 m interval along the center line from the end of the roller bucket invert and along the excavated canal to the opposite river bank. Pressure

interaction on the steep sloping "end sill" of the excavated canal and the opposite river bank will be measured to estimate fluctuations.
    - Pressure fluctuations will be measured on one of the excavated canal side slopes at 6 points equally distributed in height at two sections, one close to the bucket and the other far from the bucket, i.e. 3 point in height at each location.

- Water elevations
    - Water elevations will be measured in three section lines at 10 m intervals from the spillway crest and along the roller bucket, the excavated canal and the original river canal.

For ***part B*** the following measurements will be done:

- Water elevations
    - Water elevations will be measured in three section lines at 10 m intervals from the spillway crest and along the roller bucket, the excavated canal and the original river canal.

For each case, for both part A and part B, the flow behavior in the system will be documented with photos and videos. Maximum discharge with reservoir elevation at fuse plug elevation will be estimated. Visual observations of the roller and its characteristics will be documented.

Table 5 – Overview of discharge series 2

Discharge on spillway			**Gate operation**			**Res. elev.**	**Part**	**Power Intake operation**
	Urriðafoss		**Interlocked**					
Q_{1000}	**2250**	**m³/s**	1	2	3	HWL	A	Off
	1900	**m³/s**	1	2	3	NWL+	B	Off
Q_{50}	**1700**	**m³/s**	1	2	3	NWL	A	Off
	1300	**m³/s**	1	2	3	NWL	B	On
	1050	**m³/s**	1	2	3	NWL	A	On
	700	m³/s	1	2	3	NWL	B	On
	500	**m³/s**	1	2	3	NWL	B	On
Q_{ave}	**350**	**m³/s**	1	2	3	NWL	A	On
	200	**m³/s**	1	2	3	NWL	B	On
Q_{min}	~100	**m³/s**	1	2	3	NWL	B	On

Discharge test series 3 [DT3]

This series is designed to simulate conditions in the roller bucket and downstream canal at different gate openings and gate combinations with the reservoir at NWL. Discharge test series 3 is designed to simulate operating conditions with gates out of operation. Gates that are operated within each case will be interlocked.

Table 6 lists the discharges that will be tested. The flow behavior in the canal and river bend will be documented with photos and videos. Included in the documentation will be how the water in the basin influences the closed gates, backwater influence. Expected number of cases is 35.

Table 6 – Overview of discharge test series 3. Columns marked with x indicate a close gate.

Discharge on spillway at Urriðafoss			Asymmetric operation Gate Operation Case 1			Asymmetric operation Gate Operation Case 2			Asymmetric operation Gate Operation Case 3			Asymmetric operation Gate Operation Case 4			Asymmetric operation Gate Operation Case 5			Res. elev.	Power Intake operat ion
	1150	**m^3/s**	1	2	x	x	2	3	1	x	3	x	x	x	x	x	x	NWL	Off
	900	**m^3/s**	1	2	x	x	2	3	1	x	3	x	x	x	x	x	x	NWL	Off
	700	**m^3/s**	1	2	x	x	2	3	1	x	3	x	x	x	x	x	x	NWL	Off
	500	**m^3/s**	1	2	x	x	2	3	1	x	3	1	x	x	x	2	x	NWL	Off
Q_{ave}	350	**m^3/s**	1	2	x	x	2	3	1	x	3	1	x	x	x	2	x	NWL	Off
	200	**m^3/s**	1	2	x	x	2	3	1	x	3	1	x	x	x	2	x	NWL	Off
Q_{min}	~100	**m^3/s**	1	2	x	x	2	3	1	x	3	1	x	x	x	2	x	NWL	Off
Number of cases:			**7**			**7**			**7**			**7**			**7**				

Discharge test series 4 [DT4]

To assess the influence of tailwater sensitivity to the roller bucket performance the bucket invert elevation will be raised by 2 m from the selected bucket invert elevation and tested for the discharges listen in Table 3. No measurements will be conducted but the performance will be documented with visual observations, videos and photos.

[2.b] Detailed measurement program – Intake and SFO – Final design

Measurement and observation methods include:

- **Particle test**: particles are scattered u/s in the model for a given case and their streamlines and flow characteristics documented with photos and video. This aims at identifying stagnant velocity zones and focusing of velocity in the system. The scattering of particles will take place immediately d/s of the flow straightness structures in the model.
- **Dye test**: To assess the streamline separation immediately upstream of the SFO crest and quantify the surface layer transported by the SFO, a dye test will be performed.
- **Velocity distribution**: velocity measured close to the surface with an ADV. Measurement points are scattered u/s of the SFO with increasing density towards the intake. In total 40-50 points will be measured.
- **Documentation:** for all cases documentation will take place, this means, that videos, pictures and noted observations will be made and, if any abnormalities are identified, they will be carefully documented and supported with the suitable method of measurement, i.e. velocity or streamline tracking.

Table 7 gives an overview of the cases that will be tested in the detailed measurement program for the intake and associated surface outlet flow (SFO) structure. Most investigation effort will be focused on cases 1.1 to 1.5 (see [3]) as they represent the normal operating conditions of the structures.

The following zones have been defined:

i) Approach zone
ii) Discovery zone
iii) Decision zone

Further clarification of the zones is discussed in [3].

Measurement and observation methods include:

- **Particle test**: particles are scattered u/s in the model for a given case and their streamlines and flow characteristics documented with photos and video. This aims at identifying stagnant velocity zones and focusing of velocity in the system. The scattering of particles will take place immediately d/s of the flow straightness structures in the model.
- **Dye test**: To assess the streamline separation immediately upstream of the SFO crest and quantify the surface layer transported by the SFO, a dye test will be performed.
- **Velocity distribution**: velocity measured close to the surface with an ADV. Measurement points are scattered u/s of the SFO with increasing density towards the intake. In total 40-50 points will be measured.
- **Documentation:** for all cases documentation will take place, this means, that videos, pictures and noted observations will be made and, if any abnormalities are identified, they will be carefully documented and supported with the suitable method of measurement, i.e. velocity or streamline tracking.

Table 7 – Overview of the cases proposed to be investigated by Verkís [3]. Columns 6 and 7 indicate type of documentation that will be produced for each case.

	Q_{Intake}	$Q_{spillway}$	Q_{total}	Q_{SFO}				
Case	[m^3/s]	[m^3/s]	[m^3/s]	[m^3/s]	Particle test	Velocity distribution	Documentation	Dye test
1.1	240	0	280 + Q_{SFO}	Q_{NWL}	x	x	x	x
1.2	370	0	410 + Q_{SFO}	Q_{NWL}	x	x	x	x
1.3	370	70	480 + Q_{SFO}	Q_{NWL}	x	x	x	x
1.4	370	235	645 + Q_{SFO}	Q_{NWL}	x	x	x	x
1.5	370	515	925 + Q_{SFO}	Q_{NWL}	x	x	x	x
2.1	0	260	260 + Q_{SFO}	Q_{NWL}	x	-	x	-
2.2	0	335	335 + Q_{SFO}	Q_{NWL}	x	-	x	-
2.3	0	605	605 + Q_{SFO}	Q_{NWL}	x	-	x	-
3.1	260	0	260 + Q_{SFO}	Q_{NWL} <	x	x	x	x
3.2	370	0	370 + Q_{SFO}	Q_{NWL} <	x	x	x	x
4.1	370	0	370	0	-	-	x	-
4.2	370	270	640	0	-	-	x	-

The cases in Table 7 have the following definition and are further discussed in [3]:

1.1-1.5 Normal operating conditions of the structures
2.1-2.3 Power Plant inoperable, SFO operational
3.1-3.2 Reservoir elevation < NWL and power plant operable
4.1-4.2 SFO inoperable, intake operable

B. Roller Bucket energy dissipater for Urriðafoss Spillway - memo

NTH-60 HPP IN NEÐRI-ÞJÓRSÁ

MEMO

PROJECT NO:	07028-036	DATE.:	2012-03-01
PROJECT PHASE:	117 Líkanprófanir	NO.:	MB-0529

AUTHOR: Þorbergur Leifsson, Verkís
DISTRIBUTION: Helgi Jóhannesson LV, Kristján Már Sigurjónsson Verkis, Einar Júlíusson Mannvit.

Roller Bucket energy dissipater for Urriðafoss Spillway

1 Introduction

The spillway at Hvammur HEP was tested in hydraulic model located at Siglingamálastofnun in Kópavogur Iceland. The model test for Hvammur started early 2011 and finished in January 2012. Partly due to results of that test an alternative design of energy dissipation for similar spillway at Urriðafoss have been studied and evaluated. The options considered were shorter shallower and longer deeper conventional stilling basins, flip bucket and roller bucket (ref 1 and 2). The result of those studies is to test a Roller Bucket option at Urriðafoss. The tests will be carried out under the same contract in the first half of 2012.

This memo presents the preliminary design of the Roller Bucket option and defines the scope of the model tests.

2 Calibration of backwater condition

The expected water levels in the natural river channel downstream from the dam and down to the old national highway bridge have been calculated by using the HEC-RAS program. The location and number (St) of the cross sections are shown on *Drawing 1.* The cross sections profiles below the water surface have not been surveyed but the river bottom was assumed to be horizontal and the depth of the river were estimated based on measured water level at the right bank the 8 of May 2008 during 465 m3/s flow in the river. The observed water levels and the calibration are shown on *Figure 1*. A Manning number of M equal to 25 and 33 was used in the calculations considered to be some upper and lower limit for the expected hydraulic roughness.

The results of the calculations indicate that the water flow in the river is subcritical at the lowest sections (< St 182 to St 290) but a little supercritical or critical at most of the upstream sections for M=25, but critical or a little subcritical for M=33. The calculated water levels at St 200 to St 350 are up to 1 m lower than the observed levels. During one trial in the calibration process the bottom elevation at St 500 to St 40 were 0,2 to 1,0 m higher resulting in the calculated levels between St 200 and 350 being about 0,5 m higher than the observed values. This occurred as the subcritical flow extended further upstream. Because the flow is frequently shifting from supercritical to subcritical phase and the bottom profiles are not known it is impossible to get a perfect fit between the calculated and observed water levels at all locations. The spillway discharge canal enters the river at St 540 to St 640 and at that location the fit is better as the flow is close to critical.

Based on aforementioned calibration the water levels and velocity for different discharges are shown on *Figure 2* and *Figure 3* for manning coefficient M=25. As the flow is very close to critical the Manning coefficient has insignificant influence on the water level although the location of sub- and supercritical flow is affected.

Verkís hf.
Ármúla 4, 108 Reykjavík
+354 422 8000
verkis.is | verkis@verkis.is
Offices:
108 Reykjavík, Ármúla 4-6
108 Reykjavík, Suðurlandsbraut 4
300 Akranes, Stillholti 18
310 Borgarnes, Bjarnarbraut 8
400 Ísafjörður, Hafnarstræti 1
603 Akureyri, Austursíðu 2
700 Egilsstaðir, Kaupvangi 3b
800 Selfoss, Austurvegi 10

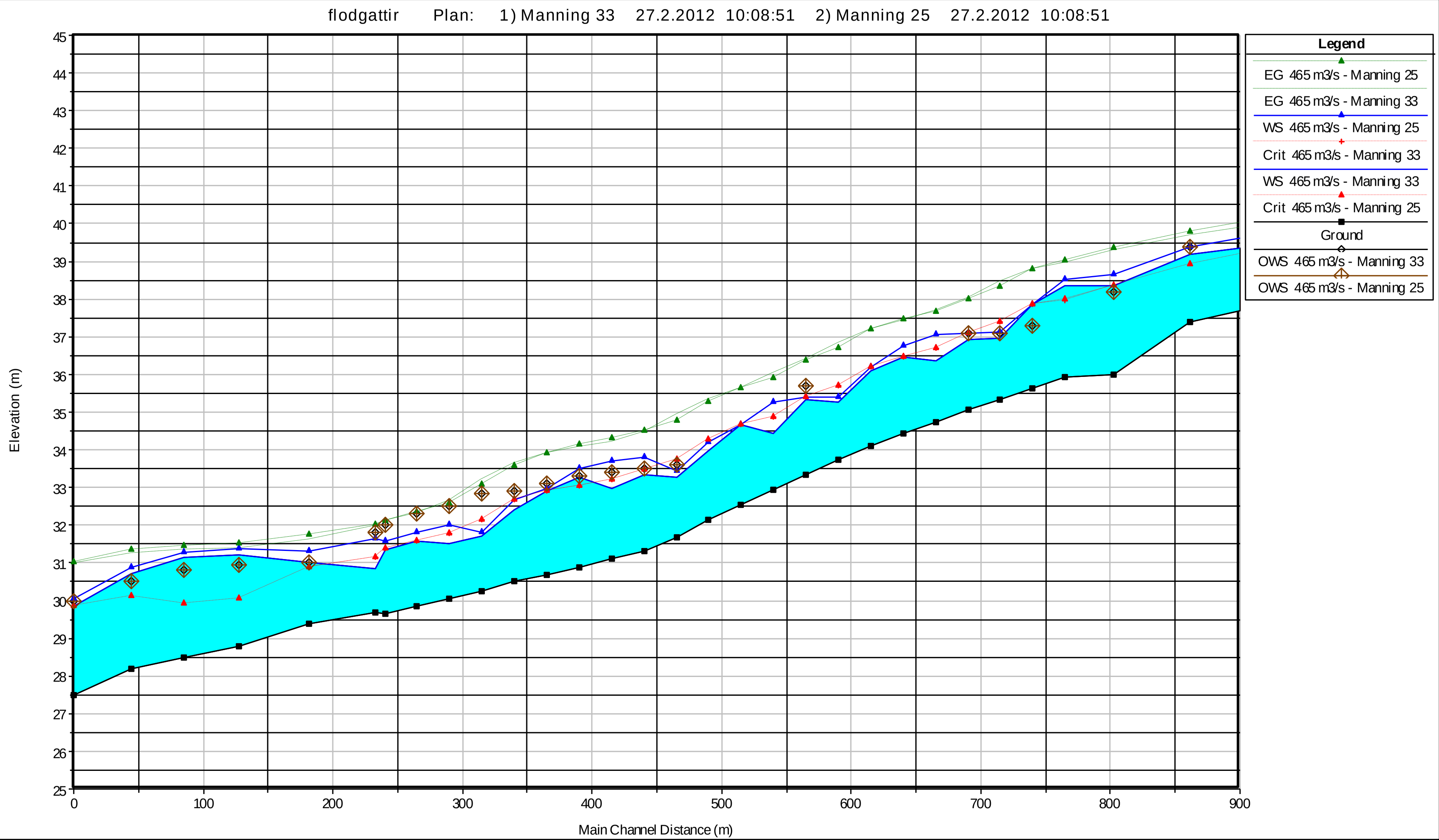

Figure 1 Final calibration of water levels for 465 m^3/s discharge and Manning number 25 and 33.

Verkís hf.
Ármúla 4, 108 Reykjavík
+354 422 8000
verkis.is | verkis@verkis.is

Offices:
108 Reykjavík, Ármúla 4-6
108 Reykjavík, Suðurlandsbraut 4

300 Akranes, Stillholti 18
310 Borgarnes, Bjarnarbraut 8
400 Ísafjörður, Hafnarstræti 1

603 Akureyri, Austursíðu 2
700 Egilsstaðir, Kaupvangi 3b
800 Selfoss, Austurvegi 10

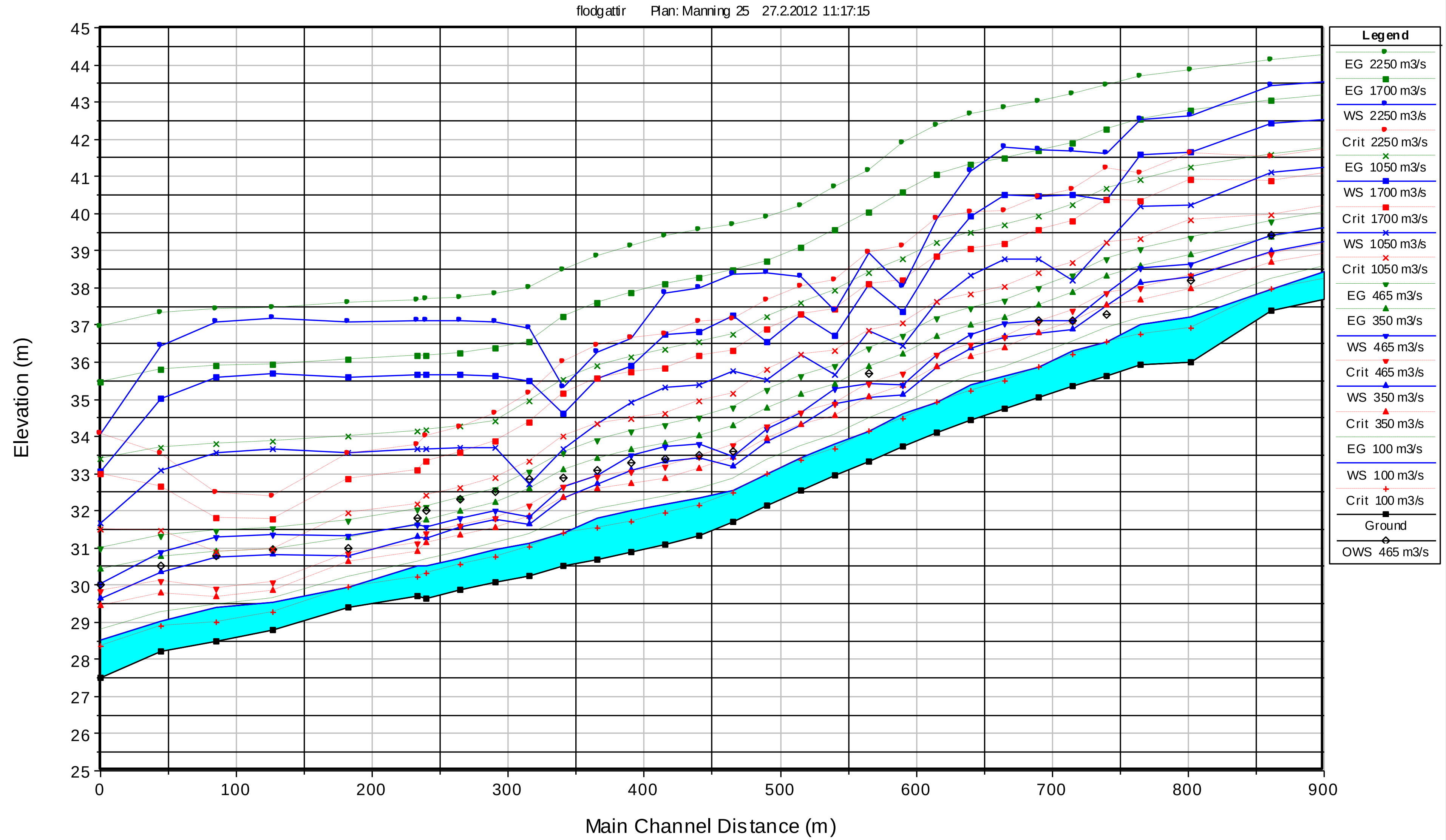

Figure 2 Profile of water level (blue), energy level (green) and critical water level (red)

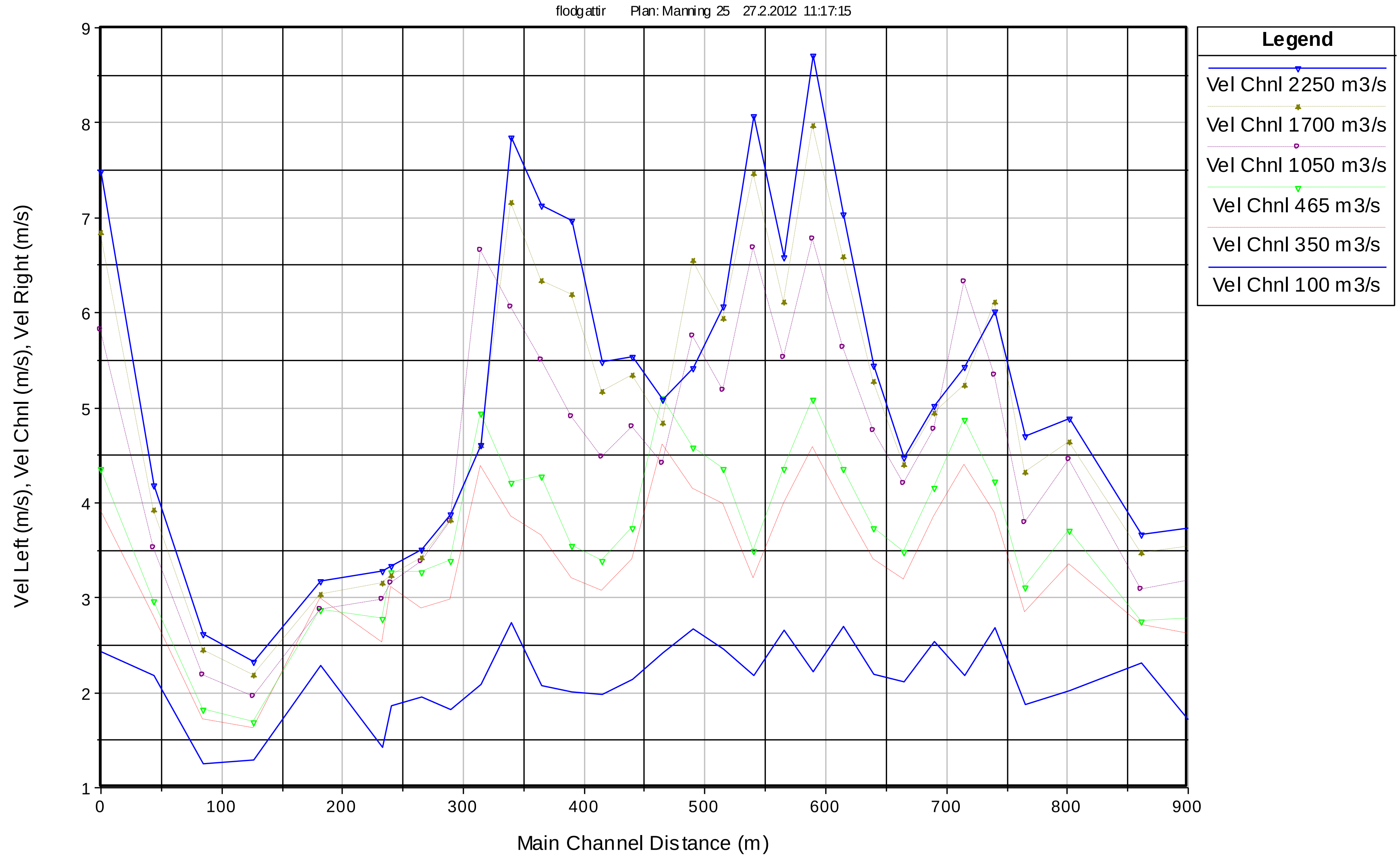

Figure 3 Average water velocity in river channel for manning M=25

The discharge values that were used in the calculations are listed in *Table 1.*

Discharge in m^3/s	Comment on flood
100	Very low flow
350	Average flow in the river
465	Flow for calibration of observed levels
1050	Average yearly maximum flood
1700	50 year flow
2250	Design flood (1000 year return period)

Table 1 Discharge used in the calculations of water levels.

After the construction of the Roller Bucket according to the layout shown on *Drawing 1* the cross-section at St 540, just downstream of where the spillway discharge canal has completely entered the river, will control the water levels upstream of it. A critical flow will exist at that section and a subcritical flow is expected at all locations upstream of it, if sweepout does not happen at the Roller Bucket and the discharge canal excavation is deep enough to prevent another hydraulic control upstream. A stagnant water level will exist in the river channel upstream of the right bank of the spillway discharge canal. The water level there will be the equal to the energy level at the critical section St 540 plus the energy loss between the two locations. It can be roughly estimated to be 0,5 to 1,5 m. The backwater level just downstream of the Roller Bucket can be estimated to be equal to the energy level at St 540 plus the headloss from it to the flow just downstream of the Roller Bucket minus the velocity head there.

The cross-section at St 540 and corresponding energy and water levels are shown in *Figure 4*, according to the same calculations as shown in *Figure 2.*

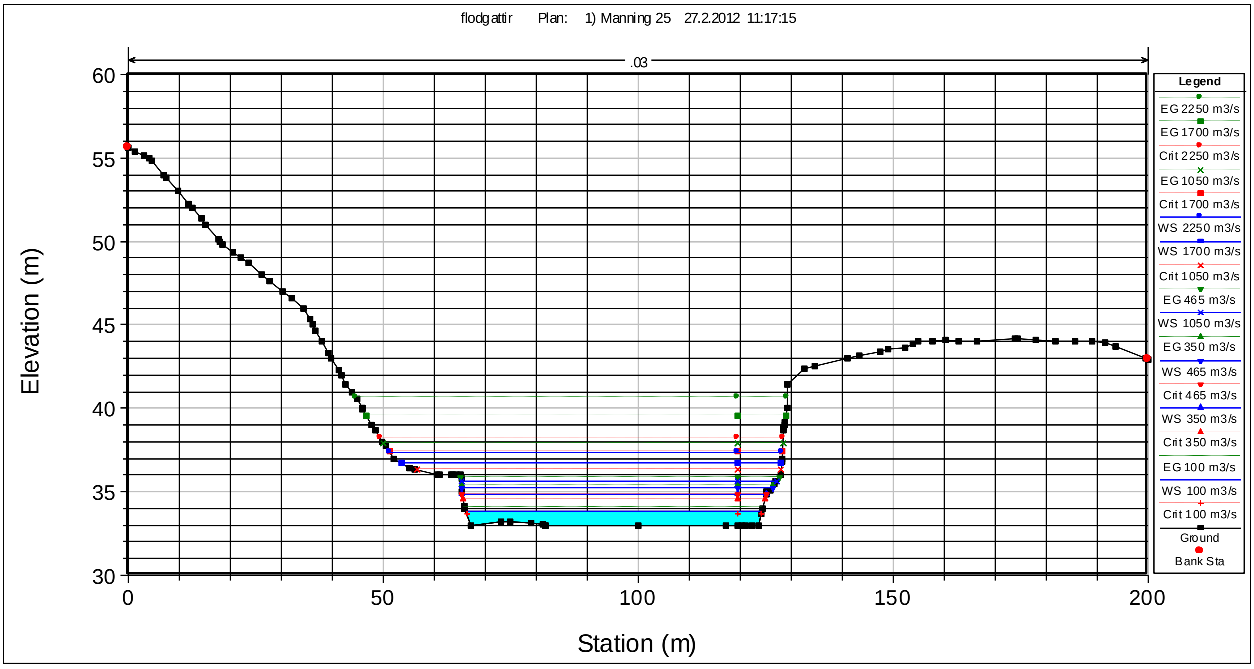

Figure 4 St 540 and calculated water level there as presented in *Figure 2*

The backwater levels according to those assumptions are presented in *Figure 5*.

Verkís hf.
Ármúla 4, 108 Reykjavík
+354 422 8000
verkis.is | verkis@verkis.is

Offices:
108 Reykjavík, Ármúla 4-6
108 Reykjavík, Suðurlandsbraut 4

300 Akranes, Stillholti 18
310 Borgarnes, Bjarnarbraut 8
400 Ísafjörður, Hafnarstræti 1

603 Akureyri, Austursíðu 2
700 Egilsstaðir, Kaupvangi 3b
800 Selfoss, Austurvegi 10

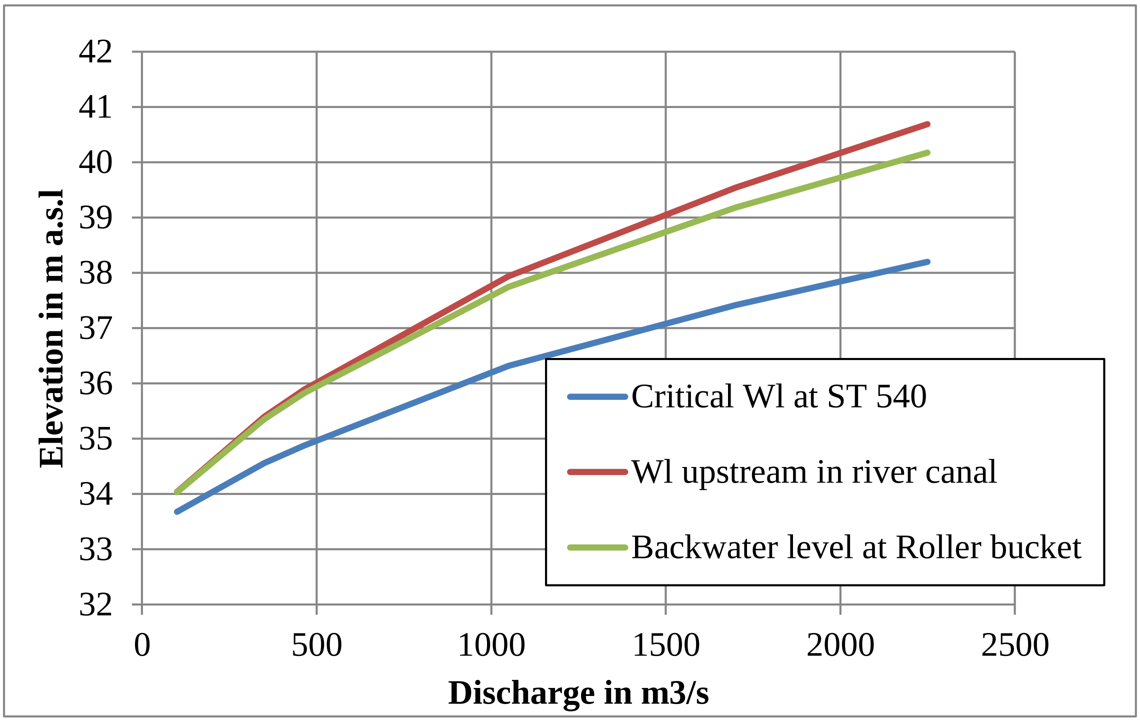

Figure 5 **Calculated and expected water levels (without addition of headloss upstream of St 540)**

The head difference between the reservoir level and the backwater energy level is up to 16 m for low flow (50-34) and down to 11,5 m for the design flood (51,5-40). This is similar differences as for the spillway at Hvammur HEP for large floods but about 4 m higher for low flow than at Hvammur HEP.

3 Roller Bucket design, guidelines and calculations

The Roller Bucket is designed according to methods given in *Ref. 3 and 4*. The definitions of variables are presented in *Figure 6.*

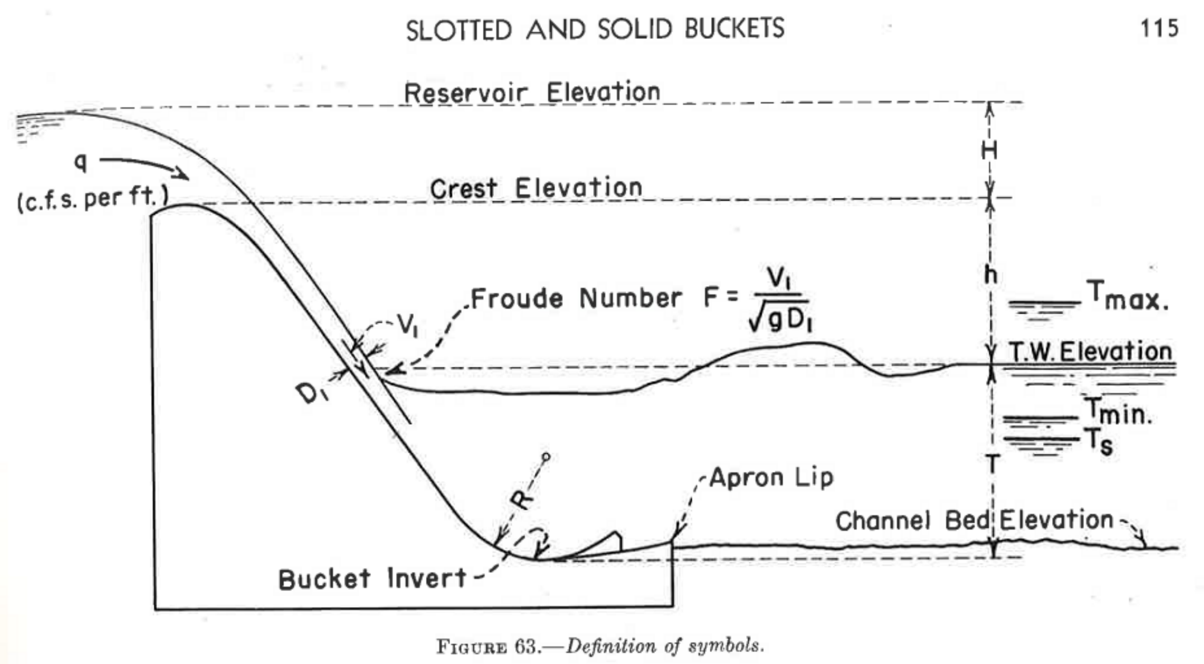

Figure 6 **Definition of variables for Roller Bucket**

Due to low head difference the Froude number F_1 is at the lower limits for the design charts provided in the references for the larges discharges. This result in the ratio between the Bucket radius and the incoming energy head ($R/(D_1+V_1^2/(2g))$) being larger than the values provided on the design charts, and thus requiring extrapolation of the charts lines.

To be able to get an adequately high tailwater level according to the estimate in *Figure 5*, a deep setting of the Roller Bucket and excavation for the discharge canal downstream of the Bucket is required. The Bucket invert elevation is set at elevation 26 m a.s.l. The results of calculations for that elevation and different discharges are presented in *Table 2*.

The last 2 columns in the table are for the case when the gates are completely open and the water level in the reservoir therefore lower than the normal Wl. of 50 m a.s.l. This might be the case during construction for the first few weeks or months after the reservoir has been filled but before the dams are finished.

The Froude number in line 7 is calculated at the elevation of the backwater. Lines 8 to 11 are only for comparison for conditions for a conventional stilling basin with bottom elevation of 26 m a.s.l.

In line 14 the minimum Bucket radius is calculated. The largest diameter is 10,5 m according to extrapolation of the lines in *Ref. 4*. The selected diameter in line 15 is a little larger or 11,0 m but less than the formula presented in *Ref. 5* ($R_{min}=5,19*(D_1+V_1^2/(2g))/F^{1,64}$). That would require a 16,8 m radius.

In lines 16 to 22 the maximum and minimum limits of the tailwater elevation are calculated. The extrapolation of the design charts are shown in Appendix A. The largest points shown in the Appendix are the ordinates used for *Table 2*. The readout for the sweepout depth and the maximum depth are the most uncertain due to the extrapolation. The readout of the minimum recommended tailwater depth is most easy as the design lines are more or less straight and can therefore easier been extrapolated.

The results of the calculations for Bucket invert elevation 26 m a.s.l are shown graphically in *Figure 7*. The results seem consistent. The sweepout depth is always a little less that the recommended minimum depth. The recommended tailwater depth is always 1 to 3 m lower than the estimated backwater elevation. Note that the expected backwater elevation is on the other hand probably 0,5 to 1,5 m higher due to headloss upstream of St 540 as said before. On the other hand downstream erosion in the river channel could lower the backwater levels.

The maximum tailwater level is always considerably higher than the expected backwater level indicating that the Bucket radius in not too small.

The result of those calculations is that the proposed layout and the level of the Roller Bucket seems to be properly chosen and within the suggested level as can be seen from extrapolation from the design graphs. A hydraulic model test is nevertheless necessary to verify and possibly improve the design.

	Bucket invert El.	26	m a.s.l	Width of bucket		42.9	m				
1	Discharge	m³/s	150	350	700	1000	1700	2250		350	700
2	Headwater level	m a.s.l	50	50	50	50	50	51.5		44.2	46.0
3	Tailwater level	m a.s.l	34.30	35.36	36.60	37.58	39.18	40.18		35.36	36.60
4	Friction loss on slope ~	m	2.10	0.74	0.30	0.16	0.06	0.05		0.74	0.30
5	V_1 (at tailwater El.)	m/s	16.3	16.5	16.0	15.5	14.5	14.9		12.6	13.8
6	D_1 (at tailwater El.)	m	0.21	0.49	1.02	1.50	2.73	3.52		0.65	1.19
7	F_1 (at tailwater El.)	-	11.3	7.5	5.1	4.0	2.8	2.5		5.0	4.0
8	V_b (at bucket invert)	m/s	18.5	20.5	20.9	21.0	20.7	21.2		17.4	18.9
9	D_b (at bucket invert)	m	0.19	0.40	0.78	1.11	1.91	2.47		0.47	0.86
10	F_b (at bucket invert)	-	13.6	10.4	7.6	6.4	4.8	4.3		8.1	6.5
11	H_2 (conjug. f. conv. stilling b	m a.s.l	26.9	27.6	28.7	29.4	31.0	32.1		27.7	28.7
12	$D_1 + V_1^2/(2g)$	m	13.8	14.4	14.1	13.8	13.5	14.8		8.7	10.8
13	$R/(D_1 + V_1^2/(2g))$ (Ref 4)	-	0.1	0.2	0.35	0.45	0.63	0.71		0.35	0.45
14	R_{min} (Fig 274 Ref 4)	m	1.4	2.9	4.9	6.2	8.5	**10.5**		3.0	4.9
15	$\mathbf{R_{selected}}$	**m**	**11**	**11**	**11**	**11**	**11**	**11**		**11**	**11**
16	$R_s/(D_1 + V_1^2/(2g))$	-	0.80	0.76	0.78	0.80	0.82	0.74		1.26	1.02
17	T_s/D_1 (Fig 69 in Ref. 3)	-		14.0	8.0	6.0	4.1	3.5			
18	H_T_s sweepout	m a.s.l		32.9	34.1	35.0	37.2	38.3			
19	T_{min}/D_1 (Fig 66 in Ref. 3)	-		13.8	8.7	6.2	4.4	3.8		9.5	6.5
20	H_T_{min}	m a.s.l		32.8	34.8	35.3	38.0	39.4		32.2	33.7
21	T_{max}/D_1 (Fig 67 in Ref. 3)	-		120.0	45.0	22.0	10.0	7.0			
22	H_T_{max}	m a.s.l		85.3	71.8	59.1	53.3	50.7			

Table 2 Calculations for Roller Bucket with invert elevation of 26 m a. s .l

Verkís hf.
Ármúla 4, 108 Reykjavík
+354 422 8000
verkis.is | verkis@verkis.is

Offices:
108 Reykjavík, Ármúla 4-6
108 Reykjavík, Suðurlandsbraut 4

300 Akranes, Stillholti 18
310 Borgarnes, Bjarnarbraut 8
400 Ísafjörður, Hafnarstræti 1

603 Akureyri, Austursíðu 2
700 Egilsstaðir, Kaupvangi 3b
800 Selfoss, Austurvegi 10

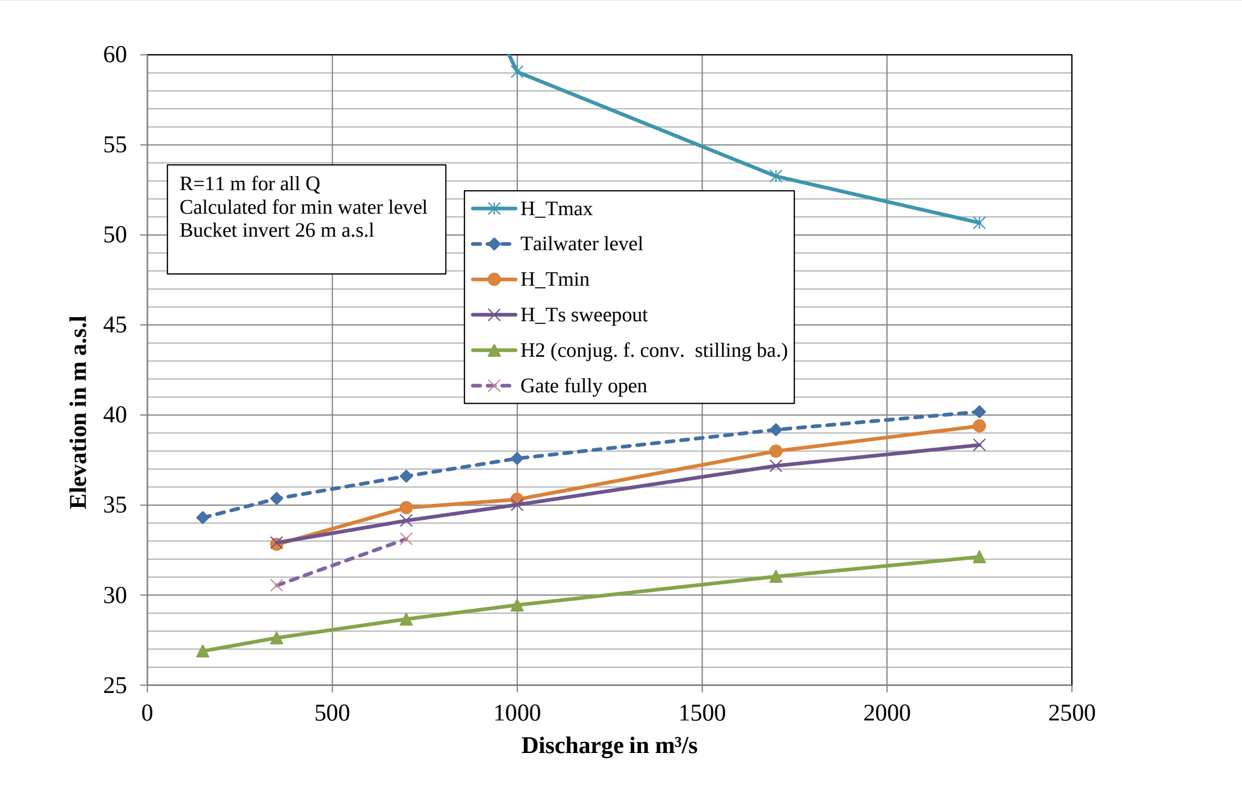

Figure 7 Result of calculated maximum and minimum required tailwater levels.

4 Proposed design of the discharge canal

The proposed design of the spillway is shown on Drawings 2 to 5, that have already been sent to the laboratory. The depth of the discharge canal to 18 m a.s.l in Drawing 2 is not the proposed design depth but the assumed lowest elevation the model must be able to represent if necessary.

A weak, ca. 4 to 5 m thick, scoria layer crosses the discharge canal. The layer is expected to be erodible by the discharge water if not protected. The bottom elevation of the layer is shown in *Figure 8*, according to rock core drillings. The thickness of the upper basalt layer on top of the scoria layer is probably only 1 to 2 m at the left bank of the river channel but probably thicker in the middle and at the right bank, but all these estimates are uncertain. The excavation of the discharge canal as shown in *Figure 8*, starts at 28 m a.s.l just downstream the concrete foundation of the Roller Bucket and extends upward with a slope of 1V:5h until it reaches the surface of the lower basalt layer. After that the excavation (erosion) follows the lower basalt layer down to the river channel. This should give the lowest backwater level at the Bucket as a hydraulic control is not created in the discharge canal according to the expected elevation of the river bottom. The flow will therefore be subcritical upstream of the St 540 section. This design is called the maximum excavation case.

Verkís hf.
Ármúla 4, 108 Reykjavík
+354 422 8000
verkis.is | verkis@verkis.is

Offices:
108 Reykjavík, Ármúla 4-6
108 Reykjavík, Suðurlandsbraut 4

300 Akranes, Stillholti 18
310 Borgarnes, Bjarnarbraut 8
400 Ísafjörður, Hafnarstræti 1

603 Akureyri, Austursíðu 2
700 Egilsstaðir, Kaupvangi 3b
800 Selfoss, Austurvegi 10

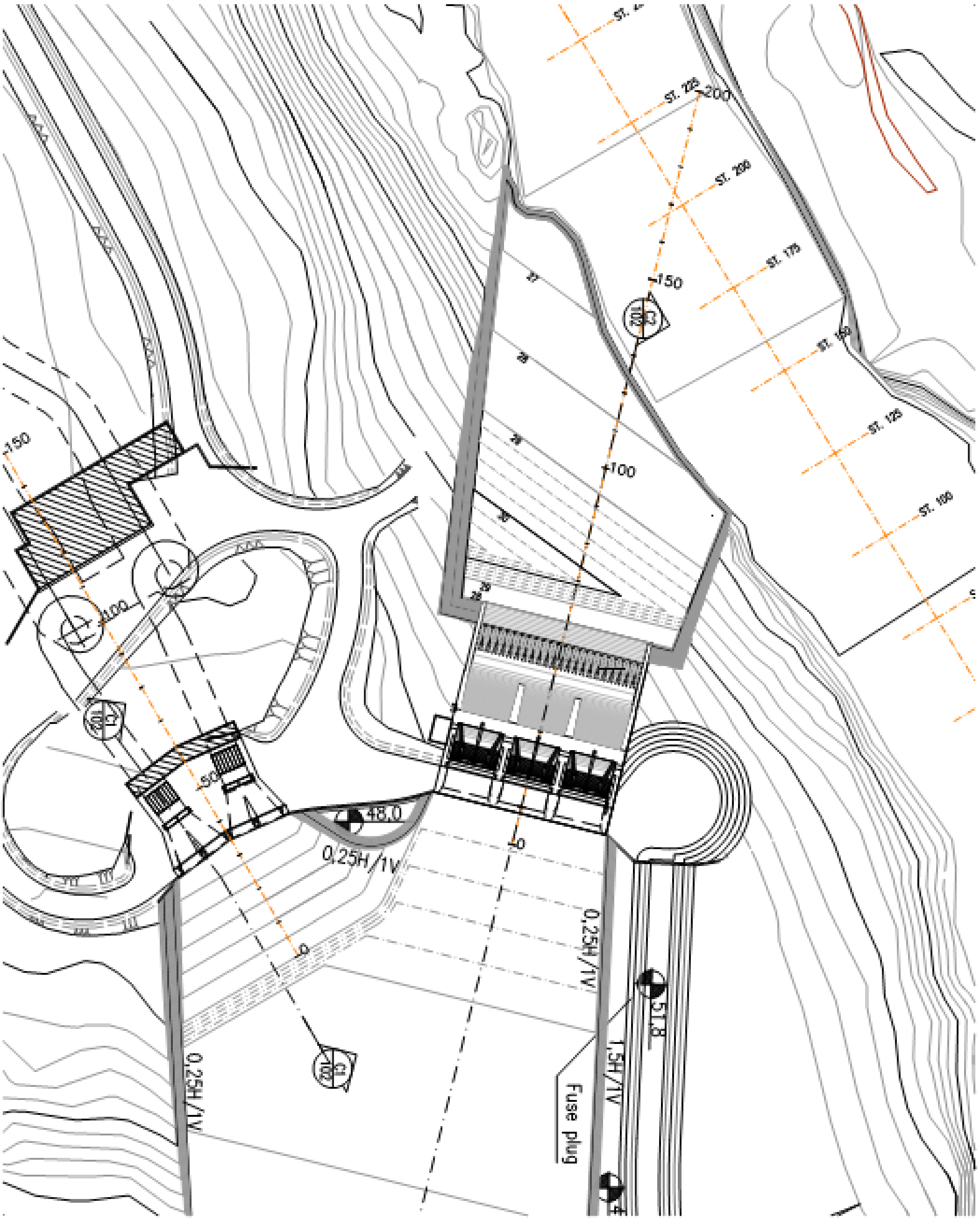

Figure 8 Roller Bucket and estimated contour lines of the discharge canal when excavated down to lower basalt layer. The maximum excavation case.

An alternative design would be to reduce the excavation to levels for example as shown on *Figure 9*. The downstream part of the canal would then be narrower and only excavated down to ca. 34 m a.s.l. A 50 m wide hydraulic control will then be created where the flow enters the river channel. The backwater level at the Bucket would be 1 to 2 m higher then shown on *Figure 5*, and a weak hydraulic jump would occur in the river channel. The benefit of this would reduced excavation cost, but more important, this would give time to investigate the rock conditions in the river channel and the discharge canal and perform proper protection and excavation, to limit the ultimate excavation/erosion to what is shown in *Figure 8*. This can be done when the river channel becomes almost dry after the station starts full operation. This limited excavation might on the other hand have unacceptable effect on the flow conditions in the river channel and possibly on the Roller Bucket. This design is called the minimum excavation case.

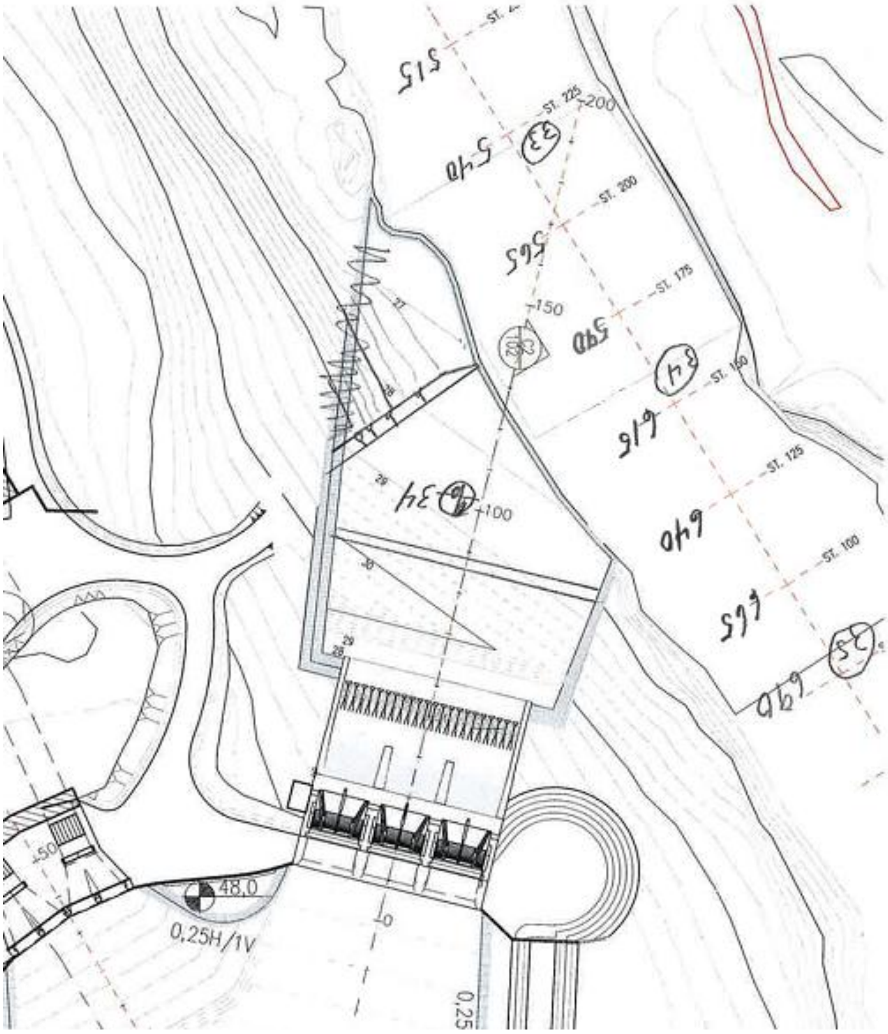

Figure 9 Proposed initial excavation. The minimum excavation case.

5 Scope and requirements of model test

The scope refers only to the Roller Bucket, the spillway discharge canal and river channel. For all upstream structures reference is made to other memorandum and the bid documents.

The general objectives of the planned Hydraulic Investigations are:

- Verification of the hydraulic performance of the hydraulic structures over the entire range of possible operating conditions
- Possible improvements and technical optimizations of the original reference design by hydraulic investigations and testing of design alternatives

In order to achieve these objectives the Contractor is encouraged to make use of his experience and qualifications and take the initiative in developing alternative options and solutions in the course of the investigations. This scope and requirements should therefore be considered as Guidelines and not strict regulations. Contributions that can result in gains of hydraulic performance and cost effectiveness are therefore desirable and welcome.

The specific scope of the planned investigations includes as a minimum:

<u>Roller Bucket (energy dissipater)</u>

1. Required bucket invert elevation possible range from 22 to 28 m a.s.l
2. Bucket radius, especially if larger radius is required.

3. Excavation/erosion of the discharge canal, closest to the Bucket (under the second roller)
4. Excavation of the downstream part of discharge canal. Minimum required initial excavation.
5. Conditions in the river channel.
6. Operation conditions for unsymmetrical gate openings.
7. Conditions for initial excavation and gates fully open and discharge 350 to 700 m^3/s.

The most important investigation is weather the second roller is properly formed and if it diverts the flow to the surface minimizing the erosion load on the bottom, and the flow conditions in the river channel, waves and load on the river banks. The maximum excavation case should be tested and optimised and if it works properly the minimum excavation case should also be tested.

6 References

1. Memo MB-0511 Ref 2, by Þorbergur Sreinn leifsson 2001-12-06.Energy dissipation for Urriðafoss Spillway.
2. Memorandum from Gunnar Guðni Tómasson, of fl. 2011-12-29. Preliminary review of proposed design at Urriðafoss HEP.
3. A.J. Petreka. Bureau of Reclamation. Hydraulic design of Stilling Basin and Energy Dissipation. Engeneering Monograph No. 25. 1978.
4. Bureau of Reclamation. Design of small dams. 1977.
5. U.S. Army Corps of Engineers. Hydraulic design of spillways. EM 1110-2-1603. 1992.

7 Attachment

Appendix A
Extrapolation on 3 design charts for *Table 2*

Drawing 1 Location and numbering of cross sections
Drawing 2 Plan of spillway and intake
Drawing 3 Plan of spillway
Drawing 4 Section in spillway and Roller Bucket
Drawing 5 Details of Roller Bucket tooths

8 Appendix A

SLOTTED AND SOLID BUCKETS 121

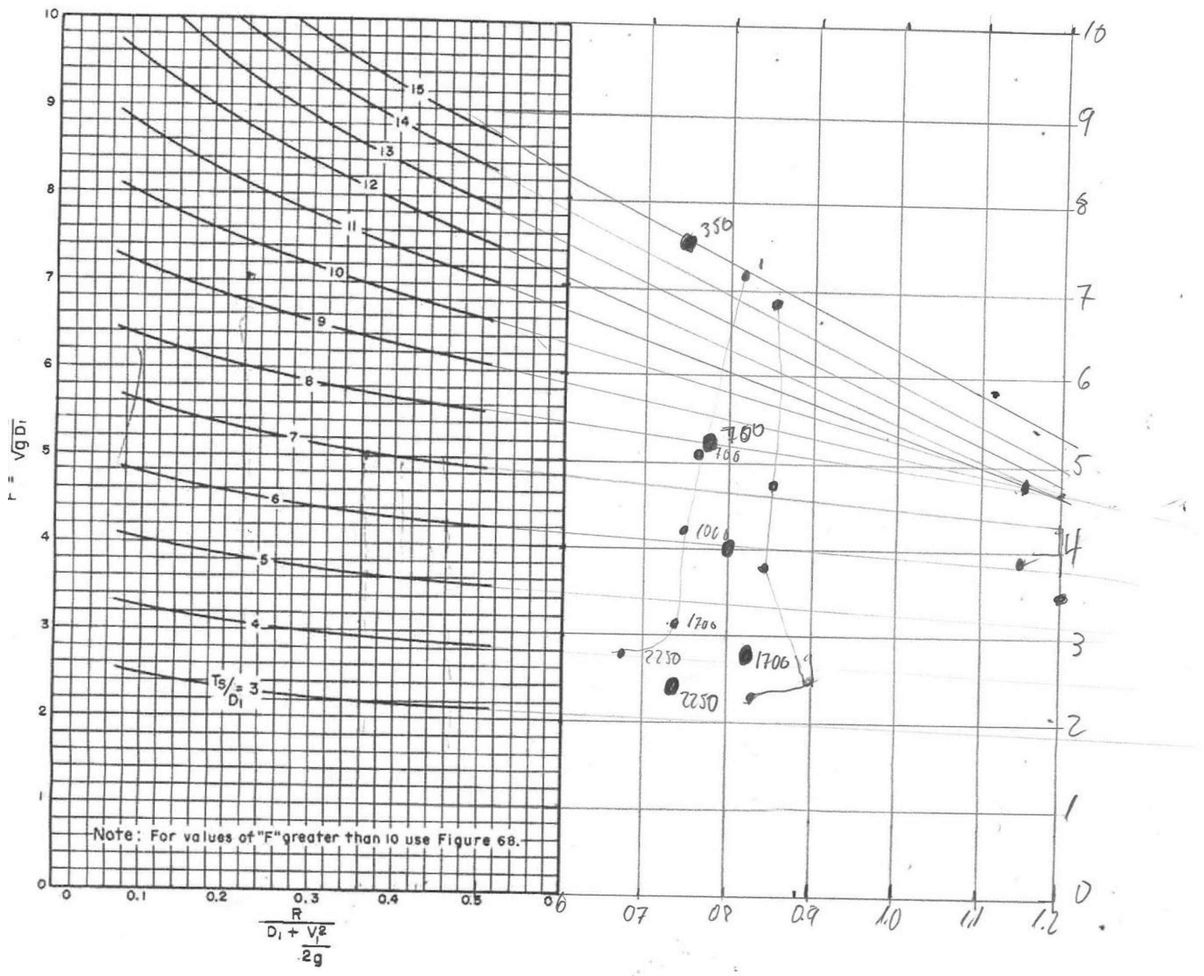

FIGURE 69.—*Tail water sweepout depth.*

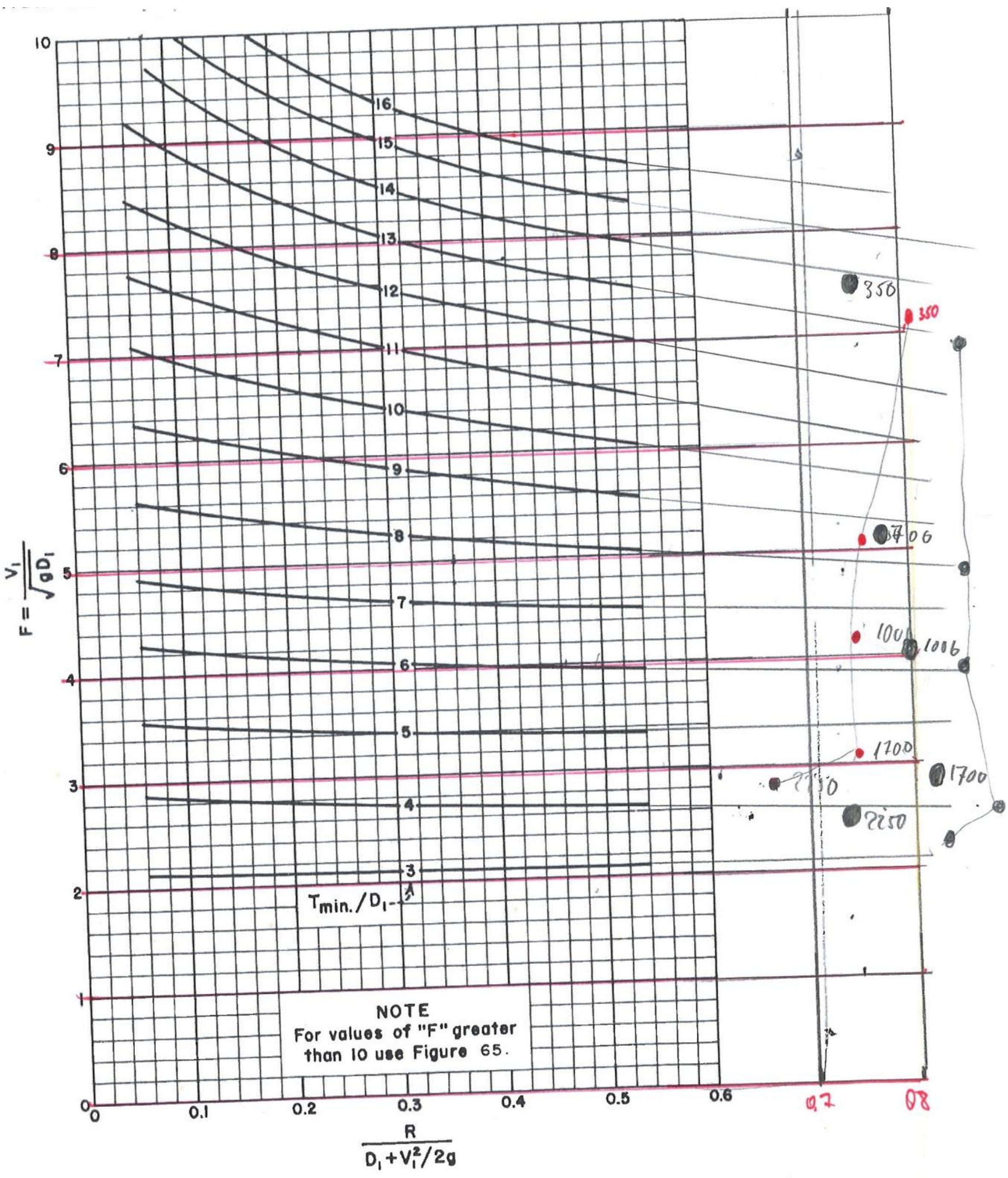

FIGURE 66.—*Minimum tail water limit.*

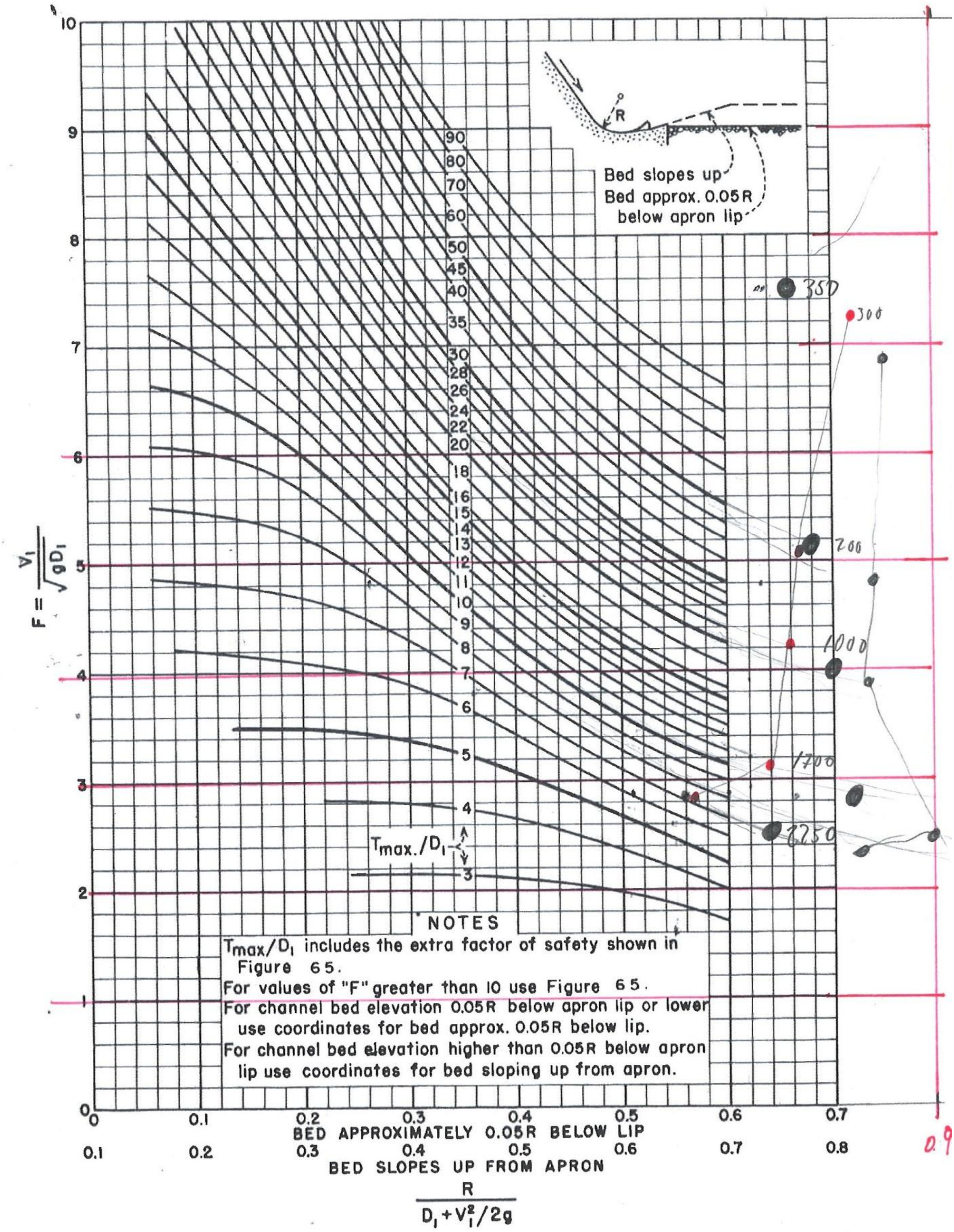

FIGURE 67.—*Maximum tail water limit.*

9 Drawings

Drawing 1

Location and numbering of cross sections

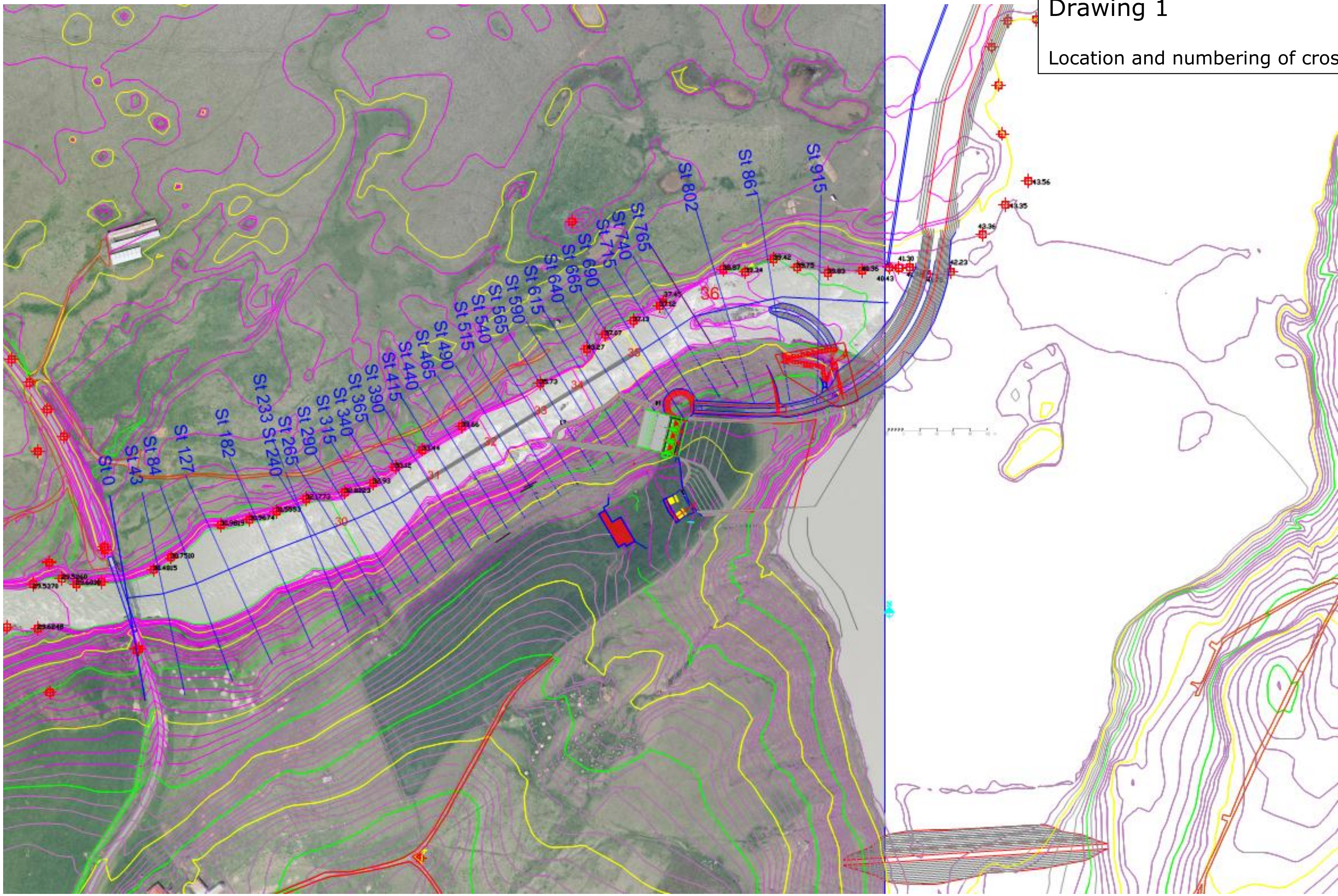

Verkís hf.
Ármúla 4, 108 Reykjavík
+354 422 8000
verkis.is | verkis@verkis.is

Offices:
108 Reykjavík, Ármúla 4-6
108 Reykjavík, Suðurlandsbraut 4

300 Akranes, Stillholti 18
310 Borgarnes, Bjarnarbraut 8
400 Ísafjörður, Hafnarstræti 1

603 Akureyri, Austursíðu 2
700 Egilsstaðir, Kaupvangi 3b
800 Selfoss, Austurvegi 10

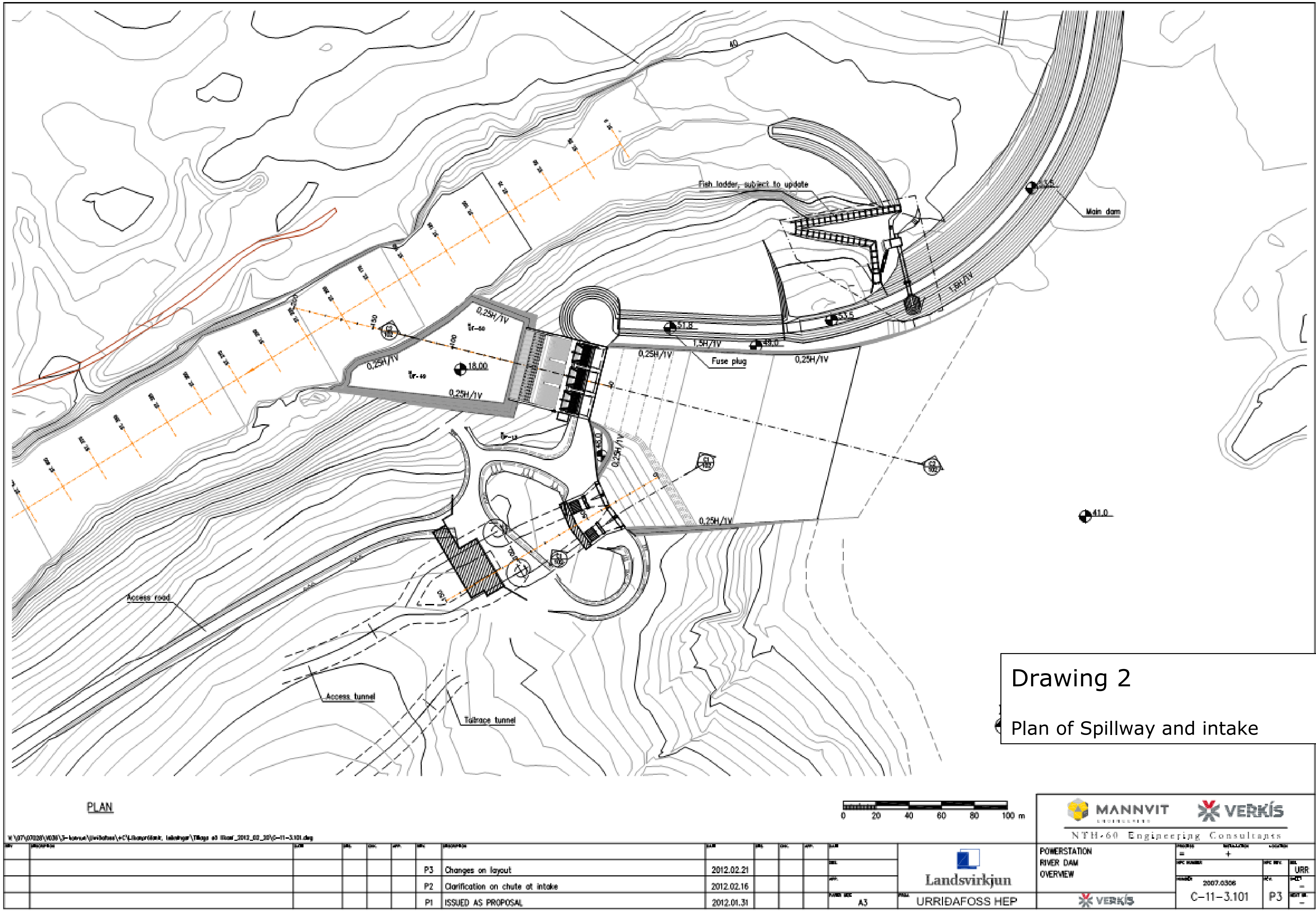

Drawing 2

Plan of Spillway and intake

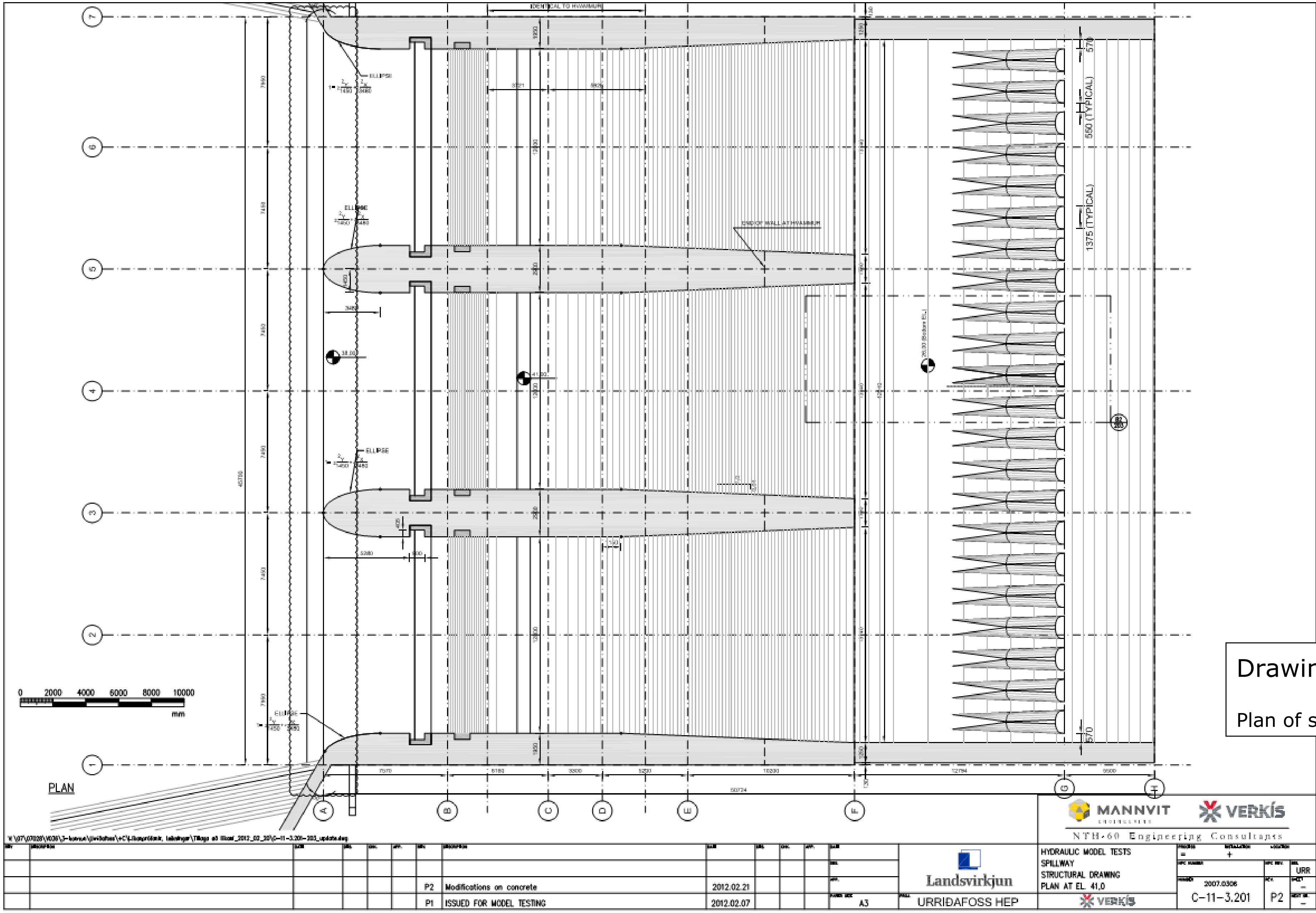

Drawing 3

Plan of spillway

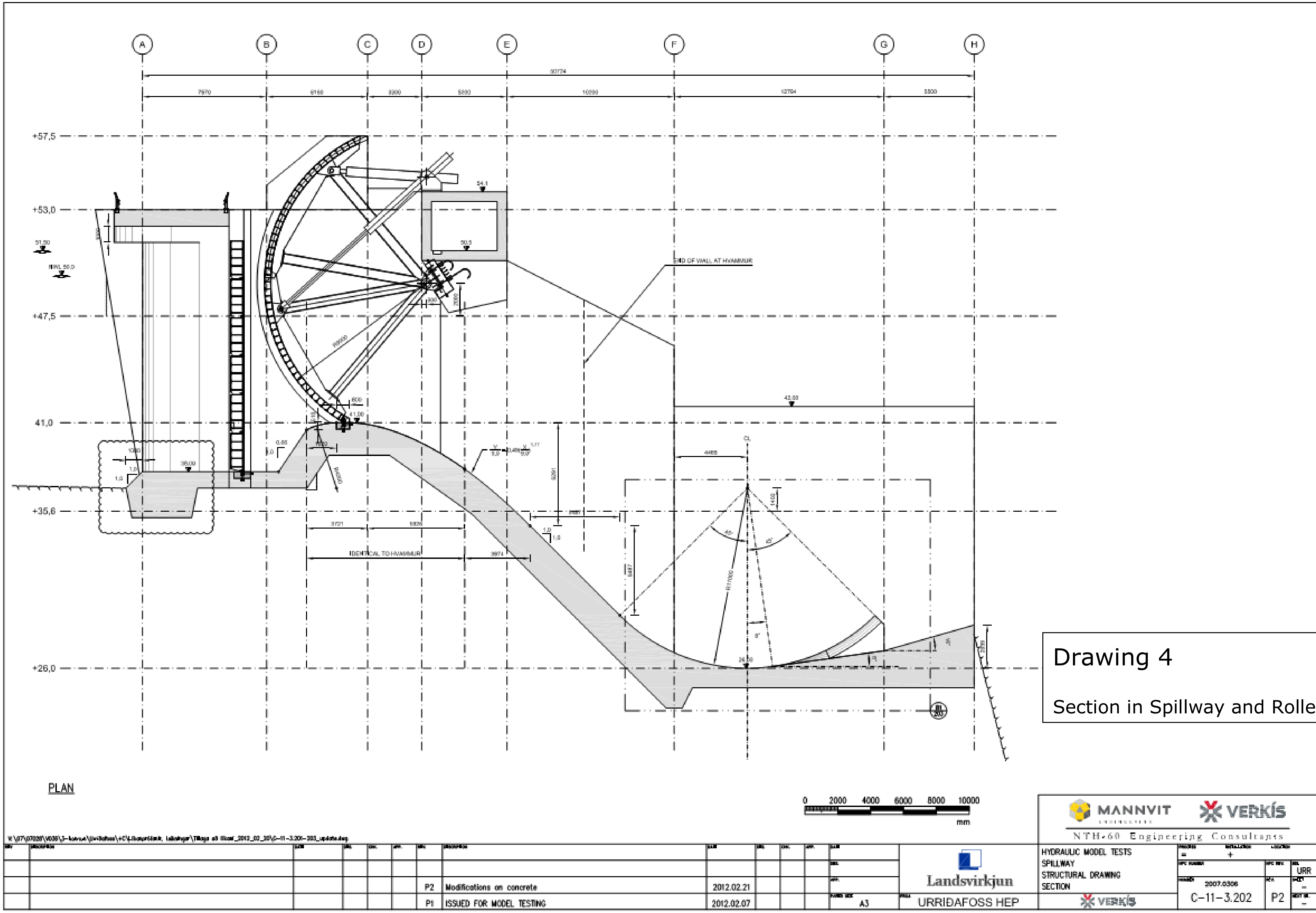

Drawing 4

Section in Spillway and Roller Bucket

Drawing 5

Details of roller bucket tooths

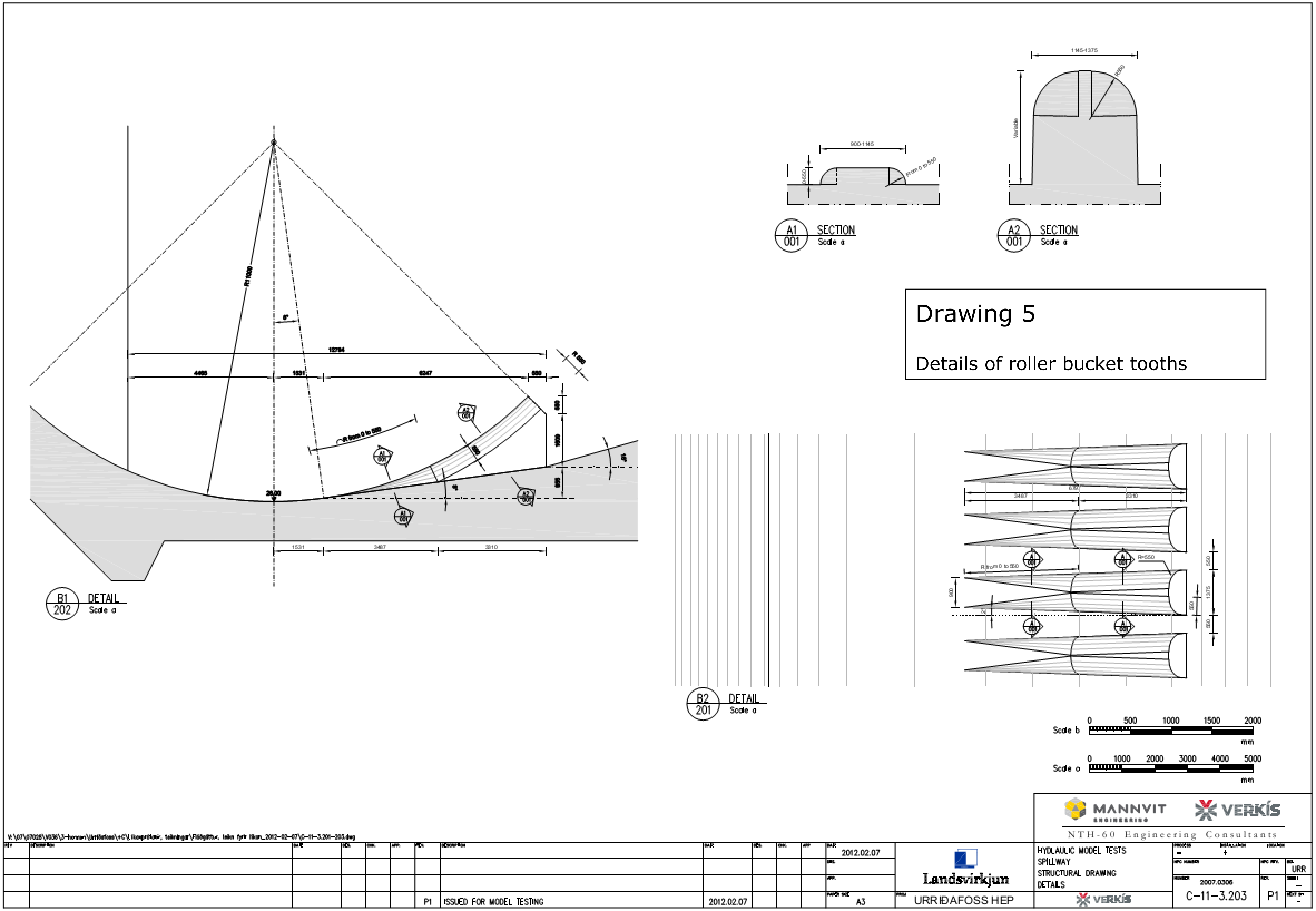

C. Tailwater level in roller bucket energy dissipation structure in Urriðafoss HEP

NTH-60 HPP IN NEÐRI-ÞJÓRSÁ

MEMO

PROJECT NO:	07028-036	DATE.:	2013-03-09
PROJECT PHASE:	117 Líkanprófanir	NO.:	MB-0603
AUTHOR:	Þorbergur Leifsson, Verkís.		
DISTRIBUTION:	Helgi Jóhannesson og Andri Gunnarsson LV, Kristján Már Sigurjónsson og Ólöf Rós Káradóttir Verkís, Einar Júlíusson Mannvit		

Tailwater level in roller bucket energy dissipation structure in Urriðafoss HEP

1 Introduction

The physical model tests of the spillway at Urriðafoss HEP are finished and the final report is being finalized. A large flood was observed in the Þjórsá river on the 26th of February 2013. It was estimated about 1300 m^3/s according to the new stage discharge relationship (VHM 30, Lykill 5). The water level in the river where the proposed spillway discharge canal will enter the river was surveyed during the flood. The expected tailwater level for the spillway can therefore be more accurately estimated based on the water level elevations during the large flood. The results of those measurements and comparison with water level estimates are presented in this Memo together with the tailwater level experienced during the model tests. Measured and calculated tailwater levels are also compared to the minimum required tailwater level (according to extrapolation of design charts) for different roller bucket elevation.

2 Measurements of water levels in Þjórsá river

The expected water levels in the natural river channel downstream from the proposed dam and down to the old national highway bridge have been calculated by using the HEC-RAS program. For location and number (St) of the cross sections, reference is made to *Drawing 1 in MB-0529 Roller bucket energy dissipater for Urriðafoss spillway 2012-03-01.*

The cross section profiles below the water surface have not been surveyed but the river bottom was assumed to be horizontal and the depth of the river was estimated based on measured water level at the right bank on May 8th 2008 during 465 m^3/s flow in the river. The river channel in the physical model was constructed according to the estimated river bed. The observed and calculated water levels are shown in *Figure 1*. A Manning number of 33 was used in the calculations.

Observed and calculated water levels in the large flood in 2013, of 1300 m^3/s, is shown on the same figure. Observations indicate that the water level at St 560 m where the spillway (discharge canal) opens into the channel is up to 1.0 m higher than has been estimated in earlier calculations, and which model tests are based on.

Verkís hf.
Ármúla 4, 108 Reykjavík
+354 422 8000
verkis.is | verkis@verkis.is

Offices:
108 Reykjavík, Ármúla 4-6
108 Reykjavík, Suðurlandsbraut 4

300 Akranes, Stillholti 18
310 Borgarnes, Bjarnarbraut 8
400 Ísafjörður, Hafnarstræti 1

603 Akureyri, Austursíðu 2
700 Egilsstaðir, Kaupvangi 3b
800 Selfoss, Austurvegi 10

VERKÍS

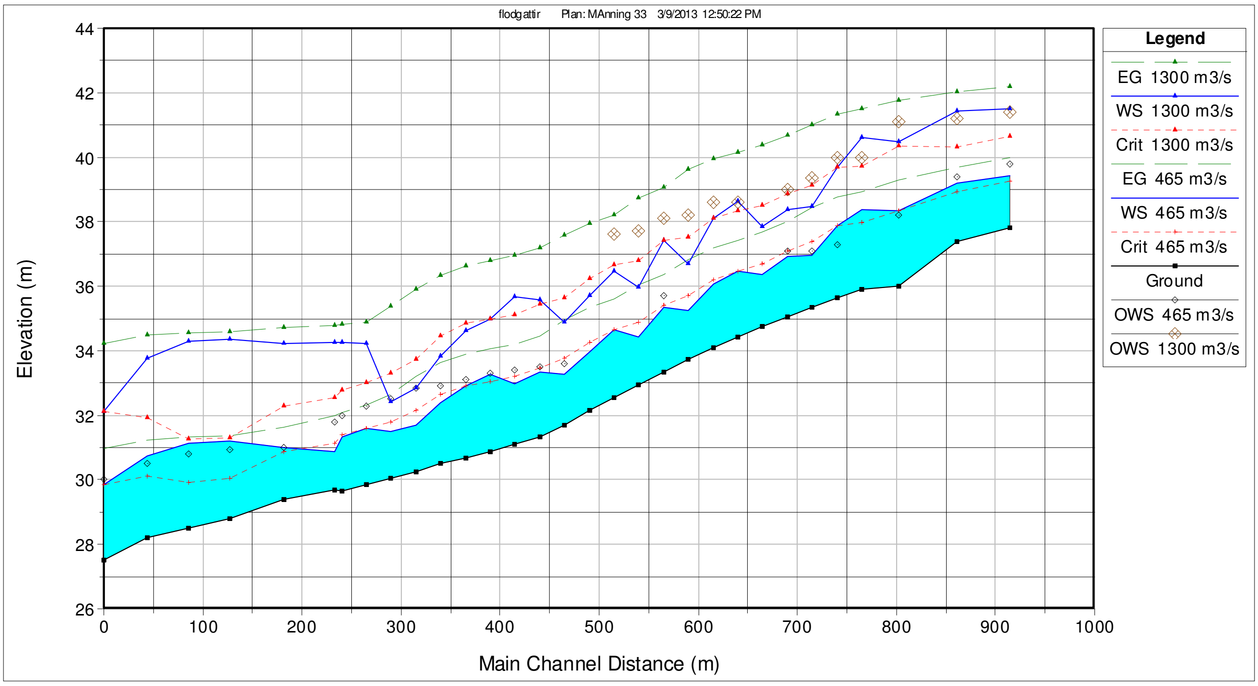

Figure 1 Observed (OWS) and calculated water level (WS) in Þjórsá river downstream of Heiðartangi dam The spillway enters the river at St 560 m. The observations and calculations are done for 465 m^3/s (old) and 1300 m^3/s discharge (new)

3 Tailwater elevations in model

Figure 2 shows the estimated tailwater level in the river using the HEC-RAS model, and the measured tailwater level in the physical model. The measured level seems to be about 1.0 m higher. The water level in the discharge canal is taken as the average value of five measured values at 40 and 50 m distance from the roller bucket (see the final report).

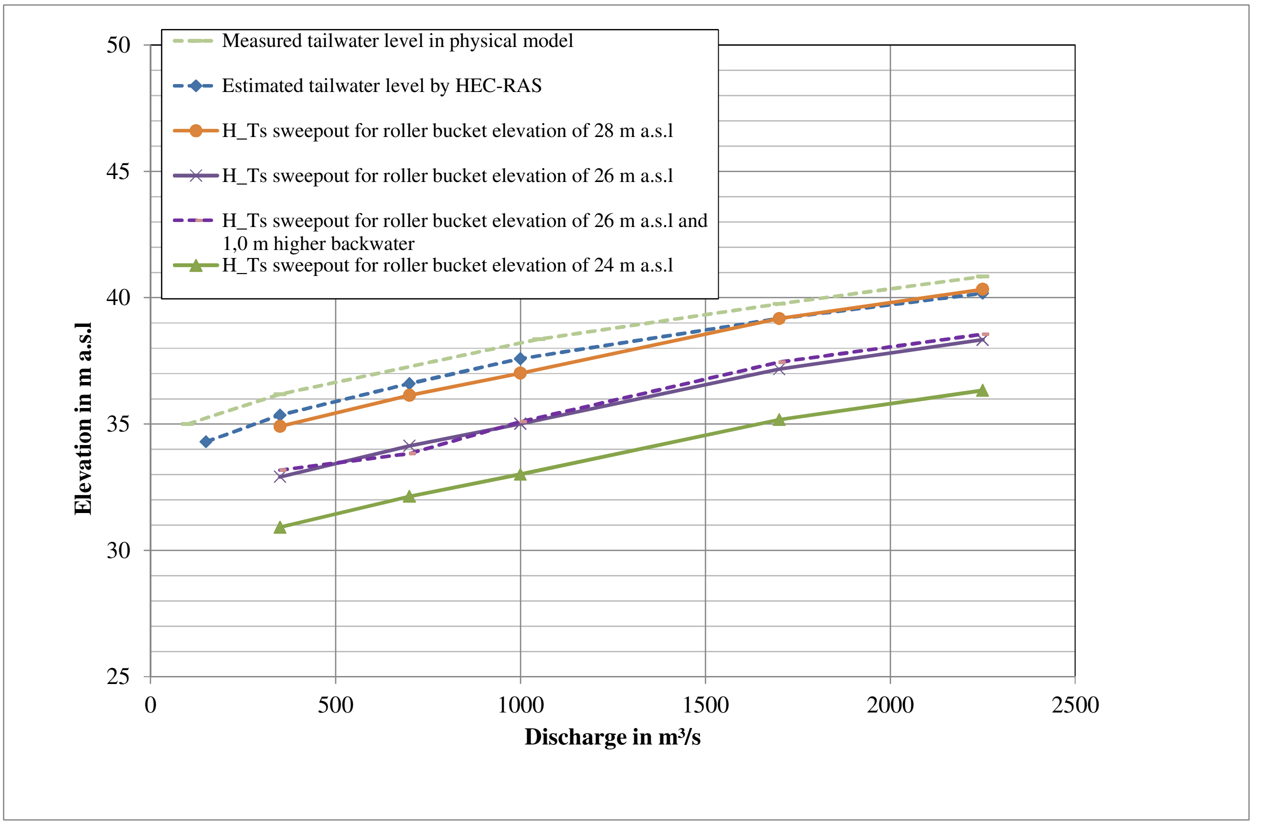

Figure 2 Estimated and measured tailwater levels in the discharge canal and the minimum tailwater level for preventing sweepout according to design charts.

The minimum tailwater elevations to prevent sweepout are shown for different roller bucket elevations; 24, 26 and 28 m a.s.l. The required elevations are the minimum sweepout elevations according to extrapolations of the design charts as shown in *MB-0529 Roller bucket energy dissipater for Urriðafoss spillway 2012-03-01*. For the 26 m a.s.l bucket elevation that was used in the final design the calculations are done for two different tailwater levels (the initial HEC-RAS estimate and the measured level in the physical model) and the results are identical as expected. The calculation imply that if the roller bucket elevation is increased or decreased by 2 m the required tailwater elevation to prevent sweepout does increase or decrease by the same amount.

Sweepout was only detected in the model tests in the largest flood and bucket elevation of 28 m a.s.l. The figure shows that the sweepout should not have happened according to the measured water level, but should have happened for this case only for the HER-RAS estimated level. The results are therefore in fairly good agreement with the calculations.

4 Conclusion

The measured tailwater level in the model seems to be about 1.0 m higher than initially estimated using HEC-RAS. However new measurements of the water level in the river during a recent large flood indicate that the actual tailwater level might also be up to 1.0 m higher than the initial estimate at least for medium and large floods. The measured tailwater level in the model is therefore probably very similar to the expected values in the prototype.

The measurements and calculations of minimum sweepout water levels seem to be in good agreement.

D. Acoustic Doppler velocimeter

D.1. Introduction

Acoustic Doppler Velocimeter (ADV) is a single point, high resolution, three dimensional current meter.

The ADV measures the velocity of water using a physical principle called the Doppler effect. If a source of sound is moving relative to the receiver, the frequency of the sound at the receiver is shifted from the transmit frequency by the amount (Sontek 2001).

$$F_{Doppler} = -F_{Source}(\frac{V}{C}) \tag{D.1}$$

where $F_{Doppler}$ is the change in received frequency, F_{Source} is the frequency of transmitted sound, V is the velocity of source relative to the receiver and C is the speed of sound in the current media.

To some extent, ADV's can substitute the roles of a range of other instruments for velocity measurements, including propeller type current meters, hot-film probes, electromagnetic current meters, and laser-doppler velocimeters, depending on the methods used to collect and process the data. The primary data collected by an ADV is a time series of velocity vector components either in 2D or 3D depending on the instrument (Wahl 2000).

The ADV is non-intrusive measurement technique, which can sample data up to 100 Hz and has a relatively small sampling volume. Location of the sampling volume varies with instrument type but is usually 5-10 from the transducer. Figure D.1 shows a setup of an ADV for laboratory use. The transducers are mounted such that their beams intersect at a volume of water located some distance away. This beam intersection determines the location of the sampling volume (the volume of water in which measurements are made). The transmitter generates a short pulse of sound at a known frequency, which propagates through the water along the axis of its beam. As the pulse passes through the sampling volume, the acoustic energy is reflected in all directions by particulate matter (sediment, small organisms, bubbles, etc.). Some portion of the reflected energy travels back along the receiver axis, where it is sampled by the ADV and the processing electronics measure the change in frequency. The Doppler shift measured by one receiver is proportional to the velocity of the particles along the bistatic axis of the receiver and transmitter (Sontek 2001).

Since their introduction in 1993, acoustic Doppler velocity meters (ADV's) have quickly become valuable tools for laboratory and field investigations of flow in rivers, canals, reservoirs, the oceans, and around hydraulic structures and in laboratory scale models. ADV's are capable of

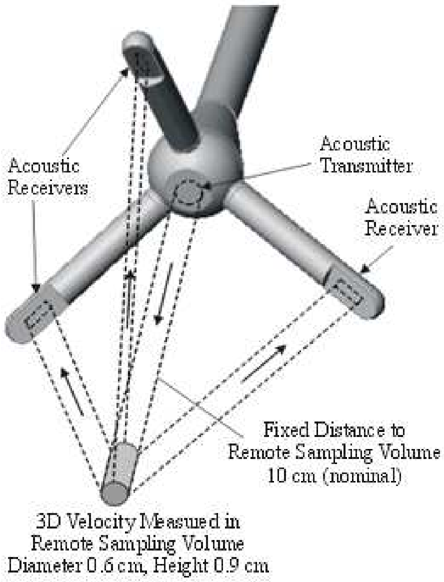

Figure D.1: *Definition sketch for an ADV*

reporting accurate mean values of water velocity in three dimensions (García, Cantero, Nino & Garcia 2005), (Liu, Zhu & Rajaratnam 2004). However in complex flow regimes with high air entrainment, such as in a hydraulic jump the instruments capability to accurately resolve flow turbulence is still uncertain. Arguments have been made by (García et al. 2005) that the ADV resolution is sufficient to capture a significant fraction of the turbulent kinetic energy of the flow. By filtration of the acquired time series the data can be corrected for spikes in the data caused by air bubbles in the sampling volume. WinADV32 is a software developed by the Bureau of Reclamation department of the U.S. Department of the Interior and is endorsed by major manufactures of ADV instruments. WinADV32 loads the raw data files from the data acquisition software and filters and processes the data. A correlation score is calculated aimed at identifying the quality of each individual measurement and compared to the sound to noise ratio (SNR) of the received signal of the ADV. Further processing thresholds are left for the user to filter the data at ones own convenience. Out through the study presented here a SonTek/YSI 16-MHz MicroADV was used, data was acquired with Sontek's HorizonADV software and processed with WinADV32 by the USBR.

D.2. Calculations with ADV

Out through this study, turbulence kinetic energy (TKE) is defined as mean kinetic energy per unit mass associated with eddies in turbulent flow. The turbulent kinetic energy is characterised by root-mean-square (RMS) velocity fluctuations in the longitudinal, lateral and vertical directions. Generally, the TKE can be quantified by the mean of the turbulence normal stresses:

$$TKE = \frac{1}{2}((\sqrt{u'^2})^2 + (\sqrt{v'^2})^2) + (\sqrt{w'^2})^2) \tag{D.2}$$

where TKE is turbulent kinetic energy per unit mass and $(\sqrt{u'^2})^2$, $(\sqrt{v'^2})^2$ and $(\sqrt{w'^2})^2$ are root mean squares of the velocity fluctuations in the longitudinal, lateral and vertical directions, respectively (Urban, Wilhelms & Gulliver 2005). Turbulence is a result of interaction between viscosity and inertial reactions and is therefore described by the Reynolds number.

Fluctuations of velocity (RMS) is calculated as shown in Equation D.3 according to Urban et al. (2005):

$$RMS[V_i'] = \sqrt{(\bar{V_i'})^2} = \sqrt{\frac{\sum V_i^2 - (\sum V_i)^2/n}{n-1}} \tag{D.3}$$

where V_i is the velocity component defined by the index i and n is number of samples for the time series. The root-mean-square of the turbulent velocity fluctuations about the mean velocity are computed for use in determining turbulence intensities and levels of turbulent kinetic energy. The RMS value is equal to the standard deviation of the individual velocity measurements and is believed to indicate energy dissipation extent.

E. Scale effects

E.1. General

In free-surface flows, gravity effects are predominant. Similarity in physical models is performed usually with a Froude similitude ensuring the ratio between inertia and gravity to be the same for the model and the prototype (ASCE 2000). Scale effects in hydraulic models are defined as distortions introduced by effects other than the dominant model law. They occur where one or more dimensionless parameter differs between the model and the prototype. In most cases scale effects are small but not always negligible (Chanson 2004). In general, for a hydraulic model with a scale factor of $\lambda = 40$, verification needs to done to ensure and realize possible scale effects and their influence on the study. Examples of scale effects include scaling from model to prototype of friction, turbulence, cavitation, air entrainment and air release, fluid structure interaction and local scouring (Khatsuria 2005).

E.2. Air Entrainment and Turbulence

The modelling of free surface and forced aeration in hydraulic jumps is unachievable with geometrically similar models as the turbulence structure and its dynamics is presented by the Reynolds number which is underestimated in Froude similarity models. Table E.1 shows comparison of the calculated Reynolds numbers for the prototype and for the model.

Table E.1: *Comparison of calculated Reynolds numbers in the prototype and the model for Q_{50} and Q_{1000}.*

	Reynolds number	
Discharge m^3/s	Prototype	Model
2250	2.8.E+07	1.1.E+05
1600	2.5.E+07	9.8.E+04

Direct scaling of air - water flow properties in hydraulic jumps is hard considering the large number of relevant parameters such as inflow depth, inflow velocity, the characteristic turbulent velocity and the boundary layer thickness. Further more air entrainment in hydraulic jumps is related by a number of dimensionless parameters such as Morton number, Froude number and Reynolds number which are impossible to satisfy all at once (Chanson & Gualtieri 2008), (Pfister & Hager 2010),(Falvey 1980), (Chanson 2006). Effect of air entrained flow on stilling basin performance is limited and can in general practical applications be assumed irrelevant (Falvey 1980).

Turbulence is characterized by the Reynolds number as it results from viscosity and inertial relations. In Froude models the Reynolds number is always smaller than that derived from the prototype and therefore turbulence properties are not expected to be correctly simulated (Khatsuria 2005). It has been shown that physical models scaled according to Froude similarity can represent measured mean values (pressure and velocity) quite correctly if the values are large enough (fully turbulent model) (Khatsuria 2005), (García et al. 2005), (Liu et al. 2004).

In the study presented in this thesis the measurements of turbulence are presented for comparison between layouts with similar flow properties but not for quantification of turbulence.

E.3. Roughness

The scaling of roughness in Froude models is derived from Manning's equation:

$$V_r \frac{R_r^{2/3} S_r^{1/2}}{M_r} \tag{E.1}$$

where subscript r indicates the ratio of prototype to model, R is the hydraulic radius, S is the friction slope and M is the Manning's M. The relation of Manning's M in prototype and model is $L_r^{1/6}$ where L_r is the scale factor. Even though this relation is fulfilled in the model (which it is usually not), the energy loss due to friction is not fulfilled as it is represented by the Reynolds number (Khatsuria 2005). By assuming k_s^{model} as 0.003 m, $k_s^{prototype}$ as 0.3 m (k_s is the equivalent surface roughness height) and by utilizing the Colebrook-White formula a friction factor for the model and prototype can be assumed in respect to the calculated Reynold numbers shown in table E.1. Calculations show that the head loss due to friction is theoretically 10-25 percent percent more in the prototype than in the model in the downstream channel for the design flood. The theoretical approach assumes all the cross section area is active in the discharge channel in dissipating energy. Observations in the physical model show stagnant flow at the sloping sides of the channel indicating that the actual participating cross section is less. It can also be assumed that the headloss in the upstream spillway approach channel is underestimated in the physical model, resulting in a slight overestimation in the dischargecapacity.

E.4. Reduced flow of Surface flow outlet (SFO)

The measured discharge capacity of the SFO at Urriðafoss HEP is about 25 % less than calculated in the original design. The designers determine the spillway SFO discharge capacity by:

$$Q = C_d(L - 2(nK_p + K_a)H)H^{1.5} \tag{E.2}$$

where Q is discharge [m^3/s], C_d is a dimensionless discharge coefficient based on various geometries of the spillway design, L is the length [m] of the spillway, n is the number of piers, K_p is a dimensionless contraction coefficient due to effect of piers, K_a is a dimensionless contraction coefficient due to side wall configuration and H is the head [m] on the spillway including the velocity head of the approach flow. This setup is adopted from Design of Small Dams, published by the USBR and provides normalized design data (Peterka 1958).

The SFO has some unconventional features in comparison with conventional free flow ogee crested spillways:

- **Crest geometry:** The crest shape follows a fixed radius and is not a conventional ogee shape profile. Both the upstream and downstream ends have a constant radius instead of a profile of a free trajectory. This could result in pressures on the spillway crest influencing the capacity of the spillway, this is though believed to have limited influence. Because of the geometric design the layout is closer to a short crest weir design than a conventional spillway design. During the physical model tests at Hvammur, the previous design version of the intake was tested. This layout had the crest at 49.0 m a.s.l. and had a sharp crested design. The discharge capacity of this design layout was found to be sufficient. These results are summarized in a review report for the intake distributed in October 2011.

- **Alignment to flow**: Another feature is that the spillway crest is not perpendicular to the approach flow. In general, recommendation is made by design guidelines that the approach flow is perpendicular to the spillway crest (USBR, 1987). Quantification of the effect on capacity is very hard but believed to have limited effect on the capacity.

- **Pier configuration:** The pier thickness is greater than recommended by various references. At URR SFO the thickness of the piers is 1.8 m while the design head is 0.9 m. This gives a ratio of 2 while the recommend ratio is 1/3 of the design head for the contraction coefficients to apply (Chow, 1959).

E.4.1. Scale effects SFO

In free-surface flows, gravity effects are predominant. Similarity in physical models is usually obtained with a Froude similitude ensuring the ratio between inertia and gravity to be the same for the model and the prototype (ASCE 2000). The model at Urriðafoss is scaled according to Froude law. Consequently, air transport, skin friction and form drag in physical models may be affected by scale effects because the internal flow turbulence is underestimated, represented by the Reynolds number while the surface tension, represented by the Weber number, is overestimated.

Table E.2: *Calculated Reynolds and Weber numbers for model and prototype at Urriðafoss HEP surface flow outlet.*

	Prototype	Model
Reynolds number, Re	1.5 E+09	6.1 E+03
Weber number, We	5.3E+04	33

Because a strict dynamic similitude exists only at a full-scale, the impact of scale effects is minimized if limitations in terms of Weber or Reynolds are respected.

In general the following classification applies:

Range of Re	
$100 < \mathrm{Re} < 10^3$	Laminar flow, boundary layer theory useful
$10^3 < \mathrm{Re} < 10^4$	Transition to turbulence
$10^4 < \mathrm{Re}$	Fully turbulent

In modeling open channel flow the model needs to have Reynolds numbers where $Re_m > 5000$ is fulfilled to ensure no scale effects to take place. (Chanson, Hydraulics of Open Channel Flow, 2004). Roughness is usually underestimated within a Froude scaled physical model. At Urriðafoss the model is made out of PVC plastic having an absolute roughness height of 0.0015 -0.007 mm while concrete, the prototype material, has an absolute roughness height of 0.3 - 1 mm (values estimated from literature). The ratio of absolute roughness height between model and prototype is therefore of the order of 100-200 but should scale according to the geometric scaling (1/40). Therefore, prototype headloss due to roughness in the intake and SFO is equal or greater than in the model. Limitations of Weber numbers for scale effects taking place can be found in various references. A Weber number between 10.5 and 13 is suggested by (Chanson,2009) and a Weber number of 12 is recommended by (Pavel Novak, 2010) to minimize risk of distortions. A minimum water depth for free flow spillways is recommended as 25 mm by ASCE (Ettema, 2000). The influences and their extents are not discussed.

E.4.2. Concluding remarks

The previous remarks lead to the conclusion that the accuracy of the model investigations is good. Precise quantification of scale effects is hardly possible, but they may account for 5-10 % reduction in discharge capacity in the model as compared to the prototype, but not all the reduction in discharge capacity experienced in the model. As discussed in the previous sections, the design of the SFO is not conventional and contraction coefficients and discharge coefficients may not directly apply to the layout of the design. Furthermore, the geometric layout of the crest has much more similarities with a broad/short crested weir than a conventional spillway profile. This is believed to account for a large part of the reduction of discharge in comparison with conventional discharge rating formulas.

F. Model construction

Building of the model started in the early February 2012 and was finished early May 2012. In Section 2.2 overview of building the model is reviewed and most elements and parts in the model described. Below are figures from the building phase, which cover the 3 month building period.

Figure F.1: *Deconstruction of Hvammur HEP physical model.*

Figure F.2: *Construction of Urriðafoss HEP physical model begins. Expansion of downstream reservoir tank and topography platform undergoing.*

Figure F.3: *Building of reservoir topography.*

Figure F.4: *Building of reservoir topography.*

Figure F.5: *Building of downstream topography begins.*

Figure F.6: *Building of downstream river section and upstream approach walls.*

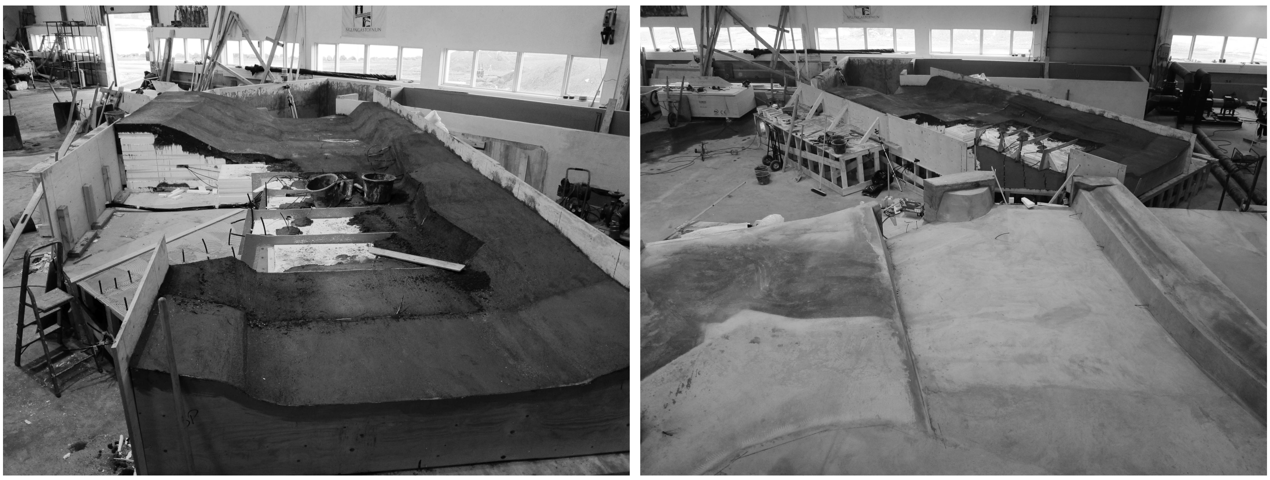

Figure F.7: *On left: Construction of downstream river section. On right: Reservoir and approach flow channel.*

Figure F.8: *On left: Overview of finished topography. On right: The spillway lowered into place.*

Figure F.9: *On left: Spillway structure and excavated channel. On right: Intake structure in place with modifications made at left approach wall.*

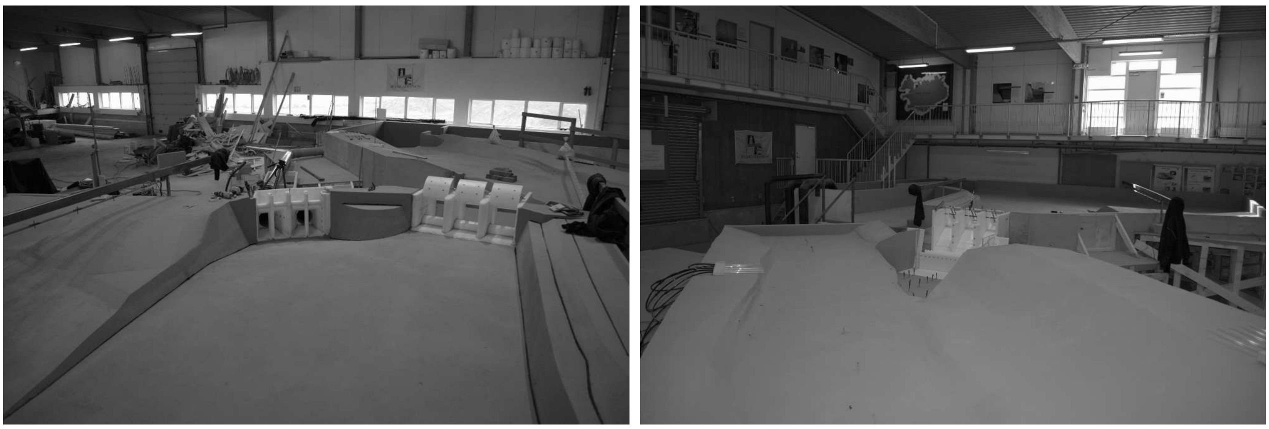

Figure F.10: *Overview of approach flow channel and downstream river section.*

Figure F.11: *Overview of Urriðafoss HEP physical model.*

G. Drawing sets

Drawings and modifications are published out through the project by the designers. Table G.1 gives an overview of the main drawings issued out through the project and details of the final design.

Table G.1: *List of drawings.*

Drawing number	Version	Description
Drawings of original design from contract documents		
G-81-3.001	B1	Overview of Urriðafoss forebay
C-81-3.002	B1	Spillway, sections
C-81-3.202	B1	Power intake, plan at el. 38.35 m a.s.l.
C-81-3.221	B1	Power intake, section
C-81-3.223	B1	Juvenile fish passage, section
Drawings of revised design		
C-11-3.101	P1	Power station, river dam, overview
C-11-3.101	P2	Power station, river dam, overview
C-11-3.101	P3	Power station, river dam, overview
C-11-3.101	P4	Power station, river dam, overview
C-11-3.103	P2	Hydraulic model tests, spillway excavation, overview
C-11-3.104	P1	Hydraulic model tests, spillway excavation, plan & section
C-11-3.103	P1	Hydraulic model tests, spillway excavation, overview
Drawings of final design		
C-11-3.101	P7	Power station, river dam, overview
C-11-3.201	P2	Hydraulic model tests, spillway, structural drawing, plan at el. 41,0
C-11-3.202	P2	Hydraulic model tests, spillway, structural drawing, section
C-11-3.203	P1	Hydraulic model tests, spillway, structural drawing, details
C-11-3.251	P4	Power station, power intake, layout, plan el. 38,35
C-11-3.252	P6	Power station, power intake, layout, plan el. 50,80
C-11-3.253	P3	Power station, power intake, layout, plan el. 53,00
C-11-3.261	P4	Power station, power intake, layout, section A1
C-11-3.271	P3	Power station, power intake, layout, section B1
C-11-3.272	P3	Power station, power intake, layout, section B2
C-11-3.273	P2	Power station, power intake, layout, section B3

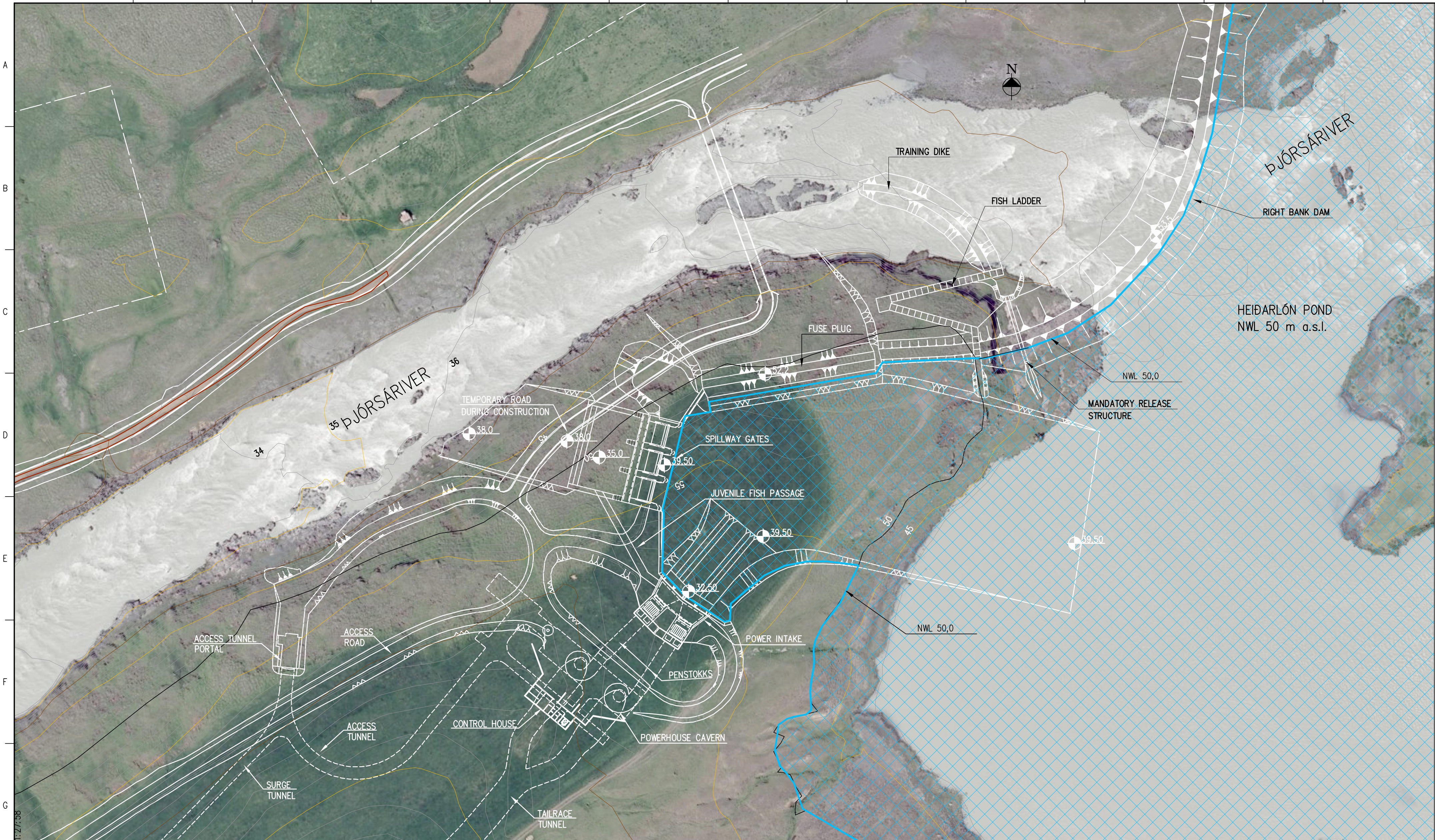

0 20 40 60 80 100 m

DRAFT

6.11.2008 11:27:58

K:\2007.03\06\vinna\Líkanprófanir\NTH-81\Drawings\Proposal\C-81-3.001b.dwg

VST Consulting Engineers Ltd. VGK HÖNNUN RAFTEIKNING HF RT

NTH-60 Engineering Consultants

REV.	DESCRIPTION	DATE	DES.	CHK.	APP.
B1	Issued for tender	2008-11-14	ÞSL	ÞSL	

DATE	2008-11-04
DES.	ÞSL
APP.	KMS
PAPER SIZE	A3

Landsvirkjun

PROJ. URRIÐAFOSS

HYDRAULIC MODEL TEST
FOREBAY
OVERVIEW
PLAN

VST Consulting Engineers Ltd.

PROCESS	INSTALLATION	LOCATION
=	+	

NPC NUMBER	NPC REV.	BDL
		URR

NUMBER	REV.	SHEET
2007.0306 G-81-3.001	B1	–

NEXT SH. –

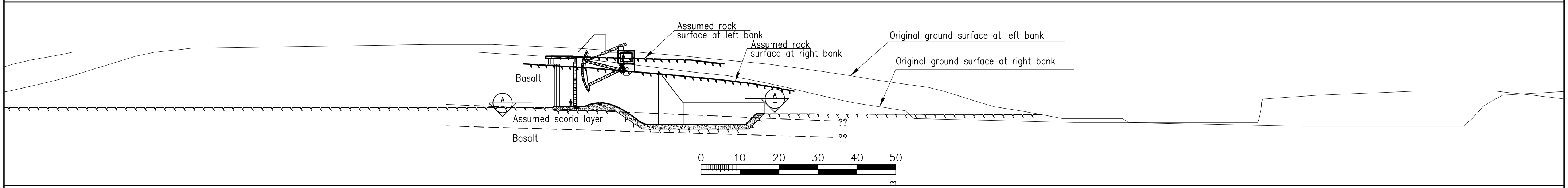

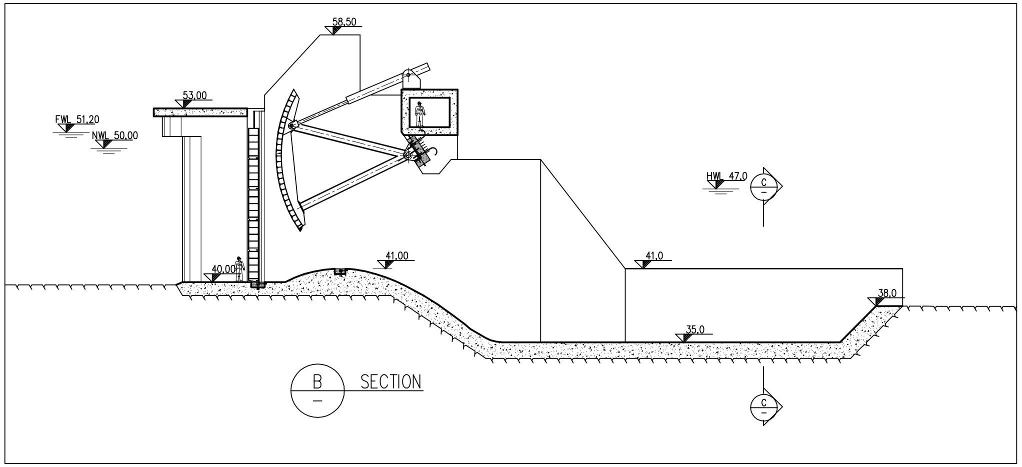

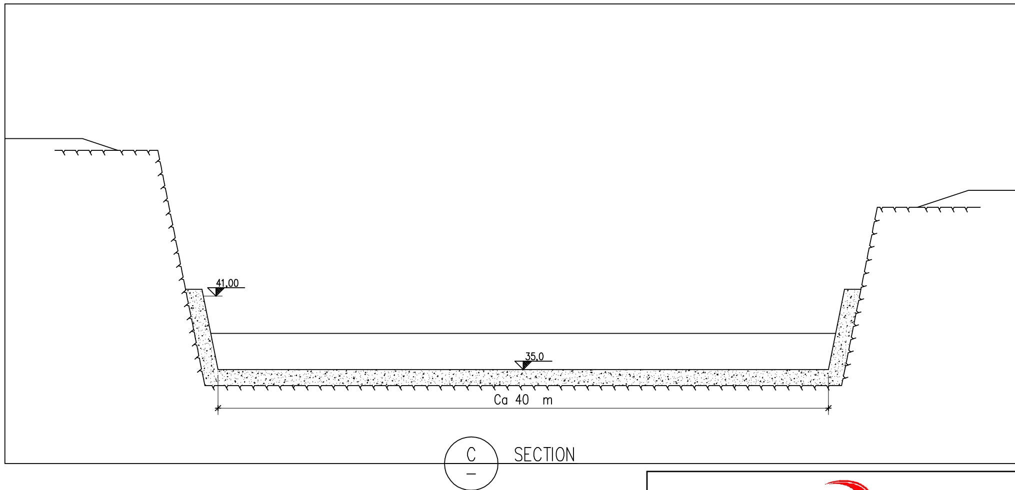

0 5 10 15 20
m

K:\2007.03\06\vinna\Líkanprófanir\NTH-81\Drawings\Proposal\C-81-3.002.dwg

VST Consulting Engineers Ltd. VGK HÖNNUN RAFTEIKNING HF

NTH-60 Engineering Consultants

REV.	DESCRIPTION	DATE	DES.	CHK.	APP.
B1	ISSUED FOR TENDER	2008-11-14	ÞSL	SH	KMS

DATE: NOVEMBER 2008
DES.: ÞSL
APP.: KMS
PAPER SIZE: A3

Landsvirkjun

PROJ.: URRIÐAFOSS

HYDRAULIC MODEL TEST
SPILLWAY
SECTIONS

VST Consulting Engineers Ltd.

PROCESS	INSTALLATION	LOCATION
=	+	

NPC NUMBER:
NPC REV.:
BDL: URR
NUMBER: 2007.0306 — C-81-3.002
REV.: B1
SHEET: –
NEXT SH.: –

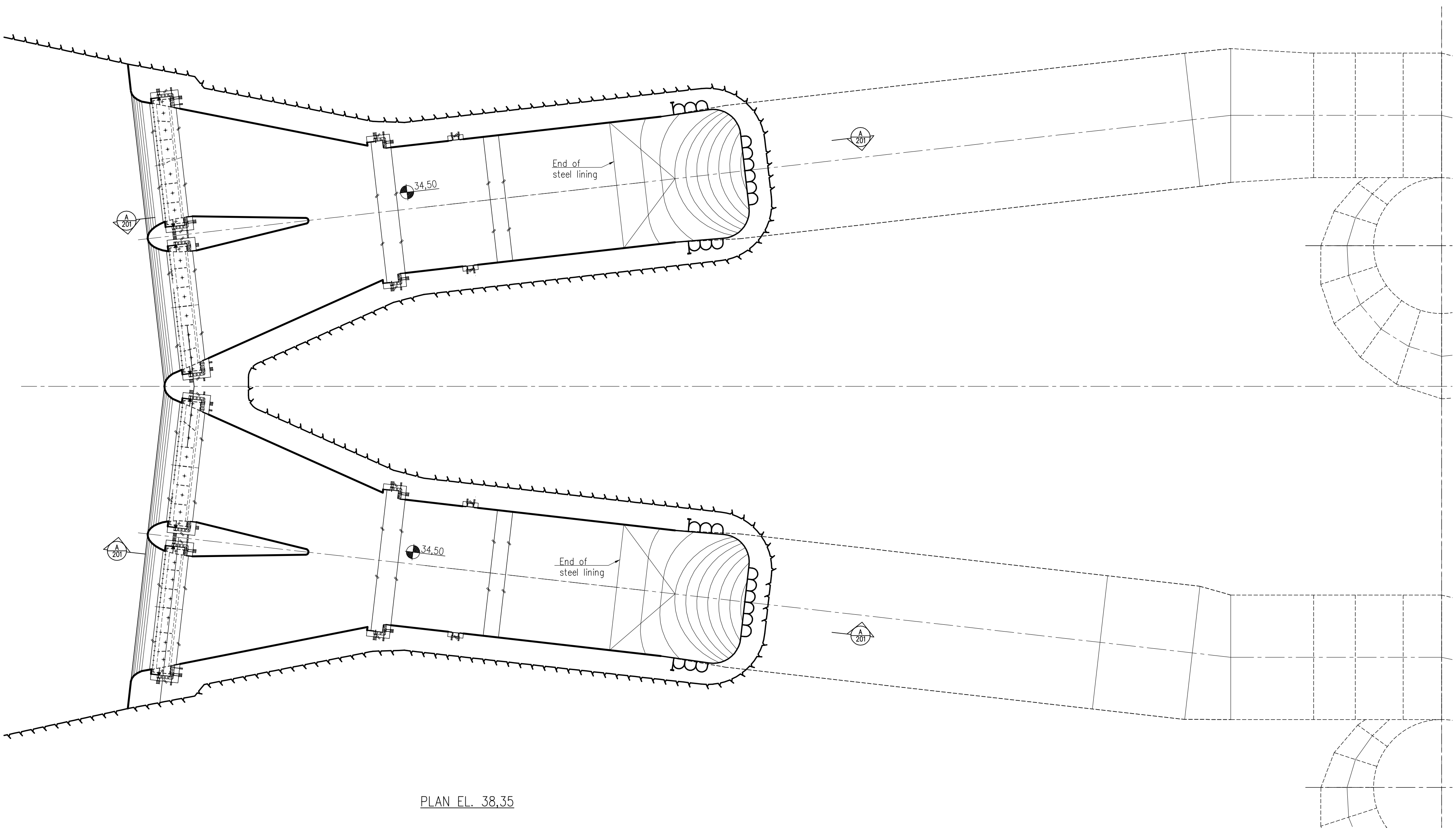

PLAN EL. 38,35

K:\2007.03\06\vinna\Líkanprófanir\NTH-81\Drawings\Proposal\C-81-3.222.dwg

REV	DESCRIPTION	DATE	DES.	CHK.	APP.
B1	ISSUED FOR TENDER	2008-11-14	SH	EBJ	KMS

DATE: NOVEMBER 2008
DES.: SH
APP.: KMS
PAPER SIZE: A3

Landsvirkjun

PROJ.: URRIÐAFOSS

VST Consulting Engineers Ltd. VGK HÖNNUN RAFTEIKNING HF RT

NTH-60 Engineering Consultants

HYDRAULIC MODEL TEST
POWER INTAKE

PLAN EL. 38,35

VST Consulting Engineers Ltd.

PROCESS: =
INSTALLATION: +
LOCATION:
NPC NUMBER:
NPC REV.:
BDL: URR
NUMBER: 2007.0306 C-81-3.202
REV.: B1
SHEET: –
NEXT SH.: –

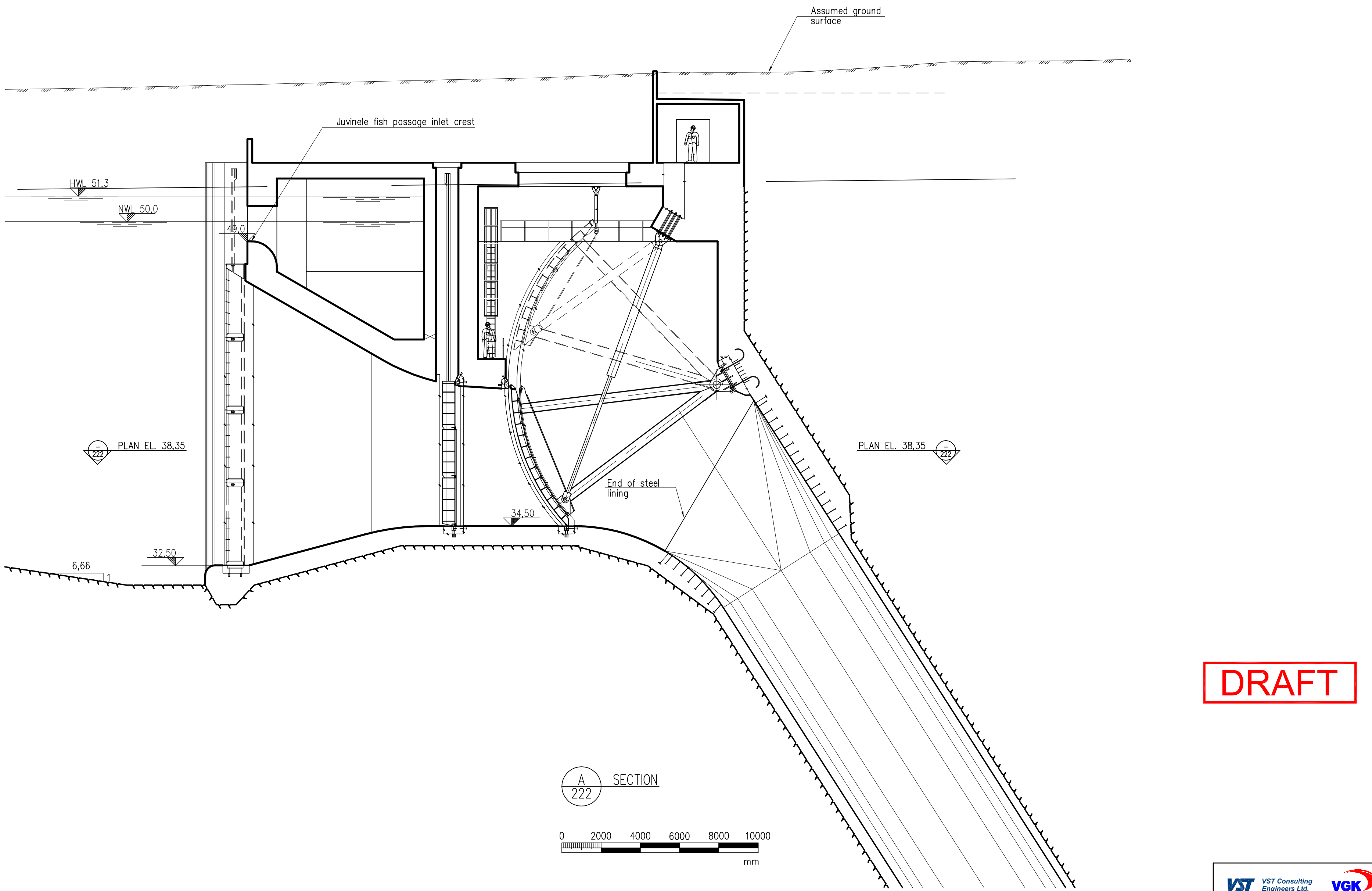

K:\2007.03\06\vinna\Líkanprófanir\NTH-81\Drawings\Proposal\C-81-3.221.dwg

REV.	DESCRIPTION	DATE	DES.	CHK.	APP.
B1	ISSUED FOR TENDER	2008-11-14	SH	EBJ	KMS

DATE	NOVEMBER 2008
DES.	SH
APP.	EBJ
PAPER SIZE	A3

Landsvirkjun

PROJ. URRIÐAFOSS

VST Consulting Engineers Ltd. VGK HÖNNUN RAFTEIKNING HF

NTH-60 Engineering Consultants

HYDRAULIC MODEL TEST
POWER INTAKE
SECTION

VST Consulting Engineers Ltd.

PROCESS	=
INSTALLATION	+
LOCATION	
NPC NUMBER	
NPC REV.	
BDL	URR
NUMBER	2007.0306 C-81-3.221
REV.	B1
SHEET	–
NEXT SH.	–

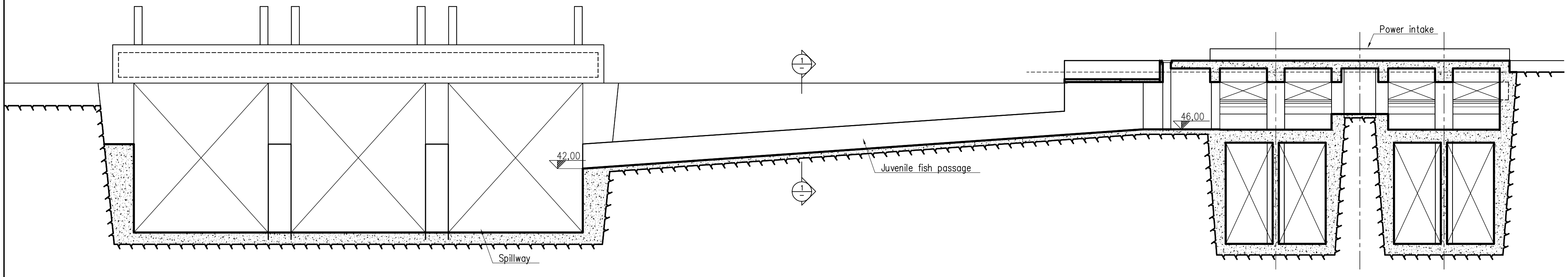

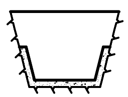

1 – SECTION

DRAFT

K:\2007.03\06\vinna\Líkanprófanir\NTH-81\Drawings\Proposal\C-81-3.223.dwg

REV.	DESCRIPTION	DATE	DES.	CHK.	APP.
B1	ISSUED FOR TENDER	2008-11-14	SH	EBJ	KMS

DATE: NOVEMBER 2008
DES.: SH
APP.: KMS
PAPER SIZE: A3

Landsvirkjun

PROJ.: URRIÐAFOSS

VST Consulting Engineers Ltd. VGK HÖNNUN RAFTEIKNING HF RT

NTH-60 Engineering Consultants

HYDRAULIC MODEL TEST
JUVINELE FISH PASSAGE
SECTIONS

VST Consulting Engineers Ltd.

PROCESS: = INSTALLATION: + LOCATION:
NPC NUMBER: NPC REV.: BDL: URR
NUMBER: 2007.0306 C-81-3.223 REV.: B1 SHEET: – NEXT SH.: –

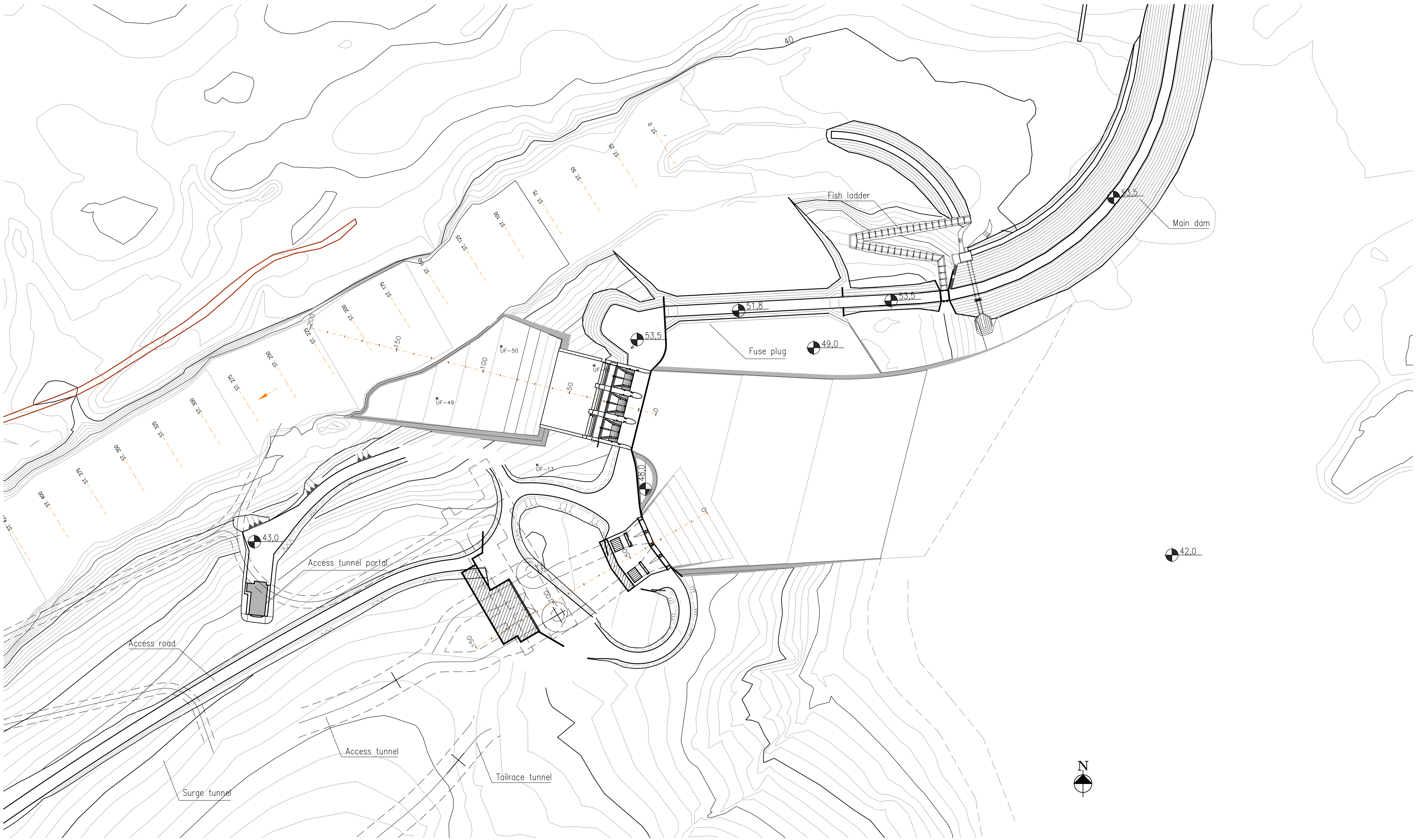

PLAN

0 20 40 60 80 100 m

V:\07\0707\0306\...\C-11-3.101-2012-01-31.dwg

REV.	DESCRIPTION	DATE	DES.	CHK.	APP.
P1	ISSUED AS PROPOSAL	2012.01.31			

MANNVIT ENGINEERING · VERKÍS

NTH-60 Engineering Consultants

Landsvirkjun

PROJ. URRIÐAFOSS HEP

POWERSTATION
RIVER DAM
OVERVIEW

PROCESS	=
INSTALLATION	+
BDL	URR
NUMBER	2007.0306
PAPER SIZE	A3
DRAWING NO.	C-11-3.101
REV.	P1
SHEET	–
NEXT SH.	–

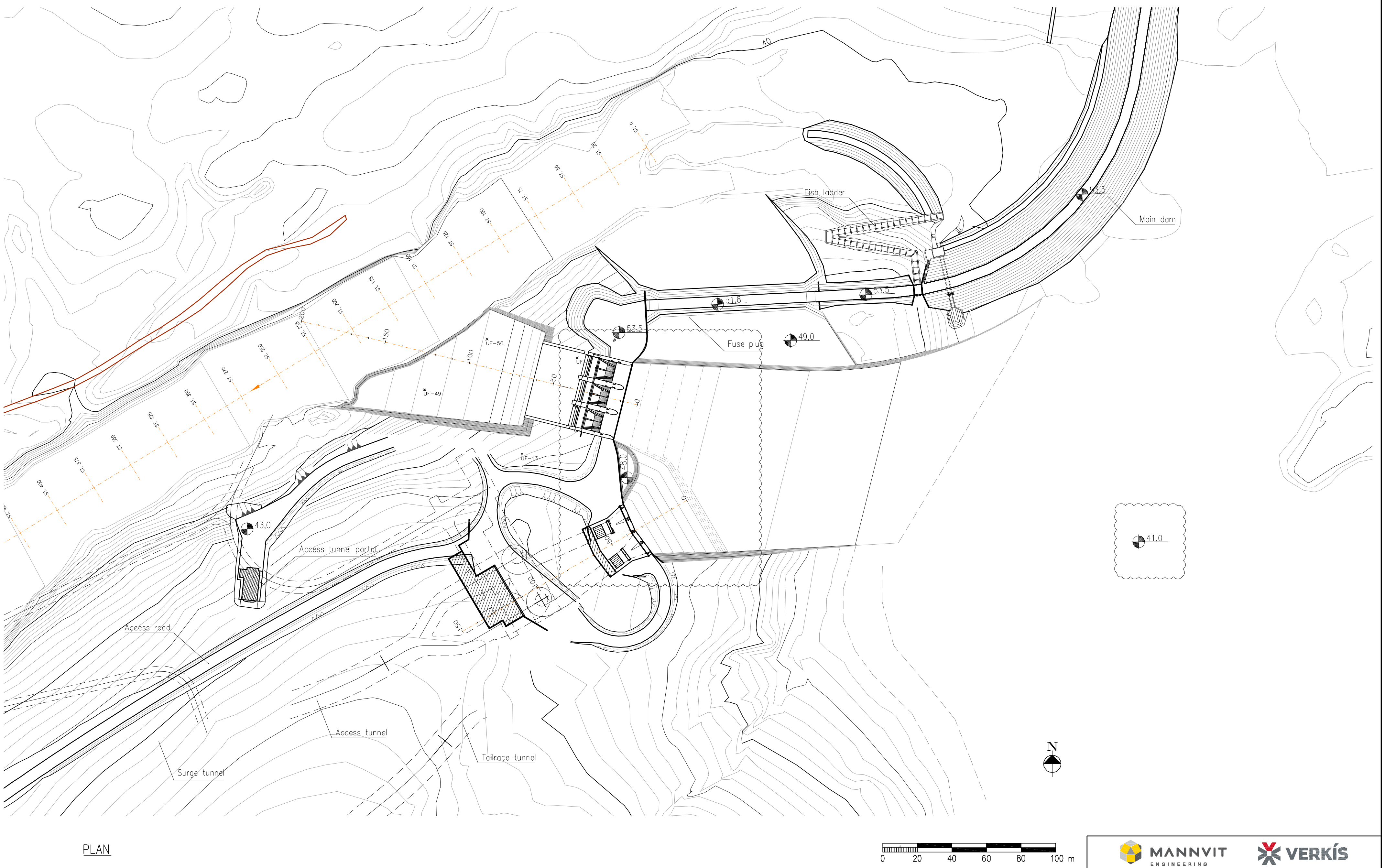

PLAN

V:\07\07028\V036\3-hommun\Urriðafoss\+C\Líkanprófanir, teikningar\LÍKANPRÓFUN_ 2012-01-31\mynd.dwg

REV.	DESCRIPTION	DATE	DES.	CHK.	APP.
P2	Clarification on chute at intake	2012.02.16			
P1	ISSUED AS PROPOSAL	2012.01.31			

PAPER SIZE A3

Landsvirkjun

PROJ. URRIÐAFOSS HEP

MANNVIT ENGINEERING — VERKÍS

NTH-60 Engineering Consultants

POWERSTATION
RIVER DAM
OVERVIEW

VERKÍS

PROCESS	INSTALLATION	LOCATION
=	+	

NPC NUMBER	NPC REV.	BDL.
		URR

NUMBER	REV.	SHEET	NEXT SH.
2007.0306 C-11-3.101	P2	-	-

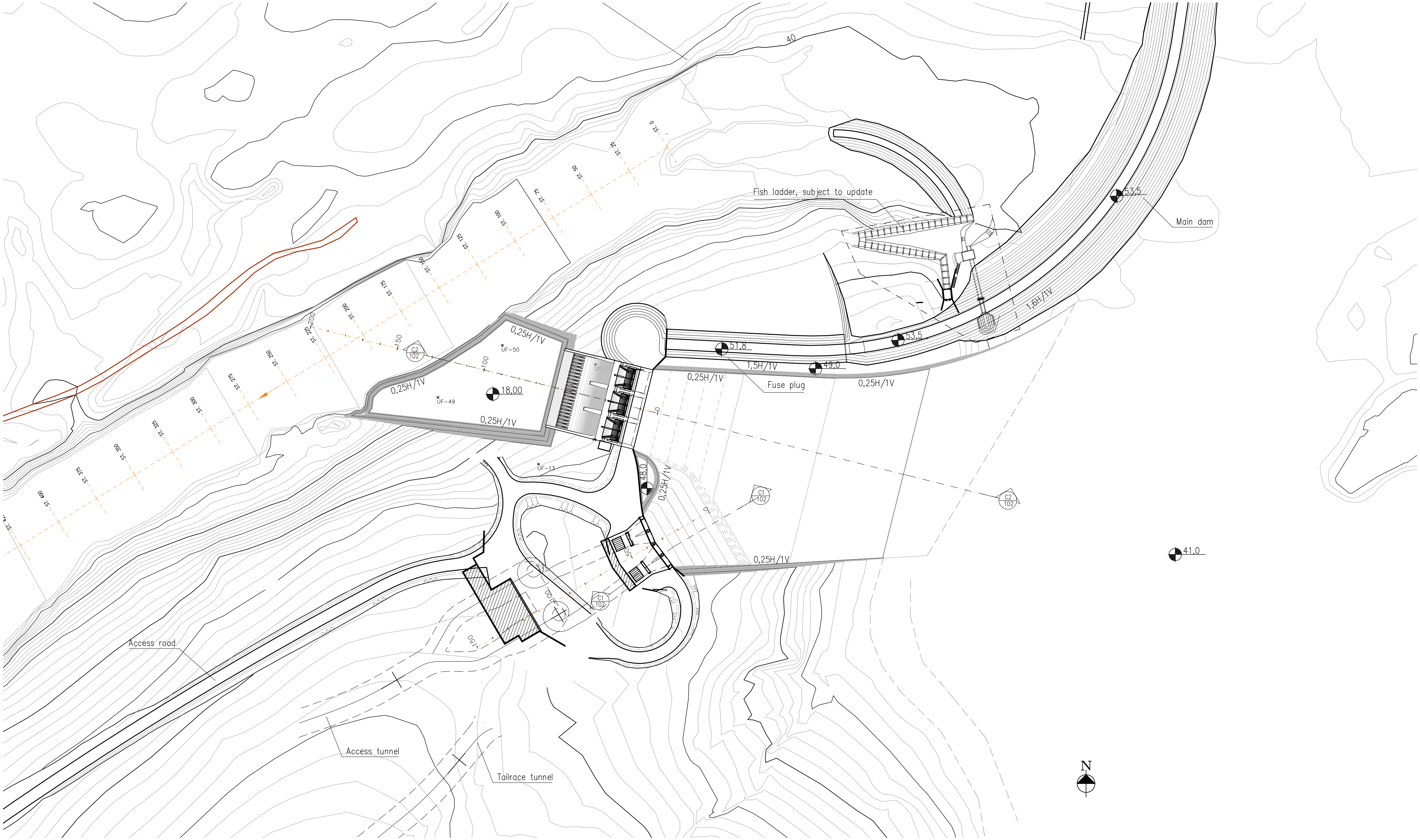

PLAN

0 20 40 60 80 100 m

MANNVIT ENGINEERING
VERKÍS
NTH-60 Engineering Consultants

V:\07\07028\V036\3-honnun\Urriðafoss\+C\Líkanprófanir, teikningar\Tillaga að líkani_2012_02_20\C-11-3.101.dwg

REV.	DESCRIPTION	DATE	DES.	CHK.	APP.
P3	Changes on layout	2012.02.21			
P2	Clarification on chute at intake	2012.02.16			
P1	ISSUED AS PROPOSAL	2012.01.31			

DATE:
DES.:
APP.:
PAPER SIZE: A3

Landsvirkjun
PROJ.: URRIÐAFOSS HEP

POWERSTATION
RIVER DAM
OVERVIEW

VERKÍS

PROCESS	INSTALLATION	LOCATION
=	+	

NPC NUMBER	NPC REV.	BDL
		URR

NUMBER	REV.	SHEET	NEXT SH.
2007.0306 C-11-3.101	P3	–	–

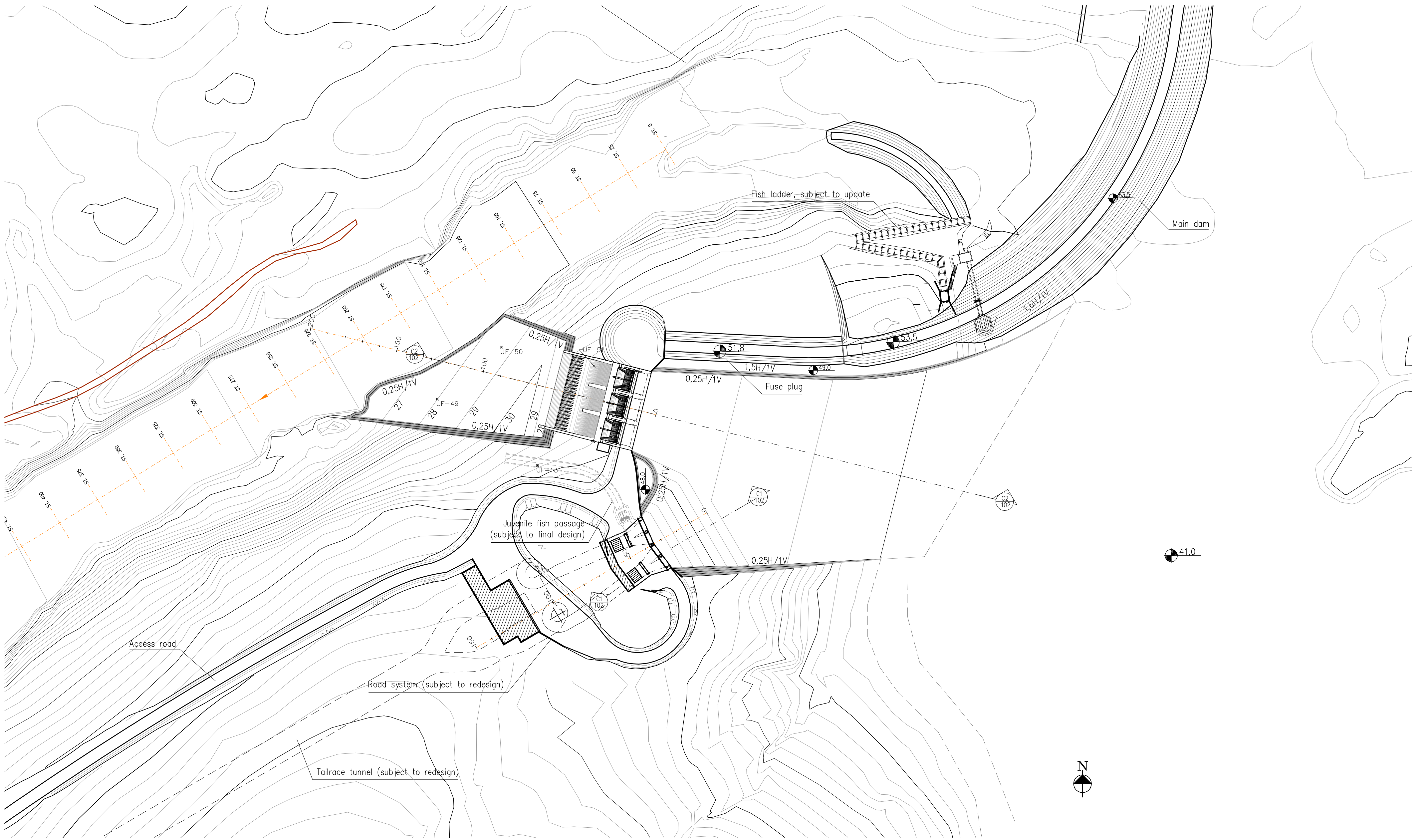

PLAN

V:\07\07028\V036\3-hönnun\Urriðafoss\+C\Líkanprófanir, teikningar\Lokateikn Líkan 2012-05-08\C-11-3.101.dwg

REV.	DESCRIPTION	DATE	DES.	CHK.	APP.
P4	Juvenile fish passage added, spillway modified	2012.05.08			
P3	Changes on layout	2012.02.21			
P2	Clarification on chute at intake	2012.02.16			
P1	ISSUED AS PROPOSAL	2012.01.31			

PAPER SIZE: A3

Landsvirkjun

PROJ. URRIÐAFOSS HEP

MANNVIT ENGINEERING — VERKÍS

NTH-60 Engineering Consultants

POWERSTATION
RIVER DAM
OVERVIEW

VERKÍS

PROCESS	INSTALLATION	LOCATION
=	+	

NPC NUMBER	NPC REV.	BDL
		URR

NUMBER	REV.	SHEET	NEXT SH.
2007.0306 C-11-3.101	P4	-	-

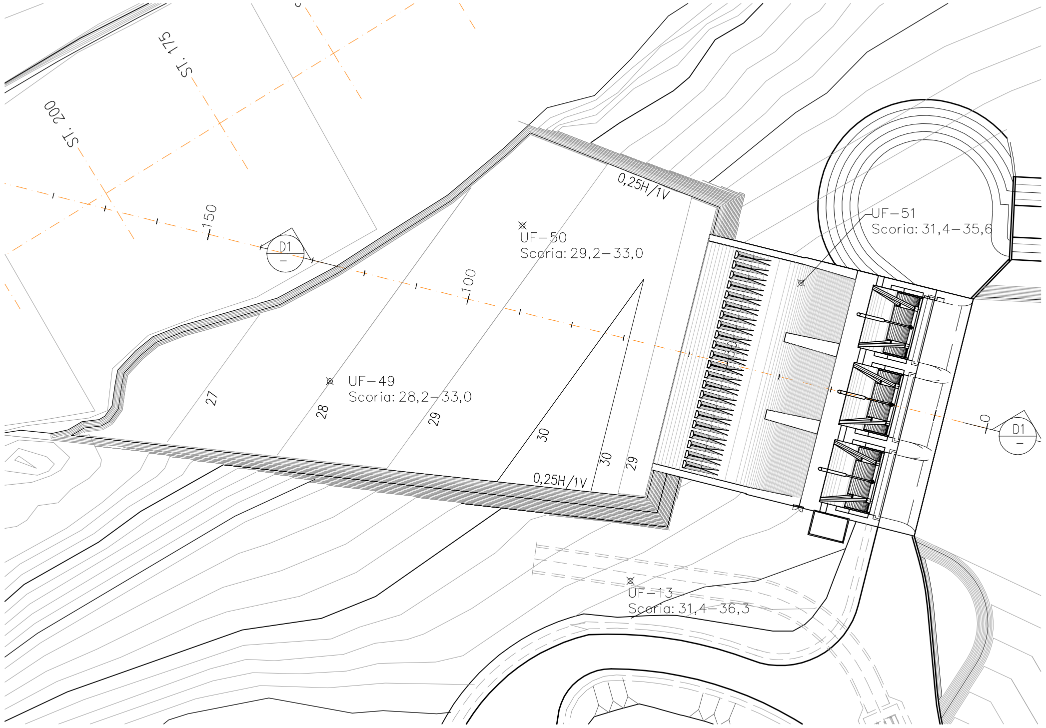

Proposal 1
Bottom of lower basalt layer

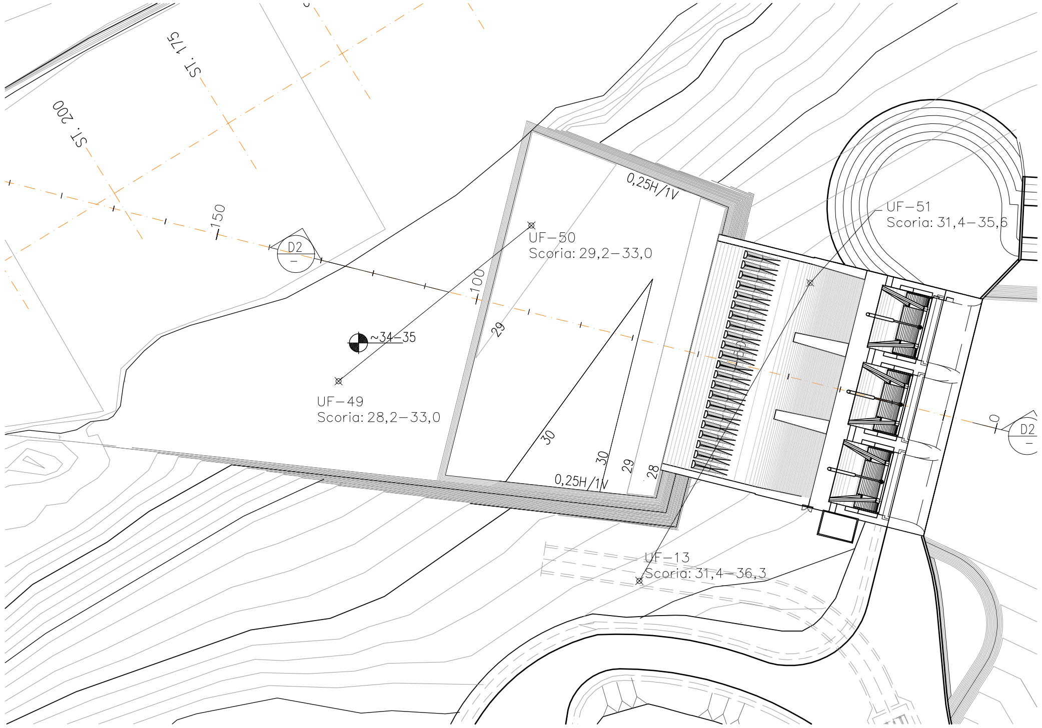

Proposal 2
Plan at EL 35,0

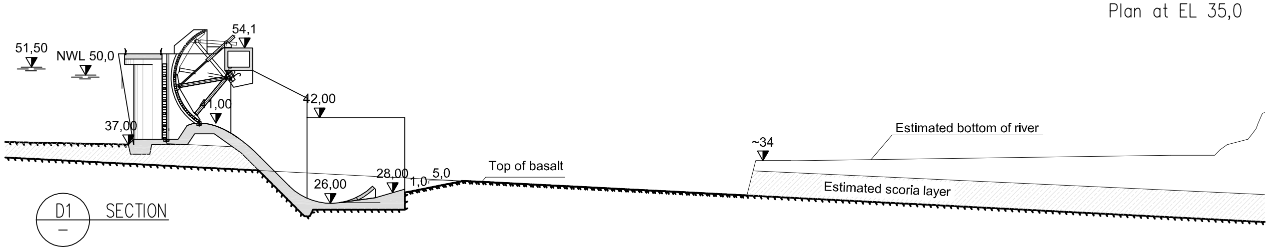

D1 SECTION

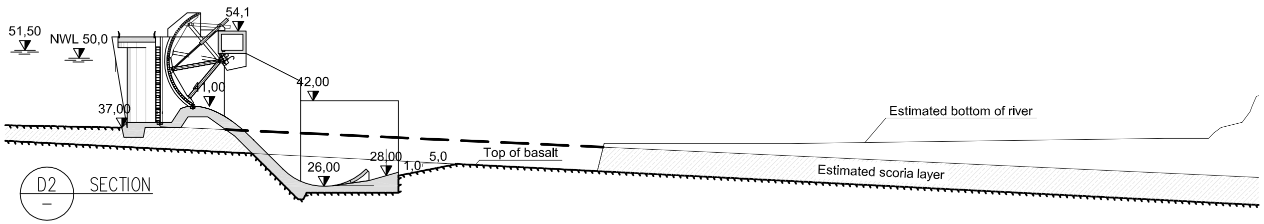

D2 SECTION

0 10 20 30 40 50
m

V:\07\07028\V036\3-hönnun\Urriðafoss\+C\Líkanprófanir, teikningar\Lokateikn Líkan 2012-05-08\C-11-3.103.dwg

P2 SCORIA LAYER ADDED ON SECTIONS 2012-05-16
P1 ISSUED AS PROPOSAL 2012.05.08
A3

MANNVIT VERKFRÆÐISTOFA
VERKÍS
NTH-60 Engineering Consultants

Landsvirkjun
URRIÐAFOSS HEP

HYDRAULIC MODEL
SPILLWAY EXCAVATION
OVERVIEW

=
+
URR
2007.0306
C−11−3.103
P2
−
−
VERKÍS

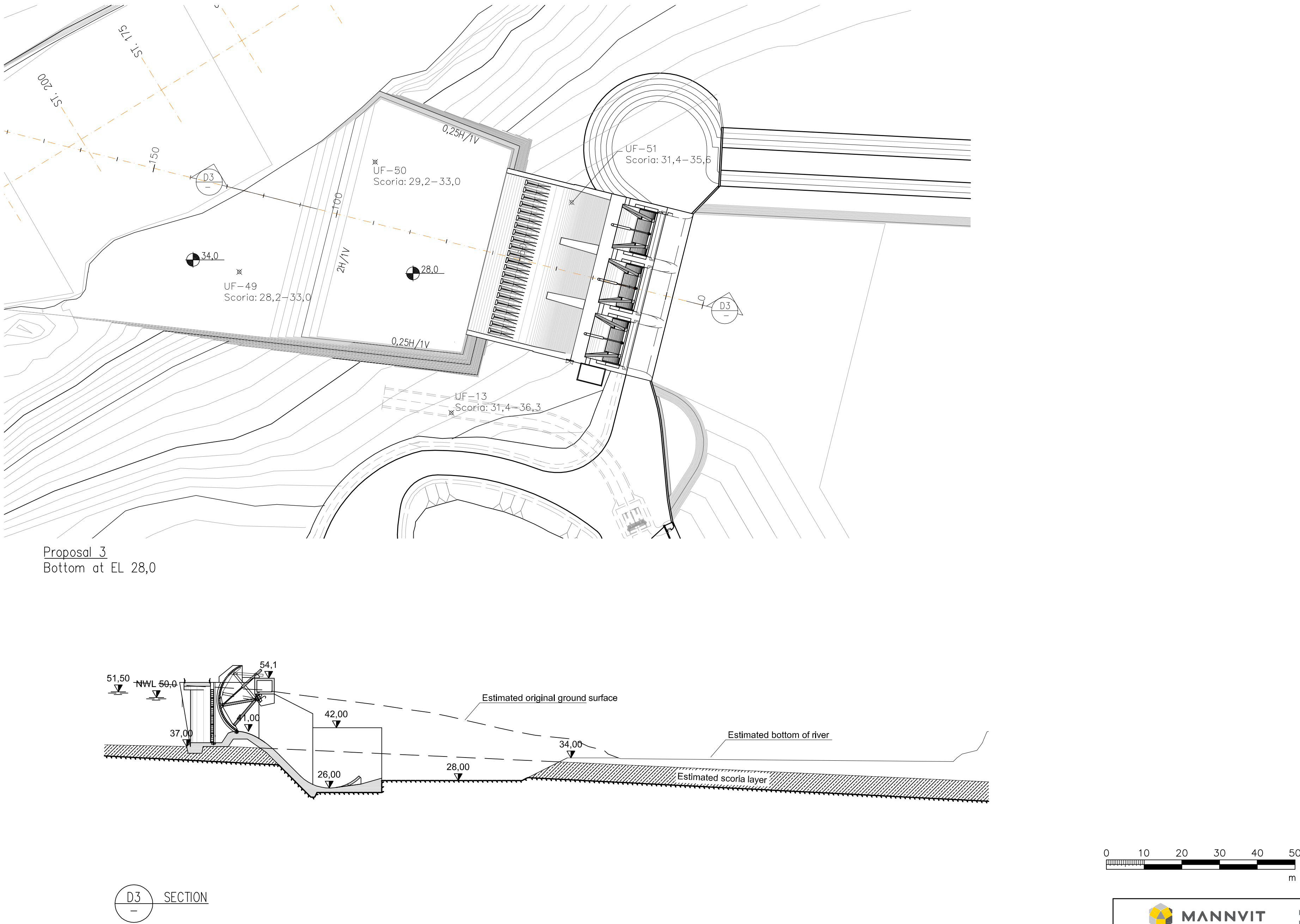

Proposal 3
Bottom at EL 28,0

D3 – SECTION

V:\07\07028\V036\3-hönnun\Urriðafoss\+C\Líkanprófanir, teikningar\2012-05-21_teikn\C-11-3.104.dwg

REV.	DESCRIPTION	DATE	DES.	CHK.	APP.
P1	ISSUED AS PROPOSAL	2012.05.22			

MANNVIT VERKÍS
NTH-60 Engineering Consultants

Landsvirkjun

PROJ. URRIÐAFOSS HEP

HYDRAULIC MODEL
SPILLWAY EXCAVATION
PLAN & SECTION

PAPER SIZE: A3
PROCESS: =
INSTALLATION: +
LOCATION:
NPC NUMBER:
NPC REV.:
BDL: URR
NUMBER: 2007.0306
C-11-3.104
REV.: P1
SHEET: –
NEXT SH.: –

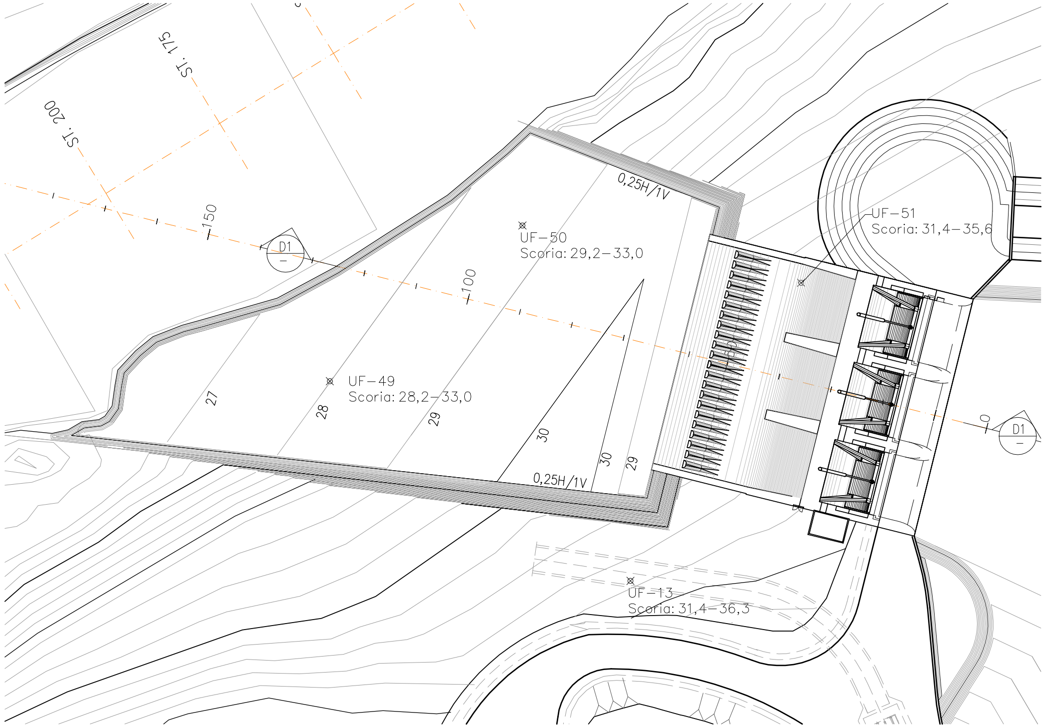

Proposal 1
Bottom of lower basalt layer

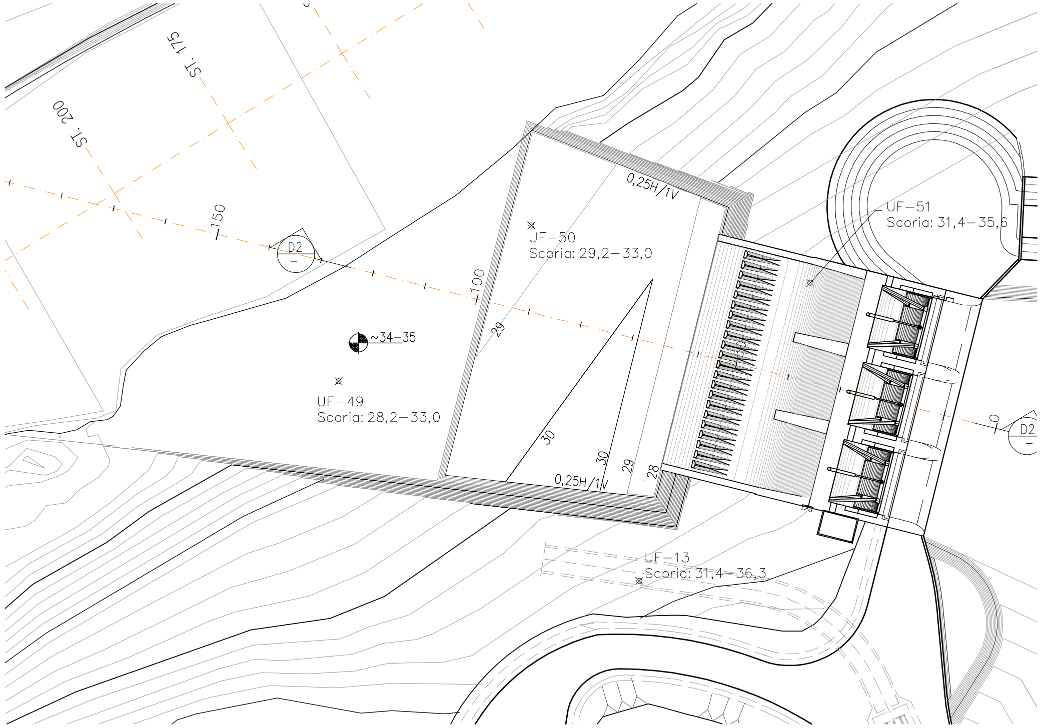

Proposal 2
Plan at EL 35,0

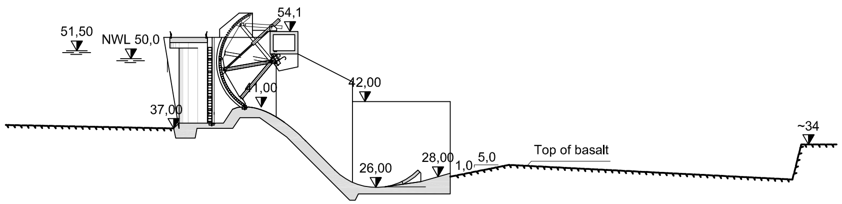

D1 SECTION

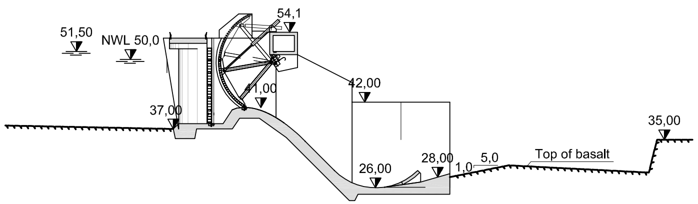

D2 SECTION

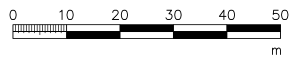

V:\07\07028\V036\3-hønnun\Urriðafoss\+C\Líkanprófanir, teikningar\Lokateikn Líkan 2012-05-08\C-11-3.102.dwg

REV	DESCRIPTION	DATE	DES.	CHK.	APP.
P1	ISSUED AS PROPOSAL	2012.05.08			

MANNVIT ENGINEERING
VERKÍS
NTH-60 Engineering Consultants

Landsvirkjun

HYDRAULIC MODEL
SPILLWAY EXCAVATION
OVERVIEW

VERKÍS

PAPER SIZE	A3
PROJ.	URRIÐAFOSS HEP
PROCESS	=
INSTALLATION	+
NPC NUMBER	
BDL	URR
NUMBER	2007.0306 C-11-3.103
REV.	P1
SHEET	-
NEXT SH.	-

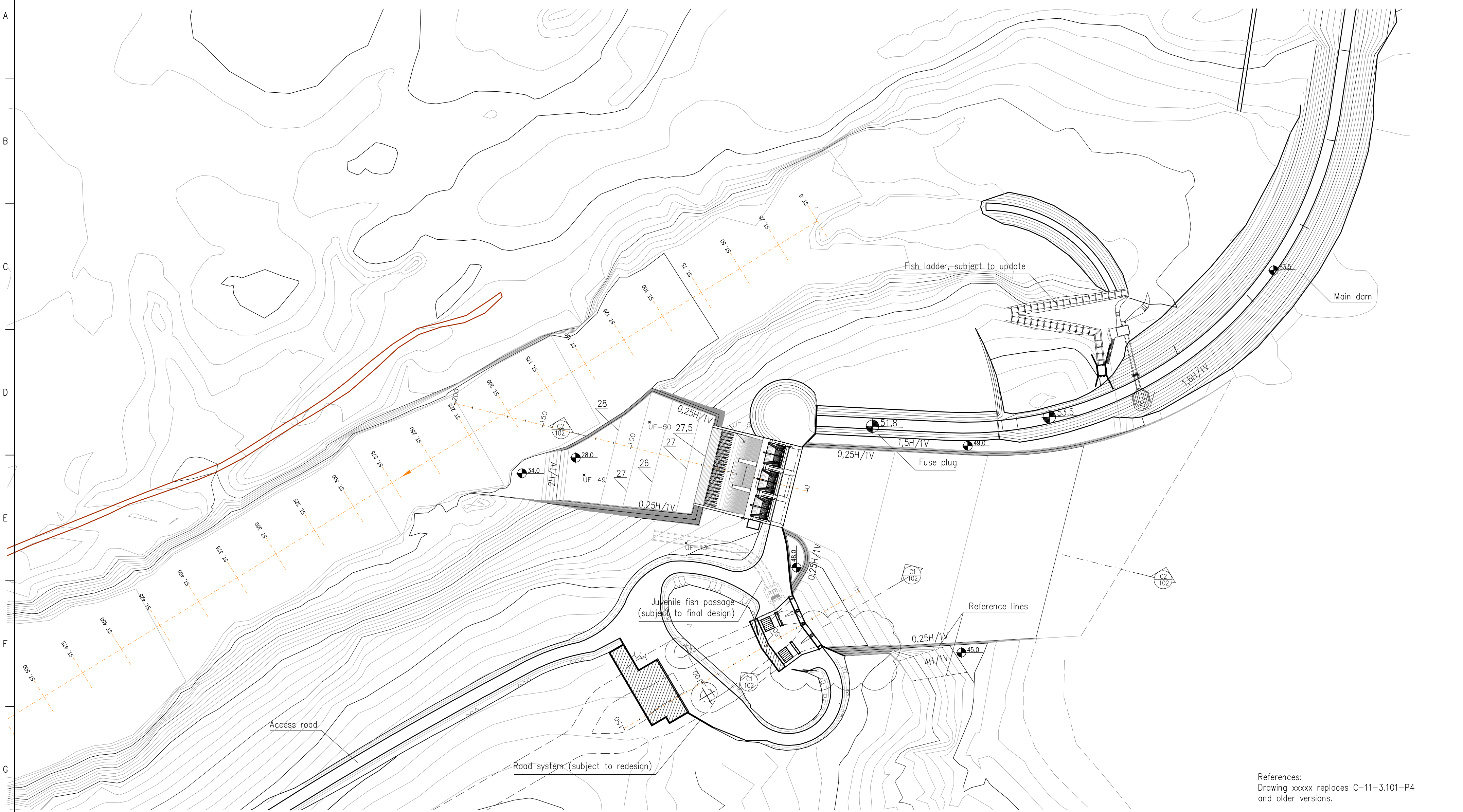

PLAN

0 20 40 60 80 100 m

V:\07\07028\V036\3-honnun\Urriðafoss\+C\Líkanprófanir, teikningar\2012-06-06\C-11-3.101-P7.dwg

REV.	DESCRIPTION	DATE	DES.	CHK.	APP.
P7	Modificationn on wall end at intake	2012-05-05			
P6	Modification on excavation	2012-06-04	ÞSL		
P5	Modifications on excavation	2012-05-30			
P4	Juvenile fish passage added, spillway modified	2012.05.08			
P3	Changes on layout	2012.02.21			
P2	Clarification on chute at intake	2012.02.16			
P1	ISSUED AS PROPOSAL	2012.01.31			

DATE 2012-06-04
DES. ÞSL
APP.
PAPER SIZE A3

Landsvirkjun
PROJ. URRIÐAFOSS HEP

MANNVIT ENGINEERING
VERKÍS
NTH-60 Engineering Consultants

POWERSTATION
RIVER DAM
OVERVIEW

VERKÍS

PROCESS = | INSTALLATION + | LOCATION
NPC NUMBER | NPC REV. | BDL URR
NUMBER 2007.0306 C-11-3.101 | REV. P7 | SHEET – | NEXT SH. –

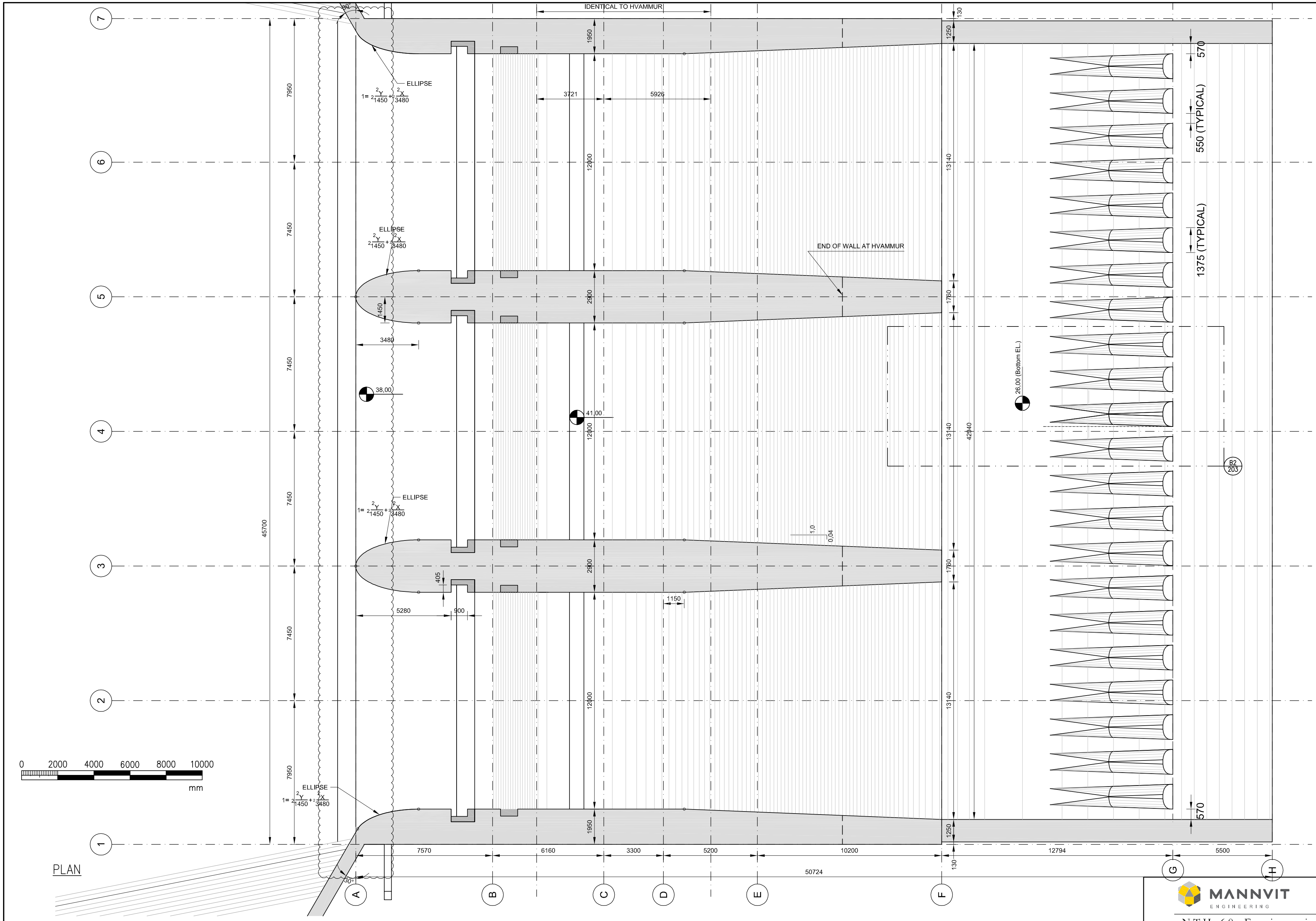

V:\07\07028\V036\3-hönnun\Urriðafoss\+C\Líkanprófanir, teikningar\Tillaga að líkani_2012_02_20\C-11-3.201-203_update.dwg

REV.	DESCRIPTION	DATE	DES.	CHK.	APP.
P2	Modifications on concrete	2012.02.21			
P1	ISSUED FOR MODEL TESTING	2012.02.07			

PAPER SIZE: A3

Landsvirkjun

PROJ.: URRIÐAFOSS HEP

MANNVIT ENGINEERING — VERKÍS

NTH-60 Engineering Consultants

HYDRAULIC MODEL TESTS
SPILLWAY
STRUCTURAL DRAWING
PLAN AT EL. 41,0

VERKÍS

PROCESS	INSTALLATION	LOCATION
=	+	

NPC NUMBER: | NPC REV.: | BDL: URR

NUMBER: 2007.0306 — C-11-3.201 | REV.: P2 | SHEET: – | NEXT SH.: –

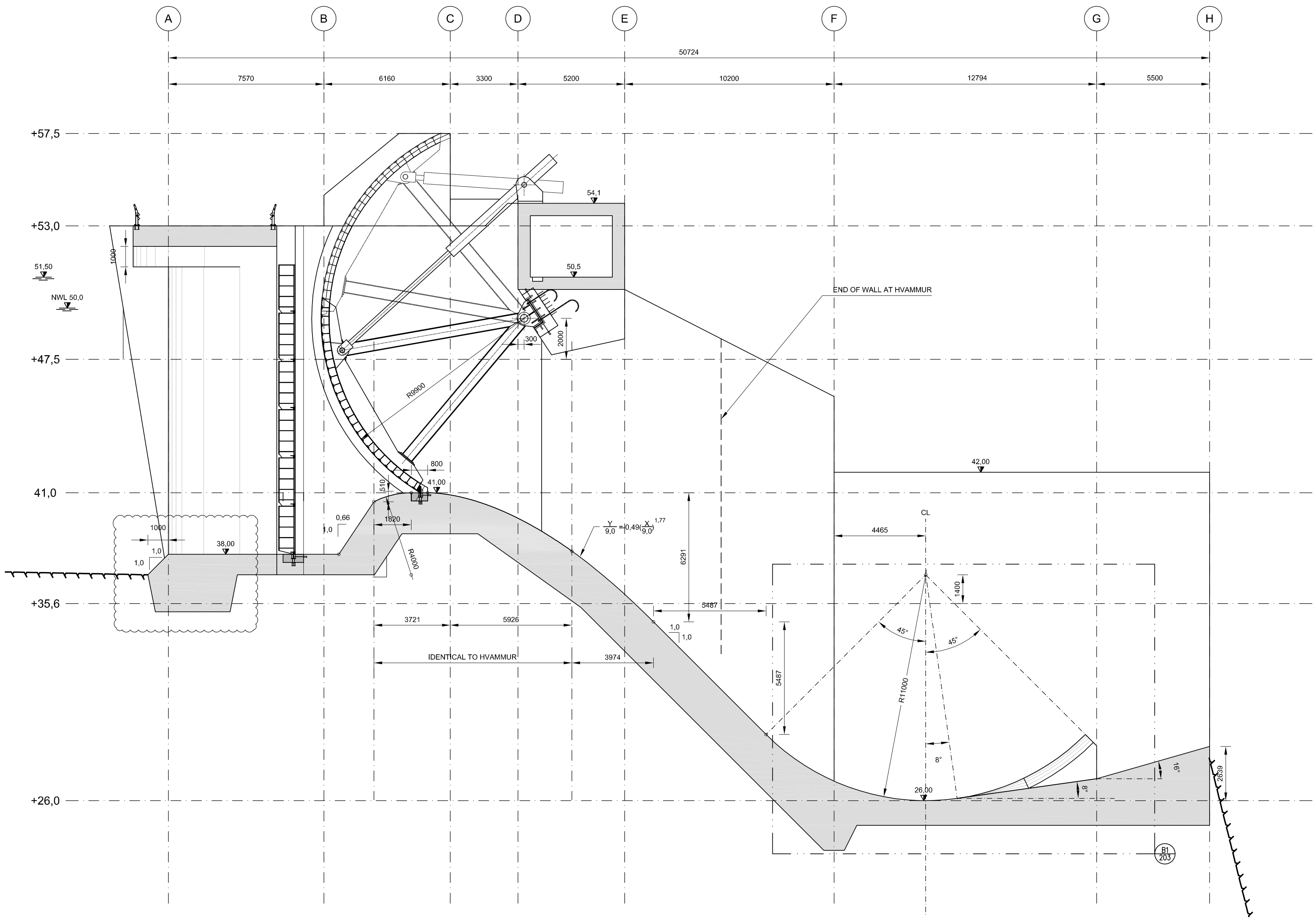

PLAN

0 2000 4000 6000 8000 10000
mm

V:\07\07028\V036\3-honnun\Urriðafoss\+C\Líkanprófanir, teikningar\Tillaga að líkani_2012_02_20\C-11-3.201-203_update.dwg

REV.	DESCRIPTION	DATE	DES.	CHK.	APP.
P2	Modifications on concrete	2012.02.21			
P1	ISSUED FOR MODEL TESTING	2012.02.07			

PAPER SIZE: A3

Landsvirkjun

PROJ. URRIÐAFOSS HEP

MANNVIT ENGINEERING — VERKÍS

NTH-60 Engineering Consultants

HYDRAULIC MODEL TESTS
SPILLWAY
STRUCTURAL DRAWING
SECTION

VERKÍS

PROCESS	INSTALLATION	LOCATION
=	+	

NPC NUMBER	NPC REV.	BDL
		URR

NUMBER	REV.	SHEET	NEXT SH.
2007.0306 C-11-3.202	P2	–	–

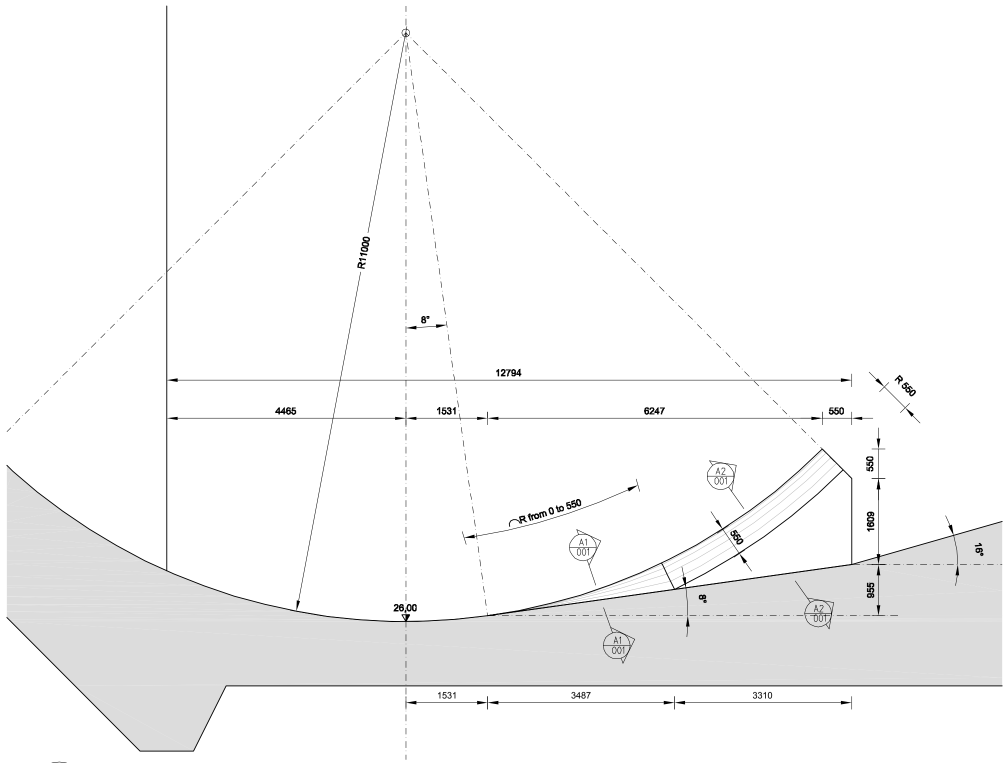

B1
202
DETAIL
Scale a

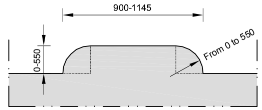

A1
001
SECTION
Scale a

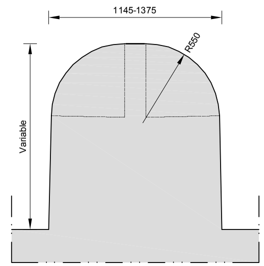

A2
001
SECTION
Scale a

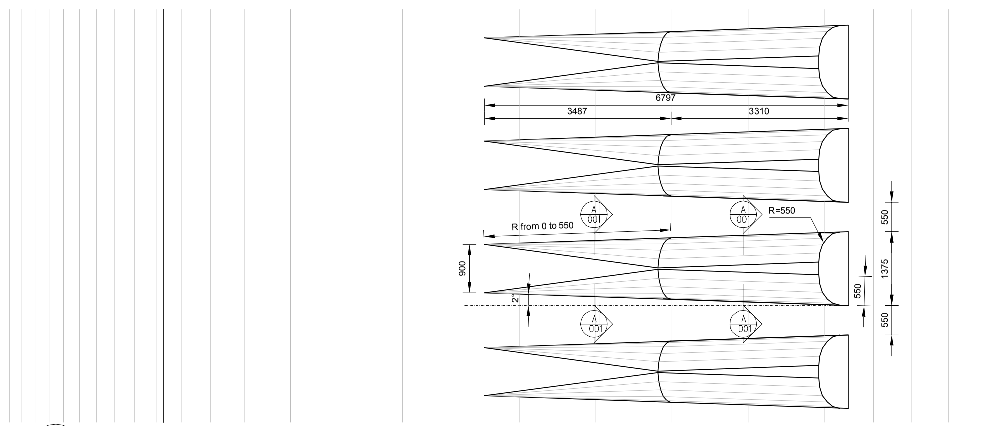

B2
201
DETAIL
Scale a

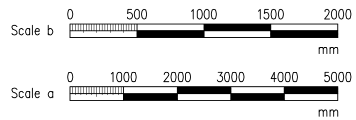

MANNVIT ENGINEERING
VERKÍS
NTH-60 Engineering Consultants

V:\07\07028\V036\3-honnun\Urriðafoss\+C\Líkanprófanir, teikningar\Flóðgáttur, teikn fyrir líkan_2012-02-07\C-11-3.201-203.dwg

REV.	DESCRIPTION	DATE	DES.	CHK.	APP.
P1	ISSUED FOR MODEL TESTING	2012.02.07			

DATE 2012.02.07
DES.
APP.
PAPER SIZE A3

Landsvirkjun
PROJ. URRIÐAFOSS HEP

HYDLAULIC MODEL TESTS
SPILLWAY
STRUCTURAL DRAWING
DETAILS

VERKÍS

PROCESS =
INSTALLATION +
LOCATION
NPC NUMBER
NPC REV.
BDL. URR
NUMBER 2007.0306
C-11-3.203
REV. P1
SHEET –
NEXT SH. –

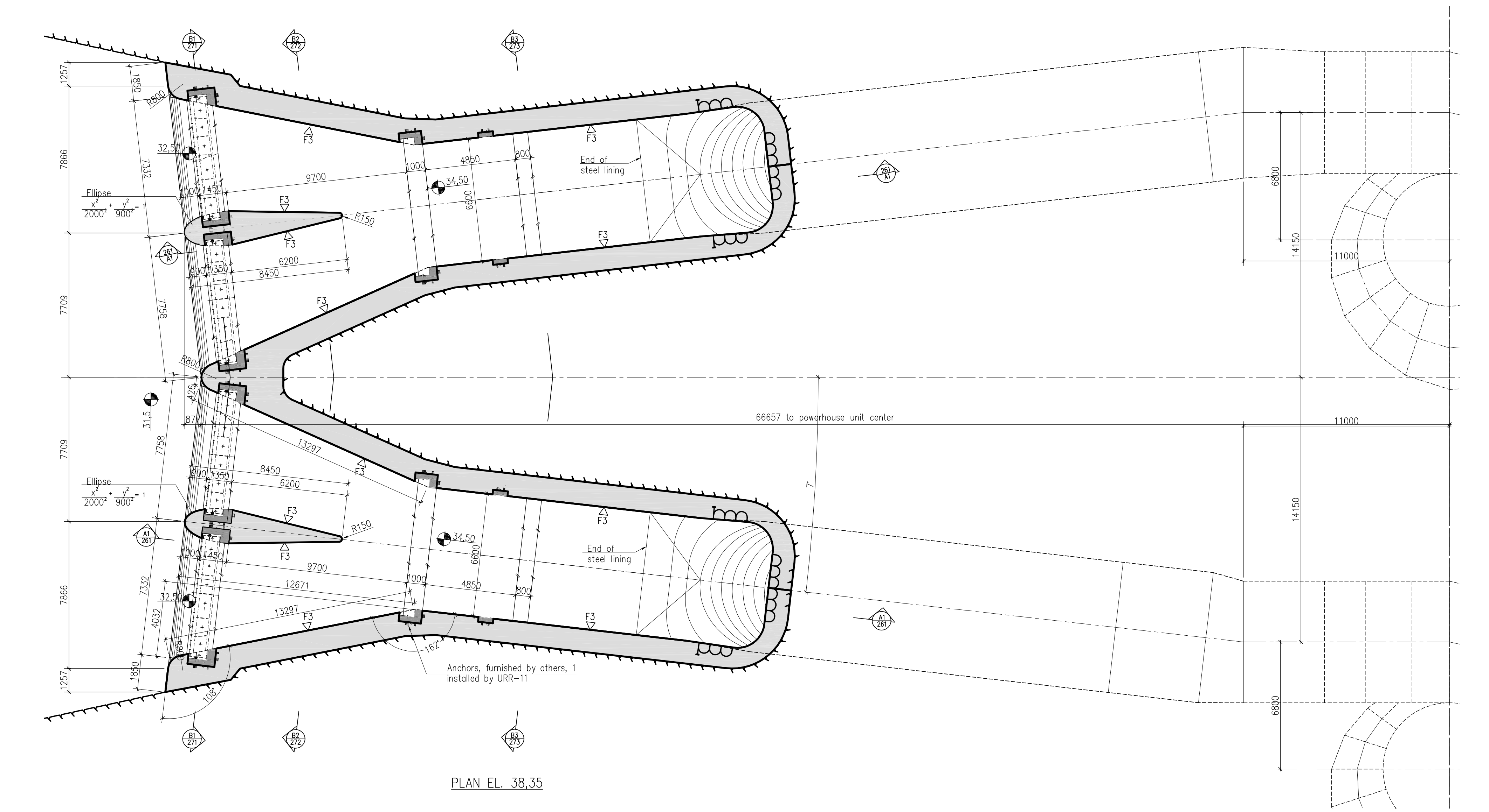

K:\2007.03\06\teikn\utbod\malt\Update\C-11-3.251.dwg

MANNVIT ENGINEERING

VERKÍS

NTH-60 Engineering Consultants

REV.	DESCRIPTION	DATE	DES.	CHK.	APP.
P4	Issued for model testing	2011-01-05	KA	þSL	
P3	Dwg. check	Oct. 2009		EBJ	
P2	Enlargement of trash racks	2008-02-19	SH		
P1	PRELIMINARY DRAWING	2008-02-01	AhS	EBJ	

DATE: JANUARY 2008
PAPER SIZE: A3

Landsvirkjun

PROJ. URRIÐAFOSS HEP

POWERSTATION
POWER INTAKE
LAYOUT
PLAN EL. 38,35

VERKÍS

PROCESS	INSTALLATION	LOCATION
=	+	

NPC NUMBER	NPC REV.	BDL
		URR

NUMBER	REV.	SHEET	NEXT SH.
2007.0306 C-11-3.251	P4	–	–

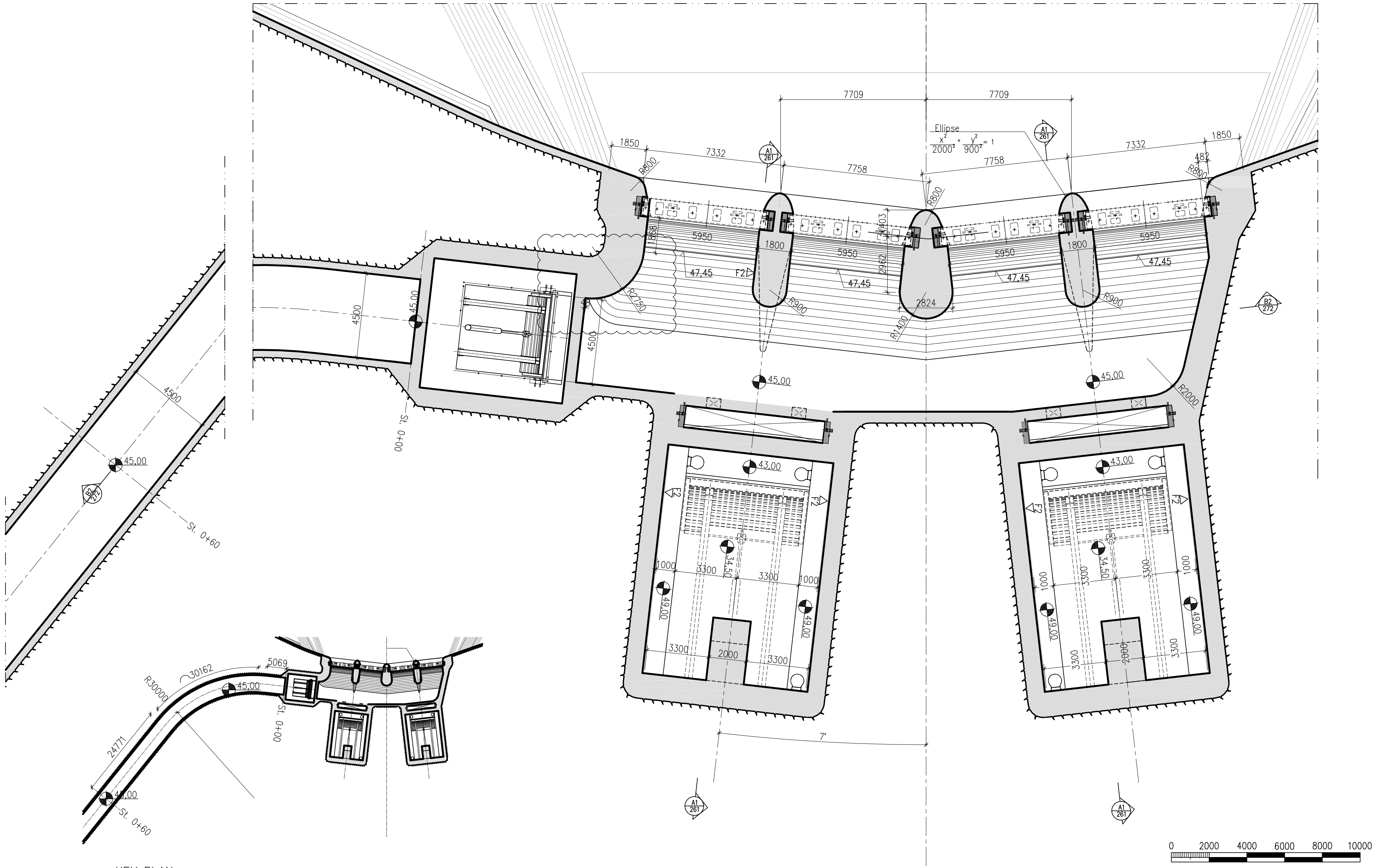

KEY PLAN

PLAN EL. 50,80

V:\11\11036\teikn\+C\C-11-3.252.dwg

REV.	DESCRIPTION	DATE	DES.	CHK.	APP.
P6	Modifications on wall end	2012.02.27			
P5	Modifications on chute	2012.02.21			
P4	Issued for model testing	2011-01-05	KA	þSL	
P3	Dwg. check	Oct. 2009		EBJ	
P2	Enlargement of trash racks	2008-02-19	SH		
P1	PRELIMINARY DRAWING	2008-02-01	AhS	EBJ	

DATE	JANUARY 2008
DES.	AhS/kjk
APP.	
PAPER SIZE	A3
PROJ.	URRIÐAFOSS HEP

Landsvirkjun

MANNVIT ENGINEERING

VERKÍS

NTH-60 Engineering Consultants

POWERSTATION
POWER INTAKE
LAYOUT
PLAN EL. 50,80

VERKÍS

PROCESS = INSTALLATION + LOCATION
NPC NUMBER
NPC REV.
BDL URR
NUMBER 2007.0306
C-11-3.252
REV. P6
SHEET –
NEXT SH. –

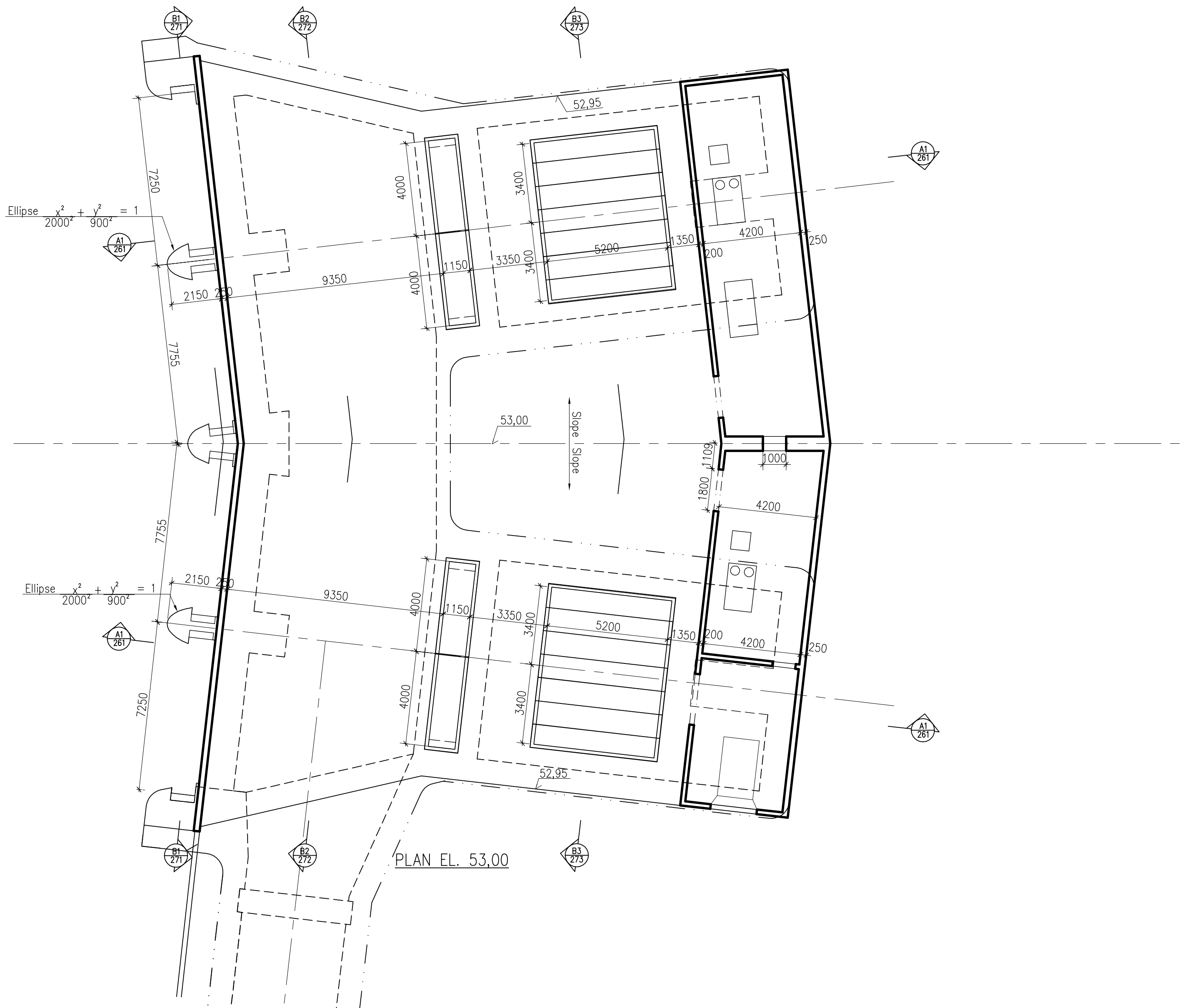

K:\2007\03\08\teikn\utbod\mat\Uppdate\C-11-3253.dwg

REV.	DESCRIPTION	DATE	DES.	CHK.	APP.
P3	Issued for model testing	2011-01-05	KA	þSL	
P2	Enlargement of trash racks	2008-02-19	SH		
P1	PRELIMINARY DRAWING	2008-02-01	AhS	EBJ	

DATE: JANUARY 2008
DES.: AhS/kjk
APP.:
PAPER SIZE: A3

Landsvirkjun

PROJ.: URRIÐAFOSS HEP

MANNVIT ENGINEERING
VERKÍS
NTH-60 Engineering Consultants

POWERSTATION
POWER INTAKE
LAYOUT
PLAN EL. 53,00

VERKÍS

PROCESS: =
INSTALLATION: +
LOCATION:
NPC NUMBER:
NPC REV.:
BDL: URR
NUMBER: 2007.0306
C-11-3.253
REV.: P3
SHEET: –
NEXT SH.: –

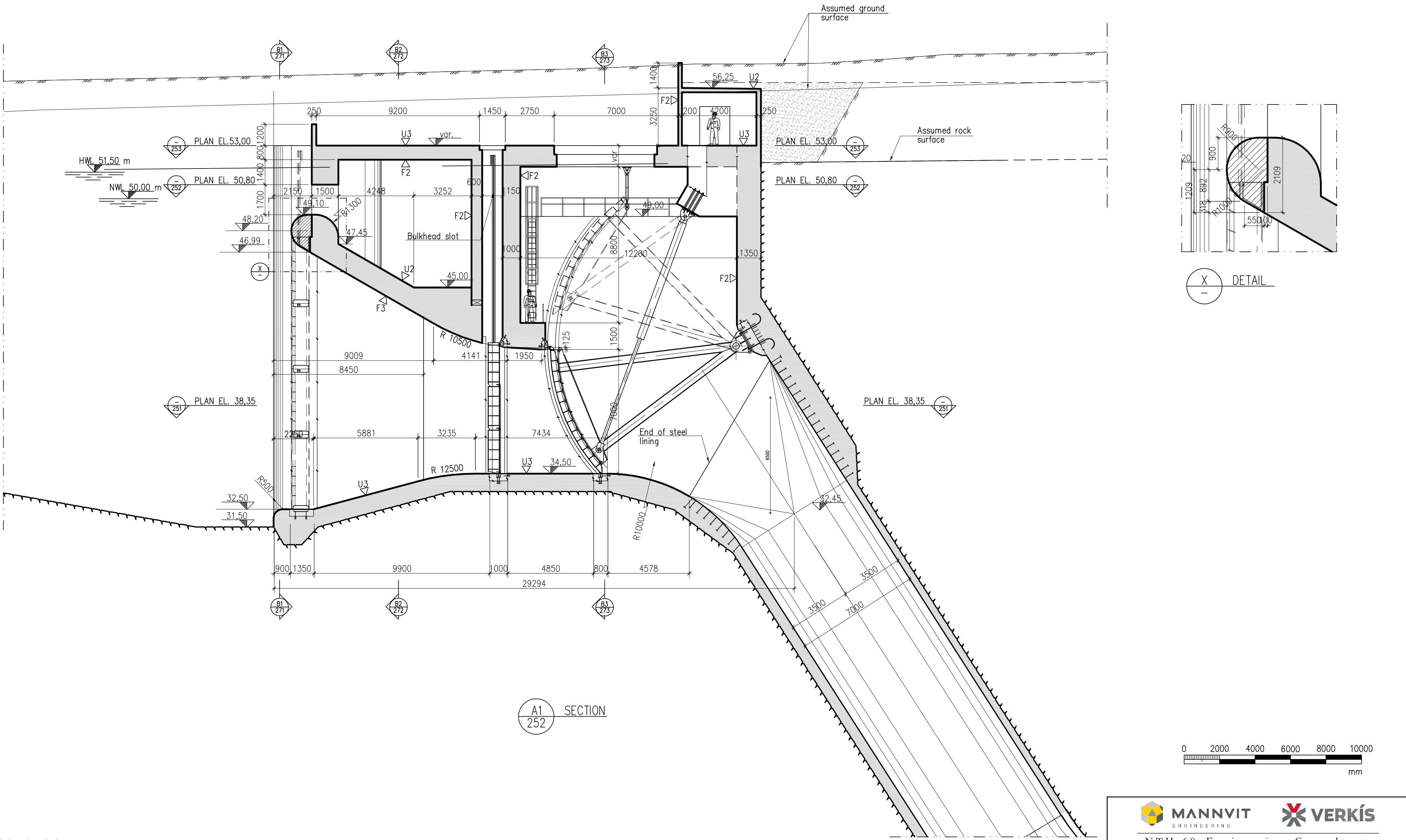

REV.	DESCRIPTION	DATE	DES.	CHK.	APP.
P4	Modifications on chute	2012-02-21			
P3	Issued for model testing	2011-01-05	KA	þSL	
P2	Enlargement og trash racks	2008-02-19	SH		
P1	PRELIMINARY DRAWING	2008-02-01	AhS	EBJ	

DATE: JANUARY 2008
DES.: AhS
PAPER SIZE: A3

Landsvirkjun
PROJ.: URRIÐAFOSS HEP

MANNVIT ENGINEERING
VERKÍS
NTH-60 Engineering Consultants

POWERSTATION
POWER INTAKE
LAYOUT
SECTION A1

VERKÍS

PROCESS	INSTALLATION	LOCATION
=	+	

BDL: URR
NUMBER: 2007.0306
C-11-3.261
REV.: P4
SHEET: –
NEXT SH.: –

V:\11\11038\teikn\v01\C-11-3.261.dwg

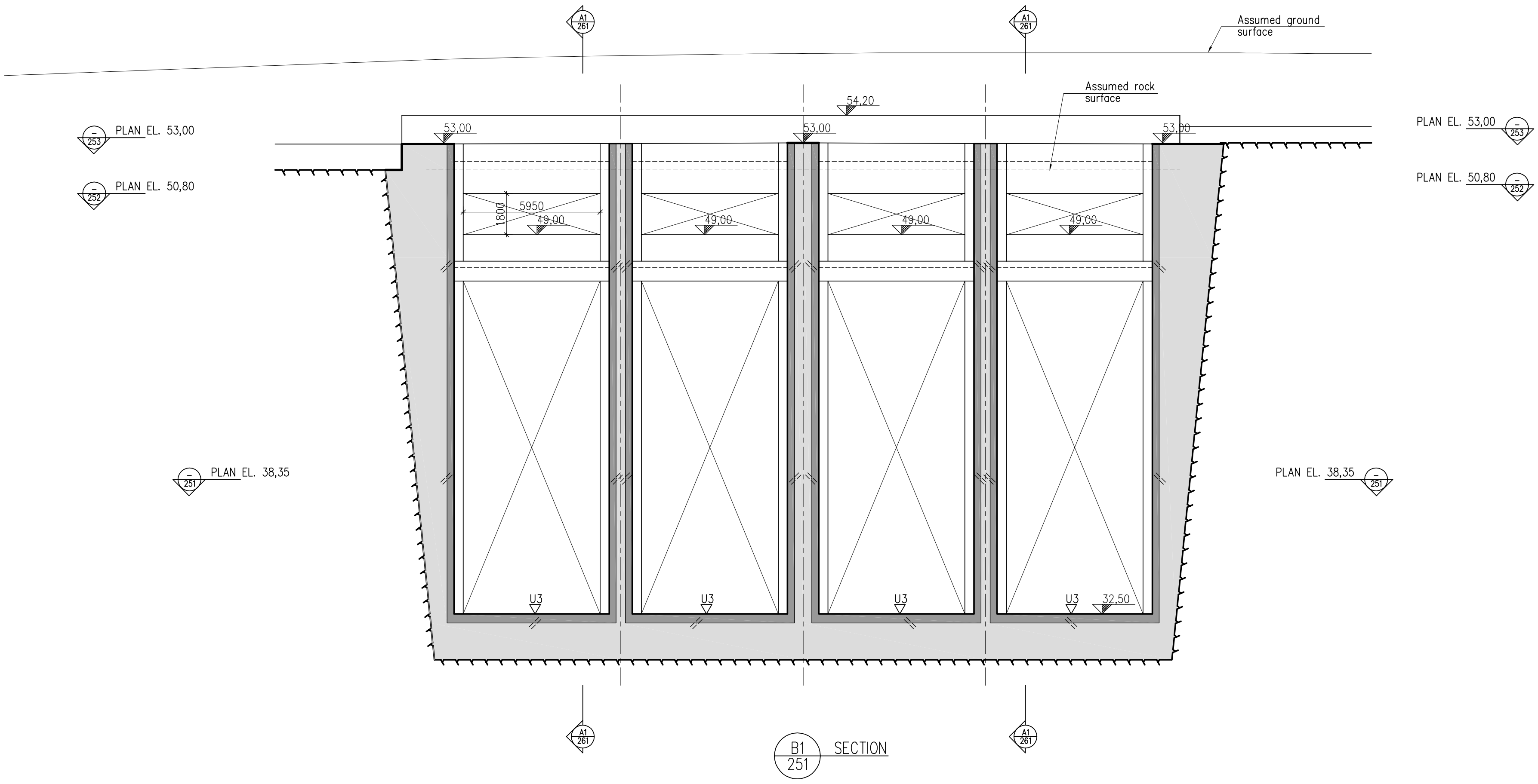

B1 251 SECTION

K:\2007\03\06\teikn\utbod\mot\Uppdate\C-11-3.271-273.dwg

REV.	DESCRIPTION	DATE	DES.	CHK.	APP.
P3	Issued for modeling	2011-01-05	KA	þSL	
P2	Enlargement of trash racks	2008-02-19	SH		
P1	PRELIMINARY DRAWING	2008-02-01	AhS	EBJ	P3

DATE: JANUARY 2008
DES.: AhS
APP.:
PAPER SIZE: A3

Landsvirkjun

PROJ.: URRIÐAFOSS HEP

MANNVIT ENGINEERING
VERKÍS
NTH-60 Engineering Consultants

POWERSTATION
POWER INTAKE
LAYOUT
SECTION B1

VERKÍS

PROCESS: =
INSTALLATION: +
LOCATION:
NPC NUMBER:
NPC REV.:
BDL: URR
NUMBER: 2007.0306
C-11-3.271
REV.: P3
SHEET:
NEXT SH.:

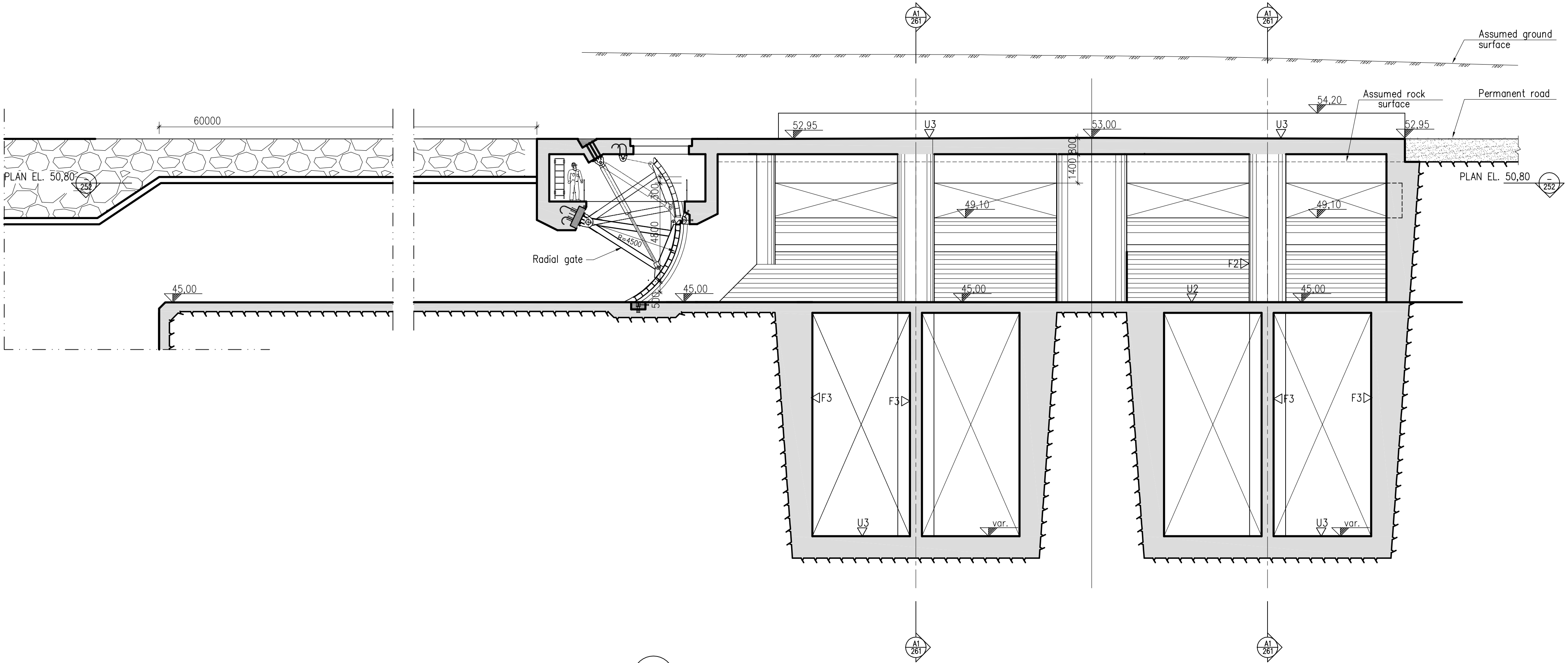

B2
252
SECTION

0 2000 4000 6000 8000 10000
mm

V:\11\11036\teikn\+C\C-11-3.272.dwg

REV.	DESCRIPTION	DATE	DES.	CHK.	APP.
P3	Modifications on chute	2012.02.21			
P2	Issued for modeling	2011-01-05	KA	þSL	
P1	PRELIMINARY DRAWING				

DATE: JANUARY 2008
PAPER SIZE: A3

Landsvirkjun

MANNVIT ENGINEERING
VERKÍS
NTH-60 Engineering Consultants

POWERSTATION
POWER INTAKE
LAYOUT
SECTION B2

VERKÍS

PROCESS: =
INSTALLATION: +
LOCATION
NPC NUMBER
NPC REV.
BDL: URR
NUMBER: 2007.0306
C-11-3.272
REV.: P3
SHEET: –
NEXT SH.: –

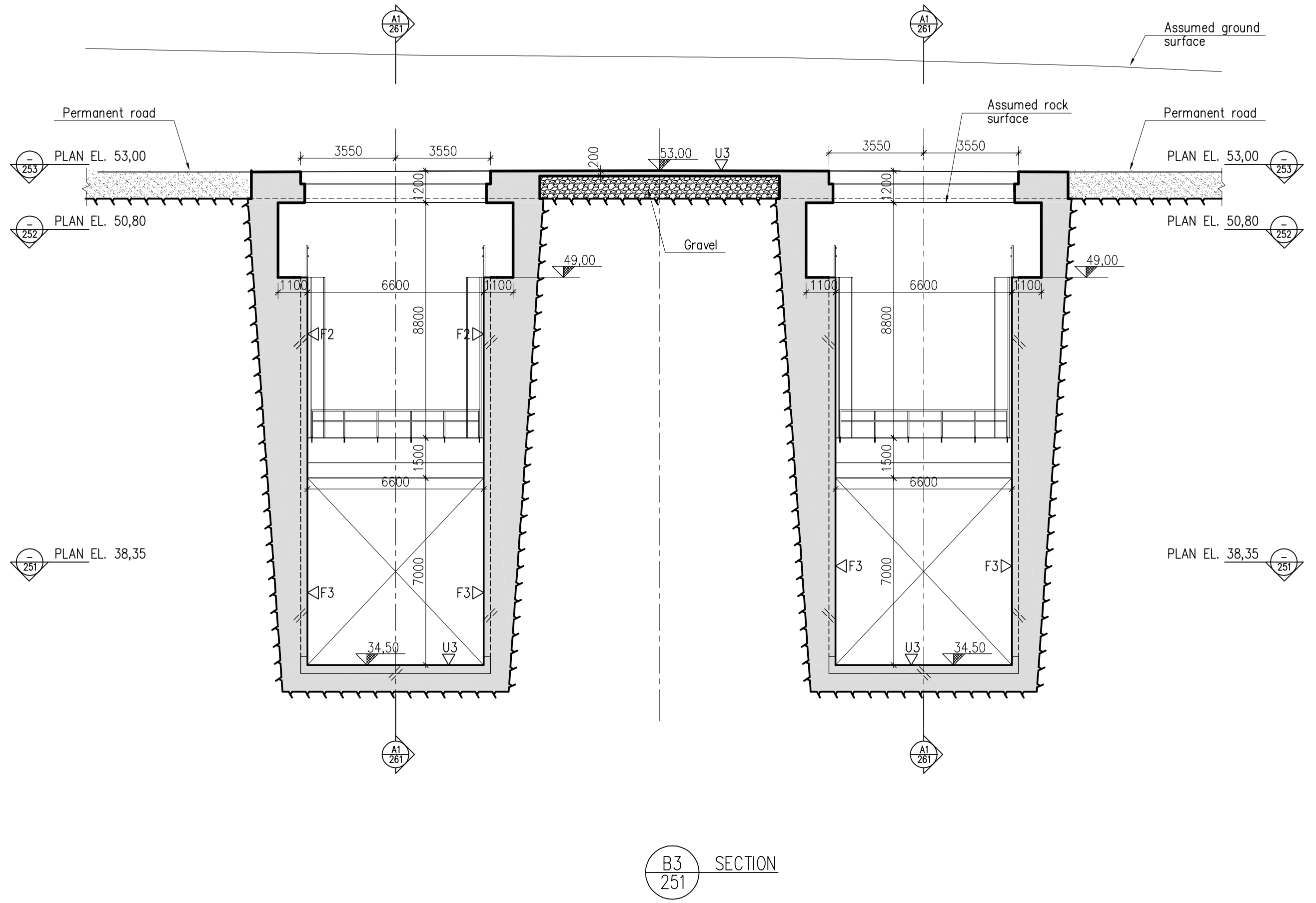

K:\2007.03\06\teikn\utbod\malt\Update\C-11-3.271-273.dwg

REV.	DESCRIPTION	DATE	DES.	CHK.	APP.
P2	Issued for modeling	2011-01-05	KA	þSL	
P1	PRELIMINARY DRAWING				

MANNVIT ENGINEERING | VERKÍS

NTH-60 Engineering Consultants

DATE	JANUARY 2008
PAPER SIZE	A3

Landsvirkjun

POWERSTATION
POWER INTAKE
LAYOUT
SECTION B3

VERKÍS

PROCESS	INSTALLATION	LOCATION
=	+	
NPC NUMBER	NPC REV.	BDL URR
NUMBER 2007.0306 C-11-273	REV. P2	SHEET – / NEXT SH. –

H. Approach flow particle test

The following drawings show results of the particle test conducted during testing of the approach flow conditions for the intake and SFO presented in Section 5.2. The drawings show general flow behaviour in the approach flow channel observed from particle tracks.

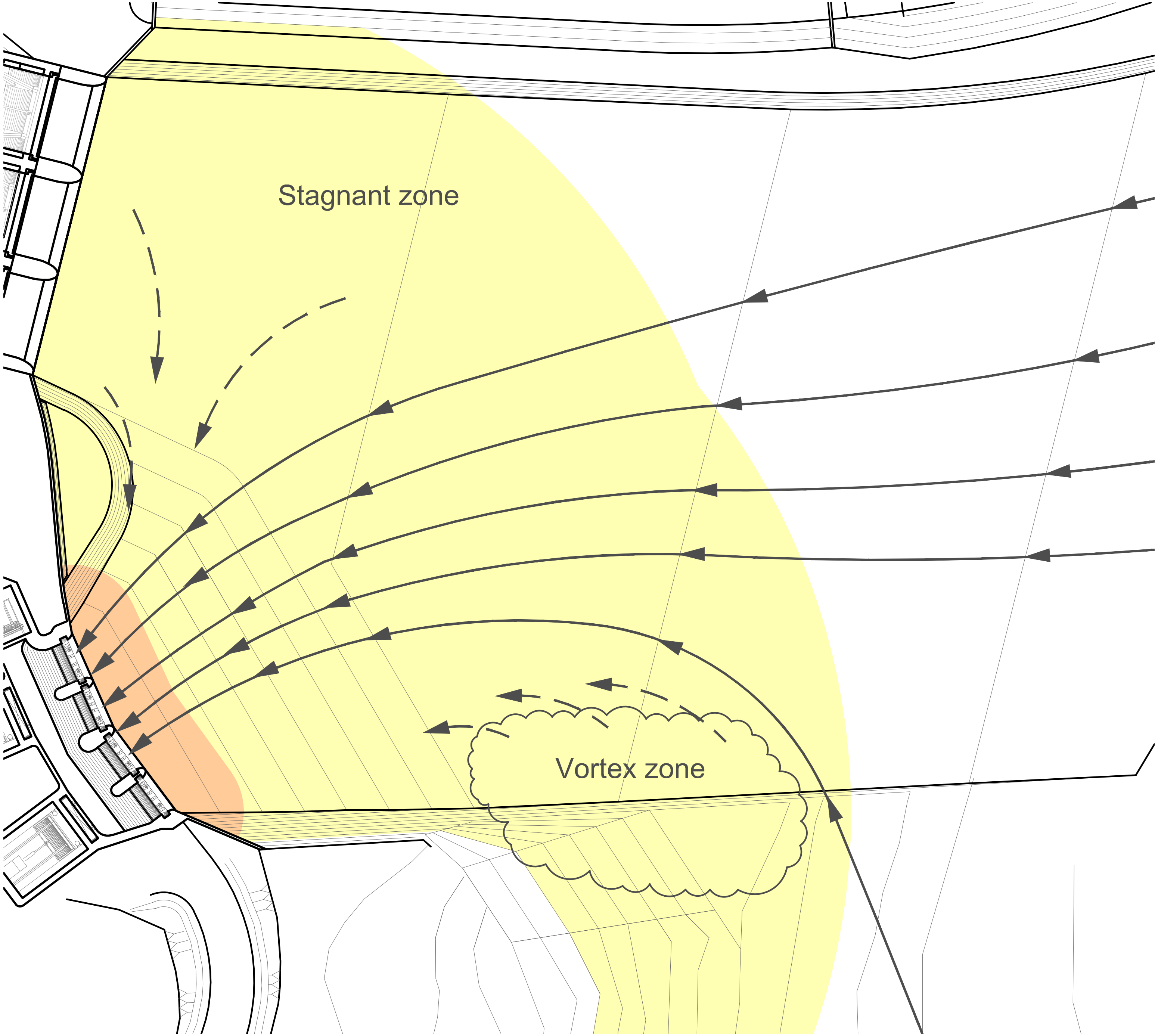

The path of the stream is estimated from visual observation of floating particles in the water surface

Decision Zone
1-10 m from SFO entrance

Discovery Zone
10-100 m from SFO entrance

RWL = 50.2 m a.s.l.
$Q_{Intake} = 240\ m^3/s$
$Q_{SFO} \approx 40\ m^3/s$
$Q_{Spillway} = 0\ m^3/s$

Surface stream patterns

Case 1.1

Landsvirkjun

UNIVERSITY OF ICELAND
SCHOOL OF ENGINEERING AND NATURAL SCIENCES
FACULTY OF CIVIL AND ENVIRONMENTAL ENGINEERING

HÁSKÓLINN Í REYKJAVÍK
REYKJAVIK UNIVERSITY

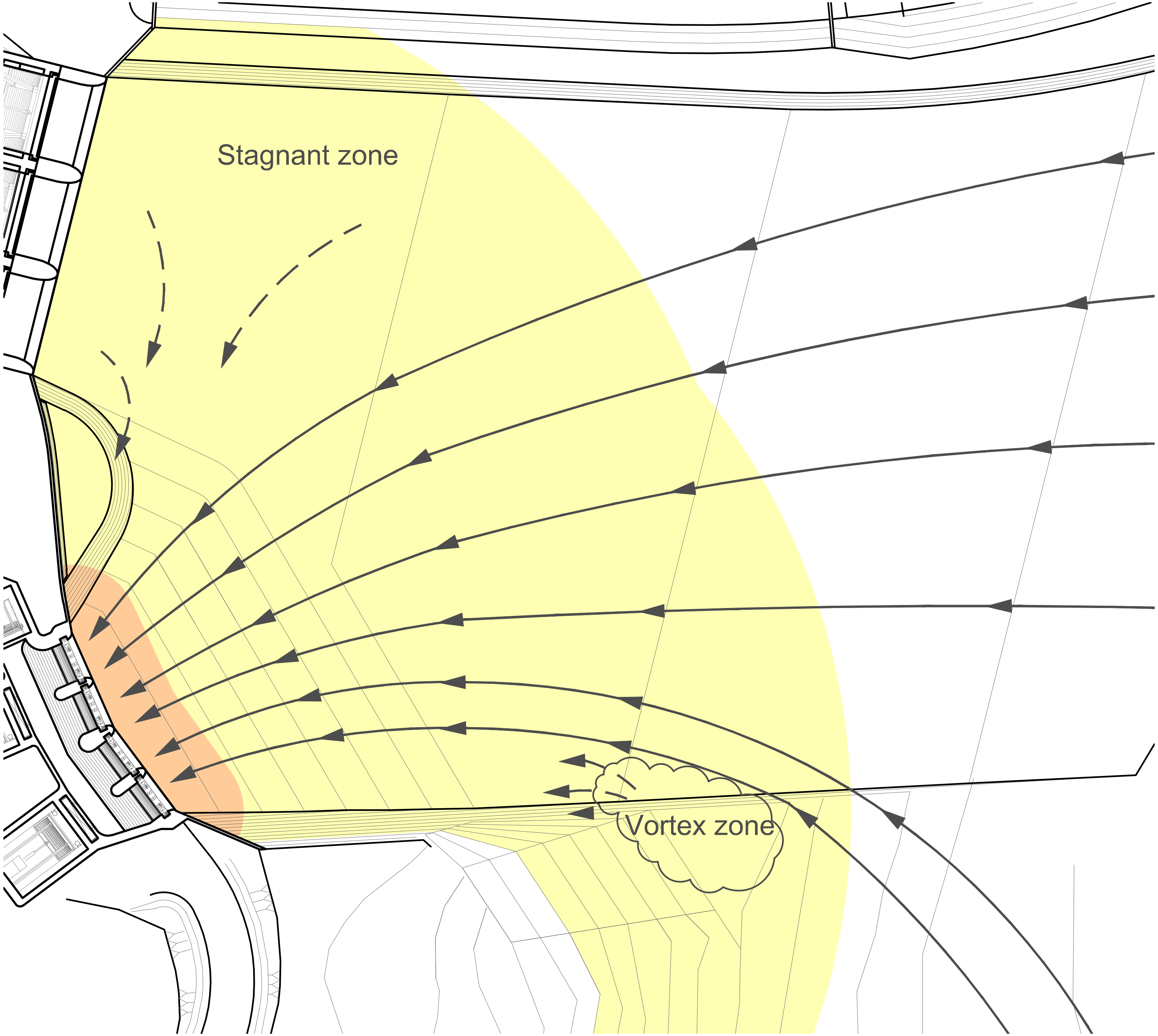

The path of the stream is estimated from visual observation of floating particles in the water surface

Decision Zone
1-10 m from SFO entrance

Discovery Zone
10-100 m from SFO entrance

RWL = 50.2 m a.s.l.
Q_{Intake} = 370 m^3/s
$Q_{SFO} \approx$ 40 m^3/s
$Q_{Spillway}$ = 0 m^3/s

Surface stream patterns

Case 1.2

Landsvirkjun

UNIVERSITY OF ICELAND
SCHOOL OF ENGINEERING AND NATURAL SCIENCES
FACULTY OF CIVIL AND ENVIRONMENTAL ENGINEERING

HÁSKÓLINN Í REYKJAVÍK
REYKJAVIK UNIVERSITY

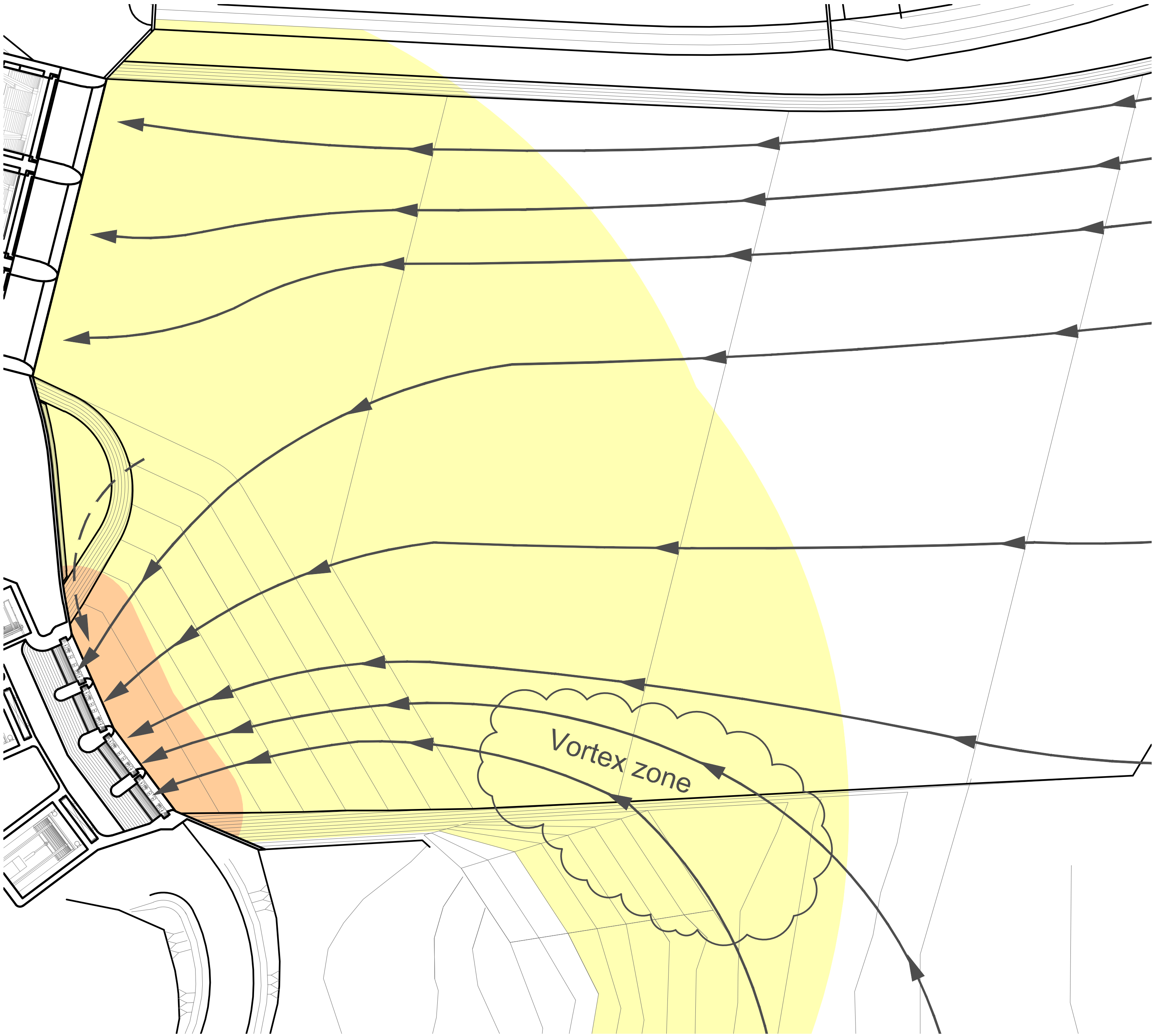

The path of the stream is estimated from visual observation of floating particles in the water surface

Decision Zone 1-10 m from SFO entrance

Discovery Zone 10-100 m from SFO entrance

RWL = 50.2 m a.s.l.

Q_{Intake} = 370 m^3/s

$Q_{SFO} \approx$ 40 m^3/s

$Q_{Spillway}$ = 70 m^3/s

Surface stream patterns

Case 1.3

Landsvirkjun

UNIVERSITY OF ICELAND

SCHOOL OF ENGINEERING AND NATURAL SCIENCES

FACULTY OF CIVIL AND ENVIRONMENTAL ENGINEERING

HÁSKÓLINN Í REYKJAVÍK

REYKJAVIK UNIVERSITY

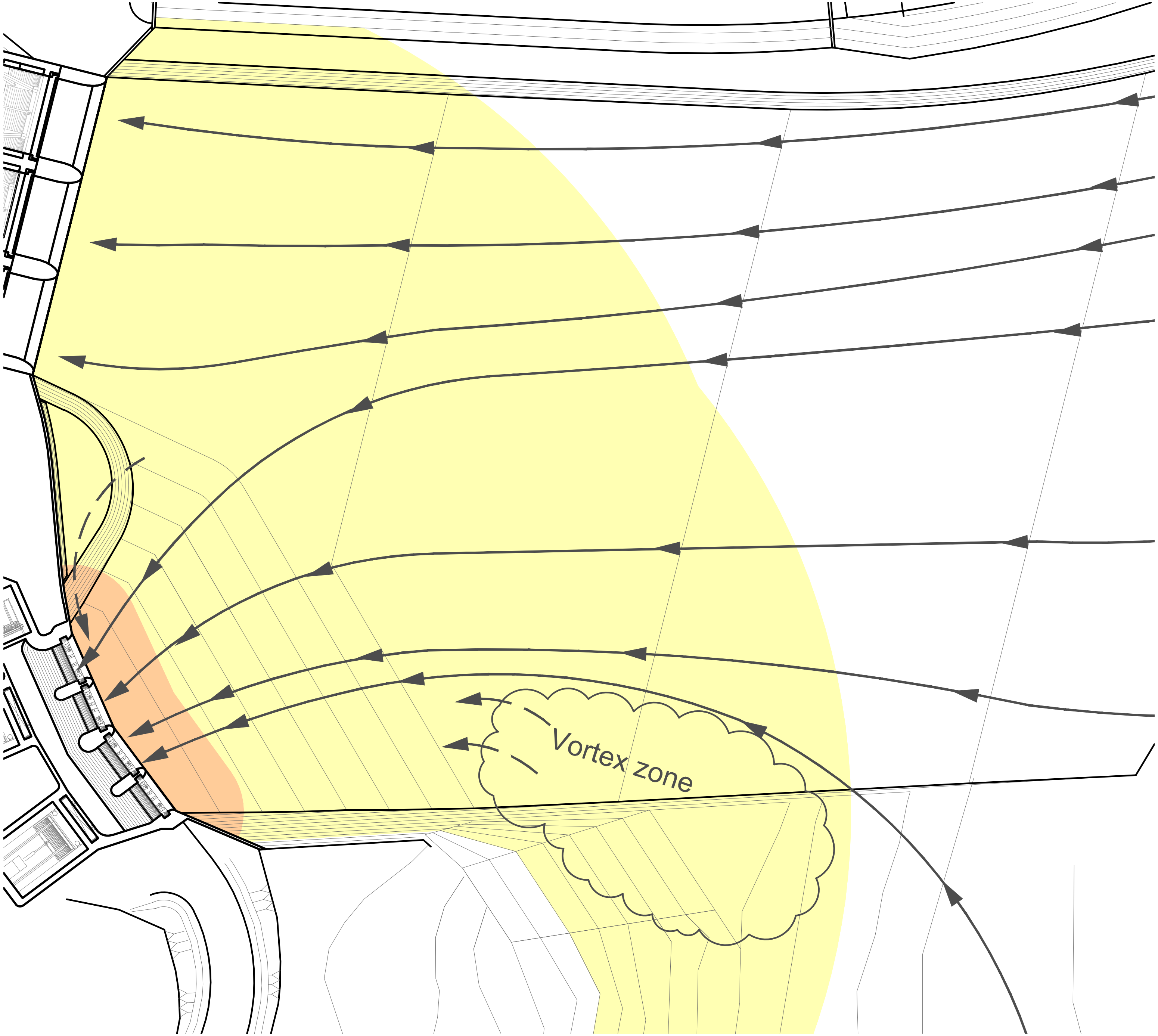

The path of the stream is estimated from visual observation of floating particles in the water surface

Decision Zone
1-10 m from SFO entrance

Discovery Zone
10-100 m from SFO entrance

RWL = 50.2 m a.s.l.
$Q_{Intake} = 370\ m^3/s$
$Q_{SFO} \approx 40\ m^3/s$
$Q_{Spillway} = 235\ m^3/s$

Surface stream patterns

Case 1.4

Landsvirkjun

UNIVERSITY OF ICELAND
SCHOOL OF ENGINEERING AND NATURAL SCIENCES
FACULTY OF CIVIL AND ENVIRONMENTAL ENGINEERING

HÁSKÓLINN Í REYKJAVÍK
REYKJAVIK UNIVERSITY

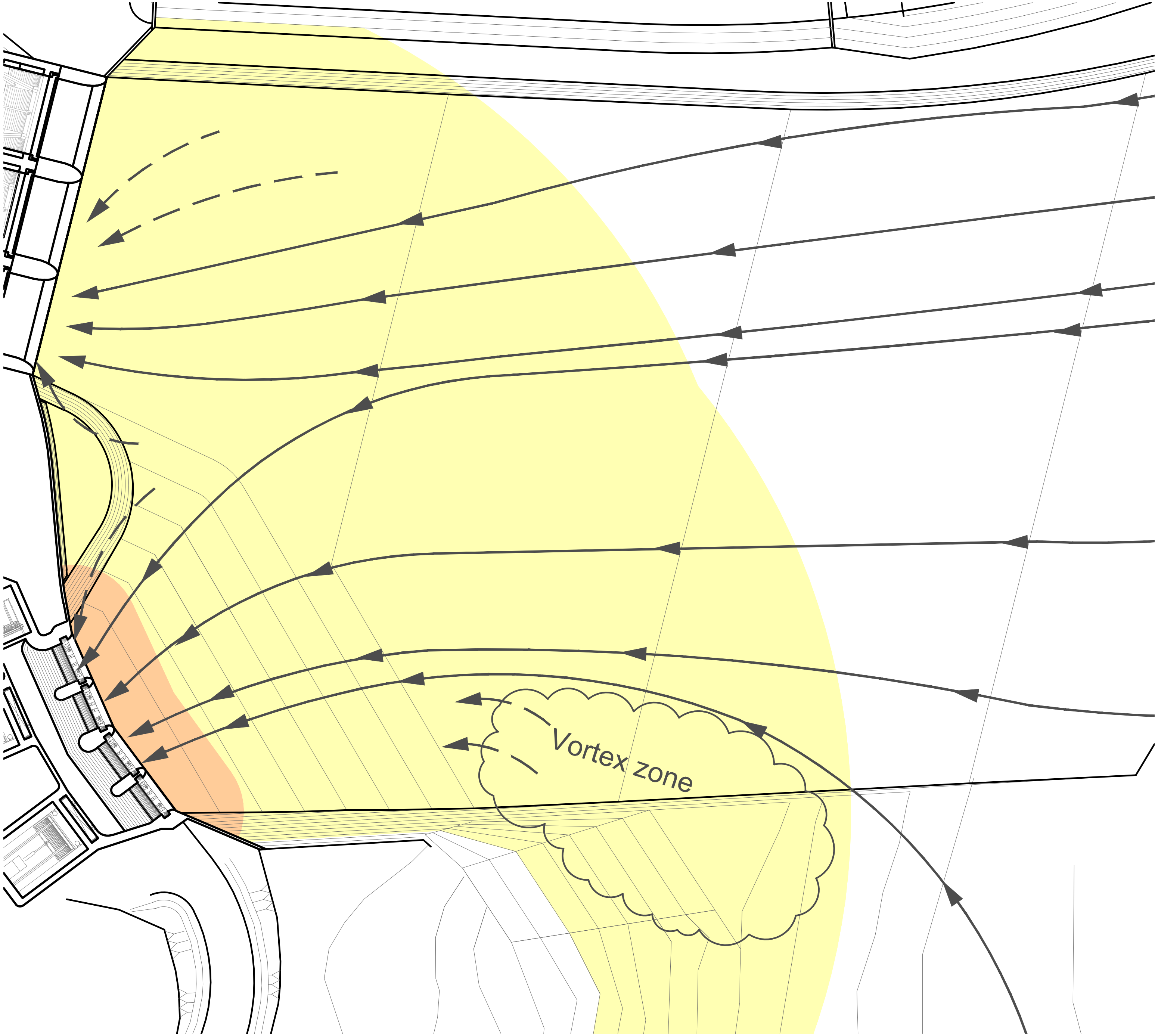

The path of the stream is estimated from visual observation of floating particles in the water surface

Spillway single gate operation

Decision Zone
1-10 m from SFO entrance

Discovery Zone
10-100 m from SFO entrance

RWL = 50.2 m a.s.l.
$Q_{Intake} = 370\ m^3/s$
$Q_{SFO} \approx 40\ m^3/s$
$Q_{Spillway} = 235\ m^3/s$

Surface stream patterns

Case 1.4 SG

Landsvirkjun

UNIVERSITY OF ICELAND
SCHOOL OF ENGINEERING AND NATURAL SCIENCES
FACULTY OF CIVIL AND ENVIRONMENTAL ENGINEERING

HÁSKÓLINN Í REYKJAVÍK
REYKJAVIK UNIVERSITY

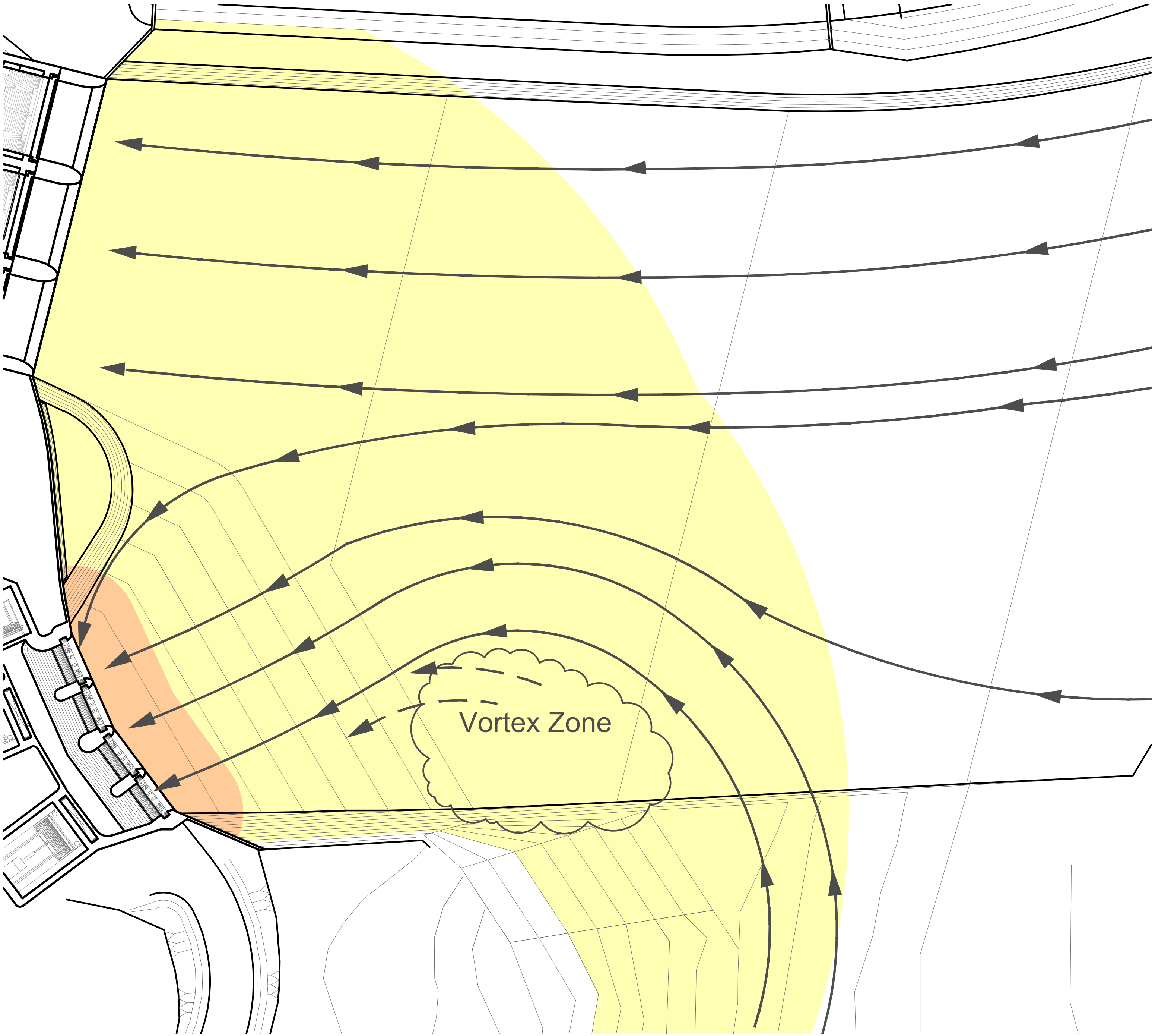

The path of the stream is estimated from visual observation of floating particles in the water surface

Decision Zone
1-10 m from SFO entrance

Discovery Zone
10-100 m from SFO entrance

RWL = 50.2 m a.s.l.
Q_{Intake} = 370 m^3/s
$Q_{SFO} \approx 40\ m^3/s$
$Q_{Spillway}$ = 515 m^3/s

Surface stream patterns

Case 1.5

Landsvirkjun

UNIVERSITY OF ICELAND
SCHOOL OF ENGINEERING AND NATURAL SCIENCES
FACULTY OF CIVIL AND ENVIRONMENTAL ENGINEERING

HÁSKÓLINN Í REYKJAVÍK
REYKJAVIK UNIVERSITY

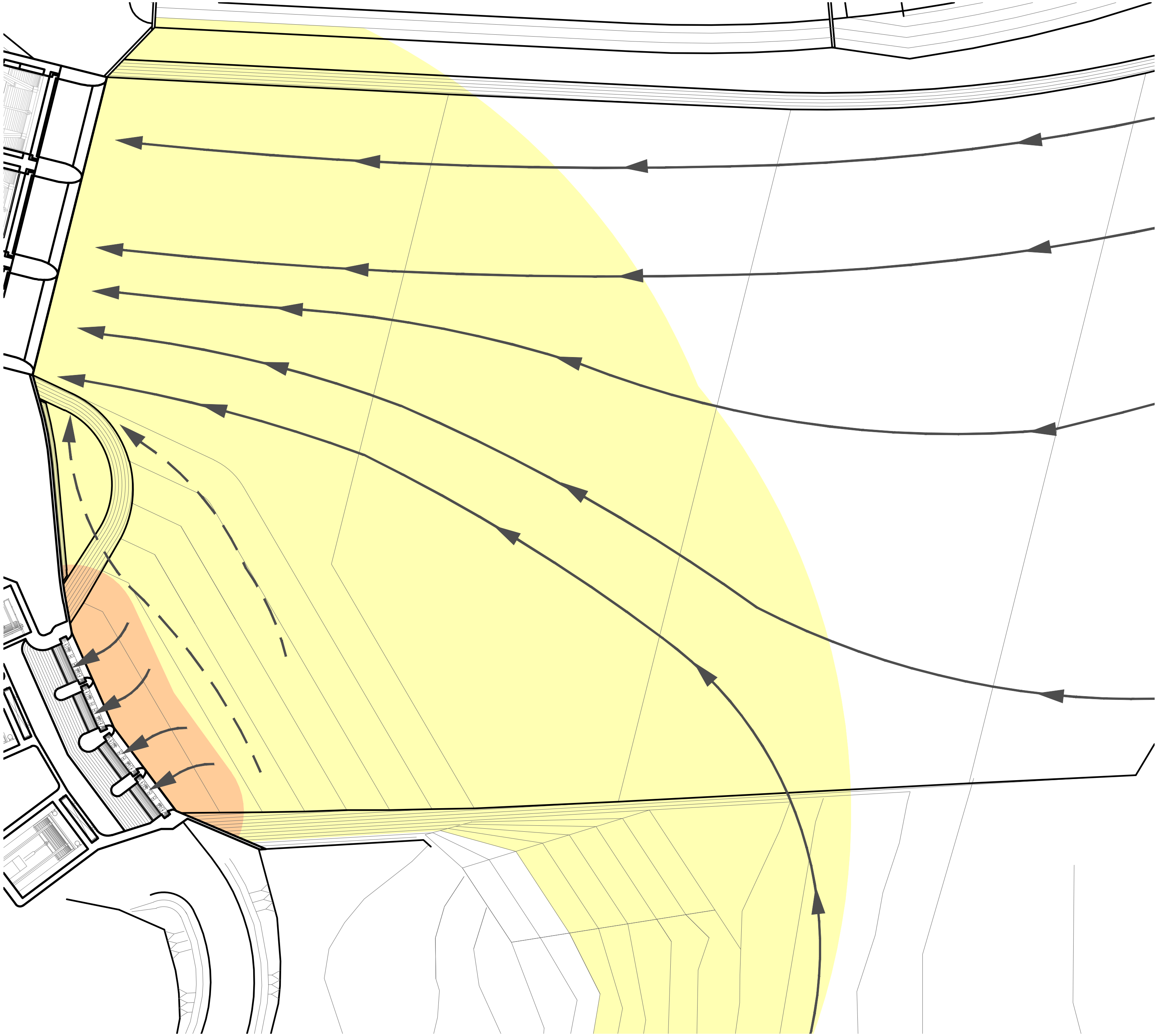

The path of the stream is estimated from visual observation of floating particles in the water surface

Decision Zone
1-10 m from SFO entrance

Discovery Zone
10-100 m from SFO entrance

RWL = 50.2 m a.s.l.
$Q_{Intake} = 0\ m^3/s$
$Q_{SFO} \approx 40\ m^3/s$
$Q_{Spillway} = 260\ m^3/s$

Surface stream patterns

Case 2.1

Landsvirkjun

UNIVERSITY OF ICELAND
SCHOOL OF ENGINEERING AND NATURAL SCIENCES
FACULTY OF CIVIL AND ENVIRONMENTAL ENGINEERING

HÁSKÓLINN Í REYKJAVÍK
REYKJAVIK UNIVERSITY

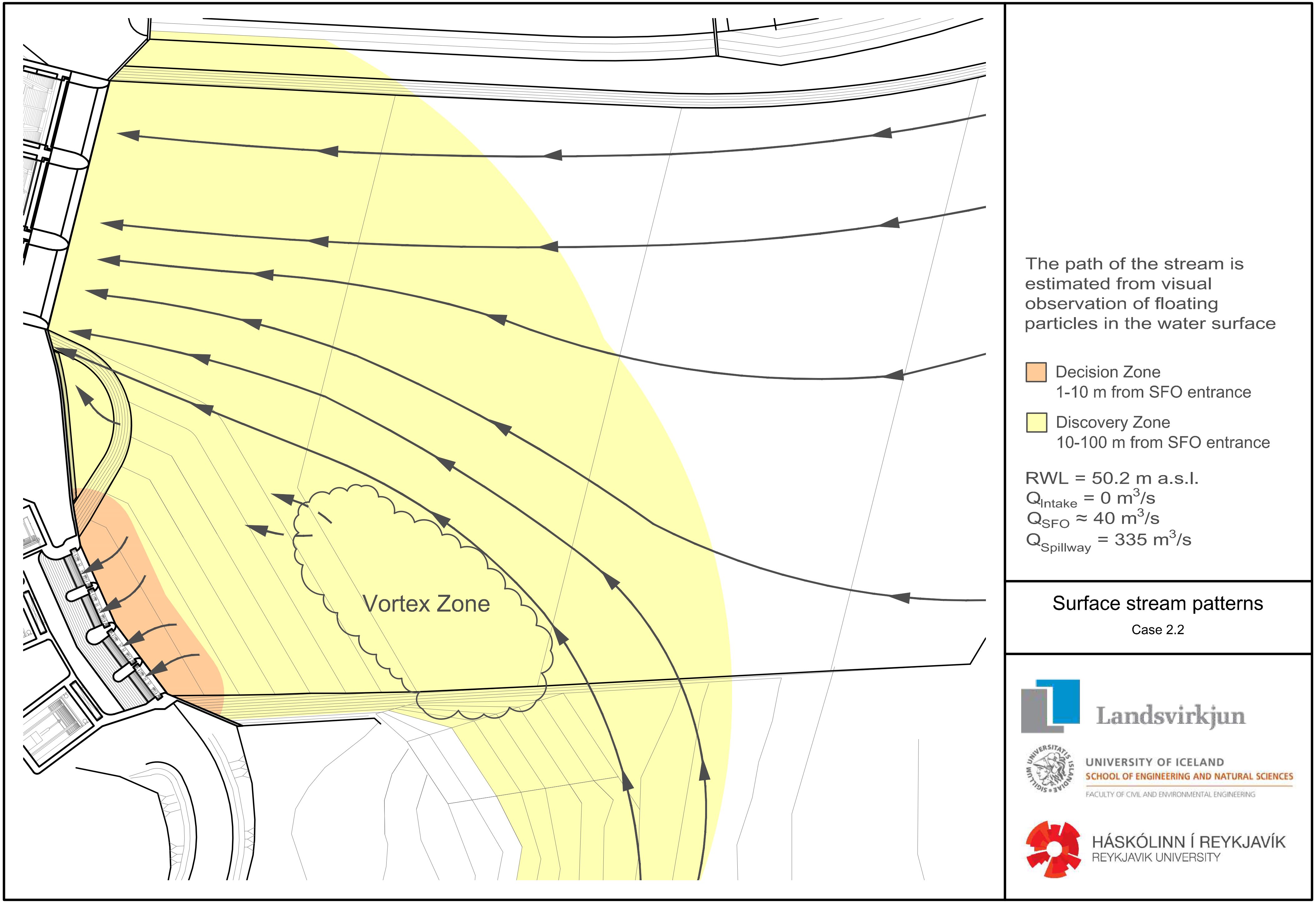

Vortex Zone
The path of the stream is estimated from visual observation of floating particles in the water surface
Decision Zone
1-10 m from SFO entrance
Discovery Zone
10-100 m from SFO entrance
RWL = 50.2 m a.s.l.
$Q_{Intake} = 0\ m^3/s$
$Q_{SFO} \approx 40\ m^3/s$
$Q_{Spillway} = 335\ m^3/s$
Surface stream patterns
Case 2.2
Landsvirkjun
UNIVERSITY OF ICELAND
SCHOOL OF ENGINEERING AND NATURAL SCIENCES
FACULTY OF CIVIL AND ENVIRONMENTAL ENGINEERING
HÁSKÓLINN Í REYKJAVÍK
REYKJAVIK UNIVERSITY

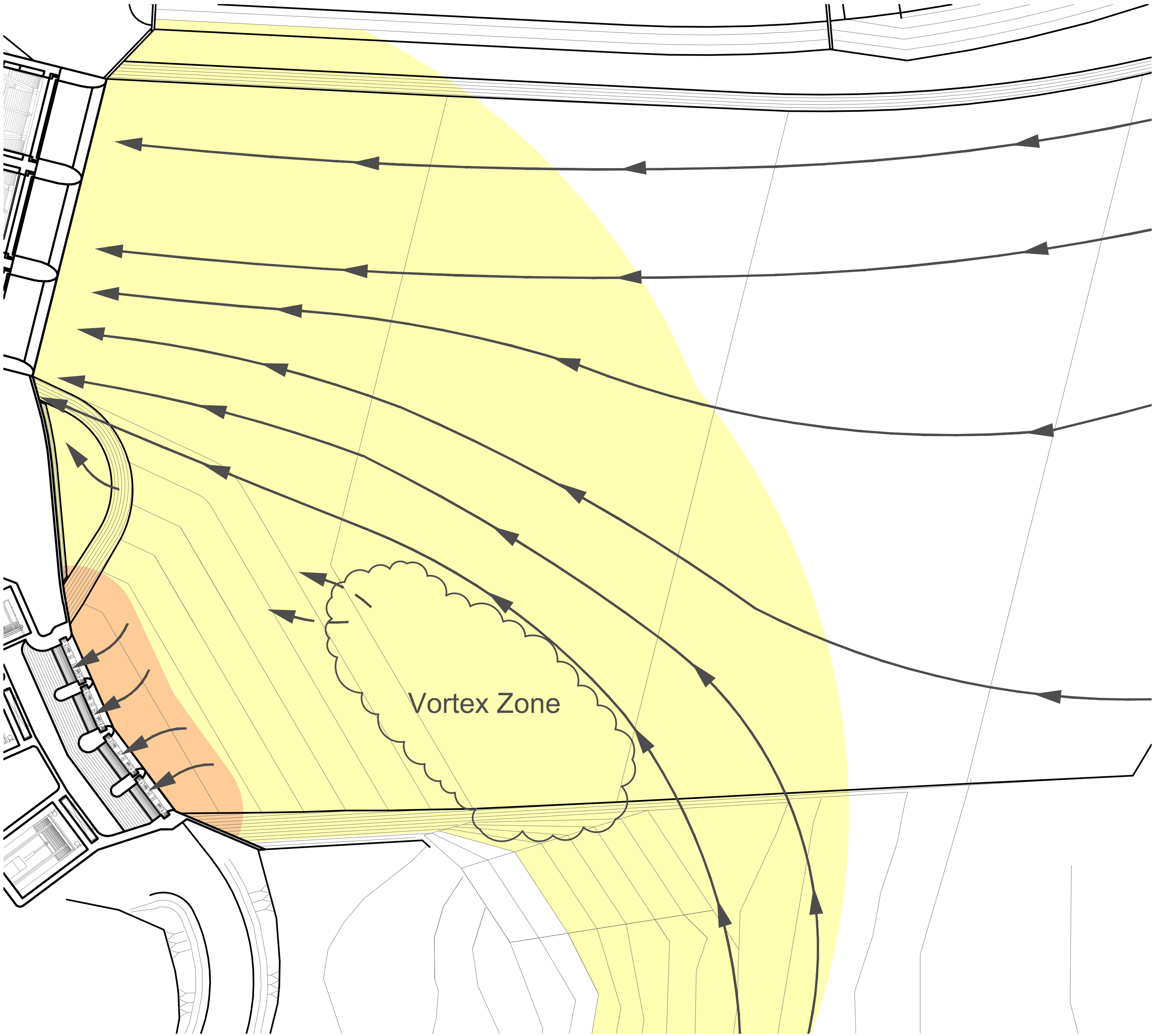

The path of the stream is estimated from visual observation of floating particles in the water surface

Decision Zone
1-10 m from SFO entrance

Discovery Zone
10-100 m from SFO entrance

RWL = 50.2 m a.s.l.
$Q_{Intake} = 0\ m^3/s$
$Q_{SFO} \approx 40\ m^3/s$
$Q_{Spillway} = 605\ m^3/s$

Surface stream patterns

Case 2.3

Landsvirkjun

UNIVERSITY OF ICELAND
SCHOOL OF ENGINEERING AND NATURAL SCIENCES
FACULTY OF CIVIL AND ENVIRONMENTAL ENGINEERING

HÁSKÓLINN Í REYKJAVÍK
REYKJAVIK UNIVERSITY

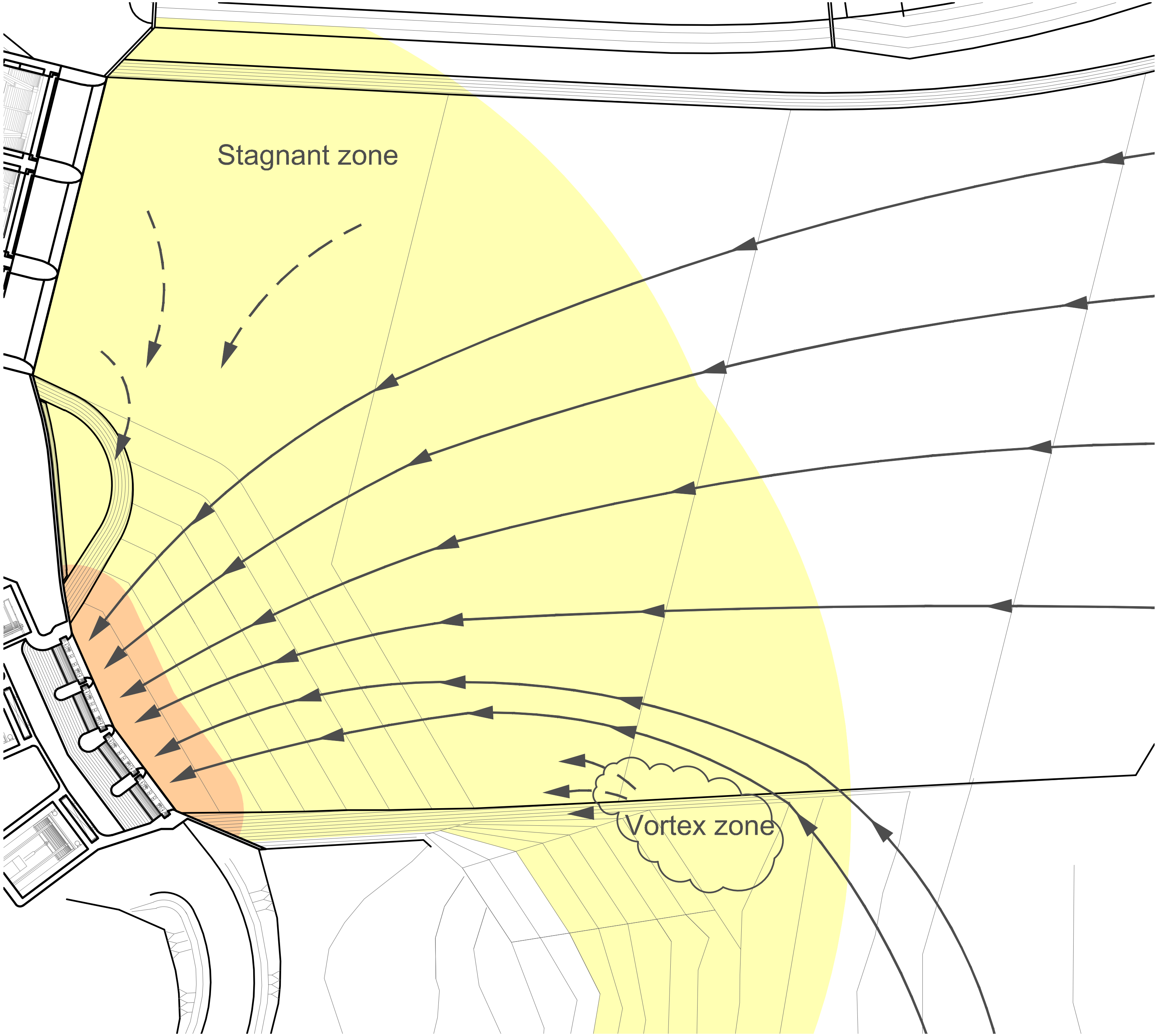

The path of the stream is estimated from visual observation of floating particles in the water surface

Decision Zone
1-10 m from SFO entrance

Discovery Zone
10-100 m from SFO entrance

RWL = 49.88 m a.s.l.
Q_{Intake} = 260 m^3/s
$Q_{SFO} \approx$ 20 m^3/s
$Q_{Spillway}$ = 0 m^3/s

Surface stream patterns

Case 3.1

Landsvirkjun

UNIVERSITY OF ICELAND
SCHOOL OF ENGINEERING AND NATURAL SCIENCES
FACULTY OF CIVIL AND ENVIRONMENTAL ENGINEERING

HÁSKÓLINN Í REYKJAVÍK
REYKJAVIK UNIVERSITY

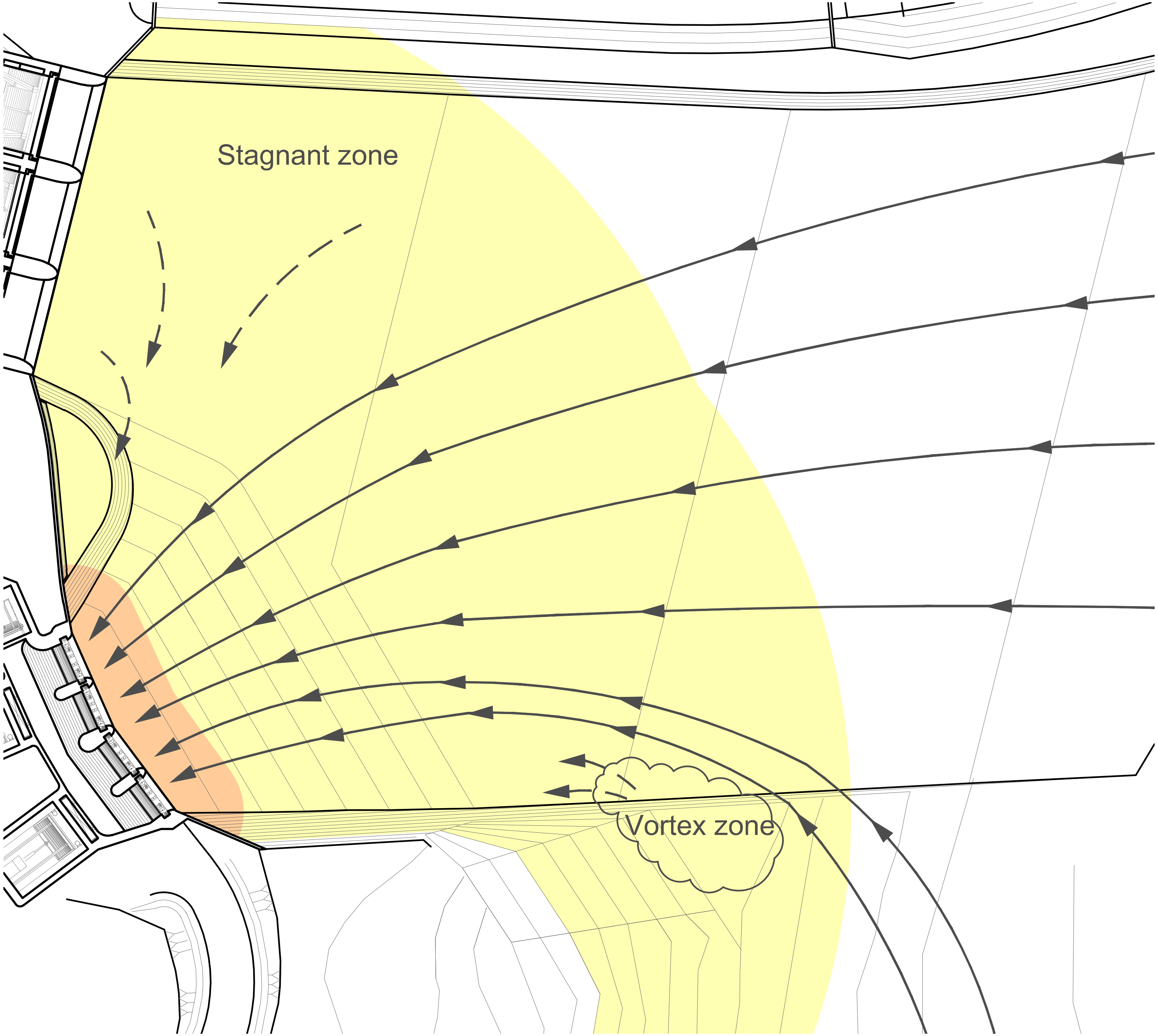

The path of the stream is estimated from visual observation of floating particles in the water surface

Decision Zone
1-10 m from SFO entrance

Discovery Zone
10-100 m from SFO entrance

RWL = 49.88 m a.s.l.
Q_{Intake} = 370 m^3/s
Q_{SFO} ≈ 20 m^3/s
$Q_{Spillway}$ = 0 m^3/s

Surface stream patterns

Case 3.2

Landsvirkjun

UNIVERSITY OF ICELAND
SCHOOL OF ENGINEERING AND NATURAL SCIENCES
FACULTY OF CIVIL AND ENVIRONMENTAL ENGINEERING

HÁSKÓLINN Í REYKJAVÍK
REYKJAVIK UNIVERSITY

I. Intake and SFO velocity distribution

In the following pages synchronized contour plots of velocity distribution in the approach flow channel are shown. The velocity distribution in the approach flow channel are discussed in detail in Section 5.3.

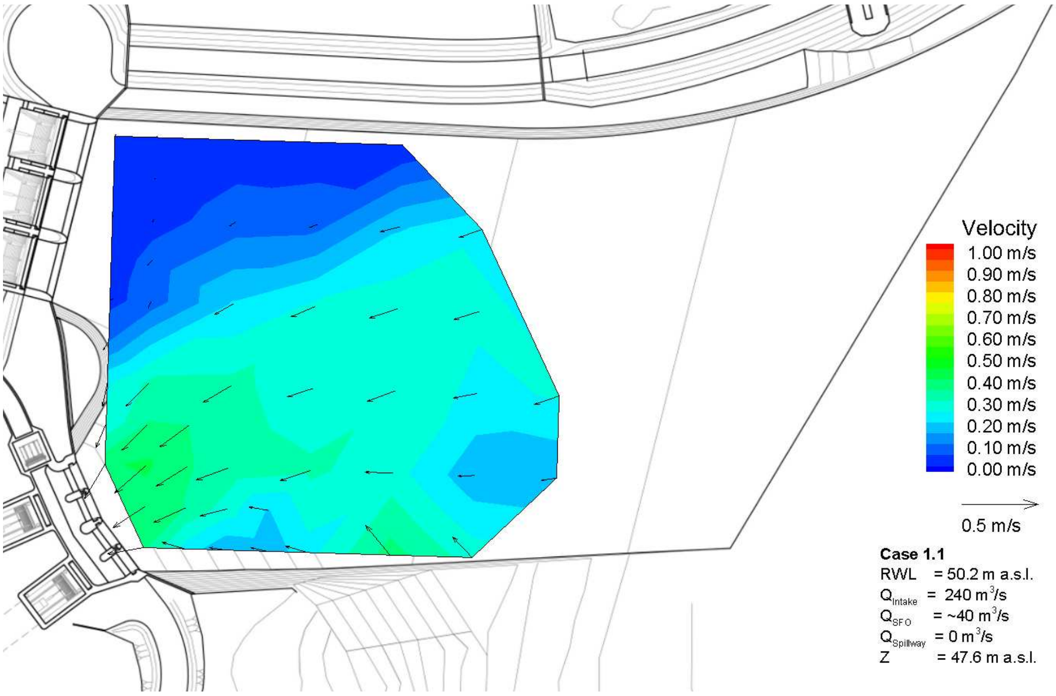

Figure I.1: *Velocity distribution in the approach flow channel for Case 1.1.*

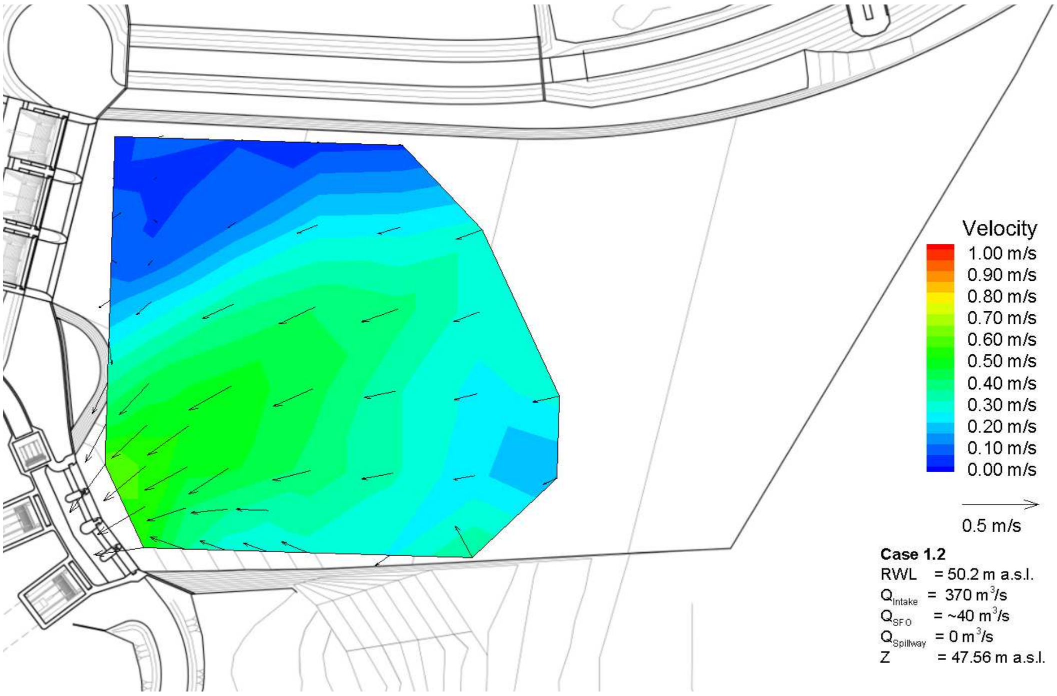

Figure I.2: *Velocity distribution in the approach flow channel for Case 1.2.*

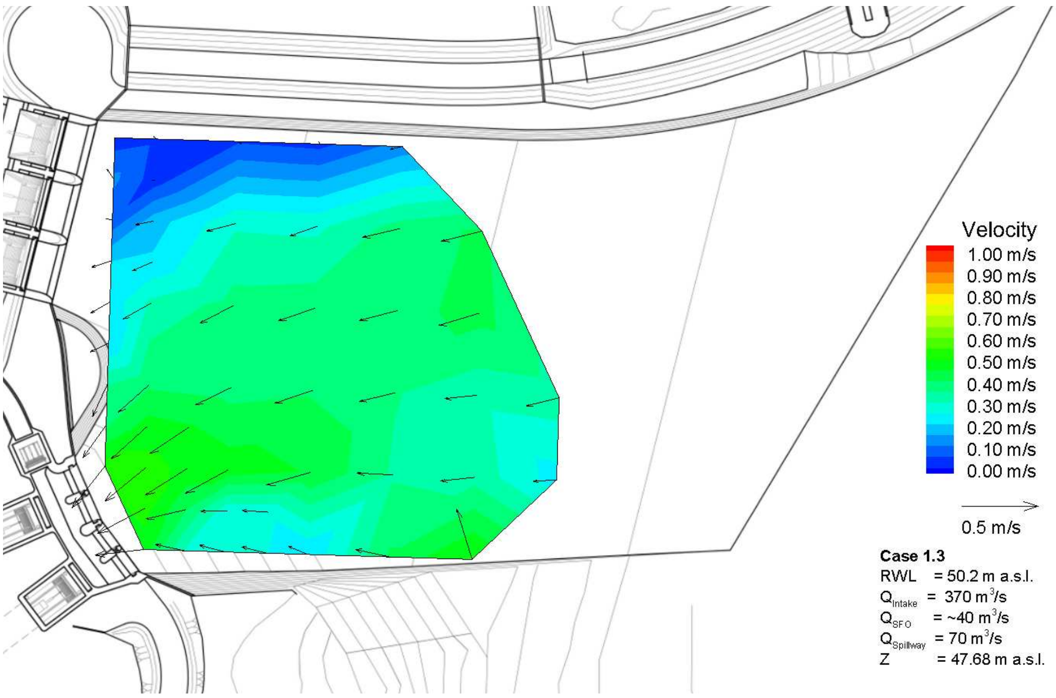

Figure I.3: *Velocity distribution in the approach flow channel for Case 1.3.*

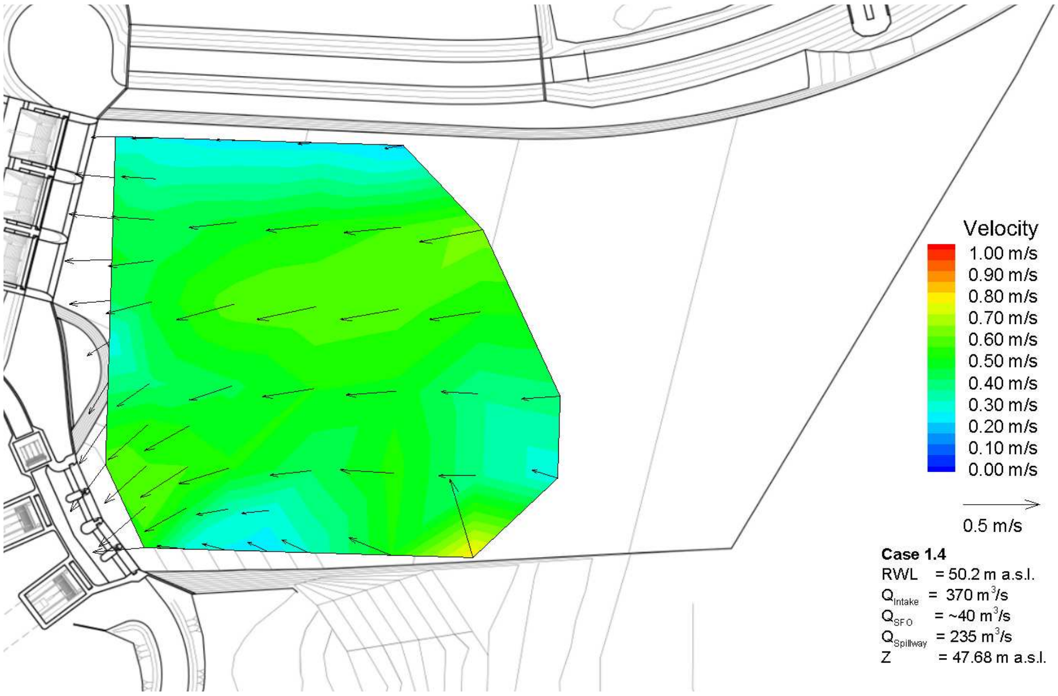

Figure I.4: *Velocity distribution in the approach flow channel for Case 1.4.*

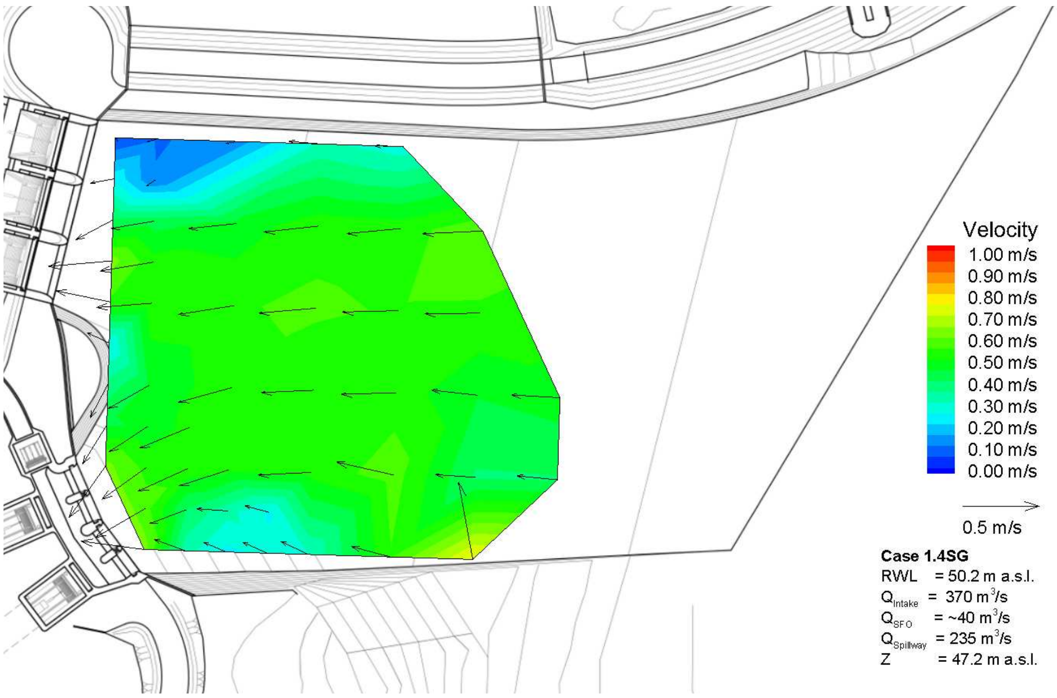

Figure I.5: *Velocity distribution in the approach flow channel for Case 1.4 SG.*

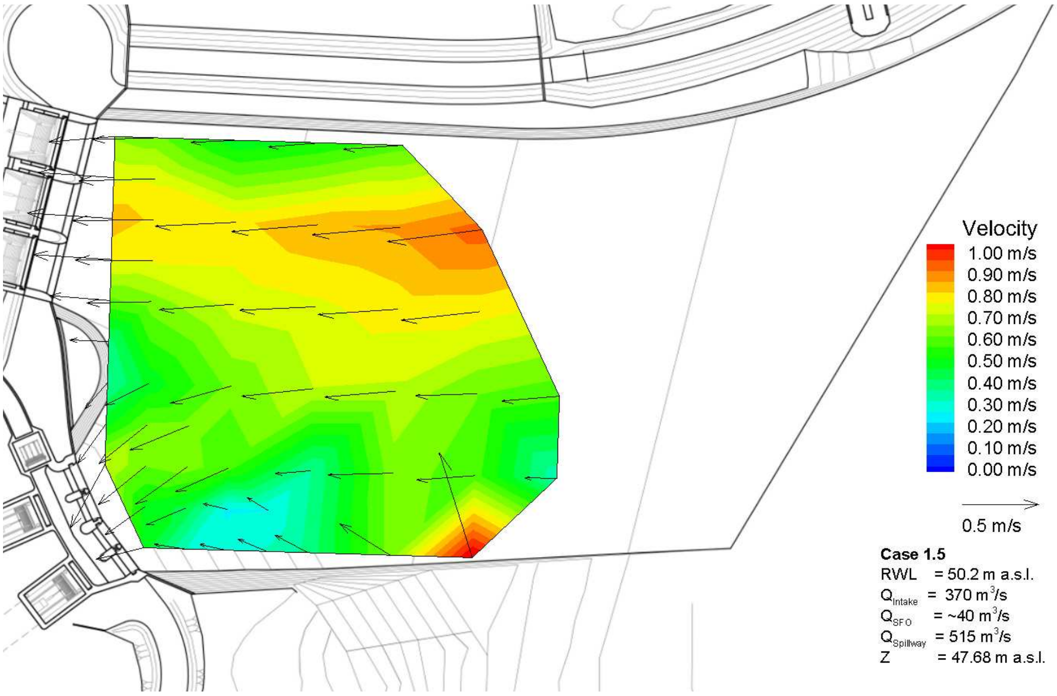

Figure I.6: *Velocity distribution in the approach flow channel for Case 1.5.*

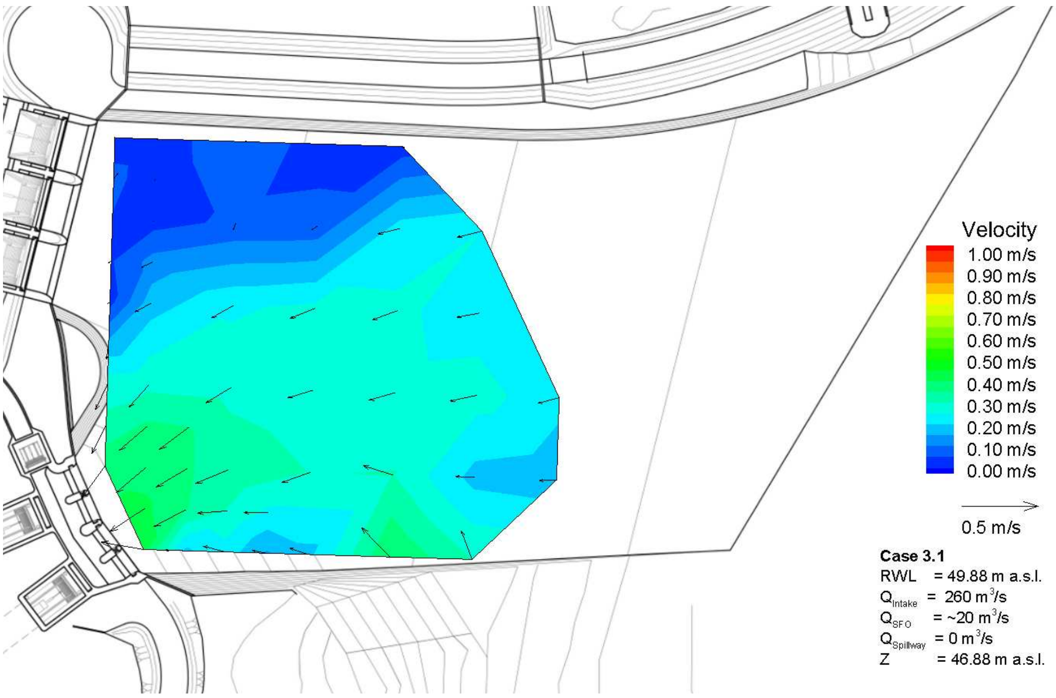

Figure I.7: *Velocity distribution in the approach flow channel for Case 3.1.*

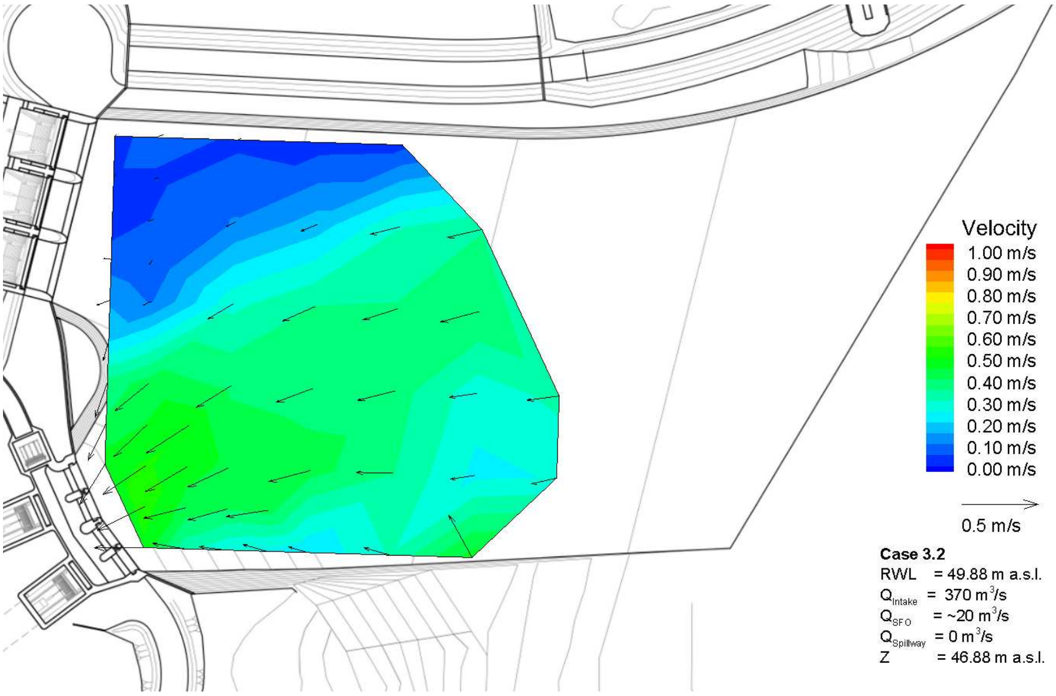

Figure I.8: *Velocity distribution in the approach flow channel for Case 3.2.*

J. Water elevations

Water elevations - Preliminary cases

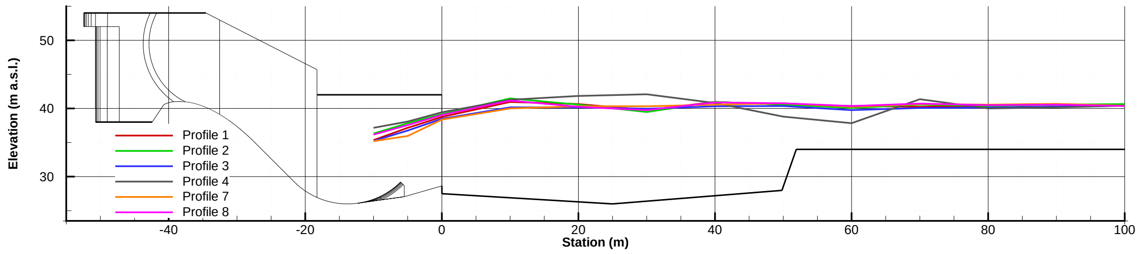

Figure J.1: *Water elevations for Section Line 1 in the downstream channel for the preliminary cases investigated in the model for Q = 2250 m^3/s..*

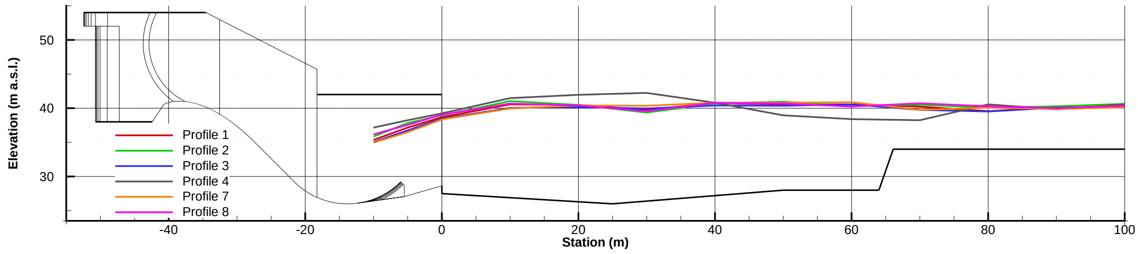

Figure J.2: *Water elevations for Section Line 2 in the downstream channel for the preliminary cases investigated in the model for Q = 2250 m^3/s.*

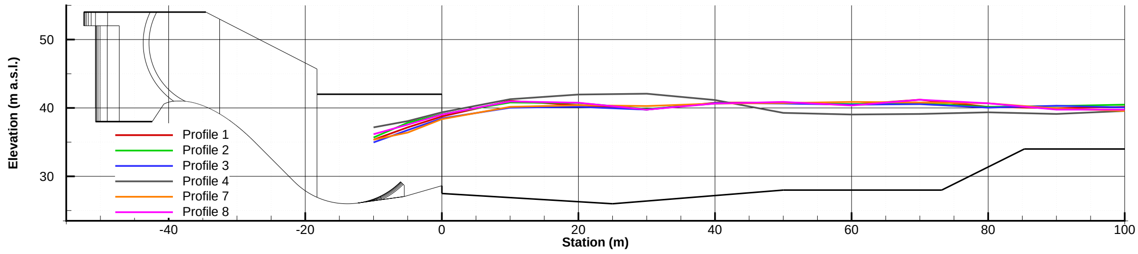

Figure J.3: *Water elevations for Section Line 3 in the downstream channel for the preliminary cases investigated in the model for Q = 2250 m^3/s.*

Water elevations - Main discharge cases

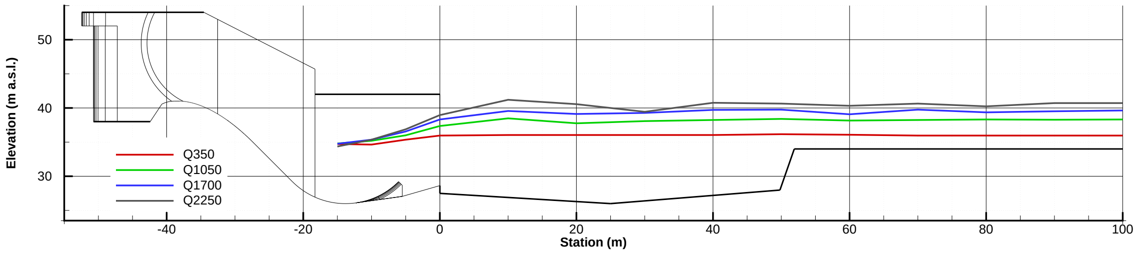

Figure J.4: *Water elevations for Section Line 1 in the system for the main discharges investigated in the model.*

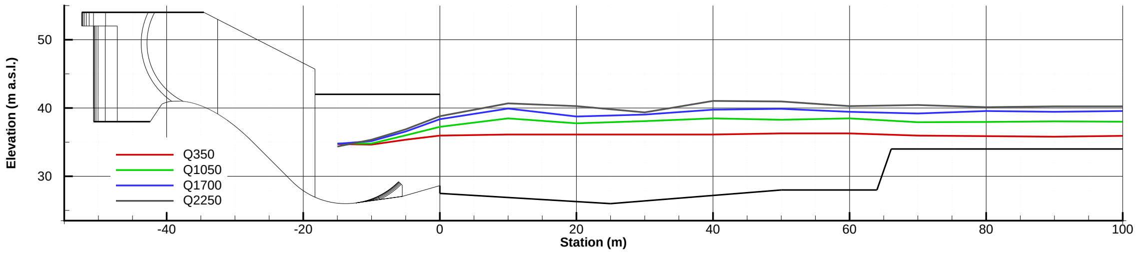

Figure J.5: *Water elevations for Section Line 2 in the system for the main discharges investigated in the model.*

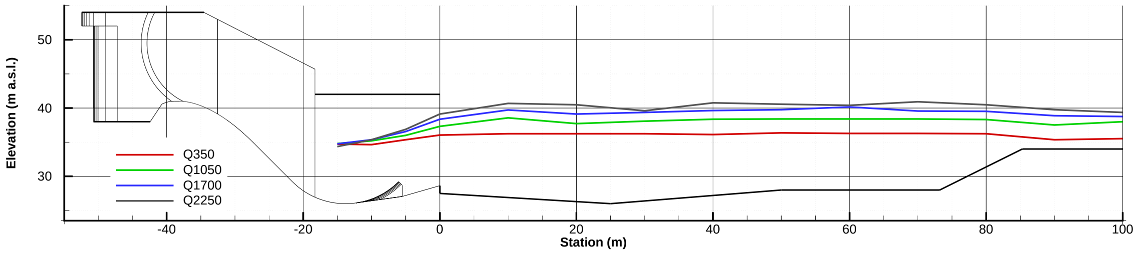

Figure J.6: *Water elevations for Section Line 3 in the system for the main discharges investigated in the model.*

Water elevations - Secondary discharge cases

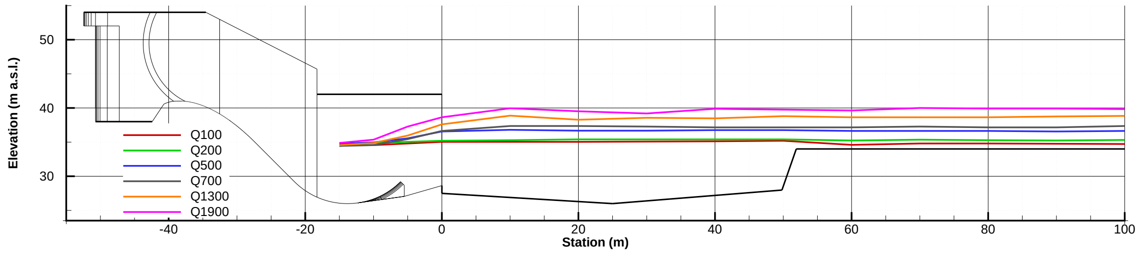

Figure J.7: *Water elevations for Section Line 1 in the system for the secondary discharges investigated in the model.*

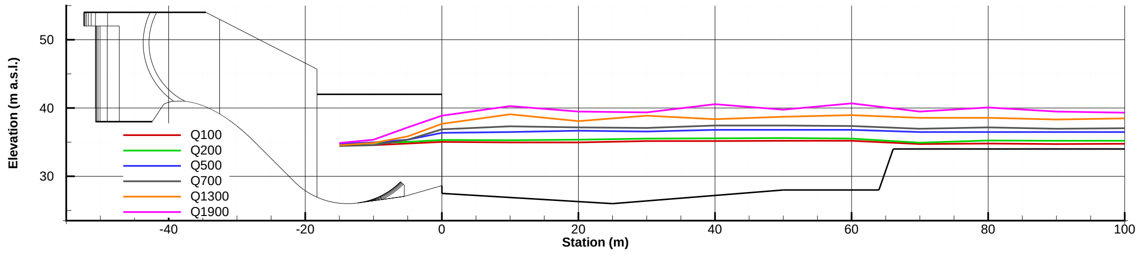

Figure J.8: *Water elevations for Section Line 2 in the system for the secondary discharges investigated in the model.*

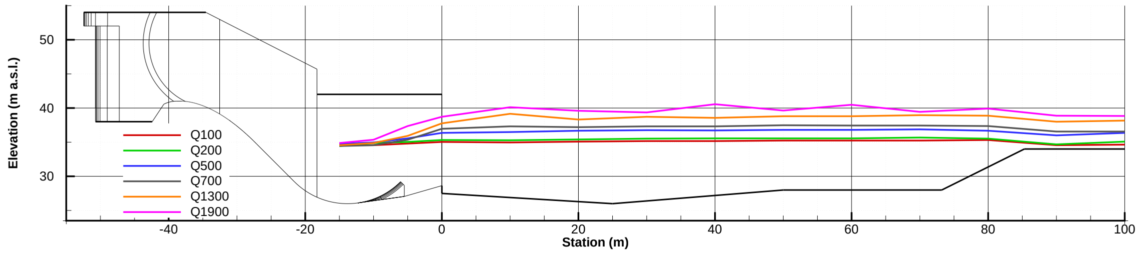

Figure J.9: *Water elevations for Section Line 3 in the system for the secondary discharges investigated in the model.*

Table J.1: *Water elevations in the downstream river sections for 350 m^3/s.*

X	Y	Water elev.	X	Y	Water elev.	X	Y	Water elev.
m	m	m a.s.l.	m	m	m a.s.l.	m	m	m a.s.l.
50.0	81.6	36.4	70.0	-15.0	36.3	110.0	0.0	35.8
50.0	47.2	36.4	80.0	-15.0	36.2	120.0	0.0	35.7
30.0	64.0	36.2	90.0	-15.0	35.4	-15.0	15.0	34.7
80.0	45.6	36.2	100.0	-15.0	35.5	-10.0	15.0	34.6
106.8	30.4	36.1	110.0	-15.0	35.8	-5.0	15.0	35.4
107.0	-34.0	35.6	120.0	-15.0	35.5	0.0	15.0	36.0
142.0	-4.0	35.4	-15.0	0.0	34.7	10.0	15.0	36.0
176.0	-37.0	33.4	-10.0	0.0	34.6	20.0	15.0	36.0
146.4	-60.0	33.4	-5.0	0.0	35.4	30.0	15.0	36.0
136.8	-40.0	34.6	0.0	0.0	36.0	40.0	15.0	36.0
-15.0	-15.0	34.7	10.0	0.0	36.1	50.0	15.0	36.2
-10.0	-15.0	34.6	20.0	0.0	36.1	60.0	15.0	36.1
-5.0	-15.0	35.4	30.0	0.0	36.1	70.0	15.0	36.0
0.0	-15.0	36.0	40.0	0.0	36.1	80.0	15.0	36.0
10.0	-15.0	36.2	50.0	0.0	36.3	90.0	15.0	36.0
20.0	-15.0	36.2	60.0	0.0	36.3	100.0	15.0	36.0
30.0	-15.0	36.2	70.0	0.0	36.0	110.0	15.0	36.0
40.0	-15.0	36.1	80.0	0.0	35.9	120.0	15.0	36.0
50.0	-15.0	36.4	90.0	0.0	35.8			
60.0	-15.0	36.3	100.0	0.0	35.9			

Table J.2: *Water elevations in the downstream river sections for 1050 m^3/s.*

X	Y	Water elev.	X	Y	Water elev.	X	Y	Water elev.
m	m	m a.s.l.	m	m	m a.s.l.	m	m	m a.s.l.
50.0	81.6	38.5	70.0	-15.0	38.4	110.0	0.0	38.0
50.0	47.2	38.5	80.0	-15.0	38.3	120.0	0.0	37.9
30.0	64.0	38.5	90.0	-15.0	37.5	-15.0	15.0	34.8
80.0	45.6	38.5	100.0	-15.0	38.0	-10.0	15.0	35.2
106.8	30.4	38.4	110.0	-15.0	37.6	-5.0	15.0	36.0
107.0	-34.0	37.3	120.0	-15.0	37.6	0.0	15.0	37.4
142.0	-4.0	37.4	-15.0	0.0	34.8	10.0	15.0	38.5
176.0	-37.0	34.9	-10.0	0.0	34.8	20.0	15.0	37.8
146.4	-60.0	35.1	-5.0	0.0	36.0	30.0	15.0	38.1
136.8	-40.0	36.5	0.0	0.0	37.2	40.0	15.0	38.2
-15.0	-15.0	34.8	10.0	0.0	38.5	50.0	15.0	38.4
-10.0	-15.0	35.2	20.0	0.0	37.8	60.0	15.0	38.2
-5.0	-15.0	36.0	30.0	0.0	38.1	70.0	15.0	38.2
0.0	-15.0	37.3	40.0	0.0	38.5	80.0	15.0	38.3
10.0	-15.0	38.6	50.0	0.0	38.3	90.0	15.0	38.3
20.0	-15.0	37.7	60.0	0.0	38.5	100.0	15.0	38.3
30.0	-15.0	38.1	70.0	0.0	37.9	110.0	15.0	38.3
40.0	-15.0	38.4	80.0	0.0	38.0	120.0	15.0	38.2
50.0	-15.0	38.4	90.0	0.0	38.0			
60.0	-15.0	38.4	100.0	0.0	38.0			

Table J.3: *Water elevations in the downstream river sections for 1700 m^3/s.*

X	Y	Water elev.	X	Y	Water elev.	X	Y	Water elev.
m	m	m a.s.l.	m	m	m a.s.l.	m	m	m a.s.l.
50.0	81.6	40.0	70.0	-15.0	39.6	110.0	0.0	39.4
50.0	47.2	39.9	80.0	-15.0	39.5	120.0	0.0	39.4
30.0	64.0	40.0	90.0	-15.0	38.9	-15.0	15.0	34.8
80.0	45.6	39.8	100.0	-15.0	38.8	-10.0	15.0	35.4
106.8	30.4	39.8	110.0	-15.0	38.9	-5.0	15.0	36.6
107.0	-34.0	37.9	120.0	-15.0	38.6	0.0	15.0	38.3
142.0	-4.0	38.8	-15.0	0.0	34.8	10.0	15.0	39.6
176.0	-37.0	35.8	-10.0	0.0	35.2	20.0	15.0	39.1
146.4	-60.0	36.0	-5.0	0.0	36.6	30.0	15.0	39.3
136.8	-40.0	37.4	0.0	0.0	38.4	40.0	15.0	39.7
-15.0	-15.0	34.8	10.0	0.0	39.9	50.0	15.0	39.8
-10.0	-15.0	35.4	20.0	0.0	38.8	60.0	15.0	39.1
-5.0	-15.0	36.6	30.0	0.0	39.0	70.0	15.0	39.8
0.0	-15.0	38.4	40.0	0.0	39.8	80.0	15.0	39.4
10.0	-15.0	39.7	50.0	0.0	39.9	90.0	15.0	39.5
20.0	-15.0	39.1	60.0	0.0	39.4	100.0	15.0	39.6
30.0	-15.0	39.4	70.0	0.0	39.2	110.0	15.0	39.8
40.0	-15.0	39.6	80.0	0.0	39.6	120.0	15.0	39.8
50.0	-15.0	39.8	90.0	0.0	39.4			
60.0	-15.0	40.2	100.0	0.0	39.6			

Table J.4: *Water elevations in the downstream river sections for 2250 m^3/s.*

X	Y	Water elev.	X	Y	Water elev.	X	Y	Water elev.
m	m	m a.s.l.	m	m	m a.s.l.	m	m	m a.s.l.
50.0	82.0	41.4	70.0	-15.0	40.9	110.0	0.0	40.4
50.0	47.0	41.1	80.0	-15.0	40.5	120.0	0.0	40.2
30.0	64.0	41.0	90.0	-15.0	39.8	-15.0	15.0	34.4
80.0	46.0	40.9	100.0	-15.0	39.4	-10.0	15.0	35.4
107.0	30.0	40.8	110.0	-15.0	39.4	-5.0	15.0	36.9
107.0	-34.0	38.4	120.0	-15.0	39.6	0.0	15.0	39.0
142.0	-4.0	39.5	-15.0	0.0	34.4	10.0	15.0	41.2
176.0	-37.0	37.0	-10.0	0.0	35.4	20.0	15.0	40.6
146.0	-60.0	36.8	-5.0	0.0	36.9	30.0	15.0	39.4
137.0	-40.0	38.1	0.0	0.0	38.8	40.0	15.0	40.8
-15.0	-15.0	34.4	10.0	0.0	40.7	50.0	15.0	40.6
-10.0	-15.0	35.4	20.0	0.0	40.3	60.0	15.0	40.3
-5.0	-15.0	36.9	30.0	0.0	39.4	70.0	15.0	40.6
0.0	-15.0	39.1	40.0	0.0	41.0	80.0	15.0	40.2
10.0	-15.0	40.7	50.0	0.0	41.0	90.0	15.0	40.7
20.0	-15.0	40.5	60.0	0.0	40.3	100.0	15.0	40.7
30.0	-15.0	39.6	70.0	0.0	40.4	110.0	15.0	40.6
40.0	-15.0	40.8	80.0	0.0	40.1	120.0	15.0	40.6
50.0	-15.0	40.6	90.0	0.0	40.2			
60.0	-15.0	40.4	100.0	0.0	40.2			

K. Velocity measurements

Preliminary design

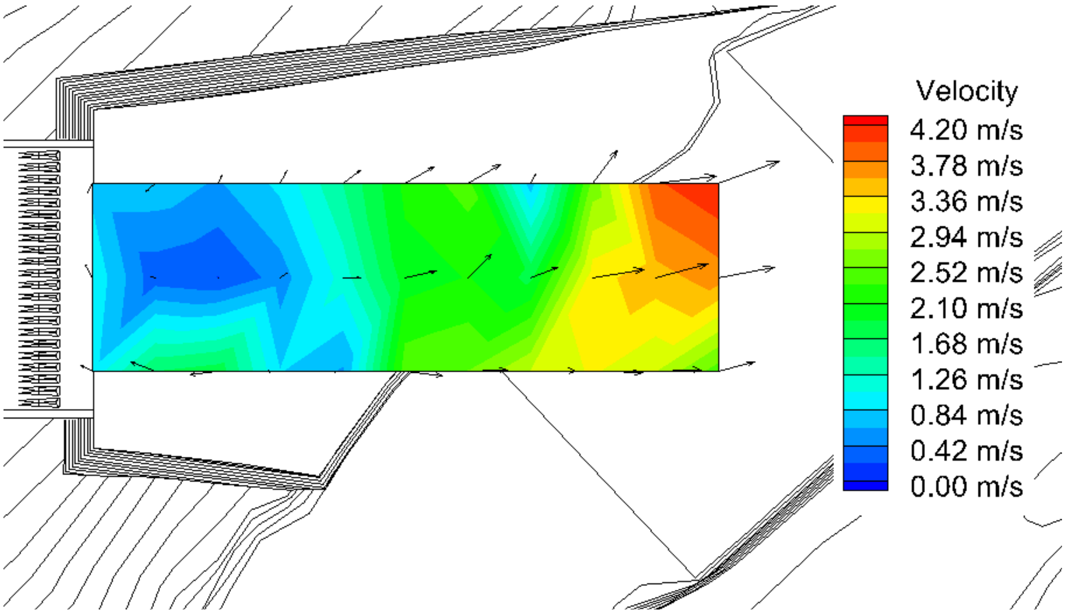

Figure K.1: *Velocity 1 m above the downstream invert for bottom profile 1.* $Q = 2250\ m^3/s$.

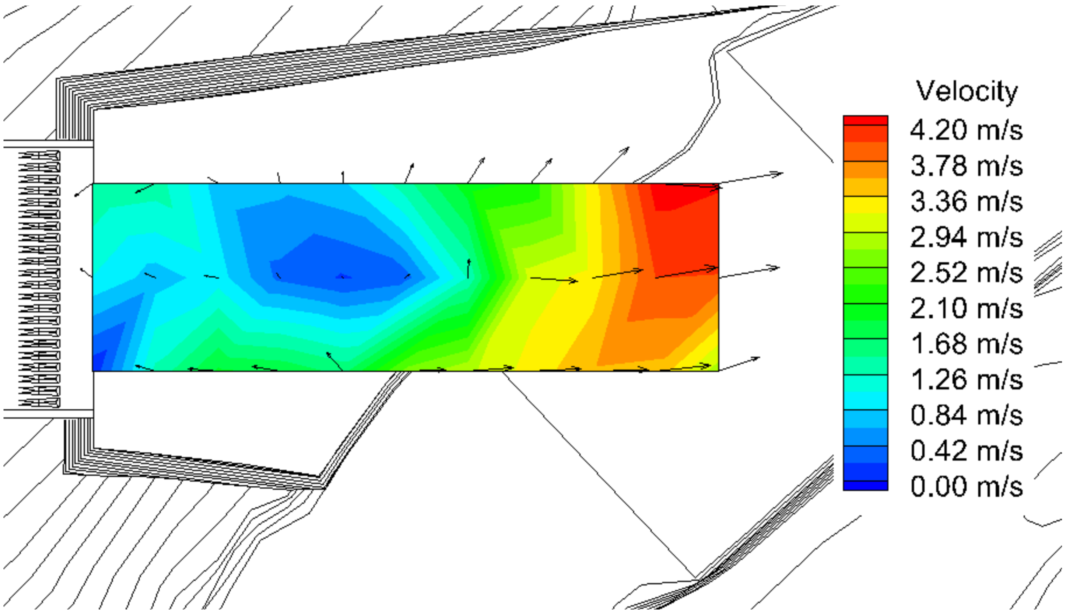

Figure K.2: *Velocity 1 m above the downstream invert for bottom profile 2.* $Q = 2250\ m^3/s$.

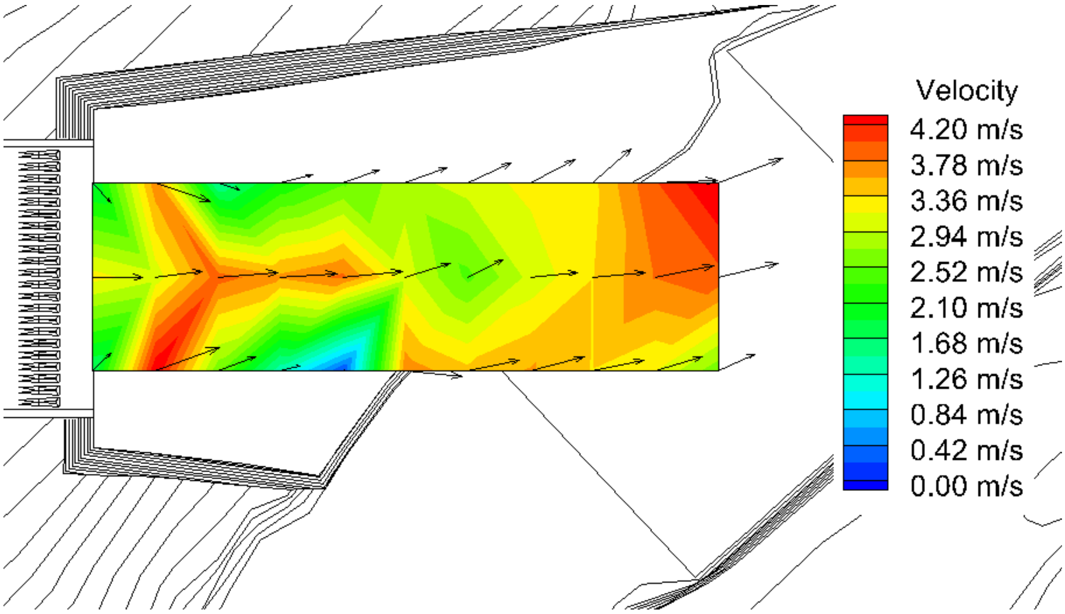

Figure K.3: *Velocity 1 m above the downstream invert for bottom profile 3. $Q = 2250$ m^3/s.*

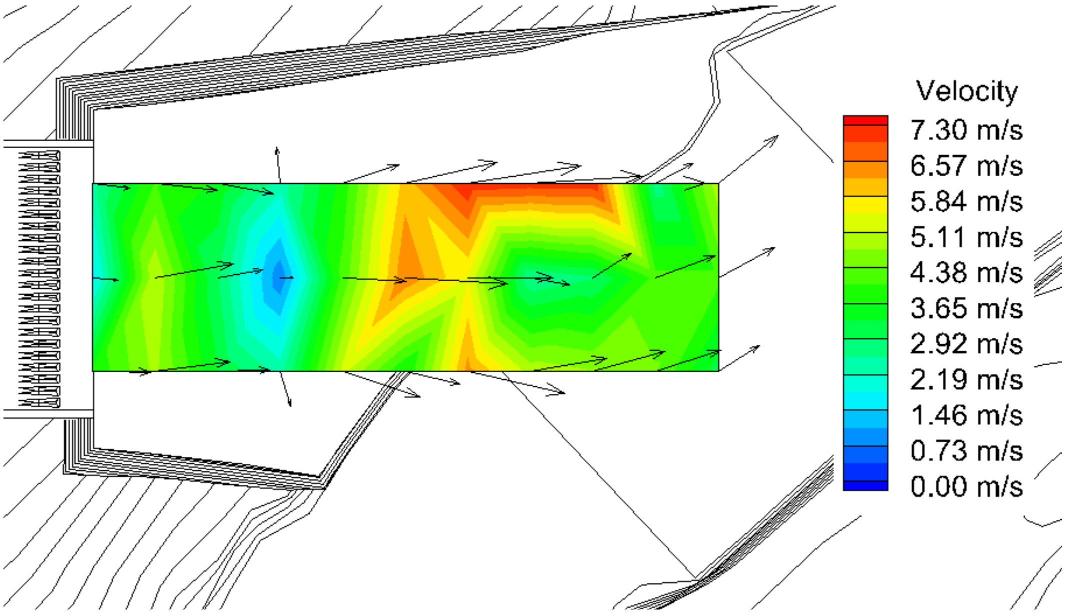

Figure K.4: *Velocity 1 m above the downstream invert for bottom profile 4. $Q = 2250$ m^3/s.*

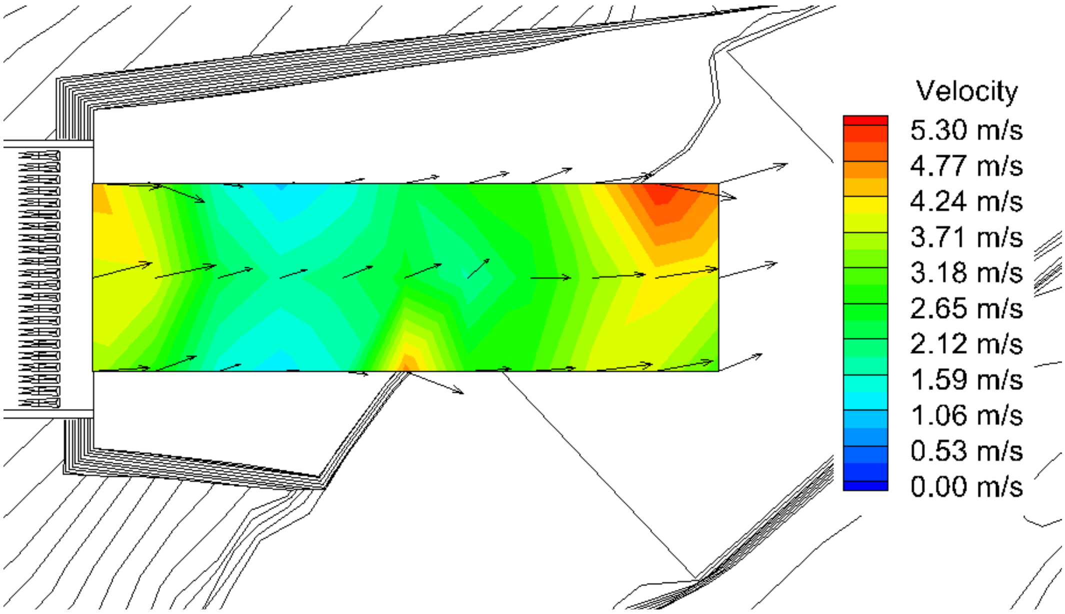

Figure K.5: *Velocity 1 m above the downstream invert for bottom profile 7.* $Q = 2250\ m^3/s$.

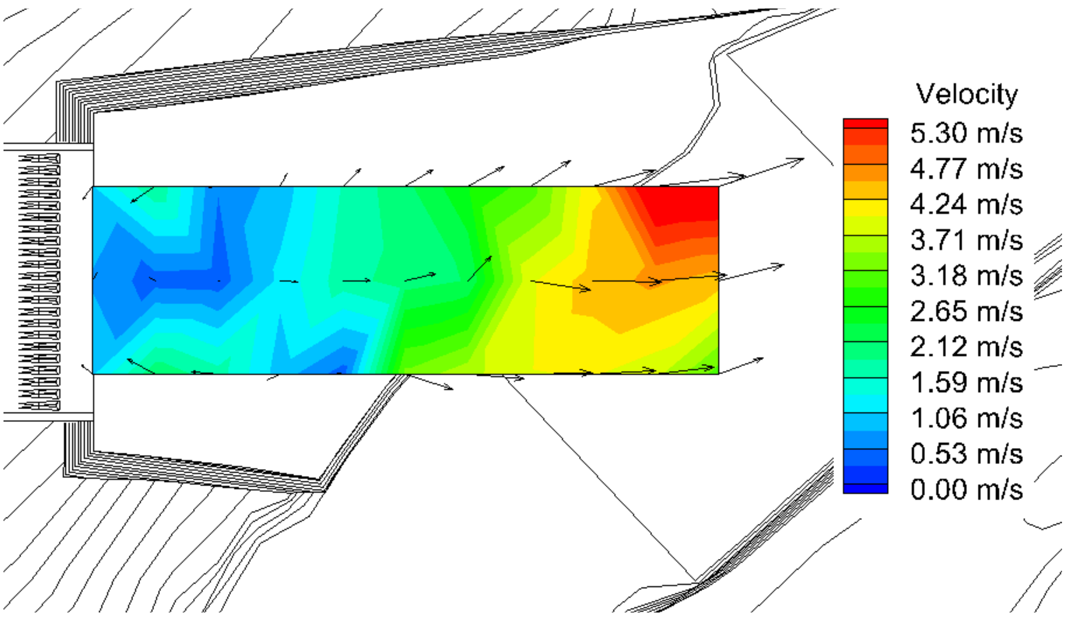

Figure K.6: *Velocity 1 m above the downstream invert for bottom profile 8.* $Q = 2250\ m^3/s$.

Final design

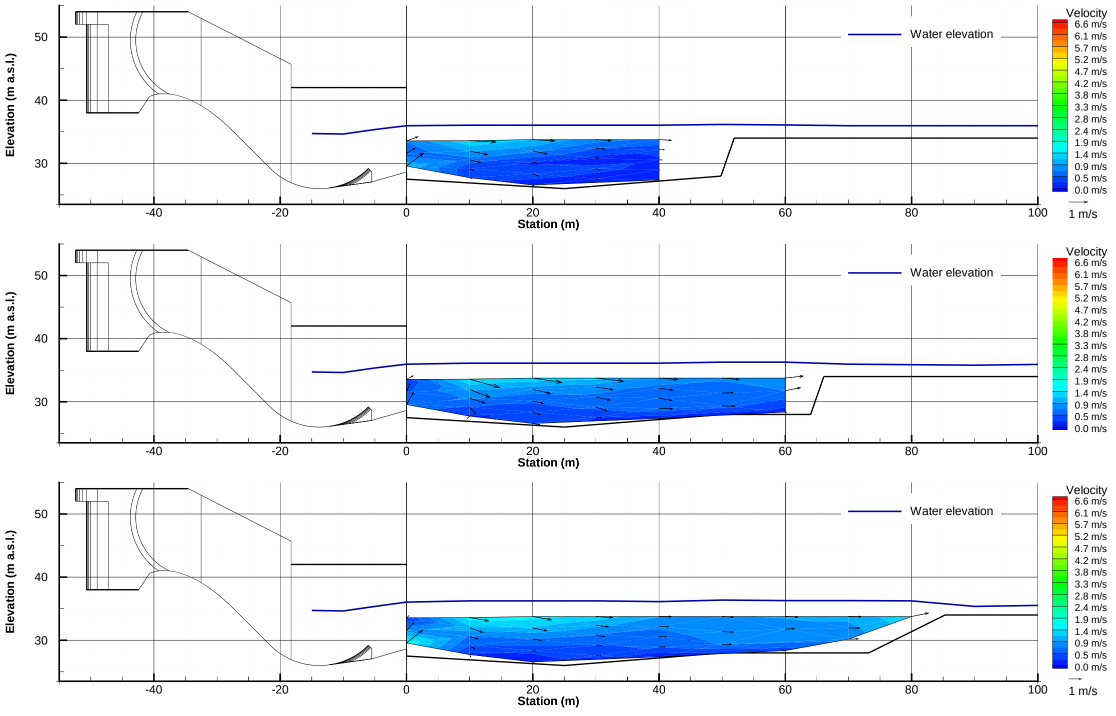

Figure K.7: *Velocity measurements in the three section lines for 350 m^3/s.*

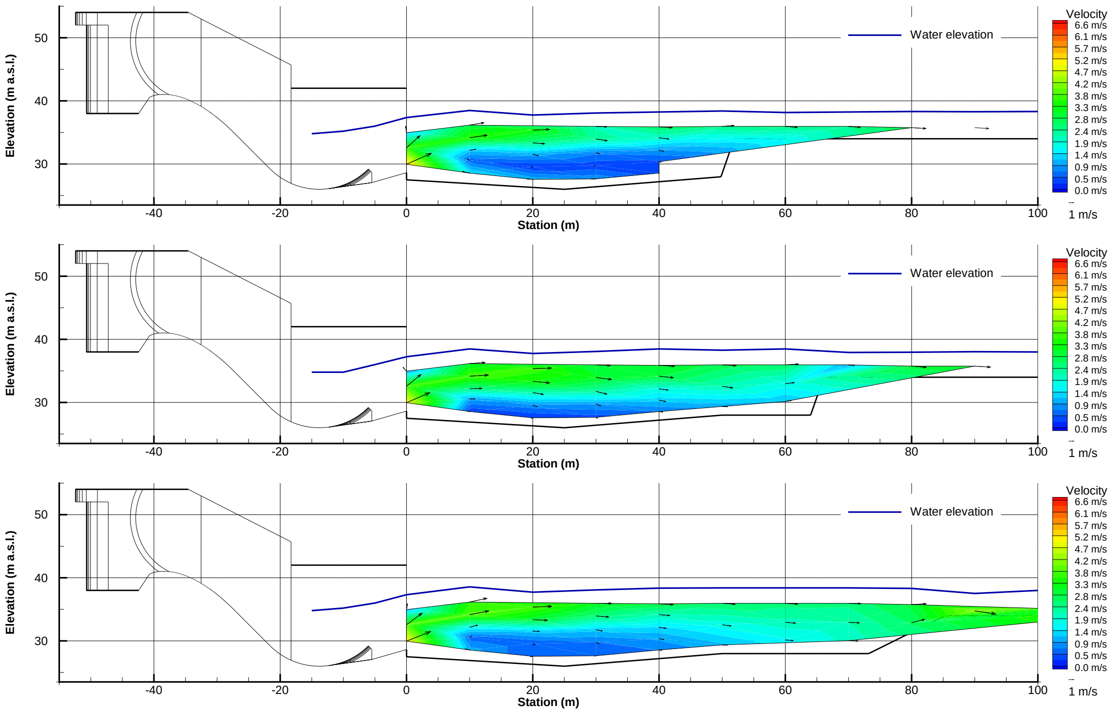

Figure K.8: *Velocity measurements in the three section lines for 1050 m^3/s.*

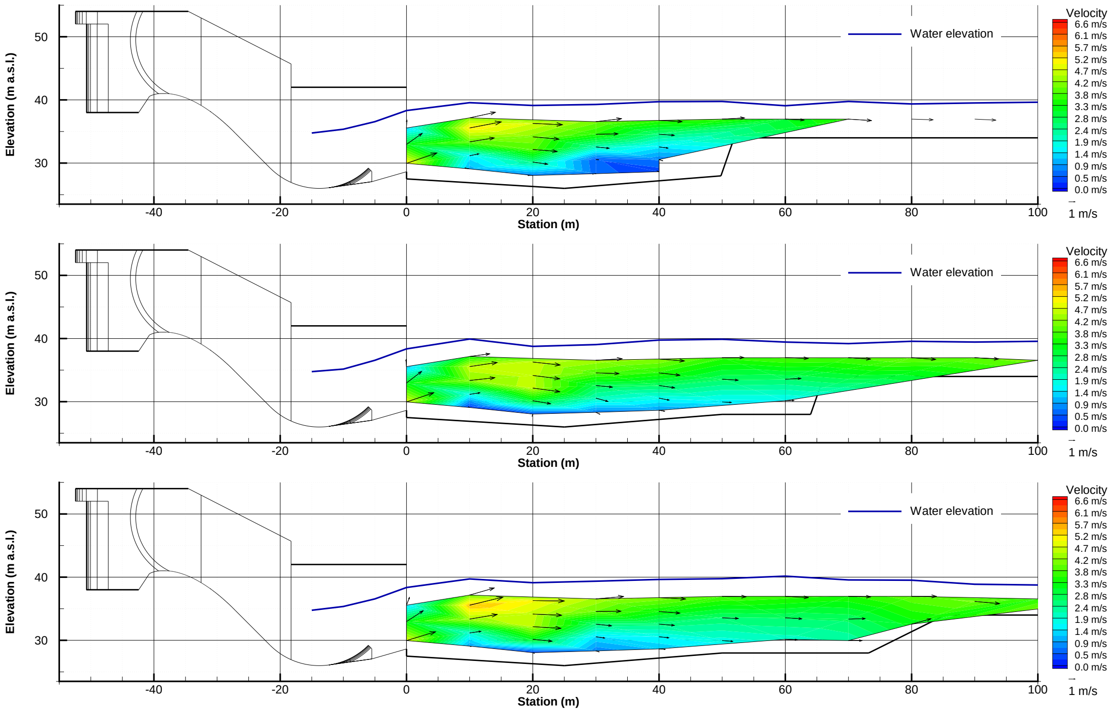

Figure K.9: *Velocity measurements in the three section lines for 1700 m^3/s.*

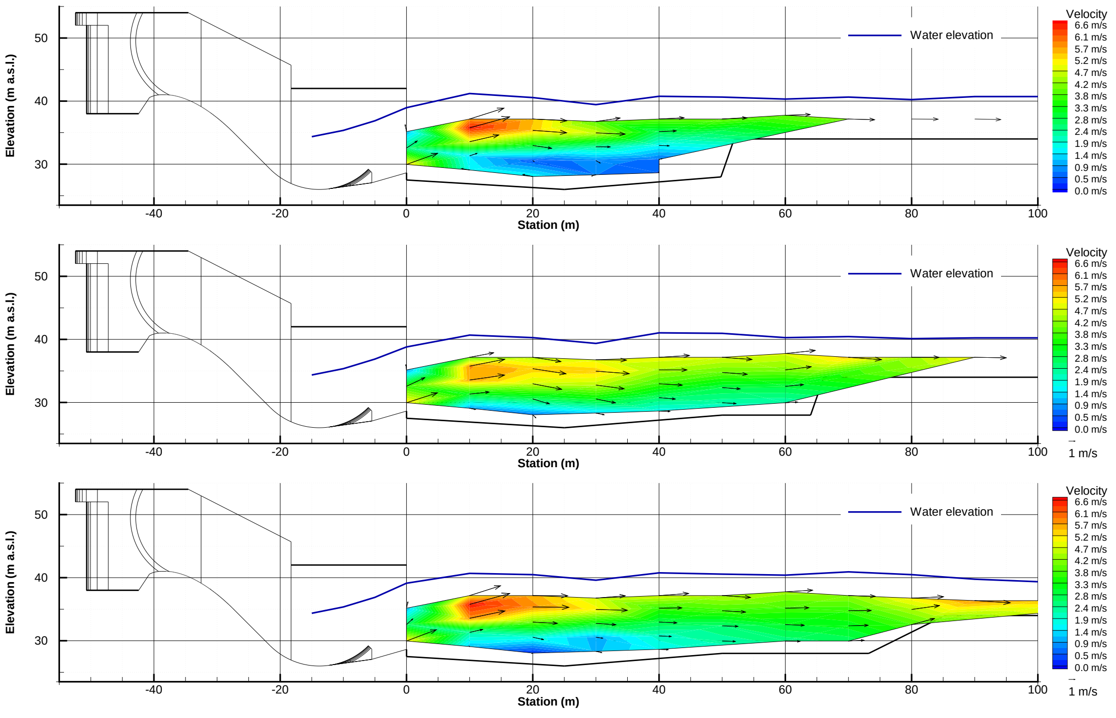

Figure K.10: *Velocity measurements in the three section lines for 2250 m^3/s.*

L. Spillway rating curves

Interlocked gate operation

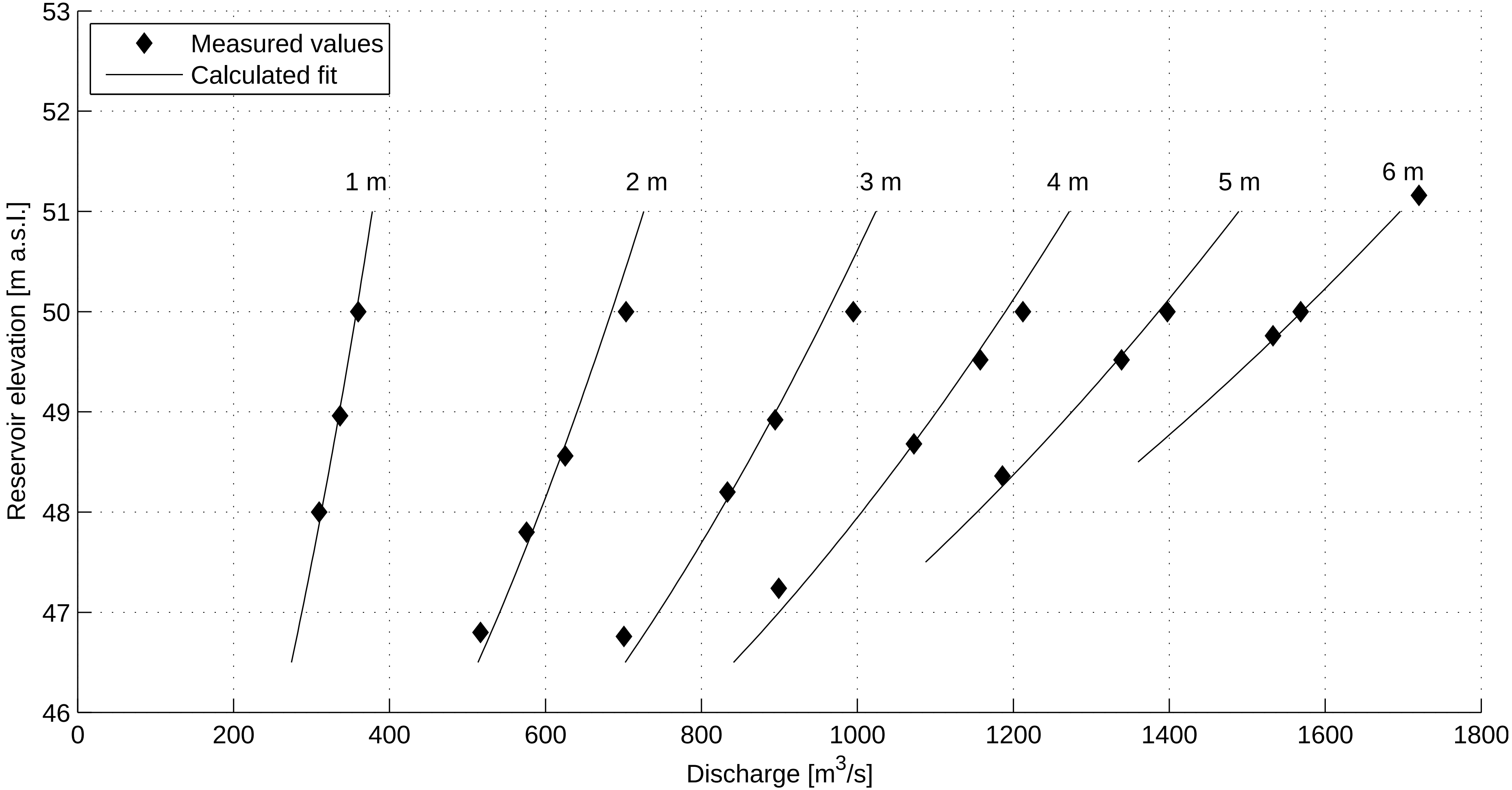

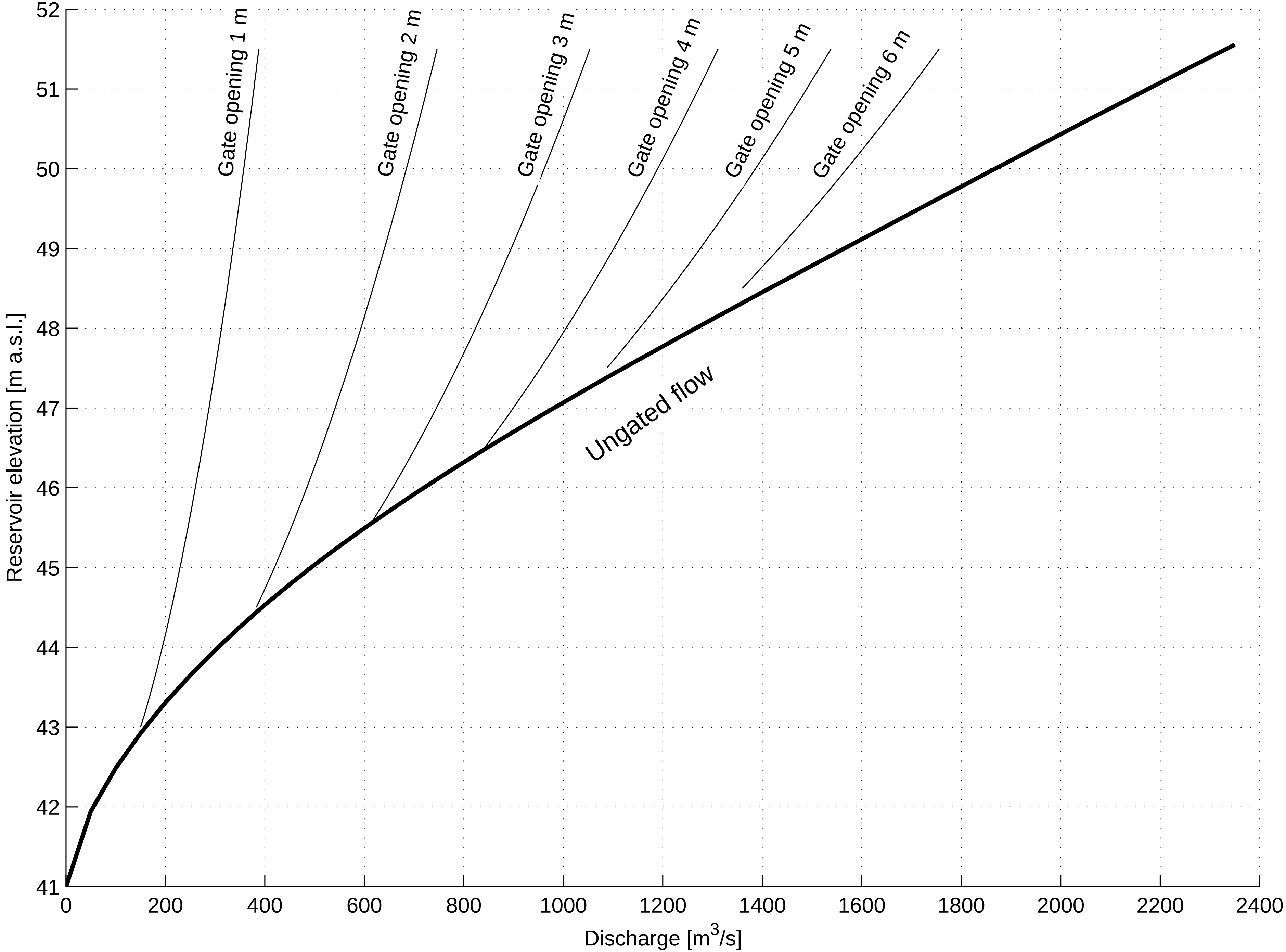
Reservoir elevation [m a.s.l.]
52
51
50
49
48
47
46
45
44
43
42
41
0
200
400
600
800
1000
1200
1400
1600
1800
2000
2200
2400
Discharge [m³/s]
Gate opening 1 m
Gate opening 2 m
Gate opening 3 m
Gate opening 4 m
Gate opening 5 m
Gate opening 6 m
Ungated flow

Single gate operation

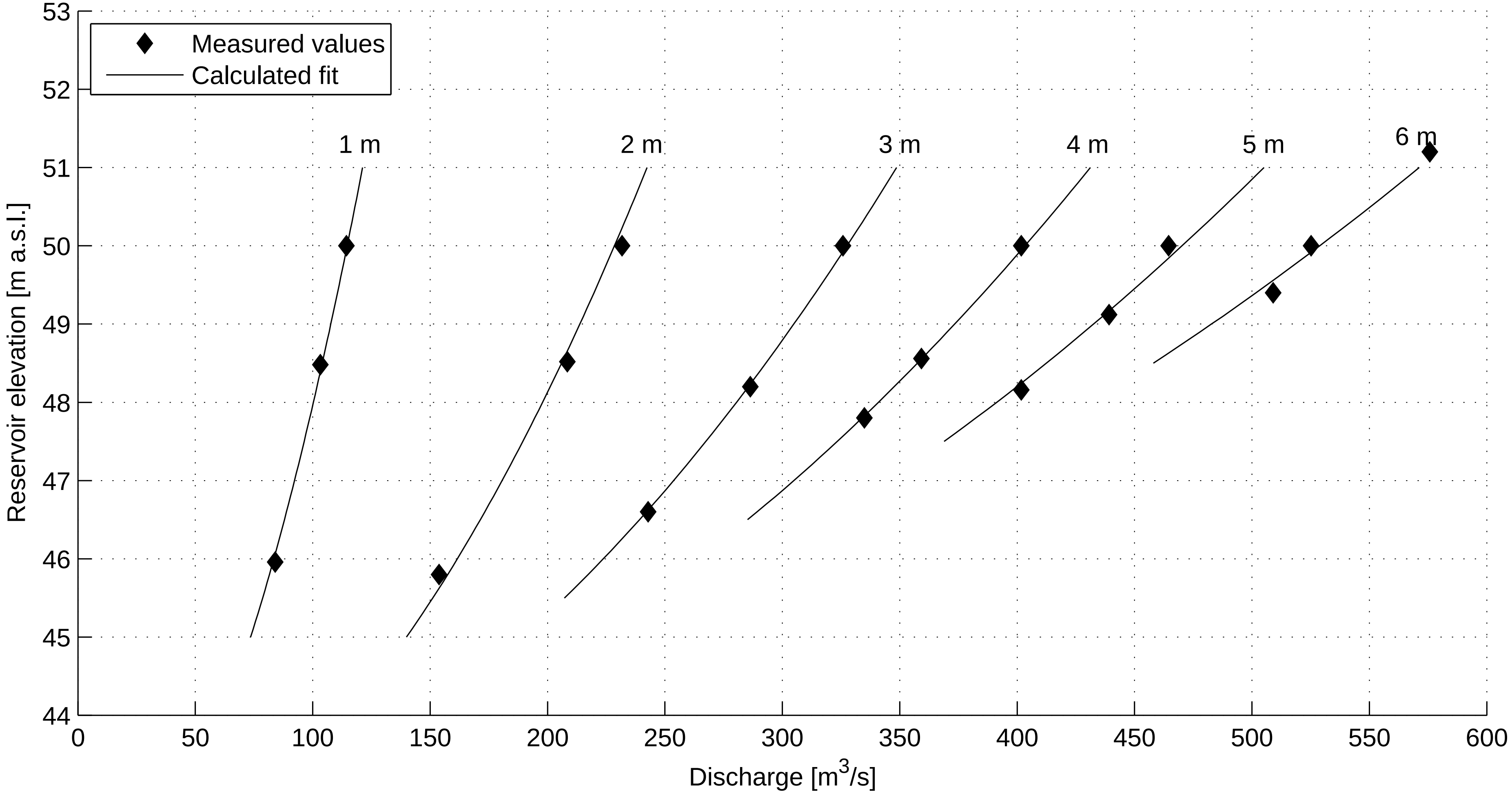

M. Video and images

Landsvirkjun

Háaleitisbraut 68
103 Reykjavík
landsvirkjun.is

landsvirkjun@lv.is
Sími: 515 90 00